University of Novi Sad
FACULTY OF TECHNICAL SCIENCES
DEPARTMENT OF PRODUCTION ENGINEERING
21000 NOVI SAD, Trg Dositeja Obradovica 6, SERBIA

UDK 621 ISSN 1821-4932

JOURNAL OF

PRODUCTION ENGINEERING

Volume 19 Number 2

Novi Sad, December 2016

Journal of Production Engineering, Vol.19 (2016), Number 2

Publisher: FACULTY OF TECHNICAL SCIENCES
DEPARTMENT OF PRODUCTION ENGINEERING
21000 NOVI SAD, Trg Dositeja Obradovica 6
SERBIA

Manuscript submitted for publication: December 20, 2016.
Printing: 1st
Circulation: 300 copies

CIP classification:

CIP – Катаголизација у публикацији
Библиотека Матице српске, Нови Сад

621

JOURNAL of Production Engineering / editor in chief Pavel Kovač. – Vol. 12, No. 1 (2009)- . – Novi Sad : Faculty of Technical Sciences, Department for Production Engineering, 2009-. – 30 cm

Dva puta godišnje (2012-). Je nastavak: Časopis proizvodno mašinstvo = ISSN
0354-6446
ISSN 1821-4932

Printing by: FTN, Graphic Center ***GRID,*** *Novi Sad*

ISSN: 1821-4932

INTERNATIONAL EDITORIAL BOARD

Editorial

The ***Journal of Production Engineering*** *dates back to 1984, when the first issue of the* ***Proceedings of the Institute of Production Engineering*** *was published in order to present its accomplishments. In 1994, after a decade of successful publication, the Proceedings changed the name into Production Engineering, with a basic idea of becoming a Yugoslav journal which publishes original scientific papers in this area.*

In 2009 year, our Journal finally acquires its present title - ***Journal of Production Engineering****. To meet the Ministry requirements for becoming an international journal, a new international editorial board was formed of renowned domestic and foreign scientists, refereeing is now international, while the papers are published exclusively in English. From the year 2011 Journal is in the data base COBISS and KoBSON presented.*

The Journal is distributed to a large number of recipients home and abroad, and is also open to foreign authors. In this way we wanted to heighten the quality of papers and at the same time alleviate the lack of reputable international and domestic journals in this area.

In this journal are published, reviewed papers from International Conference "ETIKUM 2016" which was in Novi Sad, Serbia and certain number of new scientific papers as well.

Editor in Chief

Professor Pavel Kovač, PhD,

Journal of Production Engineering
Vol.19 No.2

Contents

ORIGINAL SCIENTIFIC PAPER

Journal of Production Engineering
Vol.19 No.2
JPE (2016) Vol.19 (2) Original Scientific Paper
Madić, M., Radovanović, M., Janković, P., Petković, D., Mladenović, S.

ANALYSIS OF LASER CUTTING PROCESS BY DEVELOPMENT OF PERFORMANCE DIAGRAMS

Received: 23 June 2016 / Accepted: 08 September 2016

Abstract: *Laser cutting is an important contour cutting technology in industry. Adequate application of this technology, in terms of satisfying different quality, productivity and costs criteria, requires identification of the most suitable laser cutting conditions for each workpiece thickness and material. In this paper, on the basis of experimental results of CO_2 laser cutting of aluminum alloy and mathematical models laser, cutting performance diagrams for identification of the most suitable cutting conditions were developed. Laser cutting experimentation was based on the use of design of experiment approach by varying laser power, cutting speed and assist gas pressure at three levels. Performance diagrams, representing different laser cutting conditions, were developed considering surface roughness, kerf width and material removal rate as criteria. Three performance diagrams were used for single performance analysis and three 2D performance diagrams were used for analysis of the performance correlations.*

Key words: *laser cutting, performance diagrams, surface roughness, kerf width, material removal rate*

Analiza procesa laserskog sečenja kreiranjem dijagrama performansi. *Lasersko sečenje je važna tehnologija konturnog sečenja u industriji. Adekvatna primena ove tehnologije, u smislu zadovoljenja različitih kriterijuma kvaliteta, produktivnosti i troškova, zahteva identifikaciju najpovoljnijih uslova obrade i to za svaku vrstu materijala, kao i debljinu pripremka. U ovom radu su na osnovu dobijenih eksperimentalnih rezultata CO_2 laserskog sečenja legure aluminijuma dobijeni matematički modeli pomoću kojih su kreirani dijagrami performansi za identifikaciju najpovoljnijih uslova obrade. Eksperiment laserskog sečenja je realizovan primenom teorije planiranja eksperimenta variranjem snage lasera, brzine sečenja i pritiska pomoćnog gasa na tri nivoa. Dijagrami performansi, na kojima su prikazani različiti uslovi obrade, su kreirani uzimajući u obzir hrapavost površine reza, širinu reza i proizvodnost kao kriterijume. Tri dijagrama perfomansi su primenjena za jednokriterijumsku analizu performansi laserskog sečenja, a tri 2D dijagrama performansi su primenjena za višekriterijumsku analizu korelacija performansi laserskog sečenja.*

Ključne reči: *CO_2 lasersko sečenje, dijagrami performansi, hrapavost površine, širina reza, proizvodnost*

1. INTRODUCTION

Laser cutting is thermal based machining process involving a laser beam as a heat source. Once the beam has been generated, a lens system focuses the laser beam onto a small spot with diameter of about 0.2 mm [1] and part of the laser beam energy is absorbed by the workpiece surface due to the interaction between the electromagnetic radiation and electrons of the workpiece materials. The remaining is lost due to the reflection by the workpiece surface [2]. The absorbed energy causes melting, evaporation or chemical state change of the workpiece material which is being removed by a coaxial stream of assist gas, generating a narrow cut kerf. Figure 1 illustrates the principle of laser cutting process.

Laser cutting technology has been successfully established for processing of metal sheets and parts since the 1970s and is state-of-the-art today even in small and medium enterprises [3]. It can be used for cutting small and complex geometries on almost all categories of materials including metals, non-metals, ceramics and composites with high productivity and low costs [4]. Compared to traditional technologies, it can achieve better cut quality, smaller kerf width, localized heat affected zone (HAZ), higher accuracy of processing (narrower tolerance measures) [5]. However, laser cutting machines usually have a higher capital cost than plasma, oxy-fuel, and water-jet machines. Also, this technology is not best suited to cutting material thicker than 0.5 inches (12.7 mm) and has difficulty cutting reflective metals like copper and aluminum, where a major portion of the laser energy can be reflected away from the cut [6].

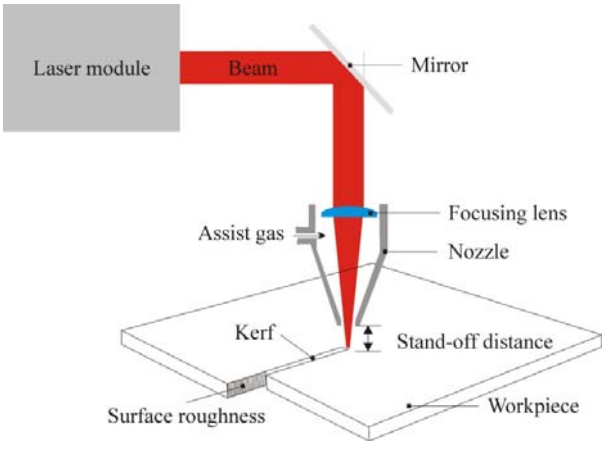

Fig. 1. Principle of laser cutting process

The laser cutting process itself is a complex machining process which is governed by a set of parameters which, both qualitatively and quantitatively, differently affect laser cutting process performances such as material removal rate (MRR), costs, processing time, cutting speed, kerf profile characteristics, HAZ, surface profile of the cut edge, dross formation, etc. In continuous wave CO_2 laser cutting operation of a given workpiece thickness and material characteristics, these performances are mostly affected by used laser cutting system (beam quality and polarization, TEM mode), main processing parameters (laser power, cutting speed, focus position), type, purity and pressure of assist gas, type and diameter of nozzle as well as standoff distance, and length and depth of focus. In order to achieve high performance laser cutting operation it is necessary to adequately set these parameters which allow a constant removal of the material from the cutting zone [7]. Otherwise, inadequate selection of cutting conditions, which can be reflected as extremely large submitted energy [8], may result in appearance of irregularities at the edges, on the cut surface, drips (solidified molten material), cracks on cut surface and other irregularities [5].

The use of laser cutting systems in manufacturing companies is usually not optimal only because there is lack of technological basis in a specific production condition [5]. But this should not be a reason for determining (near) optimal cutting conditions with the use of relatively simple optimization methods that can be readily applied by engineers, especially when expensive workpiece materials are used. In that manner laser cutting performances can be considerably improved, however, it is almost impossible to improve all performances at the same time [1, 9].

This paper presents the possibility of development and use of performance diagrams for the analysis of CO_2 laser cutting of aluminum alloy. Based on the experimental results from the full factorial design, three mathematical models, in form of regression equations, for prediction of surface roughness, kerf width and MRR were developed. Based on these models and by considering laser cutting machine constraints, in terms of selection of main laser cutting parameter values, six performance diagrams were developed. First three performance diagrams were used for the analysis of achievable surface roughness, kerf width and MRR values within covered experimental hyperspace, and the other three were used for analysis of the correlations that exist between these performances.

2. EXPERIMENTAL DETAILS

2.1 Equipment and experimental setup

The experimental trials were conducted on CNC laser cutting machine Domino Evoluzione (Prima Industries) in real manufacturing environment. The CO_2 laser cutting machine operates at 10.6 μm wavelength with a maximal output power of 4 kW in CW mode. The dimensional capacity of this machine is 3050×1540 mm with positioning accuracy axes of 0.03 mm. The laser beam was focused using a ZnSe focusing lens with focal length of 127 mm. Assist gas was suplied coaxially with the laser beam via a 2 mm diameter conical-shaped nozzle. The distance between nozzle and workpiece (stand-off distance) was controlled at 0.8 mm. In experimental trials straight cuts were performed with a Gaussian distribution beam mode (TEM_{00}) on a 3 mm thick AlMg3 workpiece material (Al 5754) by using nitrogen with purity of 99.95% as assist gas. This Al alloy has excellent corrosion resistance, especially to seawater and industrially polluted atmospheres, high ductility and elongation and good welding properties. The products manufactured from these sheets are widely used in industry, e.g. shipbuilding, automobile sector, food industry, welded structures etc.

For the purpose of experiment realization, a design of experiments (DOE) approach was adopted by taking into account laser power, cutting speed and assist gas pressure as three main factors which affect laser cutting performances to the great extent. In order to generate a uniform distribution of experimental trials within the covered hyperspace, 3^3 full factorial design plan was adopted whereas the selected input variables were varied at three levels (Table 1). Note that the range of variation for cutting speed is reduced and relatively narrow because pre-experimental trials have shown that combination of selected values of laser power and assist gas pressure with higher values of cutting speed lead to difficulties in cutting due to high reflectivity and conductivity of this aluminum alloy.

Input variables	Unit	Level 1	Level 2	Level 3
Laser power, P	kW	3	3.5	4
Assist gas pressure, p	bar	6	8	10
Cutting speed, v	m/min	3	3.25	3.5

Table 1. Laser cutting parameters used in DOE

2.2 Laser cutting performances

Laser cutting performances considered in the study included the measurement of the surface roughness, kerf width and material removal rate (MRR). Surface roughness was measured in terms of the ten-point mean roughness, R_z, using MahrSurf-XR1 measuring instrument. Each measurement was taken along the laser cut at approximately the middle of the workpiece thickness. Kerf width, which represents the top kerf width, was measured at three different places at equal distances along the length of cut using the optical coordinate measuring device Mitutoyo (type: QSL-200Z). Surface roughness and kerf width measurements were repeated so as to obtain averaged values. Based on the obtained kerf width values for different combinations of laser cutting parameters, the MRR was calculated as the product of kerf width, workpiece thickness and cutting speed.

3. MATHEMATICAL MODELS OF LASER CUTTING PERFORMANCES

For the purpose of the analysis of the laser cutting results in terms of considered performance, based on experimentally measured data and calculations, three mathematical models were developed. Mathematical models for estimation of surface roughness, kerf width

and MRR in terms of second order polynomial were obtained as follows:

$$R_z = 240.3 - 18.9 \cdot P - 4.8 \cdot p - 111.2 \cdot v + 8.3 \cdot P^2 - 0.04 \cdot p^2 + 29.5 \cdot v^2 + 2.8 \cdot P \cdot p - 19.5 \cdot P \cdot v - 0.6 \cdot p \cdot v \quad (1)$$

$$K_w = 0.62 + 1.18 \cdot P + 0.14 \cdot p - 1.76 \cdot v - 0.18 \cdot P^2 - 0.001 \cdot p^2 + 0.32 \cdot v^2 + 0.01 \cdot P \cdot p + 0.002 \cdot P \cdot v - 0.04 \cdot p \cdot v \quad (2)$$

$$MRR = 3558 + 11167 \cdot P + 1198 \cdot p - 16297 \cdot v - 1726 \cdot P^2 - 11 \cdot p^2 + 3124 \cdot v^2 + 106 \cdot P \cdot p + 116 \cdot P \cdot v - 387 \cdot p \cdot v \quad (3)$$

Prediction accuracy of the developed mathematical models was statistically tested in terms of the mean absolute percentage error (MAPE). With MAPEs less than 5 % it has been concluded that these models can be used for further analysis of the performed laser cutting experimentation.

4. RESULTS AND DISCUSSIONS

With the use of the developed mathematical models one can analyze the main and interaction effects of the laser cutting parameters on the selected performances by plotting 2D or 3D diagrams. However, the goal of the present research was to develop performance diagrams so as to be able to analyze obtainable laser cutting performances as well as their correlations. These performance diagrams are indented to show achievable laser cutting performance values with respect to different laser cutting conditions. They are valid for the covered experimental hyperspace and taking into account that laser cutting parameters such as laser power, cutting speed and assist gas pressure are adjustable in discrete domain. In the covered ranges, the laser power, cutting speed and assist gas pressure were varied at 21, 11 and 81 levels, respectively. Thus each increment in laser cutting parameter values accounts for 0.05 (kW, m/min or bar). In this way 18711 different laser cutting conditions were analyzed.

Figures 2, 3, and 4 show performance diagrams for surface roughness, kerf width and MRR for different laser cutting conditions. Each point in presented figures corresponds to a particular laser cutting condition, i.e. combination of laser cutting parameter values.

From Figure 2 it can be seen that combination 10227, corresponding to the following laser cutting parameter values (P=4 kW, p=6 bar, v=3.3 m/min), yield minimal surface roughness value of R_z=17.6 µm. On the other hand, combination 1701, corresponding to the following laser cutting parameter values (P=4 kW, p=10 bar, v=3 m/min), yield maximal surface roughness value of R_z=34.63 µm.

From Figure 3 it can be seen that combination 3403, corresponding to the following laser cutting parameter values (P=3 kW, p=6.05 bar, v=3.1 m/min), yield minimal kerf width value of K_w=0.387 mm. On the other hand, combination 1694, corresponding to the following laser cutting parameter values (P=3.65 kW, p=10 bar, v=3 m/min), yield maximal kerf width value of K_w=0.55 mm. Here it is interesting to note that minimal kerf width does not correspond to the maximal cutting speed which is the most common case.

From Figure 4 it can be seen that first combination, corresponding to the following laser cutting parameter values (P=3 kW, p=6 bar, v=3 m/min), yield minimal MRR value of MRR=3517 mm^3/min. On the other hand, last combination, corresponding to the following laser cutting parameter values (P=4 kW, p=10 bar, v=3.5 m/min), yield maximal MRR value of MRR=5211 mm^3/min.

The second part of analysis is focused on correlations between laser cutting performances. In laser cutting it is well known, as in most machining processes, that there is no particular combination of parameter values which is the most desirable with respect to different performances. Thus, process planners and engineers are often in situation to choose a particular laser cutting conditions which meet set requirements to the greatest extent. To this aim three 2D performance diagrams showing the correlations between laser cutting performances were developed (Figures 5, 6 and 7).

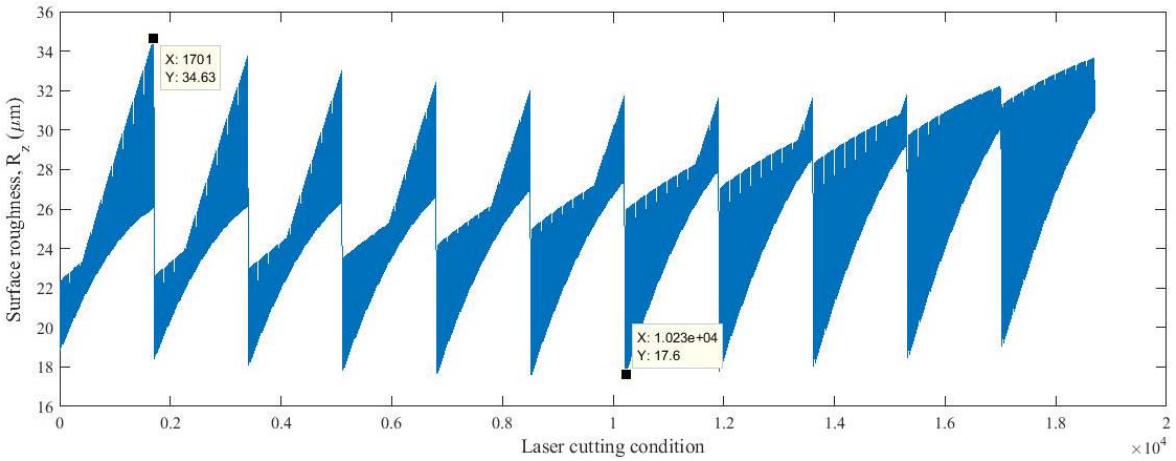

Fig. 2. Performance diagram for surface roughness

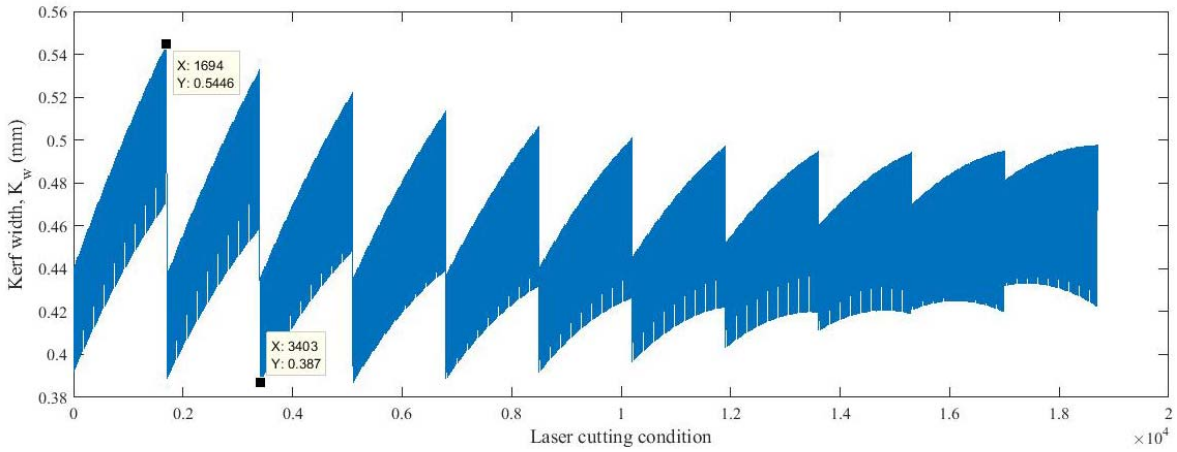

Fig. 3. Performance diagram for kerf width

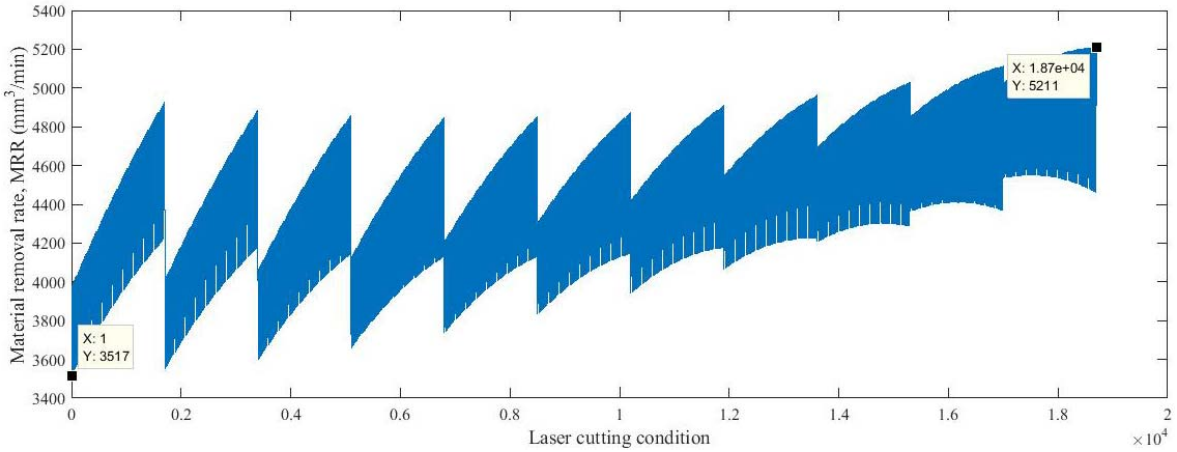

Fig. 4. Performance diagram for MRR

Here it should be noted that on these 2D performance diagrams the points on the outer edges actually represent Pareto optimal solutions. The costs of assist gas pressure were omitted in this analysis since the corresponding model is a function of only assist gas pressure.

Figure 5 presents all 18711 different laser cutting conditions while considering surface roughness and kerf width at the same time. As it is beneficial that these performances have as lower values as possible, the best laser cutting conditions, which can be regarded as near optimal, are positioned in the lower left corner. For example, the red colored point in the Figure 5, corresponding to the laser cutting condition of P=4 kW, p=6 bar, v=3.2 m/min, represents near optimal laser cutting condition which yield surface roughness value of R_z=17.77 µm and kerf width value of K_w=0.39 mm.

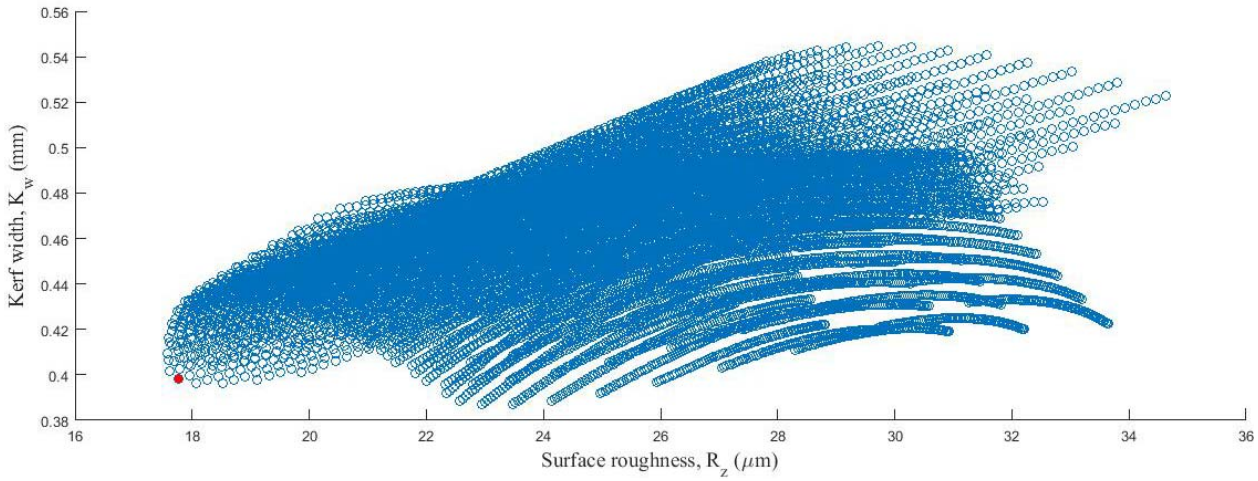

Fig. 5. 2D performance diagram showing correlation between surface roughness and kerf width

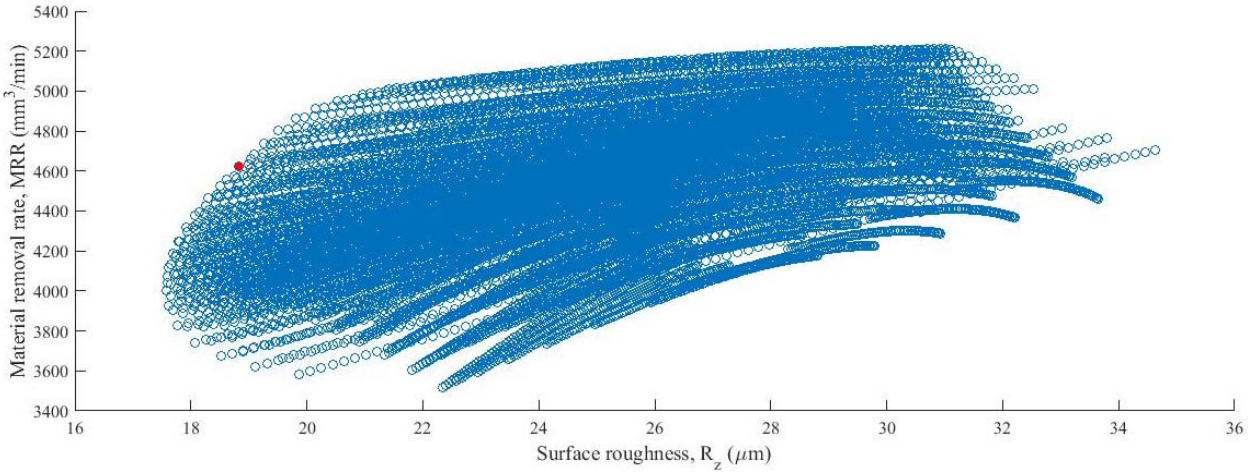

Fig. 6. 2D performance diagram showing correlation between surface roughness and MRR

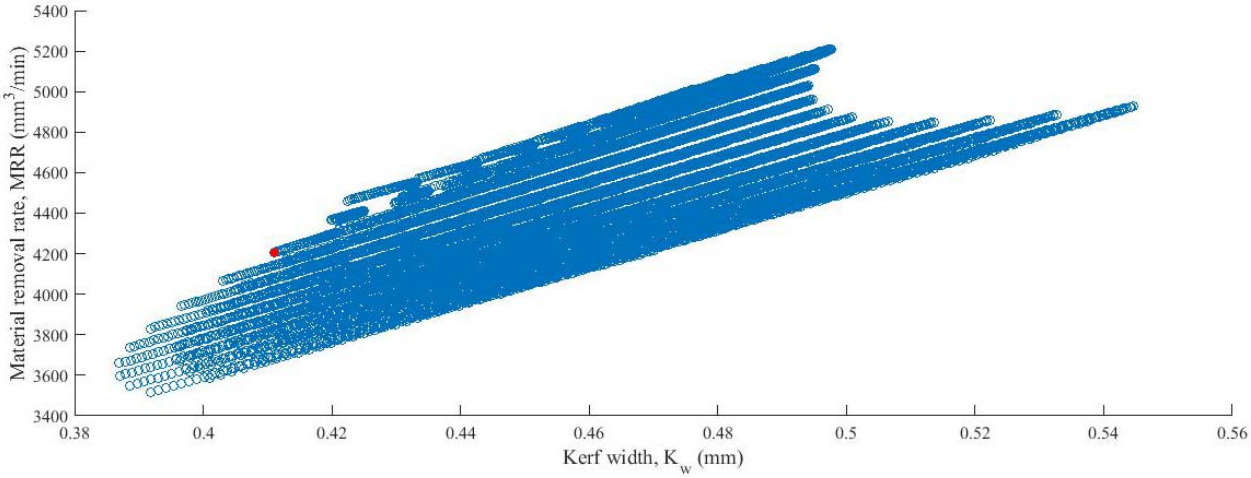

Fig. 7. 2D performance diagram showing correlation between kerf width and MRR

Figure 6 presents different laser cutting conditions while considering surface roughness and MRR at the same time. These are opposite criteria in terms of beneficial performance values, i.e. surface roughness is to be minimized while MRR is to be maximized. Therefore, the most suitable laser cutting conditions are positioned in the upper left corner. For example one can choose P=3.9 kW, p=6 bar, v=3.45 m/min which would yield surface roughness value of R_z=18.83 μm and MRR value of MRR=4625 mm^3/min. Finally, Figure 7 presents different laser cutting conditions while considering kerf width and MRR at the same time. As in the previous case, the most suitable laser cutting conditions are positioned in the upper left corner. Here it should be noted that the distinctive form of this performance diagram is due to the fact that MRR is a function of kerf width. Among a number of possible solutions one can choose P=3 kW, p=6 bar, v=3.4 m/min which would yield kerf width value of K_w=0.41 μm and MRR value of MRR=4207 mm^3/min.

5. CONCLUSION

In this paper the possibility of development and use of performance diagrams for analysis of laser cutting process was discussed in the case of CO_2 laser cutting of aluminum alloy. The performance diagrams were developed with the help of mathematical models developed upon experimental results considering laser power, cutting speed and assist gas pressure as input variables and surface roughness, kerf width and MRR as laser cutting performances. Within covered experimental hyperspace on the basis of performed analysis the following conclusions can be drawn:

- The change of laser cutting parameter values, within the covered experimental hyperspace, leads to significant changes in surface roughness values, with the difference between minimal and maximal of about 2 times. For decreasing surface roughness it is preferable to use high laser power, low assist gas pressure and intermediate cutting speed.
- The kerf width values are less sensitive to the changes in the laser cutting parameter values, i.e. different laser cutting parameter combinations. For obtaining narrower kerf width it is preferable to use low laser power, low assist gas pressure and lower cutting speed,
- Using higher values of laser power, cutting speed and assist gas pressure ensures maximization of MRR.

Based on the proposed 2D performance diagrams, the multiple near optimal laser cutting conditions for satisfying two performances at the same time can be easily identified. In this way the performance diagrams

can be used as decision making aid for process planning engineers with ultimate aim to efficiently utilize the capability of given laser cutting system and satisfy quality requirements. Finally, it has to be noted that these diagrams can be used for selection of cutting conditions so as to minimize, maximize or satisfy target values of given performances. Future work will consider development of performance diagrams for other machining processes.

6. REFERENCES

[1] Madić, M., Radovanović, M., Trajanović, M., Manić, M.: *Analysis of correlations of multiple-performance characteristics for optimization of CO2 laser nitrogen cutting of AISI 304 stainless steel*, Journal of Engineering Science and Technology Review, Vol. 7, No. 2, p.p. 16-21, 2014.

[2] Sun, S., Brandt, M.: *Laser Beam Machining*, In Nontraditional Machining Processes, p.p. 35-96, 2013, Springer, London.

[3] Goeke, A., Emmelmann, C.: *Influence of laser cutting parameters on CFRP part quality*, Physics Procedia, Vol. 5, No. 2, p.p. 253-258, 2010.

[4] Leone, C., Genna, S., Caggiano, A., Tagliaferri, V., Molitierno, R.: *Influence of process parameters on kerf geometry and surface roughness in Nd: YAG laser cutting of Al 6061T6 alloy sheet*, The International Journal of Advanced Manufacturing Technology, 2016, doi 10.1007/s00170-016-8667-4.

[5] Čekić, A., Begić-Hajdarević, D.: *Definition of mathematical models of high-alloyed steel 1.4828 in CO_2 laser cutting*, Procedia Engineering, Vol. 100, p.p. 435-444, 2015.

[6] Leahu, D., Grecu, V., Cuică, I.: *Best cutting method of a material using the decision support system*, Annals of the University of Oradea, Vol. 23, No. 3, p.p. 61-64, 2014.

[7] Petrianu, C., Inţă, M., Manolea, D.: *Laser cutting process–influence of assiting gas pressure on surface roughness at mild steel cutting*, The 4th International Conference "Advanced Composite Materials Engineering " COMAT 2012, 18- 20 October 2012, Brasov, Romania, p.p. 427-432, 2012.

[8] Wandera, C.: *Laser Cutting of Austenitic Stainless Steel with High Quality Laser Beam*, PhD Thesis, Lappeenranta University of Technology, 2006.

[9] Dubey, A.K., Yadava, V.: *Multi-objective optimisation of laser beam cutting process*, Optics and Laser Technology, Vol. 40, No. 3, p.p. 562-570, 2008.

Authors: **Dr. Miloš Madić, Prof. Dr. Miroslav Radovanović, Prof. Dr. Predrag Janković, MSc Dušan Petković, MSc Srđan Mladenović**, University of Niš, Faculty of Mechanical Engineering in Niš, Aleksandra Medvedeva 14, 18 000 Niš, Serbia, Phone: +381 18 500-687, Fax: +381 18 588-244;

E-mail: madic@masfak.ni.ac.rs
mirado@masfak.ni.ac.rs
jape@masfak.ni.ac.rs
dulep@masfak.ni.ac.rs
maki@masfak.ni.ac.rs

Journal of Production Engineering
Vol.19 No.2
JPE (2016) Vol.19 (2) Original Scientific Paper
Savkovic, B., Taric, M., Kovac, P., Nedic, B., Pucovski, V., Risteiu, M.

MODELING OF CUTTING TEMPERATURE IN TURNING OF HARDENED STEEL

Received: 03 August 2016 / Accepted: 11 October 2016

Abstract: *The paper presents, impact of cutting conditions on cutting temperature during experimental research. With aim of modeling were applied artificial neural networks and genetic algorithm during turning. Processing is performed on the hardened material using cubic boron nitride tool. Measurement of cutting temperature is performed using thermal imaging cameras positioned on the tool holder of machin tool.*
Key words: *cutting temperature, hardened material, artificial neural networks, genetic algorithm.*

Modeliranje temperature rezanja pri obradi struganjem kaljenog čelika. *U radu su prikazani uticaj režima rezanja, na temperature rezanja tokom eksperimentalnih istraživanja. U cilju modeliranja temperature rezanja primenjene su veštačke neuronske mreže i genetski algoritmi pri obradi struganjm. Obrada je vršena na kaljenom materijalu pomoću alata od kubnog nitrida bora. Merenje temperature rezanja je isvršeno pomoću termovizijske kamere postavljene na nosač alata.*
Ključne reči: *temperatura rezanja, kaljeni čelik, veštačke neuronske mreže, genetski algoritam.*

1. INTRODUCTION

The generation of heat in the cutting zone occurs as a result of work expended for metal cutting. The work is spent out on the plastic deformation of the cutting layer, and on overcoming the friction that occurs on the contact surface of the tool and workpiece. The heat generated in the chip formation zone, as well as in the contact zone of tool and chip (as well as tool and workpiece), directly affects the surface quality, accuracy and productivity of machining processes as well as other phenomena in machining.

Temperature of cutting is a very important indicator of the machining process. Mathematical modeling of this parameter is very difficult, both because of the large number of influencing factors and because of ignorance of the relations between them and difficulties in process measurement.

Nowadays, in solving such problems more frequently used systems based on artificial intelligence with which we can monitor the changes of parameters depending on the change of input, which leads to useful information and conclusions about the behavior of the cutting process.

A number of factors that influence the results obtained, it is the deviation of the experimentally obtained results from the literature values very often. It is The difference between the results show the importance of the use of artificial intelligence, and in recent years increasingly are used systems based on genetic algorithms and neuro-fuzzy systems.

2. HEAT AND TEMPERATURE OF CUTTING

The emergence of heat in the cutting zone is the result of converting mechanical energy into heat. Heat affects: the education process sawdust, wood shavings and plastic deformation factor compacted sawdust, of cutting resistance, the occurrence of deposits, the intensity of the development process of wear of cutting tools and elements of the structure and thickness of the defect layer. More than 99.5% of the energy (mechanical work) consumed in the deformation of the workpiece material and to deal with the force of friction on the contact surfaces of cutting tools wedge (pectoral and dorsal) is converted into heat [1].

Heat generated in the cutting zone leads to a warming of the workpiece, shavings and cutting tools and phenomena characteristic of temperature field and temperature.

2.1 A summary of the test of thermal phenomenon in cutting

Arsecularante [2] in its work an assessment of the recently developed semi-empirical method for predicting the durability, chip contact length and temperature. These parameters and empirical relations are used to calculate the temperature of cutting and tool life. Author of the experimental results verify these methods and use the results to predict the deformation tools. At the end of the experimental results were compared with those obtained analytically. It was noted that during cutting when the tool occurring temperature over 800 °C, diffusion occurs as a primary mechanism of tool wear, which depends on the temperature of cutting. It is therefore appropriate temperature determined by the material characteristics of the workpiece and the processing conditions. If the theory of cutting tools known dependence of the stability of the processing temperature, with known temperature, it is possible to predict the tool life with much less effort than purely empirical reasoning.

Grzesik and others. [2-5] experimentally and analytically investigated the thermodynamic effects on the angle of attack tools in orthogonal cutting. Measuring the temperatures of down to the angle of attack tools is done with thermocouples.

2.2 Thermography and thermal imaging cameras

Sometimes it is difficult to estimate the losses incurred huge damage to your device and equipment in operation, for example. Due to power failure or engine overheating in the manufacturing process, large heat losses due to some unknown damage. On some inaccessible places where is needed to determine the temperature a contact method is not suitable, we come to the use of infrared thermography (thermal imaging), Figure 1. It is known that the number of failures in the industry represents a large cost savings while using thermal imaging very big. Infrared thermography will maximize the protection devices and their accuracy, detect the causes of failures and allow repair in the most favorable time [6]. As contactless temperature measurement method is non-destructive infrared thermography enables the user to discover potential faults without requiring the production process. IC thermography image is processed in a computer with a special program and received the report of the shot.

Figure 1. Thermal imager FLIR e50

3. INTELLIGENT SYSTEMS AND ARTIFICIAL INTELLIGENCE

Artificial intelligence is often associated with the concept of knowledge. Although computer may not have the experience or be able study and learn as do men, it can use the skills that give him human experts. Such knowledge consists of facts, concepts, theories, heuristic methods, procedures and attitudes. Knowledge is information that is organized and analyzed to be understandable and applicable for solving problems or making decisions. To knowledge related to a specific problem had been applied in an intelligent system, is organized and stored in the knowledge base [7].

The in human brain is a collection of information, that is, knowledge, stored and distributed. The cancellation of a neuron does not mean that any of the information is lost, or at least are not completely. All this illustrates why people are so interested in developing new architecture, very similar neurobiological. In this sense, one can observe the main directions of development of these structures:

- Expert systems
- Fuzzy logic
- Artificial neural networks
- Genetic Algorithms
- Genetic programming

3.1 Artificial Neural Network

Important features of both biological and artificial neural networks are parallel distributed processing and distribution of information and management. The neural network there is no central control device according to an established algorithm implements a series of calculation but takes place parallel processing, where each neuron changes its state independently, on the basis of information received from the environment. This gives the neural network a higher speed, and resistance to damage in comparison to digital computers. Although the speed of processing information at a much smaller neurons than the digital computer, the parallelism of work allows the neural network work much more quickly to the results of complex tasks. Also, when is damaged part of the computer's memory, there is a current and continuing loss of information that is contained in it, while the neural network degradation of information takes place gradually, with the possibility that other parts of the network assume the role of the damaged part and compensate for lost information. The neural network has a feature adaptation to changes in the environment in which the network operates and the ability gradual improvement of network operations on the basis of previous experience, that is, learning ability [8].

Possible applications of neural networks include almost every aspect of modern life, from the recognition of printed text, handwriting and speech, through the optimization of the use of channel connections in telecommunications to financial projections and the detection of the illegal use of credit cards.

3.1.1 Model of artificial neurons

Artificial neurons, as well as biologically, has a simple structure and have similar functions as the biological neurons, neurons in Figure 2. The body is called a node or units.

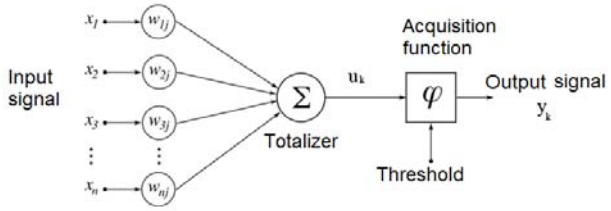

Fig. 2. Model of artificial neurons

3.2 Genetic algorithms

At the end of the 1980s, computer technology has become sufficiently developed so theoretical groundwork of genetic algorithms effectively poured into practical application. Today, genetic algorithms represent a powerful tool for solving many of the problems of engineering practice.

Genetic algorithm is the ideal scanning evolutionary process, but it is said that this is his rough approximation. If you want to simulate a real evolution, then any individual occupied a large part of the memory space, for example to map genotypes only one individual frogs, it would need about 1GB of memory space [9].

Genetic algorithms use a different approach to the problem of optimization. They do not use iterative methods of local optimization are already trying to identify solutions difficult and complex problems by referring to postulate the theory of evolution.

As it is have already said, genetic algorithms are based on the principles of evolution. Terminology and operators have been taken in the field of population genetics. The basic structure of genetic algorithm chromosome, and its utilization is called fitness (fitness). The main operators are applied to the crossing of chromosomes (crossover), mutation (mutation) and selection (selection). Crossing, mutation and selection consists of a generation, which is equivalent to one iteration in the traditional optimization techniques.

4. EXPERIMENT

For the experiment was used workpiece material standard EN 10027-1 (EN 90MnV8) or DIN V 17006-100 (DIN 90MnCrV8) diameter 36 mm, hardness of 55 HRC. Tile of cutting tool is of cubic boron nitride with negative geometry.

Machine tool on which the cutting was done is the universal lathe - Prvomajska DK480, which has the following characteristics: power 10KW, maximum turning diameter is 320 mm, maximum machining length is 2000 mm.

The selected tile of a cubic boron nitride, is shown in Figure 3, markings CNMA120404. Symbols for cutting tiles according to DIN 4983 closer to defining geometry, including: forms of tiles C → turbot; Clearance angle N→α =0˚, C→α =7˚; tolerance class M; type plates with an aperture → Form A, W, and G; the length of the cutting blade → 12.7 mm (12); the thickness of the cutting plate → 4.76 mm (04); → tool tip radius 0.4 mm (04). All tiles have a breast angle (γ = 0˚) zero.

Fig. 3. Tiles of cubic boron nitride (CBN)

Level (code)	v (m/s)	s (mm/r)	a (mm)
Upper (+ sqrt (2))	180	0,25	0,7
Upper medium (+1)	160	0,2	0,5
Medium (0)	120	0,1	0,22
Lower medium (-1)	90	0,05	0,1
Lower (-sqrt(2))	80	0,045	0,07

Table 1. Levels of factors

Prior to the experimental embodiment, the preparation of the workpiece was done. In order to get out and credible measurement results due to the workpiece is gripped in the chuck at one end and the other end rests on the cusp. It is necessary to download a specific material layer in order to avoid a throw-oval results were credible. At a length of 500 mm rods was to be divided on 24 fields in 20 mm length where the processing was performed without cooling and lubrication. Each field is planned for one experimental point. In this way, a treatment in a single clamping, and thus have provided the same conditions for all the experimental points. Table 1 shows the levels of the factors with which the experiment was performed.

By use of thermal imaging camera measured was cutting temperature in cutting interval from 6 seconds for all 24 cutting conditions shown in Table 2 and shown in Figures 4 and 5, which is still used in creating models using artificial neural networks and genetic algorithms. As input data were used in speed v, and the feed s and depth of cut, a output parameter is cutting temperature Q.

No.	v (m/s)	s (mm/r)	a (mm)	Q_{exp} (C^o)
1	90	0,05	0,1	75
2	160	0,05	0,1	80
3	90	0,2	0,1	90
4	160	0,2	0,1	115
5	90	0,05	0,5	119
6	160	0,05	0,5	134
7	90	0,2	0,5	130
8	160	0,2	0,5	155
9	120	0,1	0,22	160
10	120	0,1	0,22	162
11	120	0,1	0,22	165
12	120	0,1	0,22	131
13	80	0,1	0,22	136
14	180	0,1	0,22	180
15	120	0,045	0,22	106
16	120	0,25	0,22	147
17	120	0,1	0,07	99
18	120	0,1	0,7	164
19	80	0,1	0,22	156
20	180	0,1	0,22	200
21	120	0,045	0,22	99
22	120	0,25	0,22	180
23	120	0,1	0,07	108
24	120	0,1	0,7	164

Table 2. Input parameters of the experiment v, s, a, and the output parameter Q

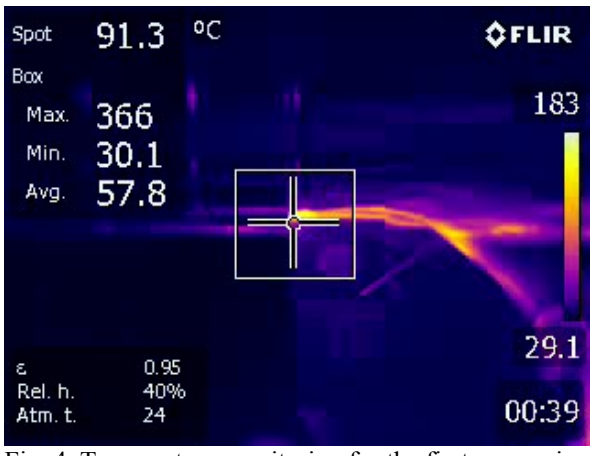

Fig. 4. Temperature monitoring for the first processing regimen

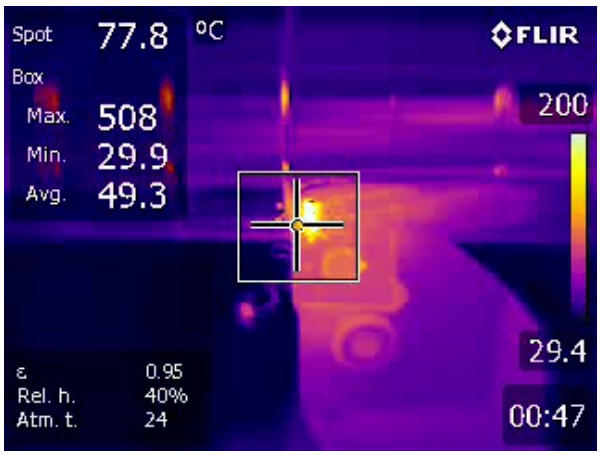

Fig. 5. Temperature monitoring for the second processing regime

5. CREATING A NEURAL NETWORK

To create and train a neural network in the MatLab was used in Neural Network Toolbox. Neural Network Toolbox includes all methods of neural networks and makes available a number of different algorithms for learning. Like other packages MATLAB, Neural Network Toolbox takes over much of the routine work so that the user can concentrate on the essential issues. NNT gives more opportunities to use MATLAB package. Tools are available for creating, visualization, simulation and implementation of different networks.

Typical fields as network name, input range, practicing function, learning, transfer functions. Selected the feed-forward, backpropagation networks.

5.1 Training and testing neural networks

After creating a neural network changes to the network training and simulation. For network training is necessary to enter input parameters and desired output. Also it is possible to define output variables which will write down the value of output, or deviation of training, figure 6.

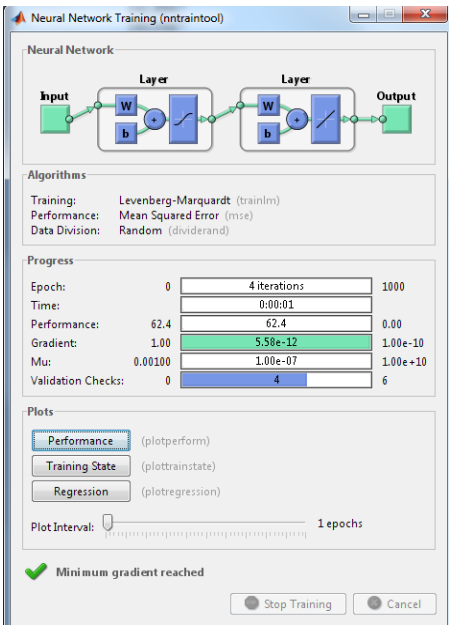

Fig. 6. The window created by neural network

For the input data used in the cutting speed v (m/s), feed s (mm/r), cutting depth a (mm), and the output cutting temperature Q (°C). The first 18 input data are used for training the neural network, and last 6 to testing the neural network.

6. MODELING FUNCTIONS GENETIC ALGORITHM

Genetic algorithm consists of several steps whose execution leads to the optimization problem, in Fig.7.

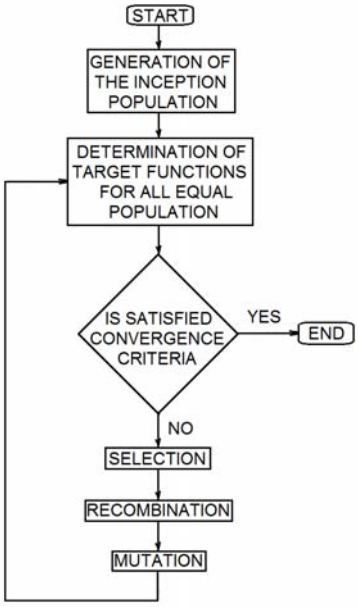

Fig. 7. Structure of the genetic algorithm

In this paper, for the modeling of tool temperature Q, used was a predefined model of the first order:

$$Q=C\cdot v^{x}\cdot s^{y}\cdot a^{z} \qquad (1)$$

The goal of optimization genetic algorithm did get solutions for coefficients C, x, y, z, such that the difference between the experimental and predicted values of the model is as small as possible [10]. Hereinafter will be described a process of posing the problem.

In the section related to the problem and its closer to first determine the size of the population changed to 50 individuals. The default value of 20 individuals is very small due to the fact that there are 4 variables. On the other hand increasing the population for faster receipt of the decision, it only makes sense to a certain value and then becomes an unnecessary burden on the computer. In this case, the figure of 50 organisms was taken as optimum on the basis of the experiments that have been performed or in the literature, and which are processed such examples.

Due to the increase in the number of organisms that make up a generation logic is to increase the number of elite organisms will be automatically transferred to the next generation. So here is this value increased to the value of the sixth.

Last but not least, it is important to define the conditions of stopping algorithm (Stopping criteria). Since we default to the value of 50 generations, to this complex problem does not mean anything, the time

interval in which evolution occurs is increased to 2000 generation. Due to very slow relative meanings optimal solutions necessary functions as Stall generations enter inf, which is in fact a number of generations. The algorithm has given a tolerance of "progress" that is, if, for a given number of generations does not happen sufficiently large changes in the results of it will be considered that he reached the optimal solution, and it will stop. With Stall generations raised on an infinite number of generations we forbade him, in fact interrupt the algorithm and thus ensure that the necessary follow all the 2000 generation.

7. ANALYSIS OF THE RESULTS

7.1 Neural networks

Table 3 shows the first 18 parameters that were used to train the neural network, and in Table 4 are shown the last 6 that were used to test the neural network.

No.	Expected Q_{Exp}	Obtained Q_{Neuro}	Error E
1	75	72,62	3,17
2	80	80,01	0,01
3	90	89,89	0,12
4	115	115,05	0,04
5	119	144,07	21,06
6	134	133,70	0,21
7	130	129,99	0,001
8	155	154,98	0,009
9	160	162,41	1,50
10	162	160,72	0,78
11	165	163,81	0,72
12	131	127,42	2,72
13	136	142,89	5,06
14	180	180,04	0,02
15	106	105,72	0,26
16	147	146,85	0,09
17	99	99,04	0,04
18	164	171,22	4,40
Average ⇒			**2,23**

Table 3. Experimental values, obtained values and the percentage deviation of training a neural network

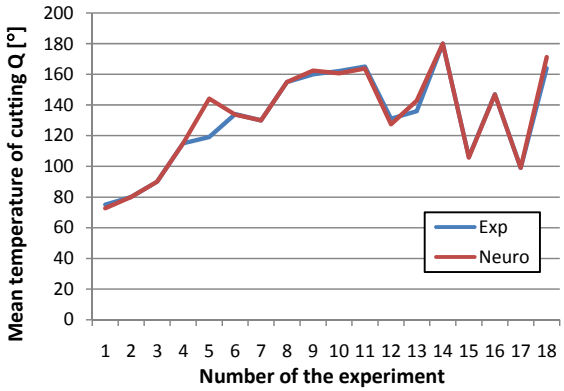

Fig. 8. Comparation of experimental temperature and temperature obtained in the training of the neural network

Figure 8 shows the diagram of the experimental attitude and the resulting temperature in the training of the neural network where it can be seen that there were deviation in the fifth experimental point but total deviation is satisfactory.

$$E = \frac{|\text{Expected}(Q) - Obtained(Q)|}{Obtained(Q)} * 100\% \qquad (2)$$

Equation (2) was used to calculate the total error Q_{Neuro} where he obtained a neural network Q_{Exp} obtained in experiment. Subtracting and dividing these values by the equation (2) for each mode is obtained E. The resultant total percentage errors **E = 2.23%**, what shows that the modeling with the help of artificial neural networks is satisfactory.

No.	Expected Q_{Exp}	Obtained Q_{Neuro}	Error E
1	156	139,28	10,71
2	200	180,92	9,54
3	99	101,45	2,48
4	180	144,34	19,80
5	108	91,82	14,97
6	164	171,75	4,72
Average ⇒			10,37

Table 4. Experumental values, obtained values and the percentage deviation of neural network test

In case the values of the test neural network overall error rate according to the equation (2) is **E = 10.37%**, which also confirms the applicability of this method of modeling.

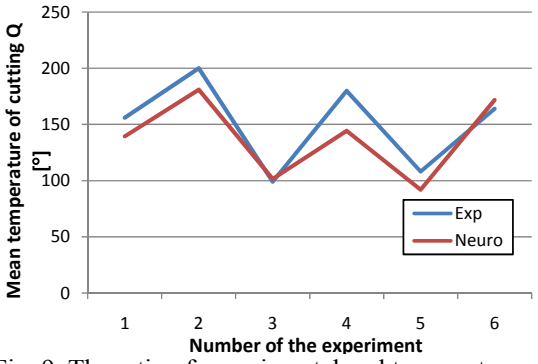

Fig. 9. The ratio of experimental and temperature obtained in the neural network testing

7.2 Genetic algorithms

Resulting coefficients for determination of temperature function Q:

C = 113.5319587
x =0.1918725394
y = 0.2024608728
z = 0.2373542486

Including these constants in the formula (2) for temperature Q calculation obtained results are shown in Table 5. It also shows the percentage and absolute deviation model obtained from the experimental values as well as the total error tolerances also expressed as a percentage. Model generated by genetic algorithms with 24 rows has an error which amounts to slightly less than 14% both in the author's opinion quite acceptable.

No.	Expected Q_{Exp}	Obtained Q_{GA}	Error E [%]
1	75	84,98	13,31
2	80	94,90	18,63
3	90	112,52	25,02
4	115	125,65	9,26
5	119	124,52	4,64
6	134	139,05	3,77
7	130	164,86	26,82
8	155	184,10	18,78
9	160	124,60	22,13
10	162	124,60	23,09
11	165	124,60	24,49
12	131	124,60	4,89
13	136	115,27	15,24
14	180	134,68	25,18
15	106	106,00	0,00
16	147	150,00	2,04
17	99	94,95	4,10
18	164	163,99	0,00
19	156	115,27	26,11
20	200	134,68	32,66
21	99	106,00	7,07
22	180	150,00	16,67
23	108	94,95	12,09
24	164	163,99	0,00
Average ⇒			**13,998 [%]**

Table 5. Experimental values of temperature and temperature obtained by genetic algorithm model

8. CONCLUSION

Neural networks and genetic algorithms was very successfully used to solve problems that are difficult to define and for mathematical modeling.

During the period of training the neural network is continuously present sets of input data (in this case the input values are speed cutting, offset and depth) and of the corresponding desired output values (in this case temperature). After training the network, it is ready for use, for information with which so far had not met that very good required parameters. Thus, well-trained neural network plays the role of an expert in a given area (in this case the choice of technological parameters of cutting).The analysis results obtained with the neural network and are satisfactory percentages of errors, or the data can give better results if you work with a larger number of input data, that is. Network needed more inputs and that would provide better results.

Due to the results obtained with small deviations in relation to the value of the model, thus conforming to criteria, it can be concluded that using genetic algorithms can solve other influential factors related to problems in production.

9. REFERENCES

[1] Nedić, B., Lazić, M.: Proizvodne tehnologije – Obrada metala rezanjem, Mašinski Fakultet Kragujevac, Kragujevac, 2007.

[2] Grzesik, W., Nieslony, P.: Physics based modelling of interface temperatures in machining with multilayer coated tools at moderate cutting speeds, International Journal of Machine Tools & Manufacture, 2004.

[3] Grzesik, W., Bartoszuk, M., Nieslony, P.: Finite difference analysis of the thermal behaviour of coated tools in orthogonal cutting of steels, International Journal of Machine Tools & Manufacture, 2004.

[4] Kovač, Savković, B., Kulundžić, N., Gostimirović, M., Hloešovsky, F., Sekulić, M.: Simulation of temperature distribution on the 3D moving cutting tool, Development in Machining Technology, Scientific Research Reports, Cracow University of Technology, Vol 5. Cracow 2015. ISBN 978-83-7242-844-8, pp. 20-26.

[5] Cica, Dj., Sredanovic, B., Kramar, D.: Prediction of cutting zone temperature in high-pressure assisted turning using ga and pso based ann, Journal of Production Engineering, 2014, Vol.17, No. 1, pp.43-46.

[6] Mitrovic, A., Kovac, P., Kulundzic, N., Savkovic, B. 3D finite element simulation of milling, Journal of Production Engineering, 2016, Vol.19, No. 1, pp.31-34.

[7] Kovač, P., Rodić, D., Pucovski, V., Mankova, I., Savkovic, B., Gostimirović, M.: A review of artificial inteligence approaches applied in inteligent processes, Journal of Production Engineering, 2012, Vol.15, No. 1, pp. 1-6.

[8] Jain K., Anil, Jianchang Mao, Mohiuddin K. M.: Artificial neural networks: A Tutorial, 1996.

[9] Kovac, P., Petrovic, V., Pucovsky, V., Bircanin, B., Savkovic B., Gostimirovic, Rokosz, K.: Energy efficiency cart modeling of solar energy collectors by genetic programming, Thermal Science, 2016, Vol. 20, Issue suppl. 2, pp. 471-479.

[10] Kovac, P., Pucovsky, V., Gostimirovic, M., Savkovic, B., Rodic, D. : Influence of data quantity on accuracy of predictions in modeling tool life by the use of genetic algorithms, International Journal of Industrial Engineering : Theory, applications and practice, 2014, Vol 21, No. 2, pp 14-21.

Authors: **Assist. Prof. Savkovic Borislav, PhD[1], Taric Mirfad, MSc[2], Prof. Kovac Pavel, PhD[1], Prof. Nedic Bogdan, PhD[3], Pucovski Vladimir, MSc[1], Prof. Risteiu Mircea PhD[4].**

[1]University of Novi Sad, Faculty of Technical Sciences, Department for Production Engineering, Trg Dositeja Obradovica 6, 21000 Novi Sad, Serbia, Phone.: +381 21 450-366, Fax: +381 21 454-495.

[2] Srednja škola metalskih zanimanja, Zmaja od Bosne br. 8, 71 000 Sarajevo, BiH

[3]University of Kragujevac, Faculty of Engineering, Sestre Janic 6, 34 000, Kragujevac, Serbia

[4],,1 Decembrie 1918" University of Alba Iulia, Computer Science Department, Str. N. Iorga nr.11-13, 510009 Alba Iulia, Romania.

E-mail: savkovic@uns.ac.rs, mirfad.taric@hotmail.com pkovac@uns.ac.rs, nedic@kg.ac.rs, pucovski@uns.ac.rs, mristeiu@uab.ro

Note: This paper presents a part of researching at the CEEPUS project and Project number TR 35015.

Journal of Production Engineering
Vol.19 No.2
JPE (2016) Vol.19 (2) Original Scientific Paper
Sruthi, B., Kilari, N., Kishore, J.S.

EXPERIMENTAL INVESTIGATION OF ABRASIVE WATER JET MACHINING PROCESSES PARAMETERS & ITS EFFECTS ON PROCESSES RESPONSES USING GREY TAGUCHI OPTIMIZATION TECHNIQUE

Received: 06 August 2016 / Accepted: 10 October 2016

Abstract: *Abrasive water Jet Machining mainly adopted by aerospace industry for cutting high strength materials and other composites. It finds most of its applications in machining of gas turbines, rocket motors, space craft, nuclear power and pumps etc., very thin stream of about 0.004 to 0.010 dia. can be cut and material loss is also less due to cutting. The aim of the work is to analysis the effect of input process parameters such as Transverse speed, Abrasive flow rate and standoff distance for achieving optimum Processes responses such as Metal Removal Rate (MRR), Surface roughness (Ra), and Kerf width simultaneously while machining on the nickel-chromium based super alloy INCONEL 825. The Design of Experiments are conducted to find the influence of processes parameters for setting optimal setting using Taguchi's concept. A series of experiments are conducted to find the optimimum parameterss. Optimization of processes parameters are predicted by using grey taguchi technique. A conformation experiment is conducted to validate the optimal level of Processes parameters prediction.*
Key words: *Metal Removal Rate, Surface Roughness, Kerf Width, Grey taguchi technique & Inconel-825.*

Eksperimentalno istraživanje procesa obrade abrazivnim vodenim mlazom i njegovog efekta na ishod procesa pomoću sive Taguči tehnike optimizacije. *Obrada abrazivnim vodenim mlazom je svoju primenu pronašla uglavnom u avio industriji kod sečenja materijala visoke čvrstoće i drugih kompozita. Svoju primenu nalazi prevashodno pri obradi gasnih turbina, raketnih motora, svemirskih letelica, nuklearnih reaktora i pumpi itd. Tanak mlaz prečnika približno od 0,004 do 0,01 se može postići i u tom slučaju je manji gubitak materijala usled sečenja. Cilj ovog rada je analiza uticaja ulaznih parametara procesa obrade kao što je brzina sečenja, količina abraziva i rastojanje mlaznice od materijala radi simultanog postizanja optimalnih izlaznih parametara procesa kao što je proizvodnost, hrapavost obrađene površine i širina reza pri obradi nikl-hrom super legure Inconel 825. Dizajn eksperimenata je sproveden radi otkrivanja uticaja parametara procesa na optimalna podešavanja korišćenjem Tagučijeve metode. Serija eksperimenata je realizovana kako bi se pronašli optimalni parametri procesa. Optimizacija parametara procesa je realizovana pomoću sive Taguči tehnike. Eksperimenti provere su sprovedeni radi potvrde optimalnih nivoa predviđanih parametara procesa.*
Ključne reči: *Proizvodnost, površinska hrapavost, širina reza, siva Taguči tehnika, Inconel 825.*

1. INTRODUCTION

Water jets were introduced in the United States during the 1970's, and were utilized merely for cleaning purposes. As the technology developed to include abrasive water jets, new applications were disco verged. The water jet process provides many unique capabilities and advantages that can prove very effective in the cost battle. Learning more about the Water jet technology gives us an opportunity to put these cost-cutting capabilities to work. Beyond cost cutting, the water jet process is recognized as the most versatile and fastest growing process in the world. No toxic gases or liquids are used in water jet cutting, and water jets do not create hazards or vapours. It is truly a versatile, productive, cold cutting process.

1.1 Working Principle of Abrasive Water Jet Machining

Water from the reservoir is pumped to the intensifier using a hydraulic pump. Water is pumped at a very high pressure about 2000-4000 bar using intensifier. When water at such pressure is issued through the orifice of about 0.2 – 0.4 mm diameter, converts the potential energy of water into kinetic energy, resulting a very high velocity jet of 1000 m/s. This high velocity of water jet when it comes out of the nozzle cuts the materials of the required size and a shape is shown in Fig. 1.

Fig. 1. Abrasive Water Jet Machining of Inconel-825

2. LITERATURE SURVEY

A lot of contributions have been made on the

optimization of process parameters of different materials by using Abrasive water jet machining and been reviewed. Some of them are discussed below.

Divyansh Patel, Puneet Tandon [1] This work explores thermally enhanced abrasive water jet machining (TEAWJM) process to improve the machining capabilities of conventional abrasive water jet machine by heating the work by an external heat source. The present work describes an experimental study of thermally enhanced machining (TEM) by adding an oxy acetylene gas welding setup as an external heat source to the machine setup which heats the work locally and temperature is measured by non-contact laser thermometer. The experimental data of cutting parameters at critical temperatures of hard-to-machine metals Inconel-718, Titanium (Ti6Al4V) and mild Steel (MS-A36) (ductile in nature) with full factorial DOE is presented here. Further, the effect of thermal treatment (during cutting) on surface morphology of the material machined has been studied for analyzing the effectiveness of the proposed methodology. Due to TEM, an increase in material removal rate, reduction in power consumption machining time is observed.

John A. Webster [2] The aerospace industry has experienced significant growth over the past decade and it is estimated that nearly 30,000 new commercial passenger aircraft will be required by 2030 to meet rising global demand. Abrasive machining is a key material removal process utilized in the production of aero engine components. Current industrial practice and perspectives relating to grinding in the aerospace sector are presented including general work piece surface integrity standards/requirements, fluid delivery systems, wheel preparation options and machine tool designs/configurations. Corresponding academic research on the mach inability of aerospace alloys and composites are critically reviewed together with recent developments involving novel/innovative grinding processes.

B.Satyanarayana, G.Srikar [3] Abrasive Water Jet Machining (AWJM) is a versatile machining process primarily used to machine hard and difficult to machine materials. The objective of this paper is to optimize material removal rate and kerf width simultaneously using AWJM process on INCONEL 718. The process parameters are chosen as abrasive flow rate, pressure, and standoff distance. Taguchi Grey Relational Analysis is opted because of multi response optimization.

From above Literature survey it is evident that Title work has been reported on Experimental Investigation on Inconel-825(Nickel Iron & Chromium based alloy) material which is used for Aeronautical, Creogenics and Chemical processing applications. Design of Experiments (DOE) is prepared in Mini-Tab Software by using Taguchi for optimizing Processes parameters like Transverse speed, Abrasive flow rate and Stand-off Distance. These processes parameters are going to be optimized based on Maximum MRR, Minimum Surface Roughness & Minimum Kerf Width after Machining is completed by conducting ANOVA & Grey Taguchi Technique [4-15].

3. EXPERIMENTAL SETUP

3.1 Work Piece Material

The material choosen is INCONEL-825 is a super alloy which is precipitation hardened material and high level of corrosive resistance. It is a Nickel-Iron-Chromium alloy with additions of molybdenum, copper and Titanium. It has good yield strength and mechanical properties even at cryogenic temperatures to moderately high temperatures. It is highly resistant to highly corrosive acids like sulphuric acid and phosphoric acids.

Fig. 2. Inconel Workpiece Before & After Machining

3.2 Micro Structure of Inonel-825

Microstructures are studied for Inconel-825 materials with Lens magnification of 5X, 10X & 20X.

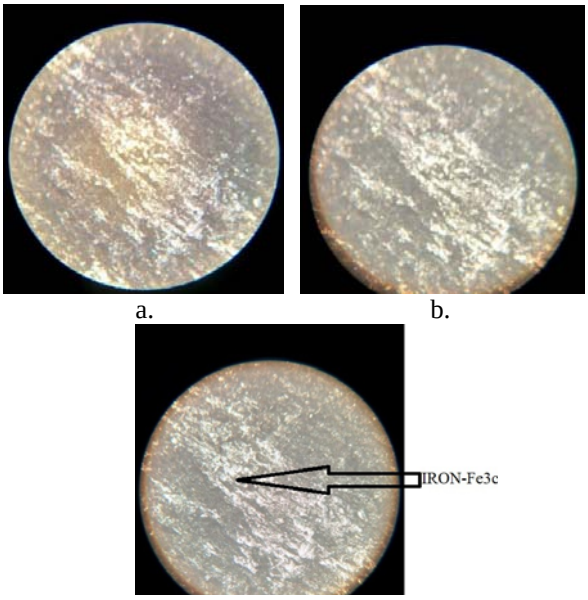

a. b.

C.

Fig. 3. Microstructures of Inconel-825 a)5X b)10X, c)15X

3.3 Abrasive Water Jet Machine Set Up

Fig.4. Excel Abrasive water Jet Machine

All experimental runs were carried out on a CNC Abrasive Water Jet Machining setup available at "EXCEL WATERJET CUTTING"- SIDCO Industrial Estate, Thirumazhisai, Chennai – 602107, Tamil Nadu, India. The WEDM machine has the following specifications.

S.No	Description	Range
1	Controlling of Machine	CNC
2	Voltage	415 V
3	Frequency	50 Hz
4	Phases	3
5	Power	547 W
6	Current	1.8 A
7	Table size	3 * 3 * 1.5
8	Travel	X-axis – 3000mm, Y-axis – 3000mm, Z-axis – 260mm
9	Nozzle diameter	1.1 mm
10	Abrasive type	Garnet
11	Abrasive size	80 Mesh
12	Orifice diameter	0.35 mm
13	Focusing tube diameter	8 mm
14	Water pressure	3500 bars
15	Water flow rate	3.5 litre/min

Table 1. Specifications of CNC Abrasive Water Jet Machine.

The work piece was mounted and clamped on the work table. A reference point on the work piece was set for setting work co-ordinate system (WCS). The programming was done with the reference to the WCS. The reference point was defined by the ground edges of the work piece. The cutting operation is done by a jet of abrasive particles and water mixture on the work piece. The input parameters like Traverse speed, Abrasive flow rate, Standoff distance are given to the CNC machine in the input panel.

3.4 Design of Experiment-DOE

The process of planning the experiment is carried out, so that appropriate data will be collected and analyzed by statistical methods resulting in valid and objective conclusions. The method of analysis depends directly on the design of experiments employed.

Most researchers identified Abrasive water jet machining process parameters that greatly affect Response parameter. The Process Parameter like Standoff distance, impact angle, traverse rate, number of passes, abrasive material, abrasive particle size, abrasive shape, and abrasive mass flow rate, focusing tube diameter and focusing tube length water pressure orifice diameter etc. In this paper we have selected process parameter as Traverse Rate (mm/min), Abrasive flow rate (gm/min) and Stand of distance (mm) to analyze its effect on MRR (gm/min) and Surface Roughness (μm) Kerf width(mm).

3.5 Control Parameters

Factor A: Transverse speed (mm/min)
Factor B: Abrasive flow rate (gm/min)
Factor C: Stand of distance (mm)

Parameter	Notation	Units	Levels				
			1	2	3	4	5
Transverse Speed	TS	mm/min	40	50	60	70	80
Abrasive flow rate	AFR	gm/min	50	100	150	200	250
Stand-off distance	SOD	mm	1.0	2.0	3.0	4.0	5.0

Table 2. Awjm Processes Parameters and their Levels.

3.6 Selection of Orthogonal Array-OA

In Taguchi method Control factors refers to input parameters for the process, and Response factors refers to corresponding output parameters for the process.

DOF for a Control Factor = No. of Levels – 1

DOF for A = 5-1 = 4

Total DOF = 12

As per Taguchi technique, the processes parameters of 5 level design has two degree of freedom (DOF) this gives a total of 5-1=4. 3 parameters are considered DOF for three processes variables for this research. The condition for selecting OA is the DOFs for selected OA must be higher than DOFs required for experiment is 12 so, the nearest OA available for satisfying the condition of selecting OA is L25

Fig. 5. Control Panel for Abrasive water jet Machine

S. No	Transverse Speed (mm/min)	Abrasive flow rate (gm/min)	Stand off distance (mm)
1	40	50	1
2	40	100	2
3	40	150	3
4	40	200	4
5	40	250	5
6	50	50	2
7	50	100	3
8	50	150	4
9	50	200	5
10	50	250	1
11	60	50	3
12	60	100	4
13	60	150	5
14	60	200	1
15	60	250	2
16	70	50	4
17	70	100	5
18	70	150	1
19	70	200	2
20	70	250	3
21	80	50	5
22	80	100	1
23	80	150	2
24	80	200	3
25	80	250	4

Table 3. Taguchi L_{25} DOE in terms of Coading Factors.

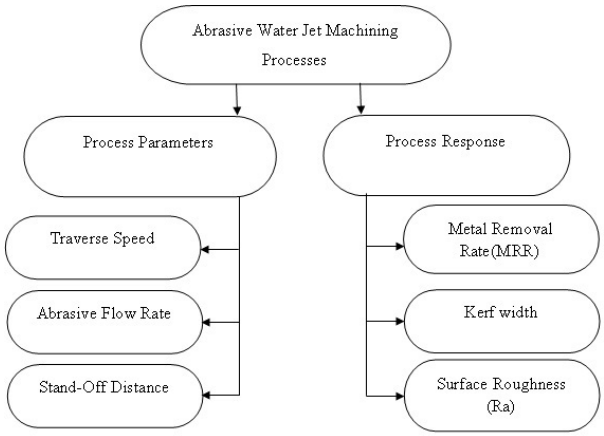

Fig. 6. Flowchart represnts Processes Parameters & Processes Responses of Experimentation.

4. RESULTS & DISCUSSIONS

Metal Removal Rate & Surface Roughness are most important criteria's, which help us determine how rough a work piece material is machined. In all the investigations it was found that the machined smoother near the jet entrance and gradually becomes rougher towards the jet exit. This is due to the fact that as the particles moves own they lose their kinetic energy and their cutting ability deteriorates. By analyzing the experimental data of the selected material, it has been found that optimum selection of the four basic parameters, i.e, water pressure, abrasive mass flow rate, nozzle transverse speed and nozzle standoff distance are very important on controlling the processes outputs such as Metal Removal Rate (MRR) & Surface Roughness (Ra). The effect of these parameters are studied while keeping the other parameters considered in this study as constant.

S.No	Transverse speed (mm/min)	Abrasive flow rate (gm/min)	Stand off Distance (mm)	Kerf width-mm	MRR-gm/mn	Surface roughness (Ra) µm
1	40	50	1	1.17	1.921	0.0145
2	40	100	2	1.20	1.826	0.0135
3	40	150	3	1.23	1.368	0.013
4	40	200	4	1.3	1.85	0.0135
5	40	250	5	1.28	4.69	0.0135
6	50	50	2	1.15	2.9	0.015
7	50	100	3	1.11	3.7	0.0145
8	50	150	4	1.14	4.5	0.0155
9	50	200	5	1.20	4.9	0.0145
10	50	250	1	1.11	4.53	0.013
11	60	50	3	0.97	3.52	0.017
12	60	100	4	1.07	4.9	0.0155
13	60	150	5	1.13	6.19	0.014
14	60	200	1	1.10	4.76	0.0135
15	60	250	2	1.12	4.84	0.013
16	70	50	4	1.1	5.71	0.0135
17	70	100	5	1.12	6.63	0.017
18	70	150	1	1.06	7.02	0.015
19	70	200	2	1.17	6.75	0.016
20	70	250	3	1.17	6.574	0.0135
21	80	50	5	1.06	5.53	0.0145
22	80	100	1	1.04	5.69	0.015
23	80	150	2	1.11	7.57	0.0135
24	80	200	3	1.13	7.037	0.013
25	80	250	4	1.16	8.087	0.015

Table 4. Taguchi'S L_{25} OA with Experimental Results

a. b.

Fig. 7. (a) Surface Roughness measurent by using Talysurf (b) Kerf width is measeured y using Vernier Callipers.

4.1 Grey Taguchi Technique

In order to investigate the significance of the process parameters on Metal Removal Rate, Kerf Width, Surface Roughness. ANOVA was performed. ANOVA table for the Grey relational grade are shown in Table 6. From these it is shows that Transverse Speed has most effecting parameter which is about 48.39% contribution on grey relational grade and following with Abrasive Flow Rate and Stand-off

Distance has effect on grey relational grade with contribution of 16.97% and 6.778%.

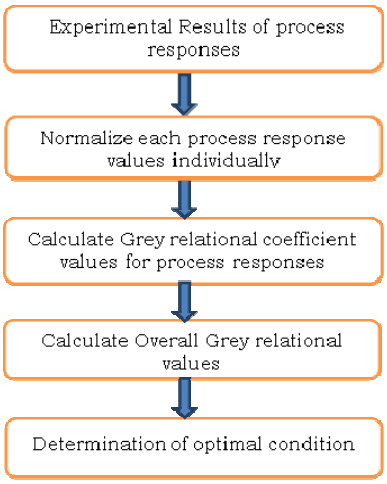

Fig. 8. Flow Chart represnts the Grey Taguchi Technique

4.2 Normalization of Experimental Results

The first step in Grey-Taguchi analysis is to normalize the experimental results of Metal Removal Rate, Kerf Width, Surface Roughness. Each response value is normalized in the range of 0 to 1. For normalizing Metal Removal Rate'Higher-the-better' is to select reperesnt in (equ.1), Kerf Width, Surface Roughness 'Lower-the-better' is to be selected in (equ.2) criterion is used.

$$X_j(v) = \frac{y_j(v) - \min y_j(v)}{\max y_j(v) - \min y_j(v)} \qquad (1)$$

$$X_j(v) = \frac{\max y_j(v) - y_j(v)}{\max y_j(v) - \min y_j(v)} \qquad (2)$$

Where, $X_j(v)$= value after normalizing data/

Grey relations generation value,

Min $y_j(v)$=smallest value of $y_j(v)$

Max $y_j(v)$=Largest value of $y_j(v)$

4.3 Grey Relational Coefficient

After normalizing the results of Metal Removal Rate, Kerf Width, Surface Roughness, the next step is calculation of grey relational coefficient values for Metal Removal Rate, Kerf Width, Surface Roughness. The grey relational coefficient $\varepsilon_j(v)$ can be calculated by using equ.3

$$\varepsilon_j(v) = \frac{\Delta_{\min} + \phi\Delta_{\max}}{\Delta_{oj}(v) + \phi\Delta_{\max}} \qquad (3)$$

4.3 Grey Relational Grade and Order

Grey relational grade for each experimental run is the average of grey relational coefficient value for a particular experimental run. Grey relational grade can be calculated by using equ.4. Higher value of grey relational grade indicates the best value, so highest grade value gives the higher order. The grey relational grade and their order is given in Table5.

EXP. No.	Grey Relational Grade	Order
1	0.459553	25
2	0.521072	19
3	0.57265	14
4	0.49447	22
5	0.548273	15
6	0.458189	24
7	0.517109	19
8	0.472264	23
9	0.499539	21
10	0.674304	4
11	0.585722	13
12	0.529562	16
13	0.603219	10
14	0.619329	9
15	0.676171	3
16	0.650284	6
17	0.516944	20
18	0.634172	8
19	0.521199	18
20	0.645919	7
21	0.598604	11
22	0.594175	12
23	0.734607	2
24	0.755251	1
25	0.655875	5

Table 5. Grey Relational Grade and Order

$$\gamma_j = \frac{1}{n}\sum_{v=1}^{n} \varepsilon j(k) \qquad (4)$$

Where, n = number of process responses

$\varepsilon_j(v)$ = Grey relational coefficient

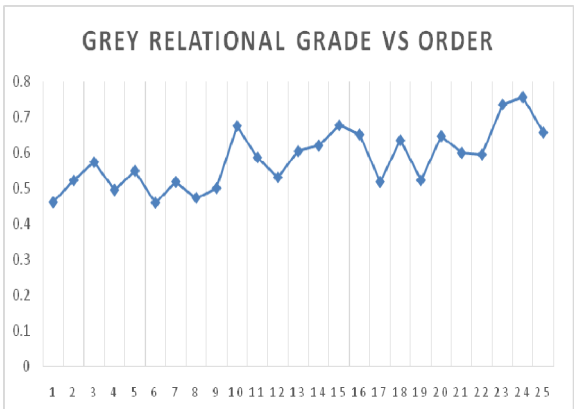

Graph.1. Graph drawn between Grey Relational Grade Vs Grey Order

Source	DF	Seq. SS	Seq. MS	F-Value	% Contribution
A	4	0.08289	0.020723	5.21	48.39
B	4	0.02907	0.007268	1.83	16.97
C	4	0.01161	0.002902	0.73	6.778
Error	12	0.04771	0.003976	--	27.85
Total	24	0.17128	--	--	--

Table 6. ANOVA for Grey Relational Grade

5. PREDICTION OF RESPONSE VALUES FOR OPTIMUM LEVELS AS PER GREY-TAGUCHI TECHNIQUE

From means of each level of process parameters we will construct a response table. For grey-relational grade. The response table for grey-relational grade is given in Table.7.

Level	Transvers Speed (A)	Abrasive Flow Rate (B)	Stand Off Distance (C)
1	0.5167	0.5500	0.6080
2	0.5240	0.5493	0.5799
3	0.6144	0.6030	0.6148
4	0.6092	0.5896	0.5600*
5	0.6672*	0.6396*	0.5688
Delta	0.1505	0.0903	0.0548
Rank	1	2	3

Table 7. Response Table for means of Grey-Relational Grade

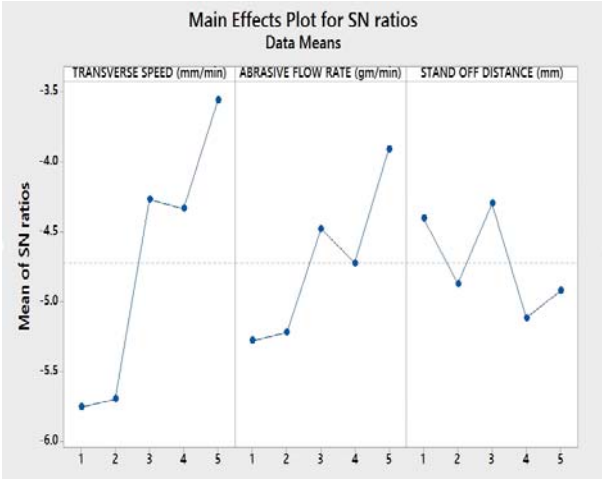

Fig. 9. Main effect plot S/N Ratio for Grey Relational Grade.

From the below Response table the optimal condition for maximizing Metal Removal Rate, minimum Kerf Width and Surface roughness simultaneously in Abrasive Water Jet Machining (AWJM) process, is found to be A5 B5 C3 i.e. Transverse speed is 80 mm/min, Abrasive Flow Rate is 250 gm/min and Stand Off Distance is 3 mm. For this optimal setting A5 B5 C4 conducted experimentation for validating results.

S.No	Process response	Optimal setting	Actual Value	Experimental Value	% of Error
1	Metal Removal Rate	$A_5B_5C_3$	8.087	7.89	2.4
2	Kerf width		1.16	1.16	0
3	Surface Roughness		0.015	0.0155	-3.33

Table 8. Optimum Parameter control level.

From the confirmation experiments, the error percentage of process responses from the predicted responses is less than 5% is acceptable.

6. CONCLUSIONS

In this present analysis of various parameters and on the basis of experimental results, analysis of variance (ANOVA), and SN Ratio the following conclusions can be drawn for effective machining of INCONEL-825 by AWJM process as follows:

1. Traverse Speed (TS) is the most significant factor on MRR during AWJM. Meanwhile Abrasive Flow Rate and Standoff distance is sub significant in influencing.
2. In case of surface Roughness Abrasive Flow Rate is most significant control factor.
3. In case of Metal Remove Rate (MRR) & Surface Roughness Transverse speed & Abrasive Flow Rate are most significant control factors.
4. The optimal condition for maximizing Metal Removal Rate, minimum Kerf Width and Surface roughness simultaneously in Abrasive Water Jet Machining (AWJM) process, is found to be A5 B5 C3 i.e. Transverse speed is 80 mm/min, Abrasive Flow Rate is 250 gm/min and Stand Off Distance is 3 mm.

7. REFERENCES

[1] D. Patel, P. Tandon"CIRP Journal of Manufacturing Science and Technology", ISSN: 1755-5817, September 10 2015.

[2] N. Tamannaee, J.K. Spelt, M. Papini," Abrasive slurry jet micro-machining of edges, planar areasand transitional slopes in a talc-filled co-polymer", Precision Engineering ,Department of Mechanical and Industrial Engineering, University of Toronto, Department of Mechanical and Industrial Engineering, Ryerson University, Toronto, Canada , Issue 24, June 2015.

[3] Fritz Klocke, Sein Leung Soo, Bernhard Karpuschewski, John A.Webster, Donka Novovic, Amr Elfizy, Dragos A. Axinte, Stefan Tönissen,"Abrasive machining of advanced aerospace alloys and composites",CIRP Annals – Manufacturing Technology, Volume 64,Issue 2, May 2015.

[4] Fang-Jung Shiou, Assefa Asmare,"Parameters optimization on Surface roughness improvement of Zerodur optical glass using an Innovative rotary abrasive fluid multi-jet polishing process", Precision Engineering,Department of Mechanical Engineering, National Taiwan University of Science and Technology, Taiwan,Issue 17, April 2015.

[5] Derzija Begic-Hajdarevic, Ahmet Cekic, Muhamed Mehmedovic, Almina Djelmic"Experimental Study on Surface Roughness in Abrasive Water Jet Cutting" 25th DAAAM International Symposium On Intelligent Manufacturing and Automation, ISSN: 1877-7058, 2015.

[6] B. Satyanarayana, G. Srikar," Optimization of abrasive water jet machining process parameters using Taguchi Grey RelationalAnalysis(TGRA)", Proceedings of 13th IRF International Conference, Pune , India, ISBN:978-93-84209-37-7, Issue 20,July 2014.

[7] Debasish ghosh, probal k. Das, b.doloi "Parametric studies of abrasive water jet cutting onsurface roughness of silicon nitride materials" all india manufacturing technology, design and research conference (aimtdr), december 12th–14th, 2014.

[8] Vijay Kumar Pal, S.K.Choudhury "Application of abrasive water jet machining infabricating micro tools for edm for producing array of square holes" all india manufacturing technology, design and research conference (aimtdr), december 12th–14th, 2014.

[9] Sreekesh K and Dr. Govindan P"A REVIEW ON ABRASIVE WATER JET CUTTING" International Journal of Recent advances in Mechanical Engineering (IJMECH), Vol.3, No.3, August 2014.

[10] M. Uthayakumar, V. Arumugaprabu, M. Kathiresan "Experimental investigation of the processparameters in abrasive waterjet cutting of redmud reinforced banana/polyester hybrid composites"all india manufacturing technology, design and research conference (aimtdr), december 12th–14th, 2014.

[11] S. R. Patel, Dr. A. A. Shaikh ,"Control and measurement of abrasive flow rate in an Abrasive Waterjet Machine",International journal of innovative Research in Science, Engineering and Technology, ISSN: 2319-8753 , Volume 2,Issue 12,December 2013.

[12] Cristian Birtu, Valeriu Avramescu," Abrasive water jet cutting Technique, Equipment, Performances", Nonconventional Technologies Review, Romania, Issue March, 2012.

[13] Veselko Mutavgjic, Zoran Jurkovic, Marina Franulovic, Milenko Sekulic, "Experimental investigation of surface roughness obtained by Abrasive Water jet machining", 15th International Research/Expert Conference, "Trends in the Development of Machinery and Associated Technology", Prague, Czech Republic, Issue 12, September 2011.

[14] M. Chithirai pon selvan and n. Mohana sundara raju "Assessment of process parameters inabrasive waterjet cutting ofstainless steel" international journal of advances in engineering & technology (ijaet), issn: 2231-1963, july 2011.

[15] Krushna Prasad Pradhan "DESIGN AND FABRICATION OFABRASIVE JET MACHINE" May 11, 2009.

Authors: **P.G.Scholar B.Sruthi[1] M.Tech, Professor Dr.Naveen Kilari[2] PhD**, **Asst.Professor Jaya Kishore Sunkara[3] M.Tech,**

[1]Sri Venkateswara College of Engineering Department of Mechanical Engineering,Tirupati, Chittor-Dist,AP, India, [2]Sri Venkateswara College of Engineering Department of Mechanical Engineering,Tirupati, Chittor-Dist,AP,India. [3]Sri Venkateswara College of Engineering Department of Mechanical Engineering, Tirupati, Chittor-Dist,AP, India

E-mail: charvi.varun@gmail.com
naveenkilari@svcolleges.edu.in
jkishore097@gmail.com

Journal of Production Engineering
Vol.19 No.2
JPE (2016) Vol.19 (2) Original Scientific Paper
Paik, N. M., Davis, R., Sahu, P., Ekka, M. N., Sudheer, D., Samson, S.

EXPERIMENTAL INVESTIGATION OF THE EFFECT OF CONTROL PARAMETERS OF EDM ON SURFACE ROUGHNESS AND TOOL WEAR RATE USING REGRESSION ANALYSIS

Received: 20 June 2016 / Accepted: 12 September 2016

Abstract: *In this paper illustration of the influence of input machining parameters on the surface roughness and Tool wear rate are determined along with regression analysis. This experiment was conducted on High Carbon High Chromium Steel (HCHCR) with Copper as tool electrode. The data collected during experimentation has been used to yield responses in respect of surface roughness and tool wear rate (TWR). The objective of this paper is to study the influence of operating input parameters of copper electrode on surface roughness of HCHCR and tool wear rate of copper followed by optimization. The effectiveness of EDM process with copper electrode is evaluated in terms of surface roughness and tool wear rate. In this work the parameters such as current, spark gap, flushing rate pulse on time, pulse off time were selected. Analysis is carried using the Anova analysis.*
Key words: *High Carbon High Chromium Steel, surface roughness, tool wear rate, EDM processs*

Eksperimentalno istraživanje uticaja kontrole parametara EDM-a na hrapavost obrađene površine i habanje alata pomoću regresione analize. *U ovom radu je dat prikaz uticaja ulaznih parametara obrade na hrapavost obrađene površine i habanje alata. Uticaj ulaznih parametara je određen pomoću regresione analize. Materijal obratka je čelik sa visokim sadržajem ugljenika i hroma (High Carbon High Chromium Steel-HCHCR) a materijal alata je bakar. Vrednosti prikupljene tokom eksperimenta su iskorišćeni radi dobijanja odziva u odnosu na hrapavost površine i habanje alata. Cilj ovog rada je istražiti uticaj proizvodnih ulaznih parametara bakarne elektrode na hrapavost obrađene površine čelika i habanje bakra. U drugom delu rada je napravljena optimizacija ulaznih parametara. Efektivnost EDM procesa sa bakarnom elektrodom je određena na osnovu hrapavaosti obrađene površine i habanje alata. U ovom radu su izabrani parametri kao što je intezitet, rastojanje alata i obratka, ispiranje, vreme pražnjenja i vreme pauze. Analiza je izvršena korišćenjem Anova analize.*
Ključne reči: *čelik sa visokim sadržajem ugljenika i hroma (HCHCR), hrapavost površine, habanje alata, EDM proces*

1. INTRODUCTION

Electrical Discharge Machining: Electrical Discharge Machining (EDM): Removal of material from the work piece by spark discharges, which are produced by connecting both tool (electrode) and work piece to a power supply. This process is also known as spark erosion. Electrical Discharge Machining (EDM) is a non-conventional machining process, where Electrically conductive materials is machined by using precisely controlled sparks that occur Between an electrode and a work piece in the presence of a dielectric fluid. It uses thermoelectric energy sources for machining extremely low machinability materials; complicated Intrinsic-extrinsic shaped jobs regardless of hardness have been its distinguishing characteristics. [1]

A. Process Parameters of EDM:

i. Voltage: It is a potential that can be measure by volt it is also effect to the material removal rate and allowed to per cycle.

ii. Current: Discharge current is directly proportional to the Material removal rate.

iii. Flushing: Flushing is the process of supplying clean filtered dielectric fluid into the machining zone.

iv. Spark gap: The Arc gap is distance between the electrode and work piece during the process of EDM. It may be called as spark gap. Spark gap can be maintained by servo system.

a. T on: The duration of time (μs) the current is allowed to flow per cycle. Material removal is directly proportional to the amount of energy applied during this on-time

b. T off: The duration of time (μs) between the sparks (that is to say, on-time). This time allows the molten material to solidify and to be wash out of the arc gap. This parameter is to affect the speed and the stability of the cut.

B. Output Parameters:

i. Tool Wear Rate: Tool wear describes the gradual failure of cutting tools due to regular operation.

ii. Surface roughness: it is a component of surface texture. It is quantified by the deviations in the direction of the normal vector of a real surface from its ideal form.

C. Cutting tools used:

Copper: copper has properties, such as its high electrical conductivity, tensile strength, ductility, creep (deformation) resistance, corrosion resistance, low

thermal expansion, high thermal conductivity, solder ability and ease of installation. Pure copper is soft and malleable. A freshly exposed surface has a reddish-orange colour.

Regression:

A statically measured that attempts to determine the strength of relationship between one dependent variable (usually denoted by y) and a series of other changing variables (known as independent variables). Regression analysis with a single explanatory variable is termed "simple regression.

Simple Regression: Simple regression also known as linear regression uses one independent variables to explain or predict the outcome of y. At the outset of any regression study, one formulates some hypothesis about the relationship between the variables of interest, here, education and earnings. Common experience suggests that better educated people tend to make more money. It further suggests that the causal relation likely runs from education to earnings rather than the other way around. Thus, the tentative hypothesis is that higher levels of education cause higher levels of earnings, other things being equal.

This linearity assumption is common in regression studies but is by no means essential to the application of the technique, and can be relaxed where the investigator has reason to suppose a priori that the relationship in question is nonlinear. Then the hypothesized relationship between education and earnings may be written

$$y = a + bx + u$$

Where,

y = the variable that we are trying to predict.
x = the variable that we are using to predict y.
a = the intercept
b = the slope
u = the regression analysis

i) Regression Analysis:

Regression analysis is a statistical tool for the investigation of relationships between variables. In this lecture, we will provide an overview of the most basic techniques of regression analysis—how they work, what they assume, and how they may go away when key assumptions do not hold. Also, of necessity, there are many important topics that including simultaneous equation models and generalized least squares. The lecture is limited to the assumptions, mechanics, and common difficulties with single- equation, ordinary least squares regression.

Step 1: Normalization of the responses (Quality Characteristics):

When the range of the series is too large or the optimal value of a quality characteristic is too huge, it will caused the influence of some factors to be overlooked. The original experimental data must be normalized to eliminate such an effect. There are three types of data normalization. The normalization is assumed by the following equations. [2]

i. LB (lower-the-better)

$$x_i(k) = \frac{\min x_i(k)}{x_1(k)} \quad \text{(i)}$$

ii. HB (higher-the-better)

$$x_i(k) = \frac{x_i(k)}{\max x_i(k)} \quad \text{(ii)}$$

iii. NB (nominal-the-best)

$$x_i(k) = \frac{\min\{x_i(k), x_{0b}(k)\}}{\max\{x_i(k), x_{0b}(k)\}} \quad \text{(iii)}$$

Here, i = 1, 2 ...m; k = 1, 2 ...n

$X_i(k)$ is the normalized data of the k^{th} element in the i^{th} sequence.

$X_{ob}(k)$ is the desired value of the k^{th} quality characteristic. After data normalization, the value of $X_i(k)$ will be between 0 and 1. The series, i=1, 2, 3,....., m can be viewed as the comparative sequence used in the grey relational analysis.

Step 2: Checking for correlation between two quality characteristics:

$$Q_i = \{x_o(i), x_1(i), x_2(i) \ldots\ldots\ldots x_m(i)\} \quad \text{(iv)}$$

Let, Where, i = 1, 2, ...n Shown above is the normalized series of the i^{th} quality characteristic. The correlation coefficient between the two quality characteristics is calculated using the following equation:

$$\rho_{jk} = \frac{\text{cov}(Q_j Q_k)}{\sigma_{Qj}\sigma_{Qk}} \quad \text{(v)}$$

j = 1,2,3....,n k = 1,2,3....,n $j \neq k$

Here, ρ_{jk} is the correlation coefficient between quality characteristic j and quality characteristic k ; cove(QjQk) is the covariance of quality characteristic j and quality characteristic k ; σ_{Qj} and σ_{Qk} are the standard deviation of quality characteristic j and quality characteristic k, respectively. [3]

The correlation is checked by testing the following hypothesis

H_o: $\rho_{j\,k} = 0$ (There is no correlation)
H_o: $\rho_{j\,k} \neq 0$(There is correlation)

Step 3: Calculation of the Principal Component Score:

i. Calculation of the Eigen value and the corresponding eigenvector β_k (k = 1, 2,.....n) from the correlation matrix formed by all quality characteristics.
ii. Calculation of the principal component scores of the normalized reference sequence and comparative sequences using the equation shown below:

$$Y_i(k) = \sum_{j=1}^{n} x_i(j)\beta_{kj} \quad \text{(vi)}$$

Where, Y_i (k) is the principal component score of the k^{th} element in the i^{th} series. X_i (j) is the normalized value of the j^{th} element in the i^{th} sequence, β_{kj} and is the j^{th} element of eigenvector β_k

iii. The principal component having highest accountability proportion (AP) can be treated as the overall quality index which is to be optimized finally. The quality loss$\Delta_{0,i}$(k)of that index (compared to ideal situation) is calculated as

$$\Delta_{\downarrow}(0,i)(k) = \left\{ {}_{\downarrow}\left(\left| y_{\downarrow} 0(k) - y_{\downarrow} i(k) \right| \right)^{\uparrow} \left(\left| x_{\downarrow} 0(k) - x_{\downarrow} i(k) \right| \right) \right\} \quad \text{(vii)}$$

a) Surface Roughness Measurement Terminology:

R_a- Arithmetic means value of the deviation of the profile within sampling length

R_z- The maximum height of irregularities is the distance b/w maximum depth of the profile peaks and profile valley within of sampling length

R_q- Square root of the arithmetic mean of the square of profile deviation (Yi) from mean within sampling length.

R_t- Total peak-to-valley height .It is the sum of the height of highest peak and the depth of deepest valley over the evaluation length. [4]

Specimen Material:

Specimen material selected for proposed research work was High Carbon High Chromium Steel (HCHCR).

i. Chemical Composition:

Element	Content (%)
C	1.40 – 1.60
Mn	0.60
Si	0.60
Co	1.00
Cr	11.00 – 13.00
Mo	0.70 – 1.20
V	1.10
P	0.03
Ni	0.30
Cu	0.25
S	0.03

Table 1. Chemical Composition of HCHCR Steel

ii. Physical Properties:

Properties	Metric	Imperial
Density	7.7 x 1000 kg/m3	0.278 lb/in3
Melting point	1421°C	2590°F

Table 2. The physical properties of HCHCR Steel

iii. Mechanical Properties:

Mechanical Properties	Metric	Imperial
Hardness, Rockwell C	62	62
Hardness, Vickers	748	748
Izod impact unnotched	77.0 J	56.8 ft-lb
Poisson's ratio	0.27-0.30	0.27-0.30
Elastic modulus	190-210 GPa	27557-30457 ksi

Table 3. The mechanical properties of HCHCR Steel

2. STRATEGY OF CONDUCTING EXPERIMENTS

*Hardness Test:*The hardness of the specimens was measured by Brinell-cum-Rockwell Hardness testing machine. This method consists of indenting the test material with a hardened steel ball indenter. The indenter is forced into the test material under a load usually 150 kgf for HCHCR and Stainless Steel. When equilibrium has reached, an indicating device, which follows the movements of the indenter and so responds to changes in depth of penetration of the indenter, is set to a datum position.

The permanent increase in depth of penetration, resulting from the application of the load is used to calculate the Brinell hardness number, which can be calculated through the following formula:

$$BHN = \frac{2P}{\pi D\left[D - \sqrt{D^2 - d^2}\right]}$$

Where,

P = Load Applied
D = Diameter of steel ball in mm
d = Diameter of indentation in mm

Calculation of Hardness Number:

Specimen 1st (HCHCR)
Applied load = 150 kgf
Diameter of the ball (D) = 3.5 mm
Diameter Of the indentation (first) = 1.9 mm
Diameter of the indentation (second) = 1.9 mm
Avg. diameter of the indentation (d) = 1.9 mm

$$BHN = \frac{2P}{\pi D\left[D - \sqrt{D^2 - d^2}\right]}$$

$$BHN = \frac{2x150}{\pi 3}.5\left[3.5 - \sqrt{3.5^2 - 1.9^2}\right]$$

$$BHN = \frac{300}{18}.22142$$

BHN = 16.464

S. no.	Specimen	BHN
1	High Carbon High Chromium Steel	16.464

Table 4. Hardness Number value of both the Specimen

3. MACHINING OPERATION ON ELECTRICAL DISCHARGE MACHINE

The total length of both material was 100X100X10 mm. Materials were cut into four pieces 25X25X10 mm each for the need of experiment set up. The work pieces (HCHCR) were fixed in Electrical Discharge Machine accordance's with experimental design and measured for surface roughness, material removal rate and tool wear rate. The factors (Current, T On, T Off, Flushing rate, Spark gape) were varied at three levels for EDM. [5]

Designing of Experiment using Regression analysis based Design of Experiment (DOE) Method:

Degrees of Freedom: Degree of Freedom in statistics is a very important value because it determines the minimum number of treatment conditions.
Degree of freedom for each factor is

$$DFA = kA - 1$$

Where k_A is the number of levels of Factor A.

In the proposed work, all the five parameters are at three levels each. Values of variables at different levels for machining on EDM of both the specimen materials are as shown in the Table 5. and Table 6.

Factors	Level 1	Level 2	Level 3
Current (A)	5.00	10.0	15.0
Spark gap (B)	0.10	0.15	0.25
Flushing rate (C)	0.50	1.00	1.50
T on (D)	4.00	5.00	6.00
T off (E)	6.00	7.00	8.00

Table 5. Factors at different levels for machining HCHCR on EDM

Factors	Level 1	Level 2	Level 3
Current (A)	10.0	15.0	20.0
Spark gap(B)	0.10	0.15	0.20
Flushing rate(C)	0.50	1.00	1.50
T on (D)	6.00	7.00	8.00
T off (E)	8.00	9.00	10.0

Table 6. Factors at different levels for machining Stainless Steel on EDM

The degree of freedom (DF) of a three level parameter is two (number of levels-3), hence total DF for the experiment is 10.

Factors	A	B	C	D	E	Total
Degree of Freedom	2	2	2	2	2	10

Table 7. Degrees of Freedom of the experiment

The selection of which Orthogonal Array to use depends upon:

i. The number of factors of interest.
ii. The number of levels for the factors of interest.

Total Degree of freedom for this experiment is 10 as shown in Table 7. As the degree of freedom required for the experiment is 10 so the orthogonal array that is to be selected should have degree of freedom higher than 10. Therefore one of the most suitable orthogonal arrays that can be used for this experiment is L27.

In this experiment, the assignment of factors was carried out using MINITAB 17 Software. The Standard L27 Orthogonal Array (Reference: Appendix A) as suggested by MINITAB using Taguchi for the particular experiment are listed in Table 8. [6]

S. no	Current (A)	Spark gap (mm)	Flushing rate (kg/cm3)	T on	T off
1	5	0.10	0.50	4	6
2	5	0.10	0.50	4	7
3	5	0.10	0.50	4	8
4	5	0.15	1.00	5	6
5	5	0.15	1.00	5	7
6	5	0.15	1.00	5	8
7	5	0.20	1.50	6	6
8	5	0.20	1.50	6	7
9	5	0.20	1.50	6	8
10	10	0.10	1.00	6	6
11	10	0.10	1.00	6	7
12	10	0.10	1.00	6	8
13	10	0.15	1.50	4	6
14	10	0.15	1.50	4	7
15	10	0.15	1.50	4	8
16	10	0.20	0.50	5	6
17	10	0.20	0.50	5	7
18	10	0.20	0.50	5	8
19	15	0.10	1.50	5	6
20	15	0.10	1.50	5	7
21	15	0.10	1.50	5	8
22	15	0.15	0.50	6	6
23	15	0.15	0.50	6	7
24	15	0.15	0.50	6	8
25	15	0.20	1.00	4	6
26	15	0.20	1.00	4	7
27	15	0.20	1.00	4	8

Table 8. Control log for the Experimental trial runs to be performed on HCHCR specimens

S. no	Current (A)	Spark Gap (mm)	Flushing rate (kg/cm3)	T on	T off
1	10	0.10	0.50	6	8
2	10	0.10	0.50	6	9
3	10	0.10	0.50	6	10
4	10	0.15	1.00	7	8
5	10	0.15	1.00	7	9
6	10	0.15	1.00	7	10
7	10	0.20	1.50	8	8
8	10	0.20	1.50	8	9
9	10	0.20	1.50	8	10
10	15	0.10	1.00	8	8
11	15	0.10	1.00	8	9
12	15	0.10	1.00	8	10
13	15	0.15	1.50	6	8

14	15	0.15	1.50	6	9
15	15	0.15	1.50	6	10
16	15	0.20	0.50	7	8
17	15	0.20	0.50	7	9
18	15	0.20	0.50	7	10
19	20	0.10	1.50	7	8
20	20	0.10	1.50	7	9
21	20	0.10	1.50	7	10
22	20	0.15	0.50	8	8
23	20	0.15	0.50	8	9
24	20	0.15	0.50	8	10
25	20	0.20	1.00	6	8
26	20	0.20	1.00	6	9
27	20	0.20	1.00	6	10

Table 9. Control log for the Experimental trial runs to be performed on Stainless Steel specimens

4. RESULTS

Following graphs are displaying the distribution of the set of data for judging the normality of the distribution of a group of residuals.

For this reason the following residuals plots consists of:

i) Histogram – is a frequency plot obtained by placing the data in regularly spaced cells and plotting each cell frequency versus the centre of the cell.

ii) Normal probability plots – since the sample sizes for residuals are generally small (less than 50) because experiments have limited treatment combinations. In present research work only twenty seve treatment combinations work chosen at a time, so a histogram may not be the best choice for judging the distribution of residuals.

Therefore normal probability plot is plotted since it is more sensitive graph.

The following steps were taken in forming following normal probability plots:

- By sorting the residuals into the ascending order.
- By calculating the cumulative probability of each residual by using the formula

$$P(ith\ residual) = i\frac{\square}{\square}(N+1)$$

Where,

P - Cumulative probability of a point.

I – order of the value in list

N – Number of entries in the list

- By plotting the calculated p values versus the residual values on normal probability paper

iii) The plots of residual versus FITS should produce a distribution of points scattered randomly about zero regardless of size of the fitted value.

After experiment the following observations were obtained where we use the array L-27 to arrange the combination of process parameters. The two output parameters are Surface Roughness (Ra) and Tool Wearing Rate (TWR).

S. no	Current (A)	Spark gap (mm)	Flushing rate (kg/cm^3)	T on	T off	Roughness (Ra)	TWR
1	5	0.10	0.50	4	6	2.91	7
2	5	0.10	0.50	4	7	2.295	10
3	5	0.10	0.50	4	8	2.595	7
4	5	0.15	1.00	5	6	3.68	0
5	5	0.15	1.00	5	7	3.465	6
6	5	0.15	1.00	5	8	3.935	12
7	5	0.20	1.50	6	6	4.07	8
8	5	0.20	1.50	6	7	3.8	6
9	5	0.20	1.50	6	8	4.36	7
10	10	0.10	1.00	6	6	6.815	6
11	10	0.10	1.00	6	7	5.245	11
12	10	0.10	1.00	6	8	5.98	12
13	10	0.15	1.50	4	6	3.22	6
14	10	0.15	1.50	4	7	4.185	7
15	10	0.15	1.50	4	8	3.575	6
16	10	0.20	0.50	5	6	4.11	5
17	10	0.20	0.50	5	7	3.56	8
18	10	0.20	0.50	5	8	4.12	6
19	15	0.10	1.50	5	6	5.12	3
20	15	0.10	1.50	5	7	5.325	5
21	15	0.10	1.50	5	8	5.62	5
22	15	0.15	0.50	6	6	7.205	6
23	15	0.15	0.50	6	7	7.14	5
24	15	0.15	0.50	6	8	5.76	7
25	15	0.20	1.00	4	6	3.5	3
26	15	0.20	1.00	4	7	4.57	3
27	15	0.20	1.00	4	8	4.72	6

Table 10. Results of Experimental trial runs performed on HCHCR specimens

Regression Analysis for High Carbon High Chromium Steel:

Source	DF	Adj SS	Adj MS	F-Value	P-Value
Regression	5	78.056	15.611	2.97	0.035
Current (A)	1	22.222	22.222	4.22	0.052
Spark gap (mm)	1	10.889	10.889	2.07	0.165
Flushing rate (kg/cm^3)	1	3.556	3.556	0.68	0.420
T on	1	9.389	9.389	1.78	0.196
T off	1	32.000	32.000	6.08	0.022
Error	21	110.463	5.26		
Total	26	188.519			

Table 11. Analysis of Variance (ANOVA)

S	R-sq	R-sq(adj)	R-sq(pred)
2.29350	41.40%	27.45%	9.40%

Table 12. Model Summary

Term	Coef	SE Coef	T-Value	P-Value	VIF
Constant	-1.09	5.18	-0.21	0.835	
Current (A)	-0.222	0.108	-2.06	0.052	1.00
Spark gap (mm)	-15.6	10.8	-1.44	0.165	1.00
Flushing rate (kg/cm^3)	-0.89	1.08	-0.82	0.420	1.00
T on	0.722	0.541	1.34	0.196	1.00
T off	1.333	0.541	2.47	0.022	1.00

Table 13. Coefficients

Regression Equation

TWR=-1.09 - 0.222 Current (A) - 15.6 Spark gap (mm) - 0.89 Flushing rate (kg/cm^3) + 0.722 T on + 1.333 T off

Obs	TWR	Fit	Resid	Std Resid
4	0.000	6.185	-6.185	-2.92 R

Table 14. Fits and Diagnostics for Unusual Observations

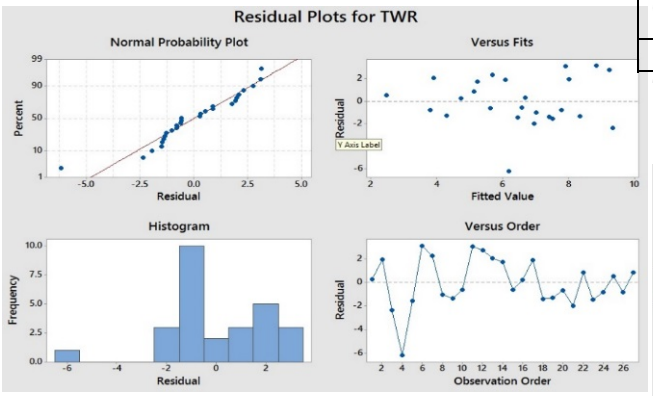

Fig. 1. Residual plots for Tool Wear Rate of HCHCR

According to ANNOVA table T off was the factor that affected Tool Wear rate significantly. While at the same time the other factors were found to be insignificant.

Roughness (R versus Current (A), Spark gap (mm), Flushing rate (k, Ton, T off) for HCHCR Steel:

Source	DF	Adj SS	Adj MS	F-Value	P-Value
Regression	5	38.7993	7.7599	26.77	0.000
Current (A)	1	17.7013	17.7013	61.06	0.000
Spark gap (mm)	1	1.4422	1.4422	4.97	0.037
Flushing rate (kg/cm^3)	1	0.0098	0.0098	0.03	0.856
T on	1	19.6460	19.6460	67.77	0.000
T off	1	0.0001	0.0001	0.00	0.988
Error	21	6.0879	0.2899		
Total	26	44.8872			

Table 15. Analysis of Variance (ANOVA)

S	R-sq	R-sq(adj)	R-sq(pred)
0.538425	86.44%	83.21%	77.80%

Table 16. Model Summary

Term	Coef	SE Coef	T-Value	P-Value	VIF
Constant	-1.85	1.22	-1.52	0.143	
Current (A)	0.1983	0.0254	7.81	0.000	1.00
Spark gap (mm)	-5.66	2.54	-2.23	0.037	1.00
Flushing rate (kg/cm^3)	-0.047	0.254	-0.18	0.856	1.00
T on	1.045	0.127	8.23	0.000	1.00
T off	0.002	0.127	0.02	0.988	1.00

Table 17. Coefficients

Regression Equation:

Roughness (Ra) = -1.85+ 0.1983 Current (A) -5.66 Spark gap (mm) - 0.047 Flushing rate (kg/cm^3) + 1.045 T on + 0.002 T off

Obs	Roughness (Ra)	Fit	Resid	Std Resid
10	6.815	5.803	1.012	2.11 R

Table 18. Fits and Diagnostics for Unusual Observations

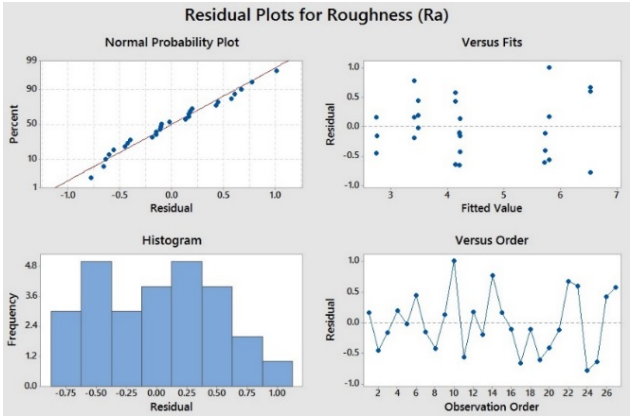

Fig. 2. Residual plots for roughness of HCHCR

According to coefficient table Current, Spark gap and Ton were the factors that affected Surface roughness significantly. While at the same time the other factors were found to be insignificant.

5. CONCLUSIONS

This comparative study utilized an efficient method for determining the optimum machining operation parameters of Electrical Discharge Machine in the different cases for Tool Wearing Rate and Surface Roughness through the use of the Response Process. The specimens chosen for the project work were High Carbon High Chromium Steel (HCHCR). The hardness tests on the specimen materials were conducted on the Hardness testing Machine at the Strength of Material laboratory, Department of Civil Engineering, S.S.E.T.,

SHIATS, Allahabad, India. The machining of specimen materials was performed on the Electrical Discharge Machine (EDM) machine (C-3822) at Rajat Engineering workshop, Kanpur, India.

Conclusions can be summed up with following:

i. The use of standard L27 orthogonal array, with five control parameters required three levels of each to design the experiment for the work pieces.

ii. In machining of HCHCR on EDM by copper tool, the cutting combination obtain for the optimal levels of the parameters were current (5Amp,10Amp,1Amp), spark gap (0.1mm, 0.15mm, 0.2mm), flashing rate (0.5kg/Cm^3, 1.0kg/Cm^3, 1.5kg/Cm^3), T On (4,5,6), T Off (6,7,8).

The present work has successfully demonstrated the application Regression method for experimental investigation of the effect of control parameters of EDM.

6. REFERENCES

[1] Amardeep Singh, Rakesh Sharma and Neel Kanth Grover (2012) recent Advancement in Electric Discharge Machining. edition12.

[2] Angelos P. Markopoulos (2008) Artificial neural network models for the prediction of surface roughness in electrical discharge machining, J Intell Manuf (2008), 19:283–292.

[3] Assarzadeh and Ghoreishi (2008) Neural-network-based modeling and optimization of the electro-discharge machining process. Int J Adv Manuf Technol (2008), 39:488–500.

[4] Ashish Khetan and Deb Sankha (2009) study on the neural network application in machining, Indian Institute of Technology Guwahati.

[5] Deepak kumar Panda and Rajat Bhoi (2005) Artificial Neural Network Prediction of Material Removal Rate in Electro Discharge Machining, Materials and Manufacturing Processes, Materials and Manufacturing Processes (2005), 20: 4, 645-672.

[6] A. Thillaivannan Rao and Rao (2010) Optimization of operating parameters for EDM process based on the Taguchi Method and Artificial Neural Network. International Journal of Engineering Science and Technology (2010), Vol 2(12), 6880-6888.

Author: **Marshal Noel Paik** Shiats, Allahabad, up, India, **Rahul Davis** Assistant professor Shiats, Allahabad, up, India, **Pritish Sahu** Shiats, Allahabad, up, India, **Miss Namlen Ekka** Shiats, Allahabad, up, India, **Darla Sudheer** Shiats, Allahabad, up, India, **Solomon Samson** Shiats, Allahabad, up, India

E-mail: marshalnoelpaik@gmail.com
rahuldavis2012@gmail.com

Journal of Production Engineering
Vol.19 No.2
JPE (2016) Vol.19 (2) Original Scientific Paper
Pawar, P., Anasane, S., Ballav, R., Kumar, A.

EXPERIMENTAL STUDY OF ELECTROLESS COPPER COATED ON ABS MATERIAL USED FOR TOOLING IN EDM MACHINING PROCESS

Received: 11 Augus 2016 / Accepted: 17 October 2016

Abstract: *In this paper, three-dimensional catia model used to make physical prototype model using fused deposition modeling rapid prototype technique. The three-dimensional prototype model made up of nonconductive ABS material. This prototype model is further coated with a 1.5mm electroless copper coating, which acts as a conductive prototype model. However, this copper coated model is used for tooling in electro discharge machining process to replicate mirror shape cavity in the mild steel material. Then calculated optimum input process parameters for higher material removal rate, lower tool wear rate and lower the surface roughness.*
Key words: *Electro Discharge Machining process, Copper, Fused Deposition Method, ABS material.*

Eksperimentalna istraživanja neelektrične depozicije bakra na ABS materijal koji se koristi kao alat u procesu elektro-erozivnog procesa obrade. *U ovom radu je korišćen trodimenzionalni CATIA model za izradu prototipa pomoću ciljne depozicije kao tehnike brze izrade prototipa. Trodimenzionalni prototip je napravljen od neprovodljivog ABS materijala. Ovaj prototip je posle neelektrično obložen sa 1,5mm bakarnog sloja koji se ponaša kao provodljiv model prototipa. Ovaj bakrom obložen model je korišćen kao alat kod elektro-erozivnog postupka obrade radi repliciranja negativa oblika u čeličnom materijalu. Na kraju je izračunat optimum vrednosti ulaznih parametara procesa radi postizanja veće proizvodnosti, manjeg habanja alata i manje površinske hrapavosti.*
Ključne reči: *Elektro-erozivni postupak obrade, bakar, metoda ciljne depozicije, ABS materijal.*

1. INTRODUCTION

Yarlagadda, P.K.D.V. et al. used a rapid tooling technique for the making of sheet drawing tool by an assortment of stereolithography and nickel electroforming method [1]. Gillot F. et al. analyzed the dimensional accuracy of electroplated copper electrodes on positive shape [2]. Dimla D. E. et al. produced EDM electrodes using two methods of rapid prototyping techniques i.e. copper coating of stereolithography models and copper coating of direct metal laser sintered models [3]. Ferreira J.C. et al. The thermojet 3D printing technique rapid prototyping method used for making tools for electrical discharge machining process [4]. Pawar P. et al. has studied the 0.5mm and 1mm electroless Cu coated on ABS material used as tooling in electro discharge machining process to replicate mirror cavity in mild steel [5, 6].

2. EXPERIMENTAL PROCEDURE

The triangular shaped CAD model is developed in the CATIA V5 software. Then this model is transferred into Stratasys FDM-DIMENSION machine to build up actual ABS (Acrylonitrile butadiene styrene) physical prototype model according to the CAD model. However, this physical prototype model was sent to Cu plating process. The Electroless copper plating was done in Metaffin Industries, Andheri, Mumbai. For initial stage, the layer thickness of Cu deposited on FDM component is to 1.5mm for the plating process of this component required 2 days for completing the plating process. The electroless Cu coated component is used as tooling in the electro discharge machine (EDM). The machine model ELECTRONICA-ELECTRAPULS PS 50ZNC die-sinking with servo head is used to produced the mirror shape in the mild steel workpiece material.

2.1 Material Removal Rate (MRR) :- The workpiece was held in a vice on the machine table. The workpiece and tools were associated with positive and negative terminals of power supply respectively. The tank was filled with EDM oil flushed through the nozzle. The depth of cut was set to 1mm. The initial weight of workpiece before the experiment was weighed using a 1mg accuracy digital weighing machine. The time taken to machine 1mm depth was recorded. The end of each experiment workpiece was removed from the machine, washed, dried and weighed on a weighing machine. The precision balance was utilized to measure the weight of the workpiece and tool material. This machine capacity is 300 grams and accuracy is 0.001 gram and Brand: Afcoset., The material removal rate was calculated using the following formula.

MRR=

$$\frac{\text{Initial weight of work piece before machining - Final weight of work piece after machining}}{\text{Machining time}}$$

gm/min

2.2 Tool Wear Rate (TWR) :- The copper coating electrode is holding on Cu holder and this holder is connected to machine spindle with the negative terminal of the power supply. The initial weight of electrode before the experiment was weighted using

0.001mg accuracy digital weighing machine. The bottom of the electrode was polished after every experiment to remove the carbon deposited on the tool surface. The tool wear rate calculated using following formula.

TWR=

$$\frac{\text{Initial weight of tool before machining} - \text{Final weight of tool after machining}}{\text{Machining time}}$$

gm/min

2.3 Surface Roughness (Ra) :- The surface roughness was measured by taking the average of the 5 readings taken along the machined surface of mild steel component using a Mitutoyo SJ 201P instrument.

3. SEQUENTIAL PROCESS OF RAPID PROTOTYPING TOOLING

3.1 Development of CAD Model:- The CAD model has designed and modeled in CAD tool CATIA-V5 software. Then this CAD modeling geometry is required to be converted into stereolithography supported format i.e. .stl format. The geometry is converted into the .stl binary format. The fig. 1 shows that three-dimensional CAD model, which is built in CATIA software.

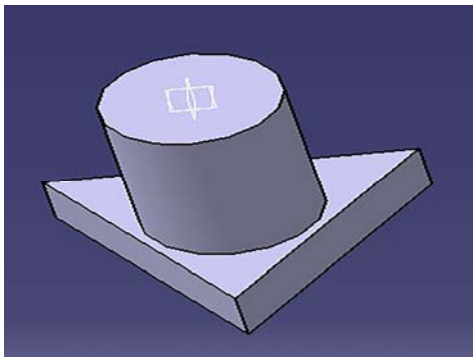

Fig. 1. 3D Triangular Shaped CAD Model

3.2 Fabrication of Rapid Prototype Model :- The Fused Deposition Modeling (FDM) RP model is fabricated by Dimension Stratsys Rapid Prototype machine, which is shown in fig. 2. The .stl file which is generated in CAD Software is processed in RP preprocessing software "CATALYST" to set the optimum build orientation and calculation of no. of layers and total build time. The machine used for this RP fabrication is a DIMENSION *BST* model, manufacturer as Stratasys, USA. The material of this prototype model is Acrylonitrile butadiene styrene.

Fig. 2. ABS Material Rapid Prototype Model

3.3 Cu Coating on FDM component :- This FDM model is further coated with Cu of 1.5 mm thickness of coating by using an electroless copper coating process. The fig. 3 shows that 1.5mm Cu coated rapid prototype tooling.

Fig. 3. Electroless Copper Coated on ABS Material and Cut section of Holding Part

3.4 Experimentation using Electro Discharge Machine :- The 1.5mm Cu coated rapid prototype component is used as tooling in the EDM machining process. The fig. 4 shows that actual experimental conditions. The fig. 5 and fig. 6 shows that machined surface according to Taguchi L9 orthogonal array input process parameters.

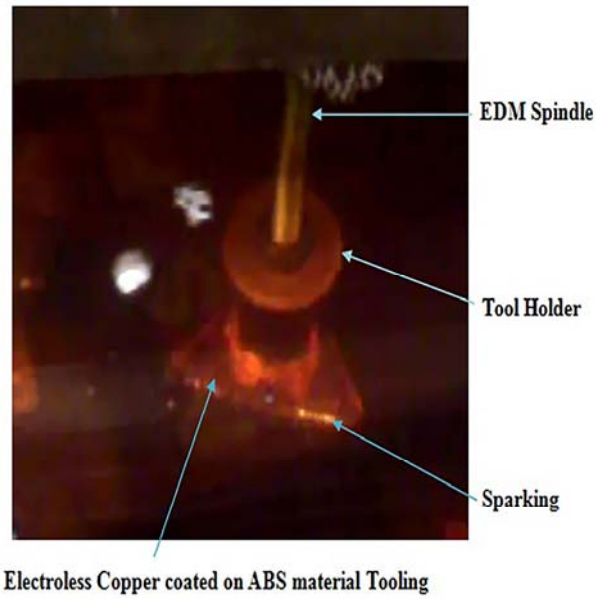

Fig. 4. Electroless Copper Coated on ABS Material used as Tooling in EDM Process

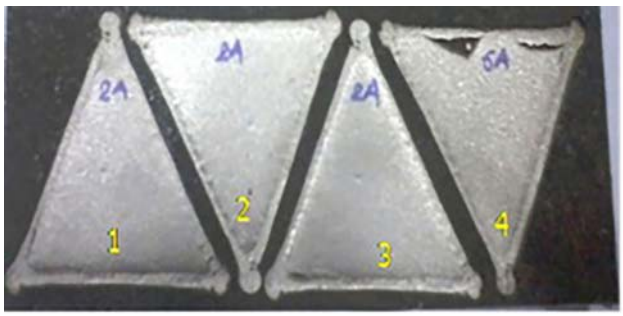

Fig. 5. Mild Steel Machined Surface 1

Fig. 6. Mild Steel Machined Surface 2

3.5 Experimentation using Taguchi L9 Orthogonal Array:- The Taguchi L9 array method was used for experimentation. The three Input factors such as current (Ip), Pulse on-time (Ton), Voltage (vg) and respective three responses are Material Removal Rate (MRR), Tool Wear Rate (TWR) and Surface Roughness (Ra). The table 1 shows that the Taguchi L9 coding system & Fig. 7 shows that input process parameters sequencing orders according to the Taguchi L9 array.

Levels	High (+1)	Medium (0)	Low (-1)
Peak current (Ip)	10	6	2
Pulse on time (Ton)	150	100	50
Voltage (Vg)	60	50	40

Table-1 Controllable parameters with their levels of experimentation

Run	Ip(A)	Ton(µS)	Vg(v)
1	1	1	1
2	1	0	0
3	1	-1	-1
4	0	1	0
5	0	0	-1
6	0	-1	1
7	-1	1	-1
8	-1	0	1
9	-1	-1	0

Run	Ip(A)	Ton(µS)	Vg(v)
1	10	150	60
2	10	100	50
3	10	50	40
4	6	150	50
5	6	100	40
6	6	50	60
7	2	150	40
8	2	100	60
9	2	50	50

Fig. 7. Taguchi L9 coding array for Experimentation

4. RESULTS AND DISCUSSION

The following observation shows that the results of MRR, TWR, and Ra is shown in Table-2. The corresponding influences on Material Removal rate (MRR), Tool wear rate (TWR) and surface roughness (Ra) has been discussed. The ANOVA Table, Response Table, Graph of SN ratio is computed by using Minitab Software.

No.	Ip	Ton	Vg	MRR (gm/min)	TWR (gm/min)	Ra (µm)
1	10	150	60	0.0560	0.00234	9.23
2	10	100	50	0.0291	0.00056	8.07
3	10	50	40	0.0204	0.002158	6.38
4	6	150	50	0.0216	0.000127	6.5
5	6	100	40	0.0192	0.00036	5.73
6	6	50	60	0.0248	0.00029	4.91
7	2	150	40	0.0063	0.0000231	2.81
8	2	100	60	0.0080	0.000117	2.62
9	2	50	50	0.0095	0.000227	2.84

Table 2. Experiemental Observations

4.1 Influence on Material Removal Rate

Taguchi method is used to analysis the results of the response of machining parameter for larger is better criteria. The analysis of variances of the factors is shown in Table 3 which is clearly indicated that pulse on time is not important for influencing MRR and Ip is most influencing factors for MRR and Vg is least significant. The delta values are Ip, Vg & Ton is 12.28, 4.36, 1.54 are respectively, depicted in Table 4.

Source	DF	Seq SS	Adj SS	Adj MS	F	P
Ip	2	241.12	241.2	120.56	15.53	**0.060**
Ton	2	4.211	4.211	2.10	0.27	0.787
Vg	2	28.757	28.76	14.37	1.85	0.351
Residual Error	2	15.523	15.52	7.761	15.53	0.060
Total	8	289.61				

Table 3. Analysis of Variance for SN ratios (MRR)

.

Level	Ip	Ton	Vg
1	-42.13	-35.45	-37.38
2	-33.25	-35.66	-34.83
3	-29.86	-34.12	-33.03
Delta	12.28	1.54	4.36
Rank	1	3	2

Table 4. Response Table for Signal to Noise Ratios

The main effect plot of an S/N ratio for MRR shown in Fig 8. The discharge current (Ip) is directly relative to MRR in the range of 2 to 6A. This is expected because an increase in pulse current creates a strong spark, which generates the elevated temperature, caused more material to melt and wear out from the workpiece. But,

with the increase in discharge current from 6A to 10A MRR increases more than previous conditions.

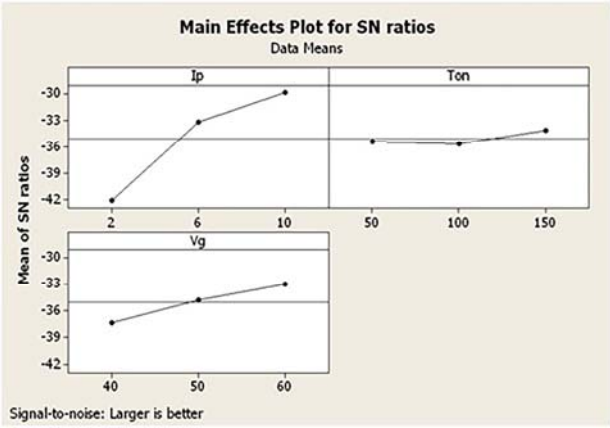

Fig. 8. Main effect plot for SN ratios (MRR)

Optimisation:- Optimum combination of SN ratios from fig. 8 is $A_1B_1C_1$ that is Ip=10A, Ton=150µs, Vg=60V. The linear regression equation for MRR is

MRR(gm/min) = - 0.0443 + 0.00340 Ip + 0.000097 Ton + 0.000715 Vg ---------- (1)

=**0.04715gm/min**

4.2 Influence on Tool Wear Rate

The Taguchi method is utilized to analyze the results of machining parameter for smaller is better criteria. The analysis of variances of the factors Ip, Ton and Vg in Table 5 is clearly indicated that the Ton and Vg are not important for influencing TWR and the value Ip is most affected the TWR. The delta values Ip, Vg and Ton are 24.42, 8.77 and 4.61 respectively depicted in table 6.

Source	DF	Seq SS	Adj SS	Adj MS	F	P
Ip	2	916.78	916.78	458.39	4.70	0.175
Ton	2	116.75	116.75	58.38	0.60	0.625
Vg	2	39.90	39.90	19.95	0.20	0.830
Residual Error	2	194.88	194.88	97.44	4.70	
Total	8	1268.3	916.78	458.39		

Table 5. Analysis of Variance for SN ratios (TWR)

Level	Ip	Ton	Vg
1	81.41	65.65	71.64
2	72.52	70.85	71.95
3	56.99	74.42	67.33
Delta	24.42	8.77	4.61
Rank	1	2	3

Table 6. Response Table for Signal to Noise Ratios

The influence of various machining parameters like Ton, Ip and Vg has a significant effect on TWR , as shown in the main effect plot for an S/N ratio of TWR in fig. 9. The increase in the discharge current gets increased the tool wear rate, Because of Ip increases the pulse energy increases and thus more heat energy is produced in the tool and workpiece interface leads to increase the melting and evaporation of the electrode. The current is directly proportional to the tool wear rate, voltage and pulse on time had no significant effect on TWR.

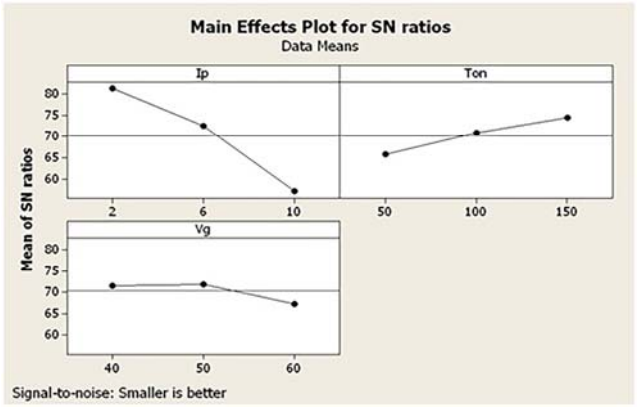

Fig. 9. Main effect plot for SN ratios (TWR)

Optimisation:- Optimum combination of SN ratios from fig. 10 is $A_3B_1C_2$ that is Ip=10A, Ton=150µs, Vg=50V. The linear regression equation for TWR is

The regression equation is TWR(gm/min)

= - 0.00059 + 0.000195 Ip - 0.000001 Ton + 0.000003 Vg ---------- (2)

= **0.00146gm/min**

4.3 Influence on Surface Roughness

Taguchi method is used to analysis the result of machining parameter for smaller is better criteria. The analysis of variances of the factors are Ip, Ton, and Vg, as shown in Table 7 is clearly indicated that the factors Ton and Vg is not significant and the value of Ip is most influencing for Ra (shown in bold). The delta values are Ip, Ton and Vg are 9.044, 1.851 and 1.076 respectively. In case smaller is better criteria, so from table 8 it is clearly defined that Ip is the most important factor then Ton and last is Vg.

Source	DF	Seq SS	Adj SS	Adj MS	F	P
Ip	2	128.9	128.85	64.429	78.80	**0.013**
Ton	2	5.139	5.139	2.5697	3.14	0.241
Vg	2	1.765	1.765	0.8827	1.08	0.481
Residual Error	2	1.635	1.635	0.8177	78.80	0.013
Total	8	137.4				

Table 7. Analysis of Variance for SN ratios (Ra)

Level	Ip	Ton	Vg
1	-8.802	-12.995	-13.411
2	-15.08	-13.889	-14.487
3	-17.84	-14.845	-13.831
Delta	9.044	1.851	1.076
Rank	1	2	3

Table 8. Response Table for Signal to Noise Ratios

The current is most significant for the surface roughness because of the high intensity of electric energy affects the Ra value. Therefore, increases current it also increases the Ra value, so it is directly

proportional to each other. The influence of various machining parameters like Ton, Ip and Vg has a significant effect on Ra , as shown in the main effect plot for an S/N ratio of Ra in fig. 10. The current increases the pulse energy and thus more heat energy is created in the tool and workpiece interface leads to surface roughness decrease when increase current and current is directly proportional to the surface roughness. The voltage & pulse on time had no significant effect on Ra.

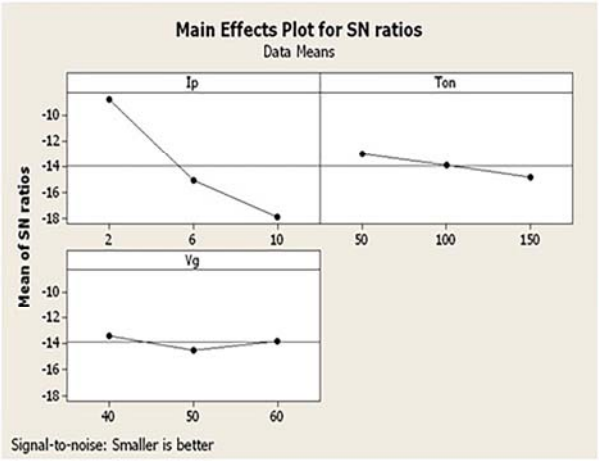

Fig. 10. Main effect plot for SN ratios (Ra)

Optimisation: - Optimum combination of SN ratios is $A_1B_3C_3$ that is Ip=10A, Ton=50µs, Vg = 40V The linear regression equation for Ra is

Ra(µm) = - 1.40 + 0.642 Ip + 0.0147 Ton + 0.0307 Vg------ (3)

= **6.983µm**

5. SURFACE TOPOLOGY

In this analyze the machined surface topology using Matazer Meatavision microscope under the 100X resolution. The machined surface obtained under 2A current input parameters having a fine surface structure which is shown in fig. 11, while the machined surface obtained under 10A current input parameters having a coarse surface structure which is shown in fig. 13.

Fig. 11. Surface Topology of 2A Current

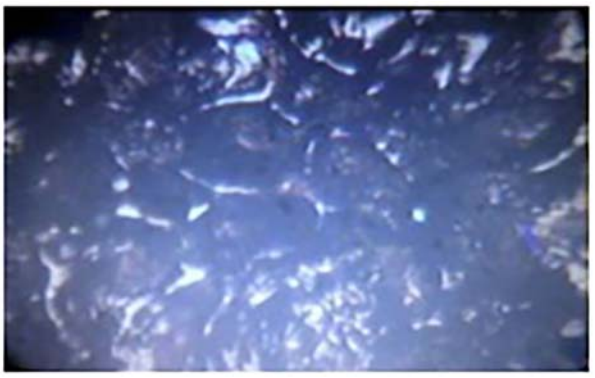

Fig. 12. Surface Topology of 6A Current

Fig. 13. Surface Topology of 10A Current

6. CONCLUSION

1) The main objective of this paper is to check the conductivity of electroplated on nonconductive material i.e. ABS Material. The Rapid prototyping tooling is used as tooling in electro discharge machining process to replicate mirror cavity in the mild steel material.

2) The experimental observations show that pulse current has the most significant effect on MRR followed by applied voltage and pulse on Time. However, the increase in discharge current from 6A to 10A MRR increases more.

3) In a case of tool wear rate increases when the pulse on time from 50 to 150us. Moreover, the tool wear rate is increased when the discharge current increases in the range from 2 to 10A due to the melting and evaporation of the tool electrode.

4) The current is the most significant factor for surface roughness because of the high intensity of electric energy effects.

ACKNOWLEDGEMENTS

This paper is the next version of the paper presented at International Conference on Precision, Meso, Micro And Nano Engineering (COPEN-8: 2013) held at National Institute of Technology, Calicut, India. paper entitled of "Experimental Investigation of Electroless Cu Coated Electrode Fabricated with FDM Rapid Prototyping Technique for Electro-Discharge Machining". The author would like to acknowledge to Mr. Sandip Anasane, Dr. Raj Ballav, Dr. Amaresh Kumar for their continuous motivational support.

9. REFERENCES

[1] Yarlagadda, P.K.D.V., Ilyas, I.P., Christodoulou, P., "*Development of rapid tooling for sheet metal drawing using nickel electroforming and stereolithography processes*, Journal of Materials Processing Technology, 111, 286-294, 2011.

[2] Gillot, F., Mognol, P., Furet, B., *Dimensional accuracy studies of copper shells used for electro-discharge machining electrodes made with rapid prototyping and the electroforming process*, Journal of Materials Processing Technology, 159, 33–39, 2005.

[3] D. E. Dimla, N. Hopkinson, H. Rothe, *Investigation of complex rapid EDM electrodes for rapid tooling applications*, Int. J. Adv. Manuf. Technol., 23, 249–255, 2004.

[4] Ferreira, J.C., Mateus, A.S., Alves, N.F., *Rapid tooling aided by reverse engineering to manufacture EDM electrodes*, Int. J. Adv. Manuf. Technol., 34, 1133–1143, 2007.

[5] Pawar, P., Anasane, S., *Experimental Investigation of Electroless Cu Coated Electrode Fabricated with FDM Rapid Prototyping Technique for Electro-Discharge Machining*, International Conference on Precison, Meso, Micro And Nano Engineering (COPEN-8: 2013), Vol-2, 639-645, 13th – 15th December, 2013, NIT Calicut, Kerala, India, ISBN-978-93-82880-91-2.

[6] Pawar, P., Anasane, S., *Feasibility study of Electro Discharge Machining Electrodes Fabricated with Rapid prototyping process using Fused Deposition Modeling*, 4th International and 25th All India Manufactuing Technology, Design and Research Conference (AIMTDR-2012), Vol-1, 637-642, December 14th -16th 2012, Jadavpur University, Kolkata, India, ISBN: 978-93-82062-75-2.

Authors: **Mr. Pravin Pawar, Ph.D. Research Scholar**, Manufacturing Engineering Department, National Institute of Technology, Jamshedpur, Jharkhand, India, Phone.: +918 863 082-001

Mr. Sandip Anasane, Assistant Professor, Department of Production and Industrial Engineering, College of Engineering, Pune, Maharashtra, India.

Dr. Raj Ballav, Associate Professor, Manufacturing Engineering Department, National Institute of Technology, Jamshedpur, Jharkhand, India, Phone.: +91-657-237-4133.

Dr. Amaresh Kumar, Head of Department and Associate Professor, Manufacturing Engineering Department, National Institute of Technology, Jamshedpur, Jharkhand, India, Phone.: +91-657-2374129

E-mail: Pravin.1900@gmail.com
ssa.prod@coep.ac.in
rballav.prod@nitjsr.ac.in
akumar.prod@nitjsr.ac.in

Journal of Production Engineering
Vol.19 No.2
JPE (2016) Vol.19 (2) Original Scientific Paper
Payal, H., Maheshwari, S., Bharti, S.P.

PARAMETRIC OPTIMIZATION OF EDM USING MULTI-RESPONSE SIGNAL-TO-NOISE RATIO TECHNIQUE

Received: 31 October 2016 / Accepted: 30 November 2016

Abstract: *The performance of electrical discharge machining (EDM) is dependent on the selection of factor/levels combinations of input parameters. The optimization of EDM process is a multi-objective optimization problem on account of the contradictory behaviour of performance measures like metal removal rate and surface roughness (MRR, SR). Many optimization technique are used for the parametric optimization of EDM that require a good amount of computational facility. In this paper, multi-response signal-to noise ratio technique has been employed to find the optimal combination of input parameters owing to its simplicity and less mathematical computation. Experiments have been designed by Taguchi's L_{36} orthogonal array. In this work, two cases are considered and the parametric level/combinations have been obtained for both the cases. Analysis of variance (ANOVA) has also been employed to find the dominant parameters and finally experimentation verification has also been performed for the validation of results obtained.*
Key words: *electrical discharge machining, Taguchi's technique, analysis of variance (ANOVA), multi-response signal-to-noise ratio (MRSN)*

Optimizacija parametara EDM-a pomoću tehnike više odazivnih odnosa signal-šum. *Performanse elektro erozivne obrade zavise od izbora kombinacija faktora/nivoa ulaznih parametara. Optimizacija elektro erozivnog procesa obrade je višekriterijumski problem optimizacije usled kontradiktornog ponašanja izlaznih parametara procesa kao što je proizvodnost i hrapavost obrađene površine. Mnogo tehnika optimizacije se koriste za optimizaciju parametara procesa obrade elektro erozijom koji zahtevaju pozamašnu količinu resursa za obradu podataka. U ovom radu je iskorišćena tehnika više odazivnih odnosa signal-šum za pronalazak optimalne kombinacije ulaznih parametara, zbog svoje jednostavnosti i manje matematičkih računanja. Plan eksperimenta je napravljen pomoću Tagučijevog L_{36} ortogonalnog polja. U ovom radu su razmatranana dva slučaja i dobijeni su rezultati nivoa/kombinacija parametara za oba slučaja. Analiza varijacije je takođe iskorišćena u cilju pronalaženja uticajnih parametara a na kraju je izvedena eksperimentalna verifikacija radi validacije dobijenih rezultata.*
Ključne reči: *elektro erozivna obrada, Tagučijeva tehnika, analiza varijacije, više odazivni odnos signal-šum*

1. INTRODUCTION

Inconel 825 is a high-temperature resistant, nickel-based super alloy with excellent mechanical and metallurgical properties like high corrosion resistance, high yield strength, resistance to oxidation. This alloy finds immense applications in aerospace, marine, spacecraft, pumps, boilers, nuclear reactors etc. [1].Due to its peculiar properties this material can't be machined on traditional machine tools [2].EDM has been used as one of the most suitable machining processes for Inconel 825.EDM process deals with material removal mechanism by the use of electrical discharges occurring between the tool electrode and the work piece with tool and electrode immersed in dielectric media. In EDM the temperature is generated around 8000-12000^{0}C which is sufficient to melt the material and evaporate from the surface. The selection of process parameters level/combinations of EDM is a challenging task as EDM is a very complex machining process. The optimization of process parameters of EDM is a multi-objective optimization problem as, in general, high MRR is required with low SR. To overcome this problem various researchers have applied many optimization techniques like Grey relational analysis (GRA), principal component analysis (PCA), simulated annealing (SA)[3-5]. Most of these techniques are based on a mathematical/statistical analysis which requires high computational skills. In this study multi-response signal-to-noise ratio (MRSN) is employed due to its easiness, simple in approach, effective. In this, technique optimal combination(s) of input parameters are obtained by converting multi-responses into a single response. Literature review shows that much work has not been reported on this technique which inspired the author to employ this technique in the multi-objective optimization of EDM. Ramakrishnan and Karunamoorthy [6] carried out the experimental runs on Inconel 718 and reported that MRR increases with a pulse on time and decrease with delay time .After that they used Multi-response signal-to-noise (MRSN) ratio to find the optimal cutting parameters. Ramakrishnan and Karunamoorthy [7] employed MRSN technique to conduct an experimental investigation on wire-EDM for heat treated steel. Bharti et al. [8] found the best input parameter combination during EDM of D2 steel by considering two cases i.e. high cutting efficiency and high surface finish. Bharti et al. [9] used this technique again in Inconel 718 by

considering three cases i.e. high cutting efficiency, high surface finish, and normal machining .In this paper, MRSN technique has been used for the optimization of multiple performance characteristics during EDM of Inconel 825. Experiments were planned according to Taguchi $L_{36}(2^1x3^6)$ orthogonal array. Seven input parameters and two performance measures have been taken for the experimentation.

2. EXPERIMENTATION

In this study, L_{36} OA based on Taguchi design was used for the design of experiments. The input parameters and their corresponding level are depicted in table 1.The machining experiments were performed on Electronica PS50ZNC die sinking machine. In this study, dielectric fluid has been taken a noise factor. The first dielectric is of IPOL Spark Erosion oil SEO-250 and the second one is commercial grade EDM oil. The study material used in the present investigation is Inconel 825, having a density of 0.00814g/mm^3 . In the present study three different tool electrodes of cylindrically shaped having diameter each of 12mm namely Copper (Cu), Copper tungsten, Cu20%W80%) and Graphite (Gr) are used. MRR is calculated by evaluating the weight loss of work piece using equation 1 respectively.

$$MRR = \frac{W_i - W_f}{\rho t} mm^3 / \min \qquad (1)$$

Where W_i and W_f are the initial and final weights of work piece in gram, ρ is the density of work piece in g/mm^3 and t is the machining time in seconds.
The centre line average (CLA) surface roughness parameter R_a was used to quantify SR.

Input Parameters	Unit	Symbol	Levels and values		
			1	2	3
Dielectric fluid	-	A	First oil	Second oil	-
Pulse-on-time(T_{on})	μs	B	20	40	75
Discharge Current(I_d)	A	C	4	8	12
Duty cycle(ζ)	%	D	10	11	12
Gap voltage(V_g)	V	E	40	60	80
Tool Electrode Material	-	F	Copper (Cu)	Copper tungsten CuW)	Graphite (Gr)
Tool electrode lift time(T_L)	sec	G	0.1	0.2	0.3

Table 1. Machining Parameters and their levels

3. OPTIMIZATION BY MRSN

In MRSN method a multi-response SN ratio is evaluated to obtain the optimal combination of process parameters. Following are the steps for MRSN.

Step 1. Normalize the loss function corresponding to each performance measures.

$$N_{ij} = \frac{L_{ij}}{\overline{L_i}} \qquad (2)$$

Where N_{ij} is the normalized loss function for the ith performance measures in the j_{th} experiment, L_{ij} is the loss function for the i_{th} performance measures in the j_{th} experiment, and L_i bar is the average quality loss function for the i_{th} performance measures.

Step 2. Evaluation of total normalized quality loss, apply a weighting method for determining the total normalized quality loss by (3)

$$TN_j = \sum_{i=1}^{p} w_i N_{ij} \qquad (3)$$

Where w_i is the weighting factor for the ith performance measures, P is the number of performance measures, j is the number of experiments.

Step 3. Evaluation of MRSN ratio
Total loss function is converted into MRSN by (4)

$$MRSN = -10\log(TN_j) \qquad (4)$$

Whereas loss function is given by (5)

$$L_{ij} = \exp\left\{\frac{-S/N}{10}\right\} \qquad (5)$$

4. RESULTS AND DISCUSSION

Table 2 shows the values of performance measures for each experimental runs. In this study, two cases have been taken from the industrial point of view. Case 1: more weightage is given to MRR in comparison to SR. Hence the weights taken are w_1=0.7, w_2= 0.3.Case 2: more weightage is given to SR in comparison to MRR.Weight w_1 denotes the weightage given to MRR and w_2 denotes the weightage given to SR. The values of MRSN for case 1, case 2 are depicted in table 2. ANOVA results and Mean MRSN ratio for case 1 are depicted in table 3 and 4. From the results of the ANOVA and Mean of MRSN ratio, it is found that discharge current is the most dominating factor, having percentage contribution of 57.79, followed by tool lift, tool material, pulse-on-time and gap voltage. Dielectric fluid and duty cycle are observed as a non-dominating factor.

The mean MRSN ratio of input parameters A to G is maximum at A2,B1,C3,D1,E1,F3 and G2.Therefore the combination A2B1C3D1E1F3G3 is recommended as the optimal factor combination for case 1.ANOVA results and Mean MRSN ratio for case 2 are shown in table 5 and 6. From the table, it is found that pulse-on-time is the dominating factor having a percentage contribution of 38.64 followed by discharge current, tool material, tool lift, gap voltage and duty cycle. The dielectric fluid is observed as a non-dominating factor. The mean MRSN ratio of input parameter A to G is maximum at

A2,B1,C2,D1,E1,F3 and G3.Therefore the the optimal factor combination for case2. recommended combination is A2B1C2D1E1F3G3 as

Exp No.	Dielectric	T_{on} (μs)	I_D (A)	ζ (%)	V_g (V)	Tool Material	T_L (sec)	MRR (mm^3/min)	SR (μm)	Case-1	Case-2
1	1	1	1	1	1	1	1	3.0631	4.347	0.014708	0.68598
2	1	2	2	2	2	2	2	4.8124	6.530	0.752782	0.14106
3	1	3	3	3	3	3	3	11.5162	7.777	2.105038	0.12675
4	1	1	1	1	1	2	2	2.1474	3.864	-0.98302	0.34939
5	1	2	2	2	2	3	3	4.3182	5.789	0.651681	0.38021
6	1	3	3	3	3	1	1	3.9810	8.284	-0.03288	-0.7152
7	1	1	1	2	3	1	2	1.1916	5.741	-3.09524	-1.5151
8	1	2	2	3	1	2	3	5.0680	6.492	0.881218	0.20220
9	1	3	3	1	2	3	1	5.5072	8.388	0.651456	-0.5084
10	1	1	1	3	2	1	3	2.2609	4.544	-0.92926	0.11289
11	1	2	2	1	3	2	1	3.4279	5.916	0.028333	0.07204
12	1	3	3	2	1	3	2	5.3038	7.859	0.683828	-0.3337
13	1	1	2	3	1	3	2	4.4451	4.644	0.988716	1.00567
14	1	2	3	1	2	1	3	4.2817	6.824	0.414079	-0.0902
15	1	3	1	2	3	2	1	1.6577	5.844	-2.05908	-0.9355
16	1	1	2	3	2	1	1	3.7465	5.287	0.389661	0.46897
17	1	2	3	1	3	2	2	5.1329	6.872	0.825359	0.04515
18	1	3	1	2	1	3	3	3.5901	5.093	0.314394	0.51409
19	2	1	2	1	3	3	3	10.4451	4.689	2.96289	1.72353
20	2	2	3	2	1	1	1	4.8870	7.426	0.598562	-0.2237
21	2	3	1	3	2	2	2	1.7625	5.605	-1.84126	-0.7447
22	2	1	2	2	3	3	1	3.3780	4.991	0.167146	0.48872
23	2	2	3	3	1	1	2	4.3688	6.204	0.59136	0.19888
24	2	3	1	1	2	2	3	2.4783	6.528	-0.96079	-0.5775
25	2	1	3	2	1	2	3	10.0142	5.387	2.627634	1.25991
26	2	2	1	3	2	3	1	1.8366	5.309	-1.67688	-0.5622
27	2	3	2	1	3	1	2	8.0770	8.386	1.371173	-0.2845
28	2	1	3	2	2	2	1	5.7410	5.488	1.414494	0.79905
29	2	2	1	3	3	3	2	2.4439	5.192	-0.79696	-0.0555
30	2	3	2	1	1	1	3	4.7907	7.432	0.550995	-0.2426
31	2	1	3	3	3	2	3	4.8455	5.530	0.996776	0.62132
32	2	2	1	1	1	3	1	2.3034	4.988	-0.94153	-0.0572
33	2	3	2	2	2	1	2	4.4988	8.635	0.17737	-0.7408
34	2	1	3	1	2	3	2	4.4204	4.995	0.890604	0.80595
35	2	2	1	2	3	1	3	2.5422	5.646	-0.7537	-0.1926
36	2	3	2	3	1	2	1	3.1368	7.081	-0.41027	-0.5039

Table 2.Parametric levels and MRSN ratios for two cases

Source	DF	Seq SS	Adj MS	F	P	Percentage Contribution
Dielectric(A)	1	0.3147	0.314	0.57	0.458	0.567737
Pulse-on-time(B)	2	1.3247	0.662	1.2	0.32	2.389835
Discharge current(C)	2	32.036	16.01	29.03	0	57.79533
Duty cycle(D)	2	0.929	0.464	0.84	0.444	1.67597
Gap voltage (E)	2	1.0622	0.531	0.96	0.397	1.91627
Tool Material (F)	2	1.9777	0.988	1.79	0.19	3.567885
Tool Lift (G)	2	5.6472	2.823	5.12	0.015	10.18787
Residual Error	22	12.138	0.551			21.89928
Total	35	55.430				100

Table 3. Analysis of Variance for MRSN in Case-1

Input Parameter	Mean S/N			Selected Level	Optimum level/factor combination
	Level 1	Level-2	Level-3		
A-Dielectric fluid	0.08899	0.27598		2	A2B1C3D1E1F3G3
B-Pulse-on-time(T_{on})	0.45376	0.04786	0.04583	1	
C-Discharge Current(I_d)	-1.14238	0.70931	0.98053	3	
D-Duty cycle(ζ)	0.40202	0.12332	0.0221	1	
E-Gap voltage(V_g)	0.40972	-0.00551	0.14324	1	
F-Tool Electrode Material	-0.0586	0.10601	0.50003	3	
G-Tool electrode lift time(T_L)	-0.15469	-0.03627	0.73841	3	

Table 4. Mean MRSN Ratio table for case-1

Source	DF	Seq SS	Adj MS	F	P	Percentage Contribution
Dielectric(A)	1	0.0808	0.080	0.47	0.501	0.536553
Pulse-on-time(B)	2	5.8191	2.909	16.8	0	38.64175
Discharge current(C)	2	1.598	0.798	4.62	0.021	10.61152
Duty cycle(D)	2	0.2384	0.119	0.69	0.512	1.583096
Gap voltage (E)	2	0.6515	0.325	1.89	0.176	4.326288
Tool Material (F)	2	1.5363	0.768	4.45	0.024	10.2018
Tool Lift (G)	2	1.3334	0.666	3.86	0.037	8.854447
Residual Error	22	3.8016	0.172			25.24454
Total	35	15.0591				100

Table 5. Analysis of Variance for MRSN in Case-2

Input Parameter	Mean S/N			Selected Level	Optimum level/factor combination
	Level 1	Level-2	Level-3		
A-Dielectric fluid	0.000342	0.095092		2	A2B1C2D1E1F3G3
B-Pulse-on-time(T_{on})	0.567191	-0.01184	-0.4122	1	
C-Discharge Current(I_d)	-0.24819	0.225871	0.16546	2	
D-Duty cycle(ζ)	0.160121	-0.02989	0.01292	1	
E-Gap voltage(V_g)	0.2379	-0.04299	-0.0517	1	
F-Tool Electrode Material	-0.21153	0.0607	0.29398	3	
G-Tool electrode lift time(T_L)	-0.08262	-0.094038	0.31981	3	

Table 6. Mean MRSN Ratio table for case-2

5. EXPERIMENTAL VERIFICATION

The results of the confirmatory experiments are represented in table 7 and 8 for case 1 and case 2 respectively. The results of the experimental findings show that there is considerable improvement in MRR, SR with respect to initial settings of the input parameter. Initial settings are taken to check the improvement in performance measures at optimum, values with respect to the initial settings. In our study case, 1 represents the high cutting efficiency (i.e more weightage is given to MRR as compared to SR), improvement in MRR (i.e.13.93%) is more than the improvement in SR (i.e.10.42%).Similarly in case 2 represents the high surface finish (i.e more priority is given to SR as compared to MRR), improvement in SR (i.e. 12.56%) is more than the improvement in MRR (i.e. 7.22%).

Initial setting		Optimum values		Improvement
		Predicted	Experimental	
Level	A2B1C2D1E3F3G3	A2B1C3D1E1F3G	A2B1C3D1E1F3G3	
MRR	10.4451	-	11.9	13.93%
SR	4.689	-	4.2	10.42%

Table 7. Results of Confirmatory Experiments for case-1

Initial setting		Optimum values		Improvement
		Predicted	Experimental	
Level	A2B1C2D1E3F3G3	A2B1C3D1E1F3G	A2B1C2D1E1F3G3	
MRR	10.4451	-	11.2	7.22%
SR	4.689	-	4.1	12.56%

Table 8. Results of Confirmatory Experiments for case-2

6. CONCLUSION

In this work, an attempt was made to employ MRSN ratio technique for determining the optimal combinations of an input parameter for the best cutting performance. MRSN technique is an effective tool

which is simple and reliable. As from industrial need two cases were taken i.e. high cutting efficiency (high MRR), high surface finish (high SR) A2B1C3D1E1F3G3, A2B1C2D1E1F3G3 are recommended as the optimum factor combination for case 1, case 2 respectively. The results show the improvement in MRR as13.93%, 7.22% in case 1 whereas in SR results shows the improvement with 10.42%, 12.56% respectively.

7. REFERENCES

[1] Aytekin, H.,Akcin, Y.: *Characterization of borided Incoloy 825 alloy*. Materials and Design, Vol. 50,p.p 515–521, 2013.

[2] Ezugwu,O.E.: *Key improvements in the machining of difficult-to-cut aerospace super alloys*. International Journal of Machine Tools & Manufacture, Vol.45, 1353–1367, 2005.

[3] Kumar, Anil Maheshwari, S. Sharma, C., Beri, N.: *A Study of Multi-objective Parametric Optimization of Silicon Abrasive Mixed Electrical Discharge Machining of Tool Steel*, Materials and Manufacturing Processes, Vol. 25,p.p 1041–1047,2010.

[4] Chakravorty, Rina, Gauri, Kumar S., Chakraborty , S.: *Optimisation of the correlated responses of EDM process using modified principal component analysis-based utility theory*, International Journal of Manufacturing Technology and Management, Vol. 26 p.p 21 – 38, 2012.

[5] Masoud Azadi Moghaddam,Farhad Kolahan, An optimized back-propagation approach and simulated annealing algorithm towards optimization of EDM process parameters, International journal of Manufacturing research,vol.10,issue3,pp.215-236,2015.

[6] Ramakrishnan,R and Karunamoorthy,L.: *Modeling and multi-response optimization of Inconel 718 on machining of CNC WEDM process* ,Journal of material processing technology,Vol. 207, 343-349, 2008.

[7] Ramakrishnan,R and Karunamoorthy,L.: *Multi-response optimization of wire EDM operations using robust design of experiments*, International journal of advanced manufacturing technology, Vol 29,issue 1,pp105-112,2006.

[8] Bharti, S. P., Maheshwari, S. Sharma, C.: *Multi-Objective Optimization of Die-Sinking Electric Discharge Machining, Applied Mechanics and Materials* ,Vol.110-116, pp. 1817-1824, 2012.

[9] Bharti, S. P., Maheshwari, S. Sharma, C.: *Multi-objective optimization of Electrical discharge machining for 718*, International Journal of Mechanical, Aerospace, Industrial, Mechatronic and Manufacturing Engineering Vol.10, No.7, 2016.

Authors:

Himanshu Payal[1], Research Scholar ,

[1]M.P.A.E. Division, Netaji Subhas Institute of Technology, New Delhi, India., **Prof.Dr. Sachin Maheshwari[1], Dr. Pushpendra Singh Bharti[2], Associate Professor,** [2]U.S.I.C.T.,Guru Gobind Singh Indraprastha university, New Delhi, India.

E-mail: himanshupayal@rediffmail.com
ssaacchhiinn@gmail.com
psbharti@rediffmail.com

Journal of Production Engineering
Vol.19 No.2
JPE (2016) Vol.19 (2) Original Scientific Paper
Sharma, S.K., Maheshwari, S.

EFFECT OF SUBMERGED ARC WELDING PROCESS PARAMETERS ON WELD COOLING TIME

Received: 28 October 2016 / Accepted: 30 November 2016

Abstract: *Cooling time of welding is a function of heat input and preheating temperature. In high heat input processes like submerged arc welding (SAW) for high strength materials which need preheating, it becomes more important to control cooling time of weld for desired properties in weld microstructure. This paper explores the relationship of cooling time of weld with SAW process parameters which decide its heat input and preheating temperature. Outcomes of this experimental investigation will help in better understanding and control of the welding process for desired results.*
Key words: *Cooling time, submerged arc welding, heat input, preheating temperature.*

Uticaj parametara procesa podvodnog ručnog elektro lučnog zavarivanja na vreme hlađenja zavara. *Vreme hlađenja zavarenog šava je funkcija unosa toplote i temperature predgrevanja. U procesima unosa velike količine toplote, kao što je podvodno ručno elektro lučno zavarivanje materijala visoke čvrstoće, postaje sve relevantnije kontrolisati vreme hlađenja zavara u cilju dobijanja željenih osobina mikrostrukture šava. U ovom radu je istraživana veza između vremena hlađenja šava i parametara procesa podvodnog ručnog elektrolučnog zavarivanja koja određuje unos toplote i temperature predgrevanja. Rezultat ovog eksperimentalnog istraživanja će doprineti boljem razumevanju i kontroli procesa zavarivanja u cilju dobijanja traženih rezultata.*
Ključne reči: *vreme hlađenja, podvodno ručno elektro lučno zavarivanje, unos toplote, temperature predgrevanja*

1. INTRODUCTION

SAW is popular for its high deposition welding rate [1]. Its field of application includes fabrication of pressure vessels, pipes and pipelines and ship building [2]. The welded components in all these applications are subjected to various critical conditions of working environment. Also, in every welding process, microstructure in weld metal as well as HAZ of joint is decided by the amount of heat input given during welding operation [3]. Further, HAZ is the critical part because of its higher susceptibility towards embrittlement or weld cracking [4]. This happens because of the microstructural changes occurring in HAZ due to thermal cycles of welding. In some materials like high strength steels and high carbon steels, preheating temperature is also given to the material to give more time for gases like hydrogen to diffuse out [5]. Hence, microstructure of welding depends upon the time taken by it to cool down from weld temperature to normal temperature. Cooling time of welding is a function of heat input and preheating temperature. In case of steel, most of microstructure changes occur between 800ºC and 500ºC [6]. Time taken by weld for cooling from 800ºC to 500ºC is also denoted as $\Delta t_{8/5.}$ During the solidification of molten material in high strength low alloy steels, critical cooling rate should be avoided. The critical cooling rate is that rate of cooling which directly produces martensite products from austenite instead of ferrite and pearlite formation through atomic diffusion [7].

In this paper, process parameters which decide the heat input of SAW process are taken into consideration. In total five variables are changed each at five intervals in which open circuit voltage, wire feed rate, welding speed, contact tube to work distance are SAW parameters and fifth variable is preheating temperature. Experiments are designed and performed according to central composite rotatable design approach of response surface methodology. Process is modeled for cooling time of weld using regression analysis.

2. MATERIALS AND METHODS

2.1 Materials

Plates of high strength low alloy steel with dimensions 300mm x 75mm x 24mm are used for laying a bead on plate surface. Combination of electrode wire and agglomerated flux is selected according to AWS A5.23: EF3EG classification. An electrode wire of 4mm diameter was used to draw higher current from power source and hence higher metal deposition rate. Chemical composition of pipeline steel as well as electrode wire is shown in table 1 while chemistry of flux used is shown in table 2.

2.2 Machine setup

SAW is carried out using ESAB-CPRA 800 (S) machine with DC power source of constant voltage type. Open circuit voltage, wire feed rate, welding speed, and contact tube to work distance are varied as SAW parameters. A finite preheat temperature was applied uniformly to each plate using a muffle furnace. Process parameters with their values at all five levels are tabulated in table 3.

2.3 Cooling time

Heat input per unit length of the welding is determined using equation 1. Mean values for arc voltage and welding current are determined by collecting the voltage-current transient data through a data acquisition system. Value of $\Delta t_{g/5}$ is calculated using equations 2 and 3.

Element	Fe	C	Si	Mn	S	P	Ni	Cr	Mo
API X80	97.39	0.053	0.225	1.59	0.005	0.0095	0.189	0.103	0.259
Electrode wire	96.37	0.13	0.22	1.73	0.004	0.007	0.93	0.03	0.53
Element	Al	Cu	Ti	Nb	Co	V	Pb	Zr	B
API X80	0.036	0.057	0.018	0.036	<0.01	0.018	<0.01	<0.006	<0.0005
Electrode wire	0.002	0.04	-	-	-	0.01	-	-	-

Table 1. Chemical composition of base plate and consumable electrode wire

Main Constituents	$SiO_2 + TiO_2$	$CaO + MgO$	$Al_2O_3 + MnO$	CaF_2	Basicity
%age	15	40	20	25	3.1

Table 2. Chemical composition for agglomerated flux

$$Heat\ input = \eta \frac{V \times I \times 60}{N \times 1000} \quad (KJ/mm) \quad (1)$$

where η = arc efficiency (1.0 for SAW process), V = mean arc voltage (V), I = mean welding current (A), N = trolley speed (mm/min).

$$\Delta t_{g/5} = \frac{Heat\ input}{2\pi\lambda} \cdot \frac{1}{\rho} \quad (\text{sec}\,onds) \quad (2)$$

$$\frac{1}{\rho} = \frac{1}{500 - T_0} - \frac{1}{800 - T_0} \quad (3)$$

where λ = thermal conductivity (50 J/s.m.°C) and T_0 = preheat temperature in °C.

2.4 Response surface methodology

RSM is a statistical and mathematical technique generally used for the analysis and modeling of problems being influenced by many process parameters [8]. A second-order model can significantly improve the optimization process due to its surface curvature and consideration of interaction amid variables [9]. The general quadratic model used in RSM is defined as-

$$y = \beta_0 + \sum_{i=1}^{k} \beta_i x_i + \sum_{i=1}^{k} \beta_{ii} x_i^2 + \sum_{i<j} \beta_{ij} x_i x_j + \varepsilon \quad (4)$$

where y denotes the desired output response, x_i denotes the process variables, k is the number of design variables, β_i is the regression coefficient and ε denotes the noise or error observed in the response. In quadratic model, higher terms are neglected and assumed to be aliased with second order terms itself.

3. RESULTS AND DISCUSSION

3.1 ANOVA analysis

Matrix of designed experiments with combination of process parameters level value and cooling time for each experiment is shown in table 4. Results of ANOVA analysis carried out on cooling time for quadraric modelling of SAW process are presented in table 5. Model is found significant with F-value 202.54. The insignificant terms are removed from the model using backward elimination method. R-square value for the model is 99% which is an indication of model's good ability to predict the response in the range of process parameters. Predicted and adjusted R-square values are also in good agreement which is always desired for a better model. Adequate precision value of the model is sufficiently high which shows its better signal to noise ratio. Quadratic modeling for actual values of process variables is shown in equation 5.

Cooling time = -66.58 +3.365*A -0.467*B +0.91*C -0.122*D +5.026*E +0.0042*A*D +0.0141*B*C -0.00199*B*D -0.071*C*E +0.0057*D*E -0.055*A^2 -0.015*C^2 +2.09e-004*D^2 -0.182*E^2 (5)

Process Parameters	Notation	Units	Levels				
			-2	-1	0	+1	+2
Open circuit voltage	A	Volt	30	32	34	36	38
Trolley speed	B	cm/min	25	30	35	40	45
Contact tube to work distance	C	mm	24	28	32	36	40
Preheat temperature	D	°C	60	120	180	240	300
Wire feed rate	E	mm/sec	20	25	30	35	40

Table 3. Process parameters and their levels used for this study

Fig. 1(a) shows the normal probability curve for cooling time model while Fig. 1(b) compares the predicted values of cooling time by the model with actual values.

Run No.	Std No	Process Parameters in Actual values					$\Delta t_{8/5}$ (sec)	Run No.	Std No	Process Parameters in Actual values					$\Delta t_{8/5}$ (sec)
		A	B	C	D	E				A	B	C	D	E	
1	12	36	40	28	240	25	16.3	17	24	34	35	32	300	30	26.19
2	26	34	35	32	180	40	15.74	18	27	34	35	32	180	30	14.35
3	28	34	35	32	180	30	14.5	19	15	32	40	36	240	25	14.06
4	11	32	40	28	240	35	16.71	20	2	36	30	28	120	25	12.12
5	16	36	40	36	240	35	18.15	21	23	34	35	32	60	30	8.16
6	1	32	30	28	120	35	12.9	22	6	36	30	36	120	35	10.71
7	32	34	35	32	180	30	14.35	23	13	32	30	36	240	35	20.11
8	3	32	40	28	120	25	8.36	24	22	34	35	40	180	30	13.1
9	30	34	35	32	180	30	14.37	25	7	32	40	36	120	35	8.82
10	10	36	30	28	240	35	24.37	26	9	32	30	28	240	25	19.38
11	14	36	30	36	240	25	20.86	27	29	34	35	32	180	30	14.35
12	17	30	35	32	180	30	11.54	28	5	32	30	36	120	25	10.47
13	20	34	45	32	180	30	10.25	29	25	34	35	32	180	20	11.13
14	8	36	40	36	120	25	8.67	30	21	34	35	24	180	30	13.36
15	19	34	25	32	180	30	18.09	31	18	38	35	32	180	30	15.02
16	31	34	35	32	180	30	14.35	32	4	36	40	28	120	35	10.44

Table 4. Central composite rotatable designed experiments with calculated cooling time.

Source	Sum of Squares	df	Mean Squares	F Value	p-value Prob > F	
Model	603.30	14	43.09	202.54	< 0.0001	significant
A-Voltage	13.16	1	13.16	61.84	< 0.0001	
B-Trolly Speed	84.71	1	84.71	398.16	< 0.0001	
C-CTWD	3.57	1	3.57	16.76	0.0008	
D-Preheat temp	446.43	1	446.43	2098.25	< 0.0001	
E-Wire Feed Rate	18.74	1	18.74	4179.75	< 0.0001	
AD	4.03	1	4.03	6261.25	0.0004	
BC	1.27	1	1.27	8342.75	0.0257	
BD	5.75	1	5.75	10424.24	< 0.0001	
CE	1.28	1	1.28	12505.74	0.0251	
DE	1.88	1	1.88	14587.24	0.0085	
A^2	1.44	1	1.44	6.74	0.0188	
C^2	1.60	1	1.60	7.53	0.0138	
D^2	16.76	1	16.76	78.79	< 0.0001	
E^2	0.97	1	0.97	4.58	0.0471	
Residual	3.62	17	0.21			
Pure Error	0.02	5	0.00			
Cor Total	606.92	31				
Std. Dev.	0.46			R-Square	0.99	
Mean	14.42			Adj R-Square	0.99	
C.V. %	3.20			Pred R-Square	0.97	
Press	19.53			Ad. Precision	57.22	

Table 5. ANOVA for response surface reduced quadratic model of cooling time

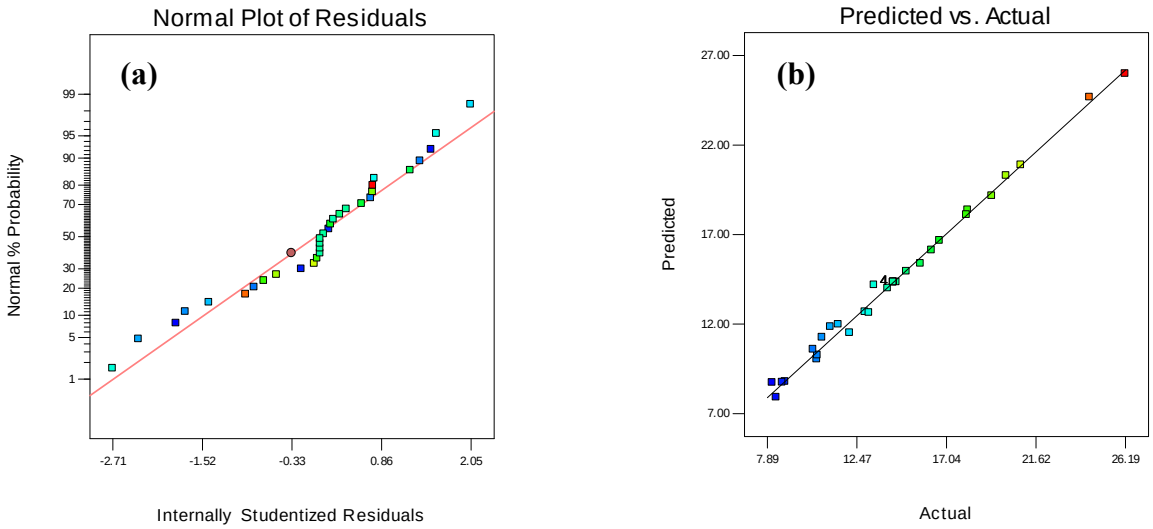

Fig. 1. Normal probability plot (a) and curve for predicted response v/s actual value (b).

3.2 Main and interaction effects

Fig. 2(a) shows the perturbation curve for main effects. Fig. 2(b-f) depicts the plots for interaction between two process variables which effects the cooling time of weld. In main effects, increase in voltage, wire feed rate and preheating temperature causes an increase in cooling time of weld. This happens because with increase of voltage and wire feed rate heat input of welding increases. As, welding current is directly proportional to wire feed rate. From equation 2, it is also clear that cooling time increases with increase of preheating temperature as it slows down the temperature gradient between two sections. However, increase in trolley speed and contact tube to work distance causes a decrease in cooling time. It can be understood as increase in trolley speed decreases the heat input to the weld joint. Similarly, with increase in contact tube to work distance welding arc widens delivering a less concentrated heat to the joint.

In the similar manner, interaction effect of any two process parameters on cooling time can be understood from the main effect of each parameter. For example, increase in preheating temperature and voltage rises the cooling time of weld and this similar pattern is visible in Fig 2(b). Similarly, in Fig. 2 (d), with the increase of preheating temperature and decrease of trolley speed, cooling time increases and it is maximum at highest level of preheating temperature and lowest level of trolley speed.

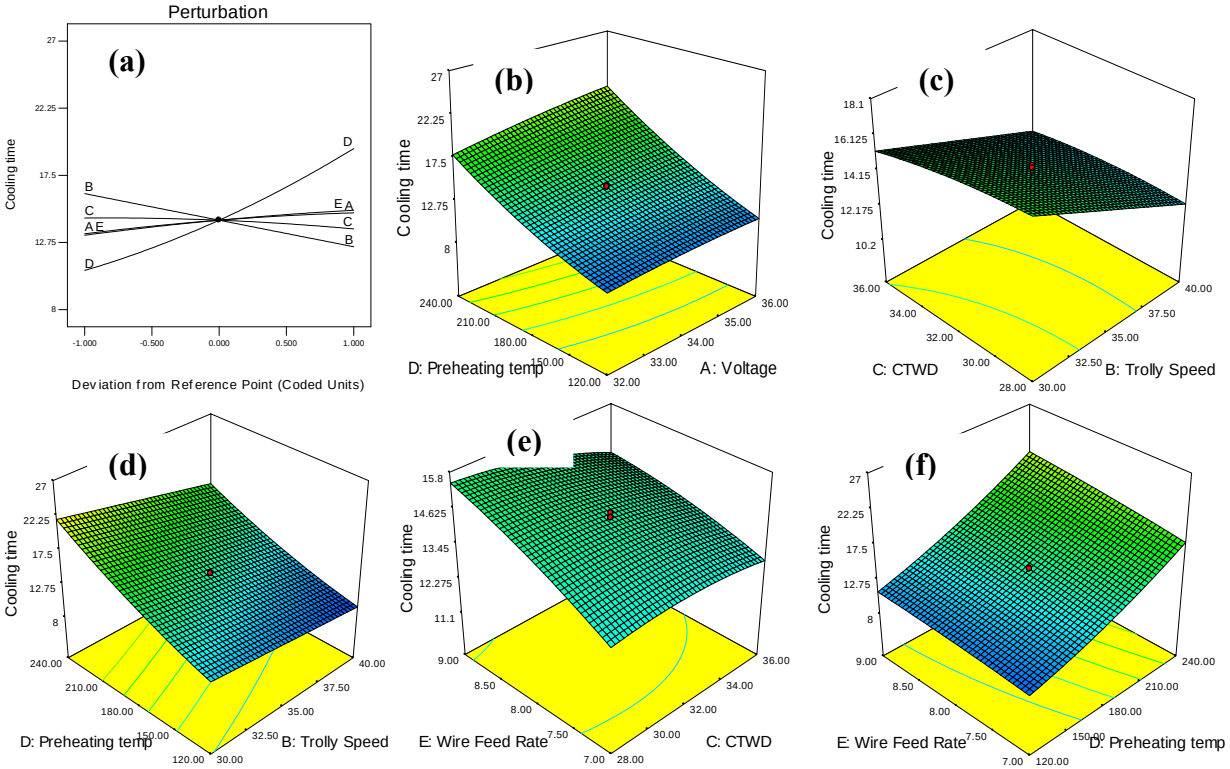

Fig. 2. 3D plots showing interaction effects between process variables for cooling time of weld.

4. CONCLUSIONS

This experimental investigation reveals the effects of SAW process parameters and preheating temperature on the cooling time of weld. Following conclusions are drawm from the study-

1. RSM can be successfully employed for the modeling of SAW process to predict the cooling time.
2. Increase in voltage, preheating temperature and wire feed rate causes an increase in cooling time of weld.
3. Increase in trolley speed and contact tube to work distance decreases the cooling time of welding process.
4. Most significant process parameters which has maximum influence on cooling time are preheating temperature and trolley speed.
5. Significant interaction effects exists between process parmaeters which affects the cooling time of weld metal.

5. REFERENCES

[1] Sharma, S.K., Maheshwari, S., Rathee, S.: *Multi-objective optimization of bead geometry for submerged arc welding of API X80 pipeline steel using RSM-fuzzy approach*, Journal of Manufacturing Science & Production, Vol. 12, p.p. 4-14, 2016.

[2] Kumar, A., Maheshwari, S., Sharma, S.K.: *Optimization of Vickers Hardness and Impact Strength of Silica based Fluxes for Submerged Arc Welding by Taguchi method,* Materials Today: Proceedings, 2, 4–5, p.p. 1092–1101, 2015.

[3] Ivanov, A.Y., Sulyagin, R. V., Orlov, V. V., Kruglova, A. A.: *Structure and Properties of Weld Joints in X80, X90, and K70 Pipe Steel,* Steel in Translation, Vol. 41, Issue 7, p.p. 611–616, 2011.

[4] Efimenko, L.A., Elagina, O.Yu., Kapustin, O.E., Vyshemirskii, E.M.: *Investigation of the weldability of high-strength pipe steels of X80 strength grade*, Welding International, Volume 24, Issue 9, p.p. 714-717, 2010.

[5] Wongpanya, P., Boellinghaus, Th., Lothongkum, G., Kannengiesser, Th.: *Effects of Preheating and Interpass Temperature on Stresses in S 1100 QL Multi-Pass Butt-Welds,* Welding in the world, Volume 52, Issue 3, p.p. 79–92, 2008.

[6] Song, S., Xu, T., Yuan, Z.:*Determination of critical time and critical cooling rate of non-equilibrium grain-boundary segregation,* Acta Metallurgica, Volume 37, Issue 1, p.p.- 319-323, 1989.

[7] Chapter 2, Fundamentals of the Heat Treating of Steel, *Practical Heat Treating, Second Edition*, ASM International. p.p.- 9-25, 2006.

[8] Montgomery, D.C.: *Design and Analysis of Experiments*, 5th Edition. John Wiley and Sons, 2005.

[9] Response Surface methodology, Chapter 3. http://www.brad.ac.uk/staff/vtoropov/burgeon/thesis_luis/chapter3.pdf (last accessed on 05-03-2016).

Authors: **Research Scholar Satish Kumar Sharma, Professor Sachin Maheshwari PhD,** Division of Manufacturing Processes and Automation Engineering, Netaji Subhas Institute of Technology, University of Delhi, New Delhi-110078, India, Phone.: +91 9996814579, Fax: +91 11 25000198.

E-mail: satishsharma847@gmail.com
ssaacchhiinn@gmail.com

Journal of Production Engineering
Vol.19 No.2
JPE (2016) Vol.19 (2) Original Scientific Paper
Khanna, P., Maheshwari, S.

EFFECT OF WELDING PARAMETERS ON WELD BEAD CHARACTERISTICS DURING MIG WELDING OF STAINLESS STEEL 409M

Received: 16 September 2016 / Accepted: 15 October 2016

Abstract: *The present trend in the fabrication industry is the use of robotics and automated welding processes to obtain high production rates and precision. To automate a welding process it is essential to establish relationship between process parameters and weld bead geometry. This will enable the prediction and control of weld bead geometry, as mechanical strength of the welds significantly depends upon the bead shape. A high quality weld can be obtained by properly adjusting the process parameters. The effect of different welding parameters therefore is needed to be determined on weld bead dimensions so that best combination of weld parameters can be selected to have a mechanically sound weld joint. Present work is an attempt to determine the effects of all these parameters on weld bead geometry. One factor at a time approach has been adopted to investigate the effect of wire feed rate, nozzle to plate distance, voltage, weld speed and gas flow rate on various weld bead aspects like weld penetration, weld bead width, reinforcement height, width to penetration ratio, width to reinforcement ratio and dilution.*
Key words: *bead geometry, weld speed, dilution.*

Uticaj parametara zavarivanja na karakteristike zavarenog šava pri MIG procesu zavarivanja nerđajućeg čelika 409M. *Današnji trend u sferi rpoizvodnje je upotreba robota i automatizovanih procesa zavarivanja radi postizanja visokih proizvodnih performansi i tačnosti. Da bi se automatizovao proces zavarivanja, neophodno je uspostavljanje veze između parametara procesa i geometrije zavarenog šava. Ovo će omogućiti predviđanje i kontrolu geometrije zavarenog šava, pošto mehanička čvrstoća zavara značajno zavisi od oblika šava. Visoko kvalitetan zavar se može postići adekvatnim podešavanjem parametara procesa. Zbog toga je potrebno odrediti efekat različitih parametara zavarivanja na dimenzije šava tako da bi se odabrala najbolja kombinacija parametara procesa radi dobijanja mehanički adekvatnog zavarenog spoja. Predstavljeni rad je pokušaj određivanja efekta svih ovih parametara na geometriju zavarenog šava. Prihvaćen je metod variranja jednog parametra ponaosob da bi se ispitao efekat brzine dodavanja žice, rastojanje šobe od ploče, brzina zavarivanja i protok gasa na različite osobine šava kao što je provar, širina šava, visina nadvišenja, odnos širine i provara, odnos nadvišenja i širine i odnos mešanja.*
Ključne reči: *geometrija šava, brzina zavarivanja, rastop*

1. INTRODUCTION

Today MIG welding has become one of the more flexible all-round welding tools in the fabrication industry [1]. This process is capable to weld all metals for which electrode wires are available [2]. The MIG semi and fully automatic versions are increasing in use and are displacing traditional oxy acetylene and SMAW processes because of reduced heat input and narrower HAZ [3]. Automatic MIG welding heads have revolutionized the fabrication industry and with the inclusion of programmable robotics, a fully automated MIG welding system makes fewer demands on the skilled labor along with consistently good quality welds at high production rates. As mechanical strength of welds is influenced not only by the composition of the weld metal but also by the weld bead shape, it is therefore essential to precisely select the process variables to have adequate control on weld bead shape in automated welding applications. To attain this, precise relationship between the process parameters and the bead parameters, as shown in Fig. 1, controlling the bead shape is to be established [4-6]. In the present case bead on plate technique is used for laying the weld beads with one process variable varied at a time for a number of tests while the remaining were kept constant.

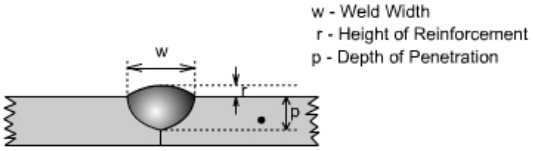

Fig. 1. Weld bead geometry

2. EXPERIMENTAL PROCEDURE

The welding was carried out on (250 mm x 150 mm x 6 mm) plates of stainless steel 409M using a setup shown in Fig. 2. The test pieces were cut from each weldment using a band saw machine and prepared by the usual metallurgical polishing procedure for macrographic investigation. The various bead parameters were measured by using a profile projector with reflecting shadowgraph technique and the observed data were utilized to present the investigation in graphical forms in Figs. 3-8. In these figures, the welding parameters are plotted on X-axis and the weld bead shape parameters on Y-axis to enable comparison of different variable's effect on bead shape parameters.

3. PLAN OF INVESTIGATION

To study the effect of welding variables on the bead geometry, investigations were carried out in the following steps:

(i) Identifying independent welding variables affecting the weld bead geometry.
(ii) Determining the useful limits of these variables.
(iii) Conducting the experiments
(iv) Recording the test observations.
(v) Graphical representation of the results.
(vi) Analysis and discussion of results.
(vii) Conclusions

Fig. 2. The experimental setup

3.1 Identifying the welding variables

Based on already existing studies [7], ease of independent control and their effect on bead geometry, six independently controllable parameters were identified namely, the wire feed rate (I), the welding speed (S), the arc voltage (V), the nozzle to plate distance (N), the electrode to work angle (θ) and the gas flow rate (G).

3.2 Selection of the useful limits of welding variables

The useful limits of the six welding variables were determined by conducting large number of trial runs. The qualifying criteria were based on the following factors [6]:

a. Stable arc
b. Spatter free welding
c. Defect free welds based on visual inspection

Based on these considerations the limits of different variables arrived at are as shown in table- 1.

Welding variables	units	symbol	Low level	High level
Wire feed rate	m/mm	I	2.8	10.8
Welding speed	cm/min	S	25	50
Arc voltage	Volts	V	22	30
Nozzle to plate distance	mm	N	10	20
Electrode to work angle	Degrees	θ	75	105
Gas flow rate	l/min	G	05	25

Table 1. limits of different welding variables.

3.3 Conducting the experiments and recording the observations

KH-400, MIG welding machine was used with flat characteristics, to conduct the experiments within the limits of variables by varying one variable at a time while keeping the others constant and repeating the same for every variable. The standard bead on plate technique was applied to lay beads lengthwise at the centre of each plate. From the middle of each plate two specimen each were cut out and were polished as per the standard metallurgical procedure and etched using an etchant (FeCl3 + HCl +H2O). The weld bead profiles were traced out at a magnification of 10X using a profile projector. The bead dimensions were noted directly from the profile projector while the bead area was calculated using a planimeter.

3.4 Graphical representation of the observations

The results obtained have been plotted graphically in Figures 3-8 to investigate the effects of different welding variables on bead geometry parameters. For the ease of understanding and meticulous study of the effects of different welding parameters on weld bead profile, the former are plotted on X- axis while the bead geometry parameters are plotted on Y-axis. This enables to study the effects of all the welding variables on each one of bead geometry parameter simultaneously. In this way, six graphs have been plotted through Figs 3-8.

3.5 Analysis and discussion of results

From the results shown in Figures 3-8, it is evident that the shape and size of the weld bead and its various geometrical ratios are influenced by different welding variables. The influence of each of these factors in the light of the results obtained are analyzed and discussed as follows;

3.5.1 Influence on weld penetration

The weld penetration increased from 1.2 mm to 2.6 mm with increase of wire feed rate. this can be attributed to increased welding current with increase in wire feed rate, that increases the arc force and heat input causing larger volume of base metal to melt and hence increased penetration.

Weld penetration increases from 1.9 mm to 2.2 mm with increase in arc voltage. This may be attributed due to the increase in heat input resulting from the rise in welding current with the rise of voltage. Weld penetration decreased from 2.3 mm to 1.7 mm with the increase in welding speed. This can obviously be attributed to reduced heat input per unit length of the weld, reducing the melting of base metal, as speed increases. Weld penetration reduces from 2.6 mm to 2.2 mm with increase in nozzle to plate distance (NPD). The reason may be with the increase in NPD the electrode extension increases that raise the circuit resistance which results in drop in current as the voltage remains the same. Weld penetration decreases slightly from 2.2 mm to 2.1 mm with the increase in electrode to work angle. This can be attributed due to decrease in heat input while changing from backhand through vertical to forehand position, as in backhand

position the arc keeps the pool molten for a longer time hence more penetration. The gas flow rate seems to have no effect on weld penetration.

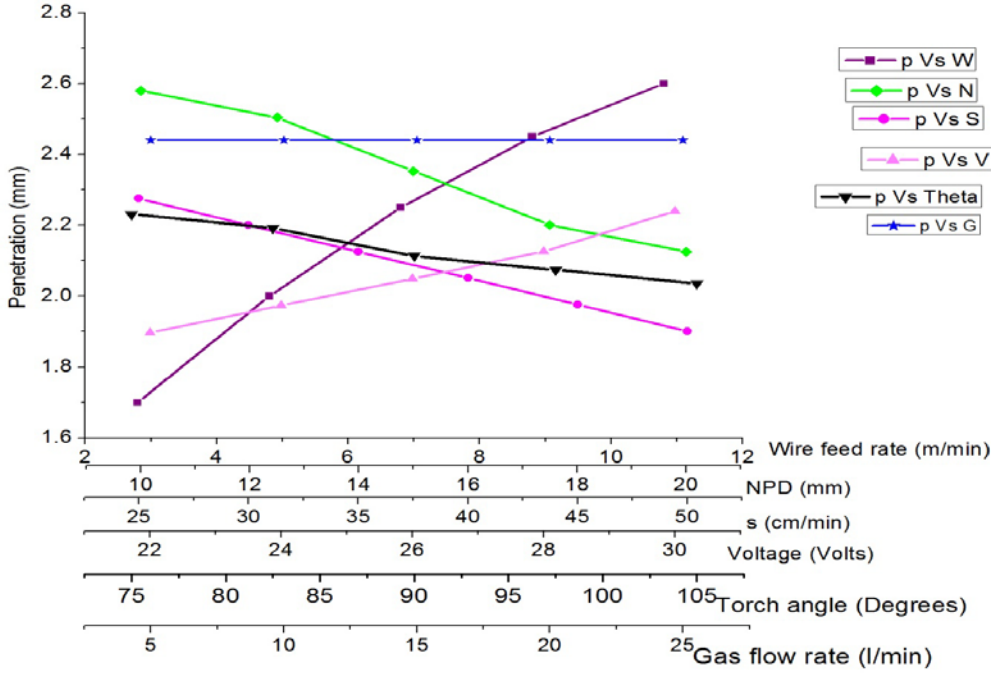

Fig. 3. Effect of welding parameters on penetration

3.5.2 Influence on reinforcement height

The reinforcement height increased from 2.7 mm to 3.9 mm with increase of wire feed rate. This can be attributed to increased volume of metal deposited per unit length of the weld.

The reinforcement height decreases from 3.6mm to 3.0mm with increase in arc voltage. This may be attributed to the increased width of the melted zone at the expense of height. Reinforcement decreased from 3.8 mm to 2.7 mm with the increase in welding speed. This can obviously be attributed to reduced heat input per unit length of the weld, reducing the amount of metal deposited. Reinforcement increased from 3.0 mm to 3.4 mm with increase in NPD. As with the increase in NPD the electrode extension increases that raise the I^2R heating causing more wire to melt before the arc formation, resulting in more metal deposition rates. Reinforcement decreases slightly from 3.6 mm to 3.3 mm with the increase in electrode to work angle. This is because in forehand position, the arc force is directed ahead of the pool and has a tendency to widen the bead, thereby reducing the reinforcement. The gas flow rate seems to have no effect on reinforcement.

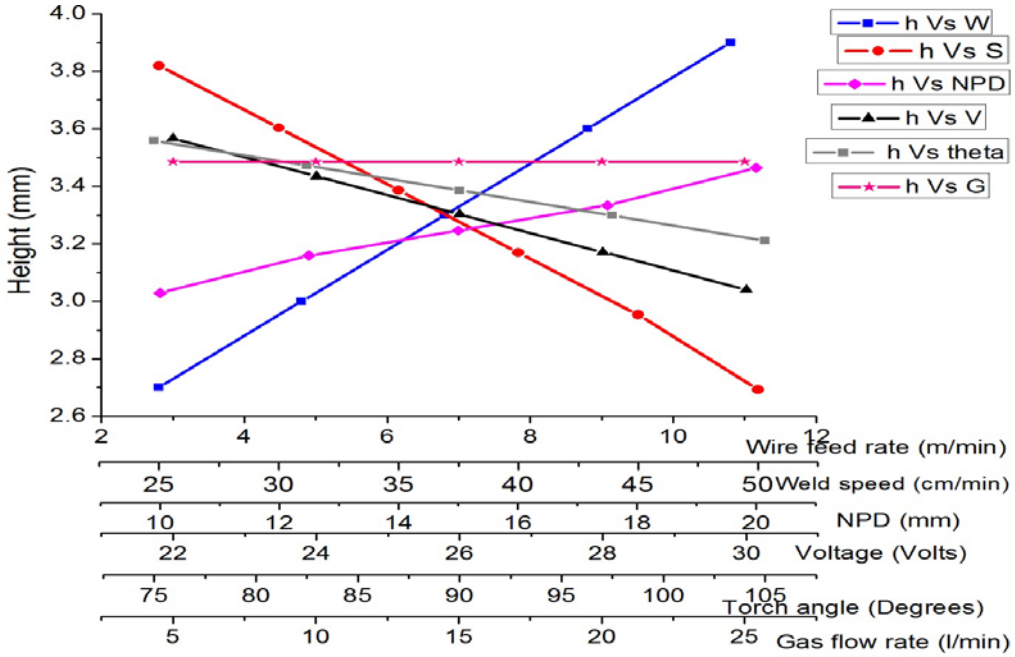

Fig. 4. Effect of welding parameters on reinforcement height

3.5.3 Influence on weld bead width

The weld bead width increased from 7.5 mm to 10.0 mm with increase of wire feed rate. This is because the higher amount of weld metal deposited due to increased current associated with wire feed rate. Width increases from 8.7 mm to 12.0 mm with increase in arc voltage. This is because at higher voltage, the arc spreads at its base thereby widening the bead. Weld width decreased from 11.5 mm to 9.0 mm with the increase in welding speed. This can obviously be attributed to reduced heat input and less filler metal is applied per unit length as speed increases resulting in a thinner and narrower bead. Weld width increases from 10.5 mm to 11.7 mm with increase in NPD. The reason may be with the increase in NPD, the spread of arc at its base increases, resulting in wider bead. Weld width increases slightly from 10.3 mm to 10.7 mm with the increase in electrode to work angle. This is because in forehand position, the arc force is directed ahead of the pool and has a tendency to widen the bead, thereby increasing the width. The gas flow rate seems to have no effect on weld width.

3.5.4 Influence on weld penetration shape factor (WPSF)

The WPSF is the ratio of weld bead width to weld penetration. It decreased from 4.5mm to 3.9mm with increase of wire feed rate. Though the penetration and width both increase with wire feed rate but the proportion of increase in penetration is more than width, therefore this decrease is observed. WPSF increases from 5.2 mm to 5.8 mm with increase in arc voltage. This is because with the increase in voltage, the proportional increase in weld width is more than that of penetration. WPSF increases with increase in welding speed, from 5.4 to 5.5 and NPD, from 4.2 mm to 6.1 mm, indicating predominance of width increase over penetration. WPSF increases from 5.2 mm to 6. 2 mm with the increase in electrode to work angle. This is because the increase in torch angle is accompanied with increase in width and decrease in penetration. The gas flow rate seems to have no effect on WPSF.

3.5.5 Influence on weld reinforcement form factor (WRFF)

The WRFF is the ratio of weld bead width to the weld reinforcement. It decreases from 2.85 mm to 2.6 mm with the increase in wire feed rate. The reason could be that with increase in wire feed rate the increase in reinforcement is more predominant over increase in width. WRFF increased from 2.3 mm to 4.1 mm with the increase in arc voltage. This is due the arc spreading effect at higher voltage that tends to flatten the bead. This sharply increases the width but reduces the reinforcement thereby increasing the WRFF. Increase in welding speed increased the WRFF from 3.0 mm to 3.5 mm because increase in width was more as compared to reinforcement height. WRFF decreased from 3.6 mm to 3.4 mm with the increase in NPD. This is because the percentage increase in reinforcement is more than that of width with the increase of NPD. With the increase in torch angle, the WRFF increases from 2.9 mm to 3.5 mm. This is because the bead width increases while reinforcement decreases with the increase in torch angle. The gas flow rate seems to have no effect on WRFF.

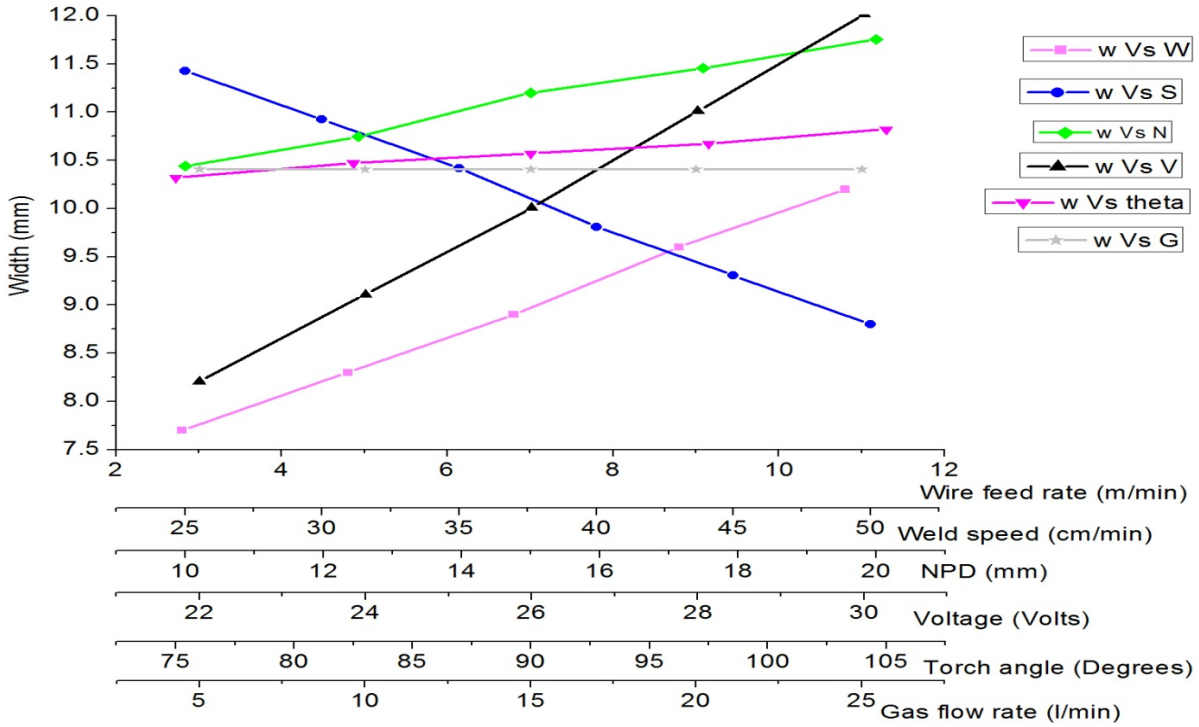

Fig. 5. Effect of welding parameters on weld bead width

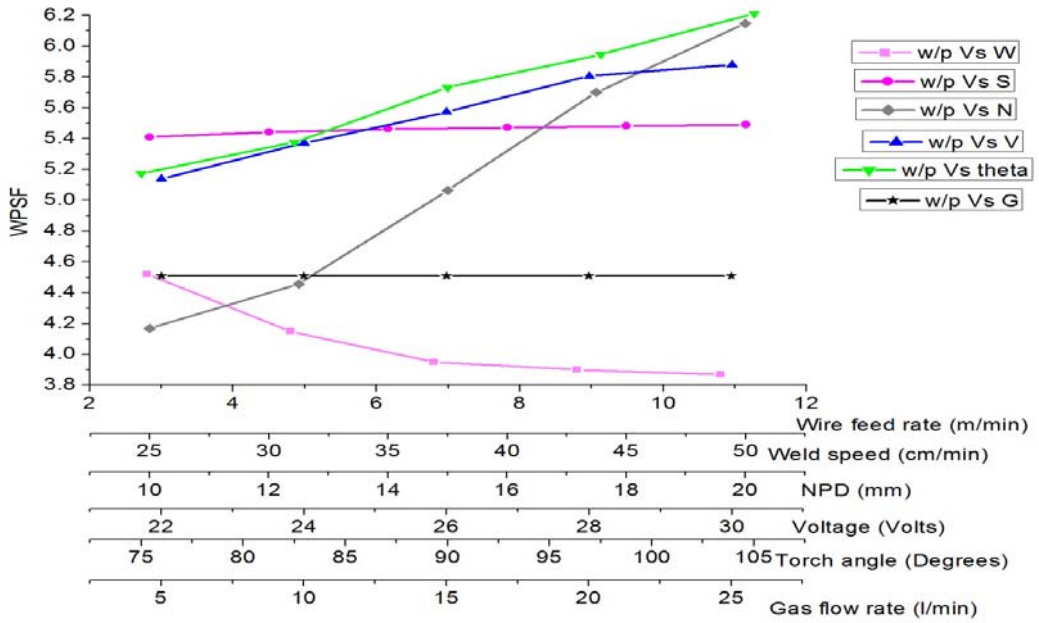

Fig. 6. Effect of welding parameters on WPSF

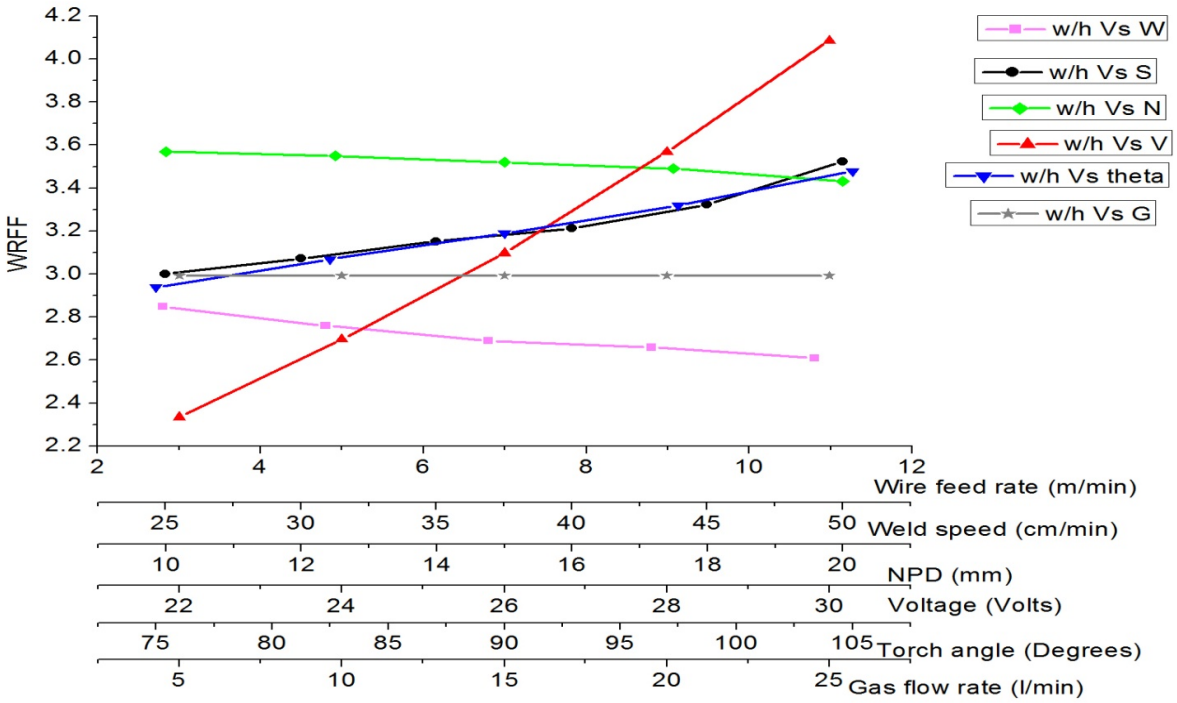

Fig. 7. Effect of welding parameters on WRFF

3.5.6 Influence on Dilution

It is the ratio of the area of base metal melted to the cross sectional area of bead. It increases from 35% to 55% with the increase in wire feed rate. The reason is the increase in area of base metal melted due to increase in welding current was more than the metal deposited. Increase in voltage has increased the dilution from 28% to 53%. The reason could be attributed to the increase in available energy which is the product of voltage and current, as voltage increases, it causes melting of more base metal and therefore dilution increases. With the increase in welding speed, the dilution reduces from 64% to 40%. The percentage increase was more in the area of weld metal deposited as compared to the base metal melted and therefore a decrease in dilution. Dilution increases slightly from 48% to 58% with the increase of NPD. It is evident that the welding current increases with the increase in NPD (6), thereby resulting in more area of base metal melted than that of deposited. Dilution reduces from 55% to 43% with the increase in electrode to work angle. As already discussed, with the increase in torch angle the amount of parent metal melted reduces, resulting in the reduction in dilution. Gas flow rate as expected has no effect on dilution within the selected range of flow rates.

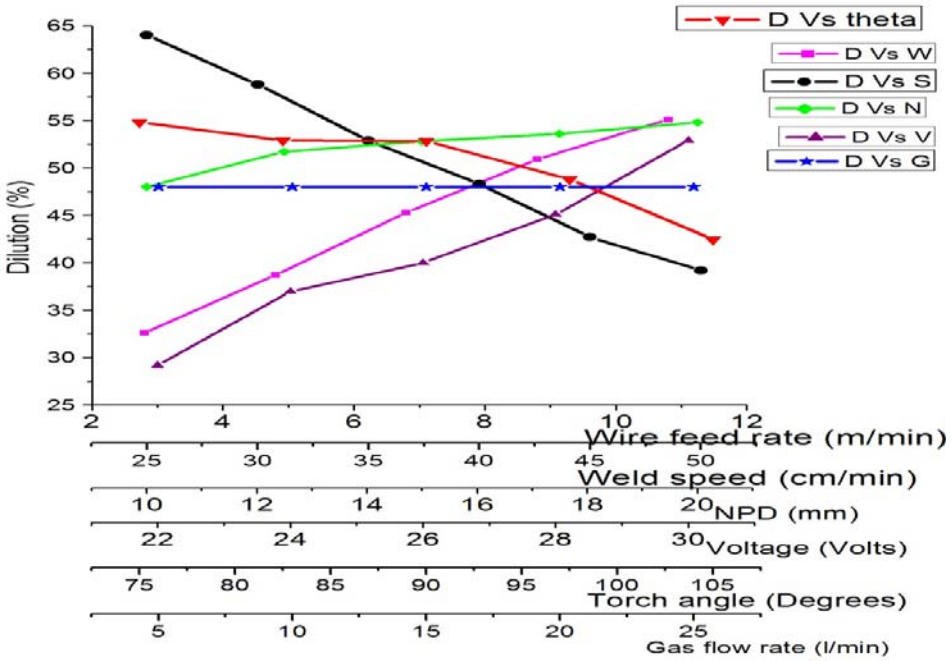

Fig. 8. Effect of welding parameters on Dilution

4. CONCLUSIONS

The following conclusions were arrived at from the results of this experiment:

1. The penetration increased with increase in wire feed rate and voltage whereas it decreased with increase in nozzle to plate distance, welding speed and torch angle.
2. The reinforcement height increased with increase in wire feed rate and nozzle to plate distance, whereas it decreased with increase in voltage, welding speed and torch angle.
3. The weld bead width increased with increase in wire feed rate, voltage, nozzle to plate distance and torch angle, whereas it decreased with increase in welding speed.
4. WPSF increased with increase in voltage, welding speed, nozzle to plate distance and torch angle, whereas it decreased with increase in wire feed rate.
5. WRFF increased with increase in voltage, torch angle and welding speed, whereas it decreased with increase in nozzle to plate distance and wire feed rate.
6. Dilution increased with increase in wire feed rate, voltage and nozzle to plate distance, whereas it decreased with increase in torch angle and welding speed.

There seems no effect of gas flow rate on any of the weld bead parameter, though at low flow rates the weld bead quality appeared to be poor because of decreased shielding effect.

5. REFERENCES

[1] Bohnart, Edward R., Welding Principles and Practices, 4th edition, McGraw Hill Education (India) Private Ltd. New Delhi, 2014

[2] Parmar, R. S, Welding Processes and Technology, third edition, Khanna Publishers, New Delhi, 2010.

[3] Davies, A.C., Welding, 10th edition, Cambridge University Press, Chennai, 2005.

[4] Murugan, N., and Gunaraj, V. Prediction and control of weld bead geometry and shape relationships in submerged arc welding of pipes. Journal of material Processing Technology, 168(2005), pp.478-484.

[5] Mandal, A. and Parmar, R.S., International Journal for the Joining of Materials, 8(2), pp 1-7, 1996.

[6] Khanna,P and Maheshwari, S., "Effects of wire feed rate, voltage and nozzle to plate distance on welding current in a MIG welding process". Proceedings of the Vth International Symposium on Fusion of Science and Technology (ISFT-2016), New Delhi, pp. 305-310, January 18-22, 2016.

[7] Pandey, S., Ph.D. thesis on "Some studies on MIG welding of Aluminum and its alloy 5083". Department of Mechanical Engineering, Indian Institute of Technology, Delhi, India, 1986.

Authors: **Pradeep Khanna, Associate Prof., Prof. Sachin Maheshwari, Ph.D**., Division of MPAE, Netaji Subhas Institute of Technology, New Delhi-110078, India.

Email: 4.khanna@gmail.com
ssaacchhiinn@gmail.com

Journal of Production Engineering
Vol.19 No.2
JPE (2016) Vol.19 (2) Original Scientific Paper
Ambedkar, B. R., Naidu, G. S., Lalitha, V.S.S., Krishna, D. M.

MICROSTRUCTURAL AND MECHANICAL PROPERTIES OF ALUMINIUM AND MAGNESIUM BIMETAL EXTRUDED COMPOSITE

Received: 23 June 2016 / Accepted: 10 September 2016

Abstract: *The purpose of this paper is to investigate the microstructural and mechanical behaviour of aluminium-magnesium (Al-Mg) bimetal extruded composite. Bimetal Extrusion is a process of simultaneously extruding two or more materials to form a single entity. A new bimetal (Al/Mg)composite containing Mg reinforcement is made through hot extrusion process. The metallurgical bond between the materials gave rise to a fully integrated and void free interface. Mg ribbons are inserted in the holes drilled in Al rod. The sample thus made is extruded at 300°C. Characterization studies of the composite revealed that there is an appropriate bonding of the matrix and reinforcement resulting in a fine grain morphology. Hardness, wear and compression tests results are presented in this paper.*

Key words: *Bimetal Extrusion, Aluminium, Magnesium, Interface-Bonding, Hardness*

Mikrostrukturne i mehaničke osobine ekstrudiranog aluminijum-magnezijum bimetalnog kompozita. *Cilj ovog rada je da ispita mikrostrukturno i mehaničko ponašanje aluminijum-magnezijum (Al-Mg) ekstrudiranog bimetalnog kompozita. Bimetalna ekstruzia je proces istovremene ekstruzije dva ili više materijala u cilju formiranja jednog entiteta. Novi bimetalni kompozit (Al/Mg) sadrži Mg ojačanja i dobijen je putem tople ekstruzije. Metalurška veza između materijala je omogućila kompaktnu i besprekidnu vezu. Mg trake su umetnute u rupe izbušene u Al šipki. Uzorak napravljen ovakvim postupkom je ekstrudiran na 300°C. Studija karakteristika kompozita je otkrila da postoji odgovarajuća veza matrice i ojačanja što rezultira finom morfologijom zrna. Rezultati ispitivanja tvrdoće, habanja i testova sabijanja su prikazani u ovom radu.*

Ključne reči: *Ekstruzija bimetala, aluminijum, magnezijum, spajanje, tvrdoća*

1. INTRODUCTION

Aluminium is the most popular metal matrix used in the fabrication of MMCs. AMCs has a wide range of applications in aerospace industry, automotive industries, in the high speed machinery, electronic packing and defence field. A composite can be said to have distinctive properties that are not obtained from any single component [2-5].Some of the major additions to aluminium include Silicon, magnesium, manganese and so on. Addition of small amounts of Magnesium enhances the properties of Aluminium.Magnesium is lighter than aluminium and is less ductile due to its hexagonal close packed crystal structure. Mg has a lower modulus of elasticity (40–45 GPa) than Al (69.6 GPa) [1]. It also has fatigue resistance and high temperature-creep resistance.A composite can be said to have distinctive properties that are not obtained from any single component [2-5].Addition of small amounts of Magnesium enhances the properties of Aluminium.

Literature studies shows that addition of Al in Mg can lead to enhanced toughness by mechanical interlocking mechanism[6]. It is also observed that rolling magnesium and aluminium to 50% reduction at 400°C followed by ARB (Accumulative Roll Bonding) resulted in the formation of $Mg_{17}Al_{12}$ and Al_3Mg_2 intermetallics[7]. Also, screw extrusion was used for producing a bimetal composite Al/Mg from granules containing aluminium alloy 6063 (AA6063) and commercial pure magnesium. The rate of growths of intermetallic compounds in different ways was found out [8]. The bimetal interface has high hardness [9-11], non-uniform deformation being adapted by the softer metal at the interface based on chemical and mechanical interactions [12,13].

2. METHODOLOGY

Sample preparation for extrusion:

An aluminium slab of 50mm diameter and 30mm height is taken and holes are drilled randomly into which magnesium ribbons are inserted. The sample is then heated in a muffle furnace above the recrystallization temperature (350^0C) and is subjected to hot extrusion at 300^0C in an extrusion.

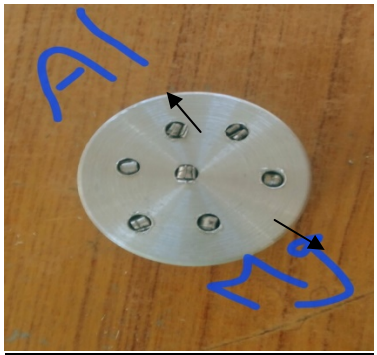

Fig. 1. Specimen before extrusion

The experiments were conducted at temperatures in the extrusion chamber high enough for generating satisfactory friction between the parts in the extruder set-up and the input materials, but at the same time low enough to avoid local melting.

2.1. Mechanical characterization:

To check the hardness profile of the extrusion product, Samples were put under Rockwell hardness testing apparatus. For Aluminium samples, $1/16^{th}$ inch diameter steel ball is used as indenter. The depth of indentation calculated, gives the Rockwell Hardness Number on B-scale.

Also, the sample hardness is examined under Vicker's hardness testing apparatus. The sample is mounted on the platform. Loading time and Load are preset as requires. Basing on the load applied, the area of indentation varies. Thus, the area of indentation gives the Vickers Hardness Number ((VHN).

Wear and compression tests were also conducted for the extruded specimens. The wear test is conducted using a pin-on-disc apparatus with 20KN and 30KN loads. The compression test is conducted using hydraulic compression testing equipment.

2.2. Microstructural analysis:

The extruded Al-Mg composite is machined to a cylinder of 20mm diameter and 30mm height. It is then polished with SiC abrasive papers of various grades. To give a scratch free surface, it is finally polished using a disc polishing machine and etched with Keller's reagent (HNO_3 5ml, HCl 3ml, HF 2ml and 190ml distilled water). The sample surface thus obtained is observed under an optical microscope.

For further information regarding the grain morphology, the sample is subjected to SEM and XRD studies.

3. RESULTS&DISCUSSIONS

3.1. Microstructure:

In order to observe the surface features, the extruded composite is observed under an optical microscope.

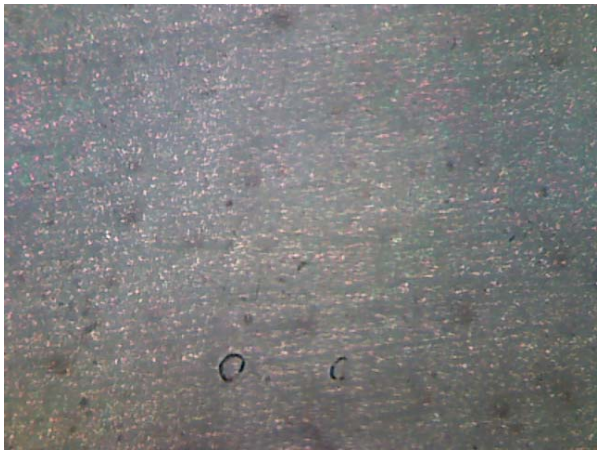

Fig. 2. Al-Mg composite at a magnification of 100X under optical microscope

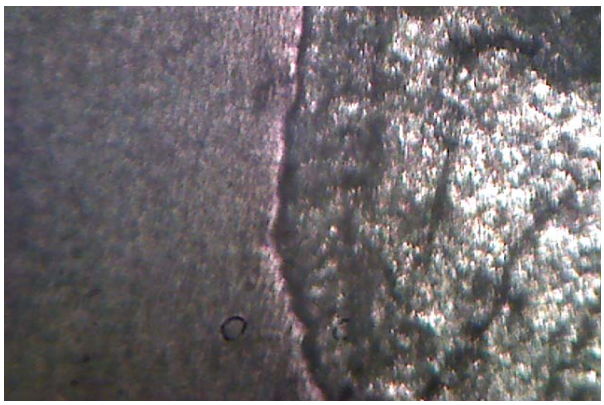

Fig. 3. Al-Mg composite at a magnification of 100X under optical microscope

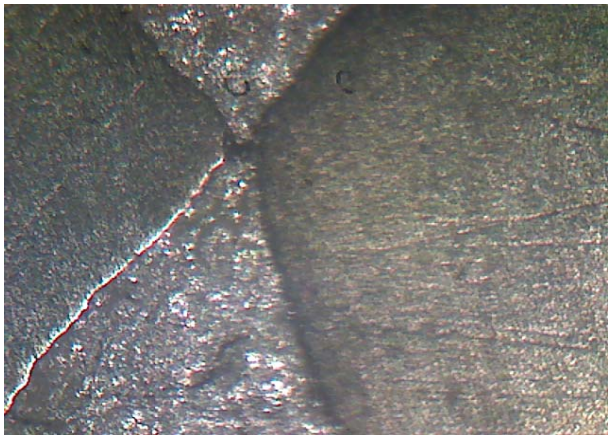

Fig. 4. Optical microscope Microstructures at a magnification of 450X

3.2 Discussion on optical microscope image results:

The composite of aluminium containing 2.5% magnesium when viewed under optical microscope at a magnification of 10X is as shown above in fig... from the figure, it is evident that there is an even distribution of magnesium in the extruded composite giving rise to a uniform structure. At a higher magnification of 450X, the microstructures observed indicates the presence of very fine grains in the extruded composite. This implies that there should be an increase in the hardness of the composite due to the presence of fine grains after extrusion, which is observed in the hardness profile in the previous section.

3.3 Scanning Electron Microscope (SEM)images:

The surface of sample containing 6.75% magnesium, as revealed by the plan-view SEM images, is smooth). In thiscase, very small particles are observed throughout the surface.

3.4 Discussion on SEM image results:

The surface of sample containing 6.75% magnesium, as revealed by the plan-view SEM images, is smooth. In thiscase, very small particles are observed throughout the surface. At a higher resolution of 20μm, the surface is relatively smooth and there is an even distribution of magnesium particles in angular form in aluminium matrix.The sample surface when viewed at various magnifications is illustrated in the following figure. Lower magnifications indicate the presence of

finely dispersed magnesium particles. At higher magnifications, the particles appear to be spherical and evenly distributed.

3.5 Chemical composition and XRD analysis:

By mixing the constituents at elevated temperatures through extrusion,intermetallic phases can be formed through diffusion. Anoverview of the relevant phases is included in the figure. From the intensity vs. diffraction angle graph, it is evident that the aluminium is the matrix in which magnesium particles are reinforced. Also, the intermetallic phase formed by magnesium with aluminium matrix is rich in $Al_{5.15}Mg_{3.15}$phase. The Al_2O_3phase formed is due to the reaction of aluminium with oxygen in the environment.

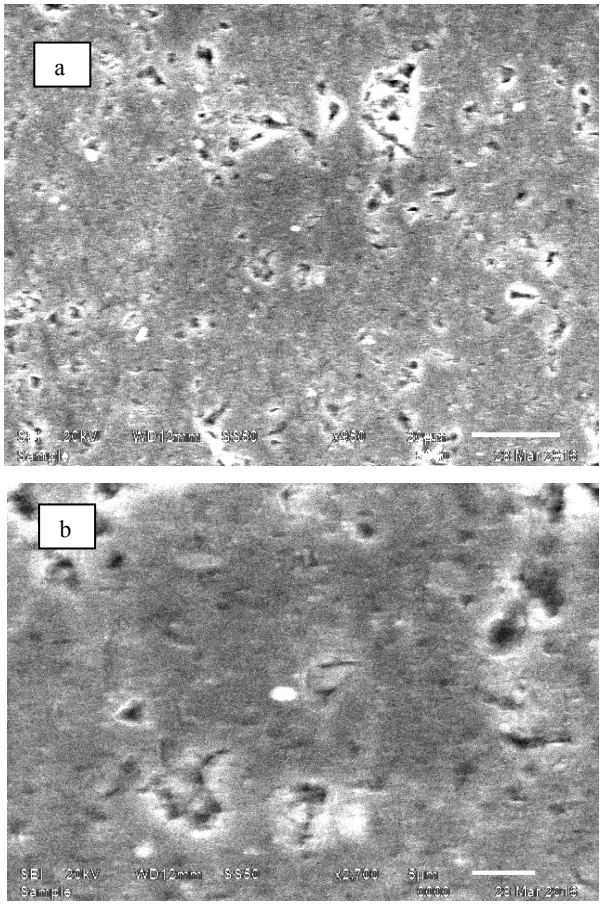

Fig. 5. SEM images at a resolution of a)20µm and b)20 µm

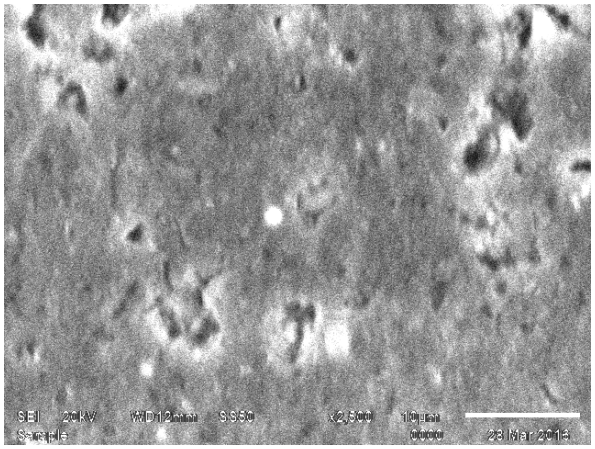

Fig. 6. SEM images at a resolution of 10 µm and 20 µm

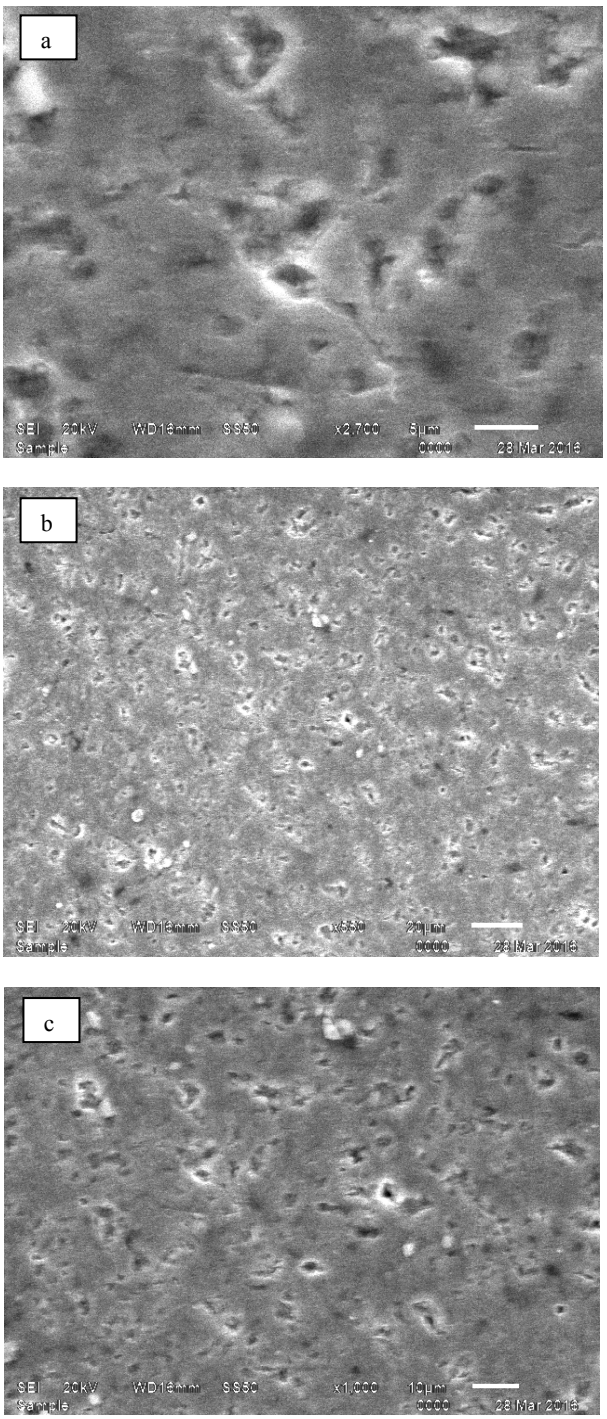

Fig. 7. SEM images at magnifications of (a) 270x, (b) 550x and (c) 1000x

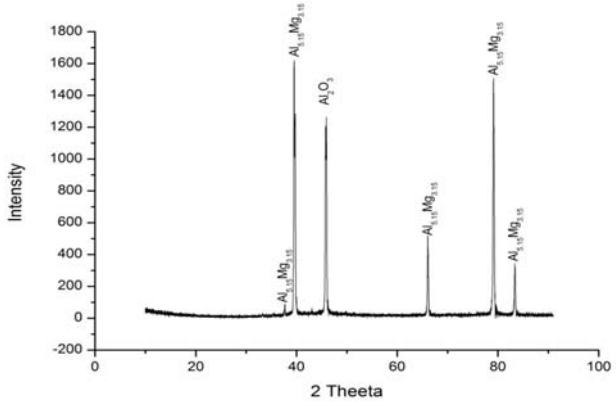

Fig. 8. Intensity versus 2θ graph

3.6 Mechanical properties and Wear Analysis :

Al-2.5% Mg composite is subjected to Rockwell hardness test to find out the overall hardness of composite before and after extrusion. The test is conducted at a load of 60Kg and the results indicate a 34% increase in the hardness of composite. Also, Vickers hardness test of the same indicated an 80.7% increase in the hardness of the composite when compared to parent metal (aluminium). Thus addition of magnesium to aluminium matrix in small amounts has brought up a huge rise in hardness profile of the parent metal. The compression test results displayed 23.8% increase in the compressive strength of the extruded specimen.

The wear test results display that there is an increase in wear resistance of the composite with a corresponding increase in time span and frictional force. The reduction in weight (wear) is found to be 0.05g for 20KN load and 0.52g for 30KN respectively.

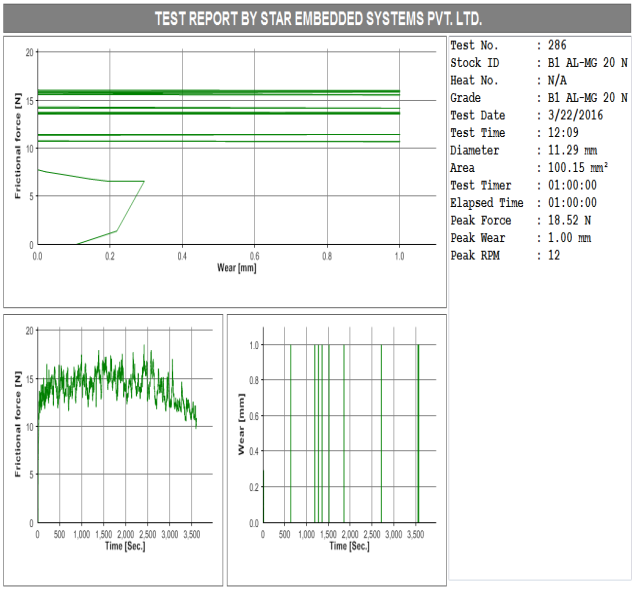

Fig. 9. Wear as a function of frictional force and time for a load of 20KN

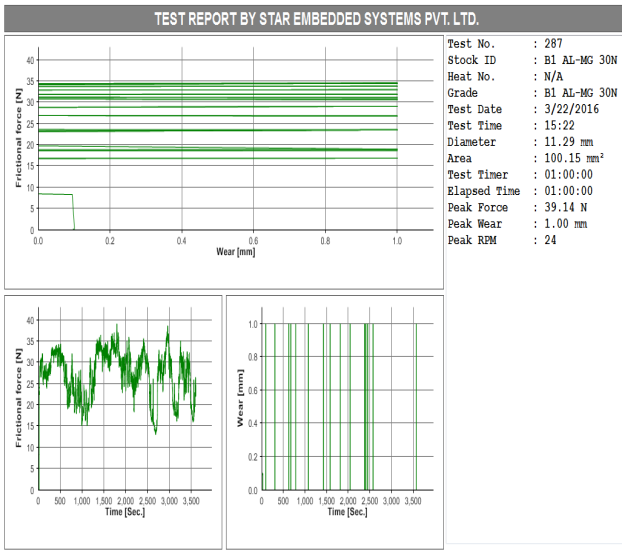

Fig. 10. Wear as a function of frictional force and time for a load of 30KN

4. CONCLUSIONS

From the results and discussions, the following conclusions are drawn.

- The production of bimetals through hot extrusion is possible.A well-mixed Al/Mg material was produced. Running extrusion at relatively high temperatures yielded a material with a quite homogeneous structure.
- It is observed that there is an overall increase in the hardness, compressive strength and wear resistance of the composite compared to base metal.
- From the SEM and XRD results, it can be concluded that there is a fine grain morphology in the extruded bimetallic composite and the respective intermetallic phases formed indicate uniform metallurgical bond between the aluminium matrix and magnesium reinforcement.
- It may be assumed that the corrosion resistance of the composite may decrease in a very percent due to the presence of magnesium in the matrix.
- Increasing the content of Mg to an Al gives promising results in regard to mechanical properties, and motivates further investigations with this novel method.

5. REFERENCES

[1] T.W. Clyne, P.J. Withers, An Introduction to Metal Matrix Composites,Cambridge University Press, Cambridge, 1993.

[2] Luo A, Perquleryuz MO. Review cast Mg alloy for elevated temperature applications. J Mater Sci 1994; 29:5259-71.

[3] LewandowskiJJ.In:Clyne TW,editor. Metal matrix composites, vol.3. Amsterdam: Elsevier; 2000. p. 151–87.

[4] Divecha AP, Fishman SG, Karmarkar SD. Synthesis of metal-matrixcomposites. J Metals 1981;33:12–15.

[5] Stephens JR. High temperature metal matrix composites for futureaerospace systems. NASA TM 1987;100–212.

[6] PARAMSOTHY M, GUPTA M, SRIKANTH N. Processing, microstructure, and properties of a Mg/Al bimetal macro composite [J]. Journal of Composite Materials, 2008, 42: 2567−2584.

[7] P. Chekhonin, B. Beausir, J. Scharnweber, C.-G. Oertel, T. Hausöl, H.W.Höppel, H.-G. Brokmeier, W. Skrotzki, ActaMater., 60 (2012) 4661-4671.

[8] M. Abbasi, A.K. Taheri, M.T. Salehi, J. Alloys Compd. 319 (2001)233–241.

[9] H. Dyja, S. Mroz, Z. Stradomski, Metalurgija 42 (2003) 185–191.

[10] E.I. Marukovich, A.M. Branovitsky, Y.-S. Na, J.-H. Lee, K.-Y. Cho, Mater. Design 27 (10) (2006) 1016–1026.

[11] A.G. Mamalis, A. Szalay, N.M. Vaxevanidis, D.I. Pantelis, Mater. Sci. Eng.A 188 (1994) 267–275.

[12] B.V. Krishna, P.Venugopal, K.P. Rao, Mater. Sci. Eng.A407 (2005) 77–83.

[13] B.V. Krishna, P. Venugopal, K.P. Rao, Mater. Sci. Eng. A 386 (2004)301–317.

Author: **Assistant Professor on contract, B. Ratna kumar Ambedkar, Dr G. Swami Naidu, V. S. S. Lailitha, D. Murali Krishna.** Department of Metallurgical engineering, JNTUK-UCEV, Vizianagaram, Phone:+918121332574

E-mail: ambi3639@gmail.com

Journal of Production Engineering
Vol.19 No.2
JPE (2016) Vol.19 (2) Original Scientific Paper
Vukman, J., Lukić, D., Milošević, M., Borojević, S., Antić, A., Đurđev, M.

FUNDAMENTALS OF THE OPTIMIZATION OF MACHINING PROCESS PLANNING FOR THE THIN-WALLED ALUMINIUM PARTS

Received: 02 August 2016 / Accepted: 13 October 2016

Abstract: *Aluminium alloy thin-walled structures are used in various branches of industry where it is required for the product to have minimal weight and meet certain mechanical characteristics at the same time. The manufacturing process of aluminium alloy thin-walled structures is usually realized by removing the material from full blanks, even up to 95% of their weight, requiring high manufacturing productivity and thus resulting in machining errors and deformations of the workpiece structure. The aim of this work is related to the improvement of technological preparation of production of aluminium alloy thin-walled structures, with the consideration of fundamentals of the optimization of machining process planning for these structures.*
Key words: *Machining process planning, optimization, thin-walled aluminum parts*

Osnove optimizacije tehnoloških procesa obrade tankozidnih aluminijumskih delova. *Tankozidni delovi od legure aluminijuma primenjuju se u raznim granama industrije gde je bitno da proizvodi budu što manje mase, a da pri tome zadovoljavaju određene konstrukciono-tehnološke karakteristike. Proces proizvodnje tankozidnih struktura najčešće se realizuje skidanjem materijala iz punih pripremaka, čak i do 95% od njihove težine, što zahteva visoku proizvodnost, usled čega se mogu javiti greške obrade i deformacije strukture obradka. Cilj ovog rada se odnosi na unapređenje tehnološke pripreme proizvodnje tankozidnih struktura od legura aluminijuma, odnosno prikaz osnova optimizacije tehnološkog procesa njihove obrade.*
Ključne reči: *Tehnološki proces obrade, optimizacija, tankozidni aluminijumski delovi*

1. INTRODUCTION

On economical level, today's market requires efficient production and rapid adaptation to customer requirements. Methods based solely on the analysis of obtained results are outdated and inefficient in modern business conditions. Production must be predicted, planned, prepared and organized in more detail, and the results achieved by using specific methods and resources should be measured and compared with the data planned in appropriate functions of production system. Special importance in the development and improvement of production has the function of technological production preparation [1, 2].

Two main activities within the technological preparation of production refer to the design and optimization of production processes. When developing the technological preparation and its integration with other functions and activities of the global business environment, numerous methods and techniques are considered, such as feature technology, techno-economic optimization methods, artificial intelligence methods, agent-based methods, internet-based method, method based on the STEP standard, etc. [2-5].

Aluminium alloy thin-walled structures are used in various branches of industry where it is important for products to weigh less, and to meet certain construction-technological characteristics at the same time. The main subject of this research refers to the representation of basic construction-technological characteristics of aluminum alloy thin-walled parts, as well as the introduction of the methodology for optimizing machining process planning for these parts, with the cosideration of conducted research and obtained results.

2. BASIC CONSTRUCTION-TECHNOLOGICAL CHARACTERISTICS OF THIN-WALLED PARTS

Machining of thin-walled structures is performed by removing material from full blanks, up to 95% of its weight. Manufacturing process for such complex structures is time consuming and very demanding. Due to the large amount of material removal it is necessary to achieve high productivity [6, 7, 8]. On the other hand, high productivity limits the lack of stiffness of thin walls, which leads to the occurrence of errors in the machining process [9]. In addition to this, moreover, permanent deformations of structures can appear which may also cause the incidence of reject parts. Numerous factors of the machining process planing may be affected by these problems, such as the elements of machining system (machines, tools, fixtures), cutting parameters, tool path strategies, fluids for cooling and lubrications, etc. [10]. Previously identified forms of thin-walled structures produced by machining processes can vary from line forms, rectangular forms to triangular, hexagonal and complex geometric forms.

2.1 Basic constructional characteristics of thin-walled parts

The division of thin-walled parts is done on the basis of several recommendations. Fitzgerald [11]

proposed a guide for noticing the difference between the thin-walled and thick-walled cylinders on the basis of distributing constant voltage through the wall. The theory of thin-walled cylinders and spheres is based on the assumption which indicates that the wall thickness to diameter ratio of 1/10 represents a separating line between the thin-walled and thick-walled cylinder. Yang [1 1] gave recommendations about distinction between super-thin, thin and thick plates. These recommendations are as follows:

- Super- thin plates = h/p < (1/100);
- Thin plates = (1/100) ≤ h/p ≤ (1/5) i
- Thick plates = h/p > (1/5).

Where: *p – the shortest distance between two edges on the plate and* h - *plate thickness*

The above recommendations can be regarded as a general definition of the wall thickness. However, due to increasing demands in terms of accuracy of a machined surface, the machining of thin-walled parts is increasingly viewed from the aspect of whether the wall bends or not, i.e. how much it bends and whether it affects the machining accuracy. To be more specific, elastic deformation of thin-walled part may be greater or equal to the allowed tolerance requirement and can be written as:

$$\delta \geq T$$

Where: *δ - elastic deformation of the wall and T - allowed machining tolerance.*

2.2 Main reasons for appearance of deformation while machining thin-walled parts

There are many factors that affect the accuracy of machining thin-walled parts, among which the following are the most influential [13]:

- Stress and deformation;
- Deformations induced by vibration;
- Wrong direction of chip flow;
- Thermal deformation and
- Inadequate machining strategy.

Figure 1 shows the factors that affect the deformation when machining the thin-walled parts [14].

Fig. 1. Deformation factors in machining of thin-walled parts [14]

Due to poor stiffness of thin-walled structure there is a stong possibility for the occurrence of deformations during the machining process, which also results in the occurrence of errors in shape, position and tolerances as well as surface quality [14, 15, 16]. Figure 2 shows measurement, shape and position errors that occur during the machining of line-type thin-walled parts. The material in the shaded area *MNOP* is planned for removal, figure 3b. However, by the influence of forces that occur in the milling process, thin wall bends, where the point *M* moves to point *M* ', while the point *N* moves to point *N*′ in the same way. A result of wall deflection (wall bending) leads to material removal in the area MN'OP which results in the occurrence of mentioned errors in NON'.

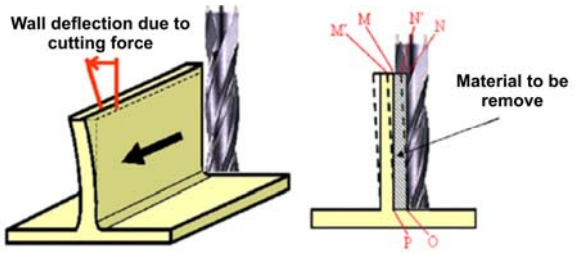

Fig. 2. Errors in the machining of thin-walled structures [15] (a) deflection of wall resulting from milling force (b) displacement points during machining

Deformations that occur in the curves of thin-walled parts are mainly influenced by cutting forces [16]. Cutting forces are directly related to machining parameters, which indicates that the selection of appropriate machining parameters is of crucial importance. Stiffness of thin-walled parts is small, however, it changes significantly for different tool positions during the machining process. In addition, as stiffness constantly changes along with the process of removing material from the workpiece, different tool paths lead to different inclinations of thin-walled structures. Therefore, the selection of an appropriate machining strategy, or tool path is also of crucial importance.

Compared to the flat (line type) thin-walled structures, curved, i.e circular thin-walled structures are more stable (stiff) because of the structure that is similar to the triangle, as shown in the Figure 3 [17]. When applying cutting force on point *A,* material on *AJ* and *AC* sides applies the radial (passive) force. Also, when material absorbs enough power to balance with the cutting force, it results in a small material bending. However, when applying cutting force on the free end or near the free end such as on the points C or J, passive force is insufficient to resist the cutting force in such conditions. This leads to the occurrence of deformations in order to establish the force balance, which affects the reduction in the amount of material removal, figure 4.

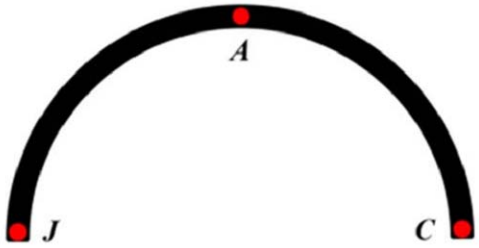

Fig. 3. 2D representation of deformation in the horizontal direction [17]

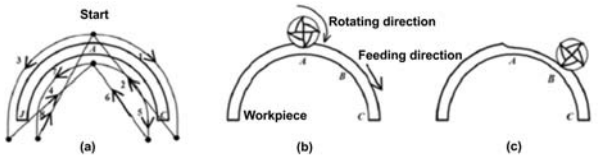

Fig. 4. Machining process from high to low stiffness [17] (a) tool path, (b) starting point and (v) machining direction

3. FUNDAMENTALS OF THE OPTIMIZATION OF MACHINING PROCESS PLANNING FOR THE THIN-WALLED PARTS

3.1 Methodology preview

Optimization theory as a scientific discipline has been increasingly adopted in solving engineering problems, where on the basis of set optimization criteria, specific optimization methods are used for finding the best solution of a selected object of optimization for specfic conditions. In accordance with the established objective an appropriate methodology for the optimization of process planning of thin-walled structures will be developed. Main stages of this methodology are the following: *Defining the optimization tasks; Design of variants of process plans with specific constraints; Setting the experiment plans; Executing the experiments; Measuring and analyzing the experimentation results; Evaluating the results and applying specific optimization methods; Mathematical modeling; Verifying mathematical models and developing a knowledge and database of parameters of the process planning as the basis for developing a CAPP system*.

3.2 Preview of previous research

On the basis of the proposed methodology preliminary research was conducted as a part of the extended research aimed at the improvement of technological preparation of production of the thin-walled structures.

The object of the research in this paper considers the line-type aluminum alloy thin-walled structures, with wall thickness of 0.5 - 1.5 mm and moderate height relative to the wall thickness (L:a=30:1). The main optimization task refers to the definition of the influence of tool path strategy, wall thickness (a) and feed rate value (f) on machining time (T), wall thickness accuracy (Δa), perpendicularity and flatness accuracy (Δb and Δc), as well as surface roughness (Ra), and it is solved using the experimental optimization method, Fig. 5. The parameters Δa, Δb, Δc and Ra can be seen as controlled parameters with defined limit value intervals. The development of appropriate mathematical models for the given output parameters is predicted as an output result.

Three variable factors are assumed within the experiment plan, two of them are numerical and one non-numerical factor, with the total of 33 experiments. The first numerical factor is the thickness of the line-type thin-walled structure (a), with the lower limit value of 0.5 mm and the upper limit value of 1.5 mm. Other factor is the numerical value of the milling feed rate (f), whose lower limit is 150 mm/min, and the upper limit value is 350 mm/min. For the third non-numerical factor three different tool path strategies are selected, based on the recommendations from the literature [18] for machining thin walled structures: *Tool path strategy 1 (Parallel Spiral)*; *Tool path strategy 2 (Zigzag)*; *Tool path strategy 3 (True Spiral)*.

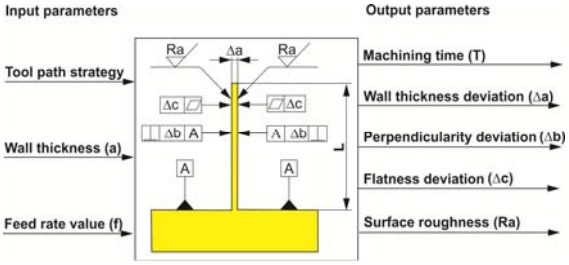

Fig. 5. Optimization task

3.2.1 Machining process planning

This stage encompasses the modelling of the thin-walled structures of appropriate dimensions, as well as the design of the variants of the machining process planning with the corresponding factors of tool path strategies and feed rate, according to the defined experiment plan. The main output result of this stage are the numerical controlled (NC) programs for the machining of 33 samples on the selected CNC machine. In defining the global machining strategy, the sequence of the execution of machining passes is adopted, as in Fig. 6.

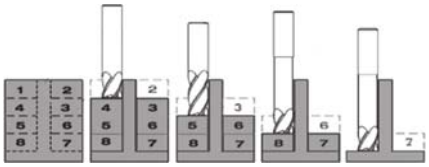
Fig. 6. The sequence of executing machining passes for the thin-walled aluminum structure

3.2.2 Executing the experiment and representing main results

Blanks for the machining of samples have a prismatic shape with (70×40×40) mm dimensions, while the material used for machining is alluminium alloy Al 7075 (AlZnMgCu1.5). For the execution of the experiment, CNC machining center is used - NUMA EMCO Concept Mill 450 and the slot milling cutter with identification R216.32-10025-AK32A – by Sandvik Coromant manufacturer.

The analysis of the results indicate that the selection of the optimal tool path strategy and feed rate values in the process of machining the thin-walled structures achieve significant savings in terms of machining time, while satisfying the accuracy of the wall thickness, perpendicularity and flatness, as well as the accuracy of surface roughness.

4. CONCLUSIONS

Based on the literature analysis it can be concluded that the area of production-machining of thin-walled structures has been the subject of research for many years. It was identified that no single approach exists

that could be implemented in the field of technological preparation of production of the observed parts.

In this paper, the main constructional-technological characteristics of aluminum alloy thin-walled parts are represented. Also, the methodology for the optimization of machining process planning for the observed parts is introduced with the short summary of the conducted research. This methodology will be significantly upgraded in the future in order to represent the competitive methodology for improving the technological preparation of machining the thin-walled parts, through the application of some of the listed methods and techniques, such as feature technologies, techno-economic optimization methods, STEP-NC standard, etc.

5. REFERENCES

[1] Scallan, P.: *Process planning: The Design/Manufacture Interface*, MA: Butterworth-Hienemann, Boston, 2003.

[2] Lukić, D.: *Development of a Genaral Technological Preparation of Production Model*, PhD thesis, Faculty of Technical Science, Novi Sad, 2012.

[3] Xu, X., Wang, L., Newman, S.T.: *Computer-Aided Process Planning - A Critical Review of Recent Developments and Future Trends*, International Journal of Computer Integrated Manufacturing, Taylor & Francis, Vol. 24, No. 1-3, pp. 1-31, ISSN 0951-192X, 2011.

[4] Borojević, S.: *Development of an System for Simultaneously Product and Process Planning Design*, PhD thesis, Faculty of Technical Science, Novi Sad, 2015.

[5] Milošević, M.: *Collaborative System for Process Planning of Product Manufacturing Based on Internet Technologies*, PhD thesis, Faculty of Technical Science, Novi Sad, 2012.

[6] Hirsch, J., Al-Samman, T.: *Superior light metals by texture engineering: Optimized aluminum and magnesium alloys for automotive applications*. Acta Materialia, Vol. 61, No. 3, pp. 818-843, 2013 DOI:10.1016/j.actamat.2012.10.044.

[7] Scippa, A., Grossi, N., Campatelli, G.*: FEM based cutting velocity selection for thin walled part machining*. Procedia CIRP, Vol. 14, pp. 287–292, 2014. DOI:10.1016/j.procir.2014.03.023.

[8] Huang, X., Sun, J., Li, J.: *Effect of initial residual stress and machining-induced residual stress on the deformation of aluminium alloy plate*. Strojniški vestnik - Journal of Mechanical Engineering, Vol. 61, No. 2, pp. 131-137, 2015. DOI:10.5545/sv-jme.2014.1897.

[9] Zhou, X., Zhang, D., Luo, M., Wu, B. (2014). *Toolpath dependent chatter suppression in multi-axis milling of hollow fan blades with ball-end cutter*. The International Journal of Advanced Manufacturing Technology, Vol. 72, No. 4, pp.: 643-651, 2014. DOI:10.1007/s00170-014-5698-6.

[10] Izamshah, R., Mo, J.P.T., Ding, S. (2011). *Hybrid deflection prediction on machining thin-wall monolithic aerospace components*. Proceedings of the Institution of Mechanical Engineers, Part B: Journal of Engineering Manufacture, vol. 226, no. 4, p. 592-605. DOI:10.1177/0954405411425443.

[11] Fitzgerald, R.W.: *Mechanics of materials, 2nd edition*, Addison-Wesley Publishing Company Inc., Massachusetts, USA, 1982.

[12] Yang, G.: *Elastic and plastic mechanics*, People Education Published Inc., PRC, 1980.

[13] Zhang, D., Gao, K., Zhou, T.: *Discussion on NC machining process of thin walled parts technical measures*, Applied Mechanics and Materials, Trans Tech Publications, Switzerland, Vol. 701-702, pp. 864-868, 2015. DOI:10.4028/www.scientific.net/AMM.701- 702.864

[14] Bing, D., Guang-bin, Y., Yan-qi, G., Jun-peng, S., Yan-qi, G., Xue-mei, W., Yu-xin, L.: *Machining Surface Quality Analysis of Aluminum Alloy Thin-Walled Parts in Aerospace*, International Journal of Security and Its Applications, Vol.9, No.11, pp. 201-208, 2015.

[15] Izamshah, R.R.A.: *Hybrid Deflection Prediction for Machining Thin-Wall Titanium Alloy Aerospace Component*, PhD. Thesis, School of Aerospace, Mechanical and Manufacturing Engineering RMIT University, 2011.

[16] WojciechowskI, S.: *The estimation of cutting forces and specific force coefficients during finishing ball end milling of inclined surfaces*, International Journal of Machine Tools and Manufacture, Vol. 89, pp. 110-123, 2015.

[17] Gao, Y.Y., Ma, J.W., Jia, Z.Y., Wang, F.J., Si, L.K., Song, D.N.: *Tool path planning and machining deformation compensation in high-speed milling for difficult-to-machine material thin-walled parts with curved surface*, The International Journal of Advanced Manufacturing Technology, Vol. 84, Issue 9, pp. 1757–1767, 2016.

[18] Hirsch, J., Al-Samman, T.: Superior light metals by texture engineering: *Optimized aluminum and magnesium alloys for automotive applications*. Acta Materialia, vol. 61, no. 3, pp. 818-843, 2013, DOI:10.1016/j.actamat.2012.10.044.

Authors: M.Sc. Jovan Vukman, Assist. Professor Dejan Lukić, Assist. Professor Mijodrag Milošević, Associate Professor Aco Antić, M.Sc. Mića Đurđev, University of Novi Sad, Faculty of Technical Sciences, Department for Production Engineering, Trg Dositeja Obradovića 6, 21000 Novi Sad, Serbia, Phone.: +381 21 485-2331, Fax: +381 21 454-495. ***Assist. Professor*** Stevo Borojević, University of Banja Luka, Faculty of Mechanical Engineering, Vojvode Stepe Stepanovića 71, 78000 Banja Luka, Republic of Srpska, BiH, Phone.: +387 51 433 068

E-mail: vukman@uns.ac.rs; lukicd@uns.ac.rs; mido@uns.ac.rs; stevoborojevic@hotmail.com; antica@uns.ac.rs; mdjurdjev@live.com

Note: This paper is part of a research on project "Modern approaches to the development of special bearings in mechanical engineering and medical prosthetics," TR 35025, supported by the Ministry of Education, Science and Technological Development, Republic of Serbia.

Journal of Production Engineering
Vol.19 No.2
JPE (2016) Vol.19 (2) Original Scientific Paper
Agarski, B., Budak, I., Ilic Micunovic, M., Imamovic, N., Kosec, B., Kljajin, M., Vukelic, Dj.

INTERNAL NORMALIZATION IN LIFE CYCLE ASSESSMENT USING THE MULTI-CRITERIA ANALYSIS APPROACH

Received: 28 June 2016 / Accepted: 15 September 2016

Abstract: *Mandatory and optional elements can be distinguished in life cycle impact assessment. The focus of this research is on the optional step of normalization. External and internal normalization approaches can be performed in order to normalize the impact categories results. Internal normalization is based on multi-criteria decision analysis, where the alternatives values are compared to other alternatives values without using the external reference. In this paper, different approaches for internal normalization in life cycle impact assessment have been investigated and compared through the comparative example of different materials production phase. The results show that internal normalization is a good practice to visually display the characterization results. Internal normalization has lower uncertainty level, and its use is recommended in uncertain cases, where similar rankings result in difficult interpretation of results.*
Key words: *normalization, life cycle assessment, multi-criteria analysis*

Interna normalizacija u ocenjivanju životnog ciklusa primenom pristupa višekriterijumske analize. *Prilikom ocene uticaja životnog ciklusa mogu se razlikovati obavezni i opcioni elementi. Fokus ovog istraživanja je na opcionom koraku normalizacije. Eksterni i interni pristup normalizacije moše se primeniti kako bi se normalizovali rezultati kategorija uticaja. Interna normalizacija je zanovana na višekriterijumskoj analizi, gde se vrednosti alternativa porede sa vrednostima ostalih alternativa bez primene eksterne reference. U ovom radu, različiti pristupi interne normalizacije u ocenjivanju uticaja životnog ciklusa su istraženi i poređeni u uporednom primeru proizvodne faze različitih materijala. Rezultati prikazuju da interna normalizacija je dobra praksa za vizuelni prikaz rezultata karakterizacije. Interna normalizacija ima manji nivo nesigurnosti i njena upotreba je preporučljiva u slučajevima nesigurnosti, kada sličan rang uzrokuje tešku interpretaciju rezultata.*
Ključne reči: *normalizacija, ocenjivanje životnog ciklusa, višekriterijumska analiza*

1. INTRODUCTION

Life cycle assessment (LCA) is the most comprehensive and credible method for assessing the environmental impact of processes during their entire life cycle. In order to consider environmental, technical, economic, and social aspects in LCA, comprehensive evaluation methods are required and multi-criteria analysis (MCA) methods present a suitable tool for sustainability and LCA [1, 2, 3, 4, 5].

Considering the benefits of using both MCA and LCA methods in sustainability assessments, several applications of MCDM and LCA are described below. Simple Additive Weighting (SAW), one of the simplest MCA methods, was used in Ecoindicator 99, ReCiPe and other Life Cycle Impact Assessment (LCIA) methods for obtaining the life cycle total environmental impact [6]. The possibility of combining LCA and MCA was discussed by Hermann et al. [7]. Myllyviita et al. [8] applied MCA in LCA to identify and weigh impact categories in order to assess the environmental impacts of biomass production. On the other hand, Milani et al. [1] applied MCA on LCA results in order to select the optimal material. Domingues et al. [9] presented a methodology for classification of light-duty vehicles according to their environmental impacts; their classification was based on Life-Cycle Impact Assessment indicators and vehicle operation indicators which were aggregated with a MCA method. Herva and Roca [10] conducted a comprehensive review of combined approaches where multi-criteria analysis was combined with environmental evaluation tools: ecological footprint, LCA and environmental risk assessment. In this respect, they reviewed the applicability of multi-criteria analysis in decision support systems in the particular areas of application.

LCA consists of mandatory and optional elements. Within this research the focus is on the optional step of normalization. In general, normalization methods allow different impact categories to be compared to each other. While there are several approaches in order to normalize impact categories results, external and internal normalization can be distinguished. The most common practice for normalization in life cycle impact assessment is external normalization where the results of the impact categories from the study are compared with the reference value (for example environmental impacts in the region of interest). Internal normalization is based on MCA, where the idea is to compare the one alternative value to other alternatives instead of using the external reference. Here, different approaches for normalization in life cycle impact assessment have been investigated and compared through comparative example of different materials production phase. This research aims to help the decision makers in interpretation phase of LCA

encouraging them to use different approaches for normalization in order to achieve several perspectives of life cycle impact assessment normalization results.

2. METHODS AND MATERIALS

2.1 Methods

Figure 1 shows the conections between the LCA and MCA methods in order to provide internal normalization in life cycle impact assessment.

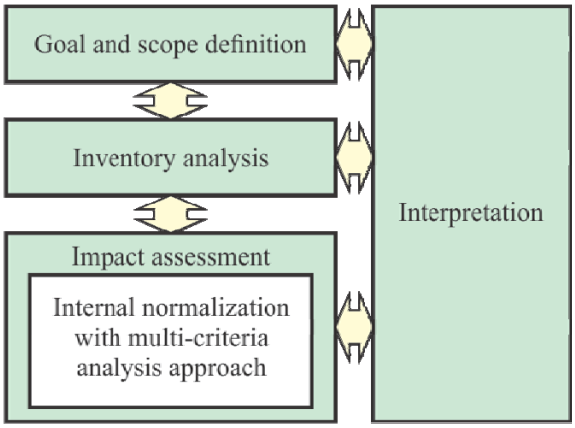

Fig. 1. Internal normalization in LCA using the MCA approach

Although the proposed MCA approach could be applied on every LCIA method, in this research, CML 2001 [11] was selected as LCIA method. For normalization of characterization results the following equations (equations 1, 2, 3, 4) for external and internal normalization (linear 1, linear 2, vector) were used, respectively:

$$N_{ij}^{Ext} = CF_j \cdot a_{ij}, \quad i = 1, 2, ..., n; \quad j = 1, 2, ..., m; \tag{1}$$

$$N_{ij}^{Int,L1} = 1 - \frac{\max_i a_{ij} - a_{ij}}{\max_i a_{ij}} \tag{2}$$

$$N_{ij}^{Int,L2} = 1 - \frac{\max_i a_{ij} - a_{ij}}{\max_i a_{ij} - \min_i a_{ij}} \tag{3}$$

$$N_{ij}^{Int,V} = \frac{a_{ij}}{\sqrt{\sum_{i=1}^{n} a_{ij}^2}} \tag{4}$$

where are: N^{Ext} – external normalization results, CF – characterization factor, N^{Int} – internal normalization results ($L1$ – linear 1, $L2$ – linear 2, V - vector), a_{ij} – characterization results, n – number of compared products/processes, m – number of impact categories.

2.2 Materials

The following numerical example shows the comparison of LCA results of four similar paper production, each with mass of one kilogram: newsprint paper without deinking, newsprint paper with deinking, recycled paper without deinking, recycled paper with deinking. Production of these products include European production of newsprint or recycled paper with or without the use of deinked pulp. Included processes are: transports to paper mill, wood handling, mechanical pulping and bleaching, deinking of waste paper (depending on the product), paper production, energy production on-site, and internal waste water treatment. The data for the inventory of these products were obtained from Ecoinvent Database v2.0 [12].

3. RESULTS

For LCA calculations SimaPro 8.0 software was used. Figures 2, 3, 4, and 5 show LCA results: external normalization, internal normalization - linear 1, linear 2 and vector. Considered impact categories in CML 2001 are:

- Abiotic depletion (AD),
- Abiotic depletion - fossil fuels (AD(FF)),
- Global warming (GWP100a),
- Ozone layer depletion (ODP),
- Human toxicity (HT),
- Fresh water aquatic ecotoxicity (FWAE),
- Marine aquatic ecotoxicity (MAE),
- Terrestril ecotoxicity (TE),
- Photochemical oxidation (PO),
- Acidification (A), and
- Eutrophication (E).

4. DISSCUSSION AND CONCLUSIONS

In life cycle assessment, normalization can be understood as an interpretation aid because it serves to better understand the relative magnitude of an environmental impact. The overall results for the presented normalization approaches, considering all the impact categories, show that the recycled paper with deinking has the highest environmental impact, while the recycled paper without deinking has the lowest environmental impact.

External and internal normalization approaches provide completely different results and can not be interpreted on the same manner. When characterized results from life cycle impact assessment are presented without normalization, interpretation may not be transparent. Therefore, internal normalization, based on multi-criteria decision analysis, is often used in LCA software's for more understandable visualization of characterization results. The external normalization provides information about the impact on the specific geographic area or population, however, this results have larger uncertainties because of the use of normalization factors. Internal normalization is good practice to visually display the characterization results. Internal normalization has lower uncertainty level, and it's use is recommended in uncertain cases, where similar rankings result in difficult interpretation of results.

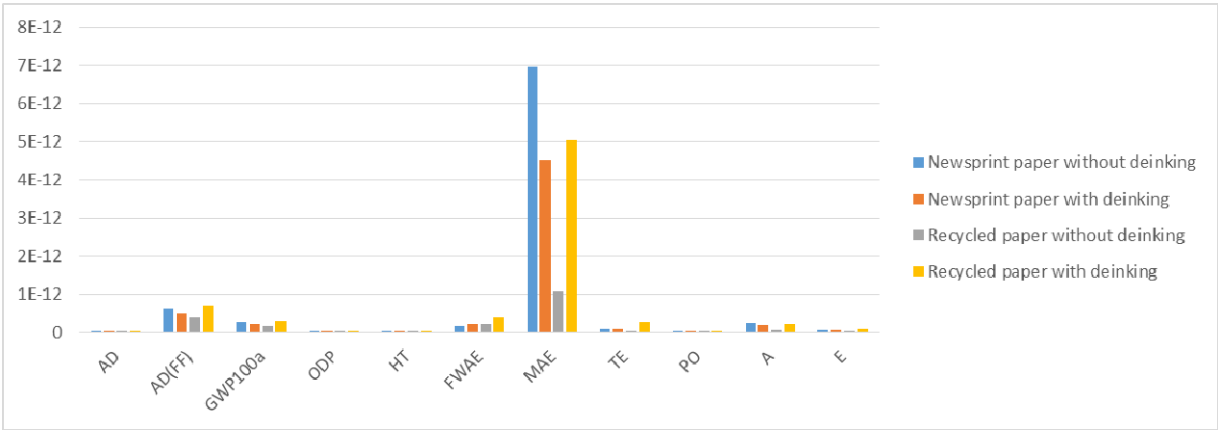

Fig. 2. External normalization

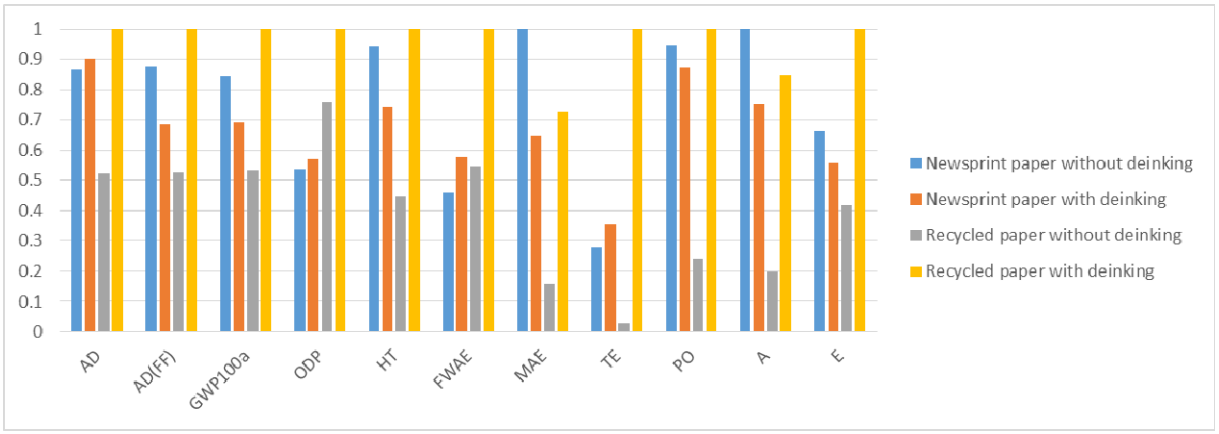

Fig. 3. Internal normalization – linear 1

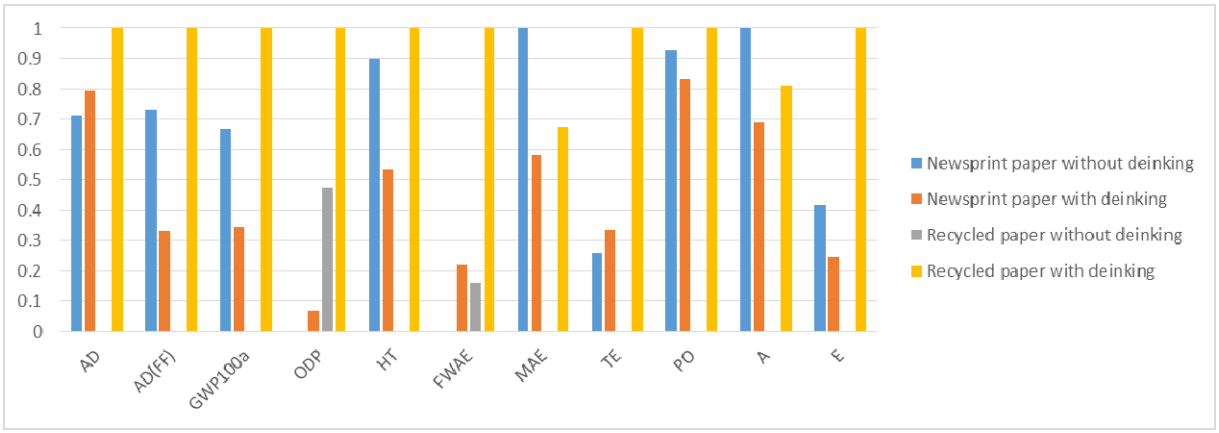

Fig. 4. Internal normalization – linear 2

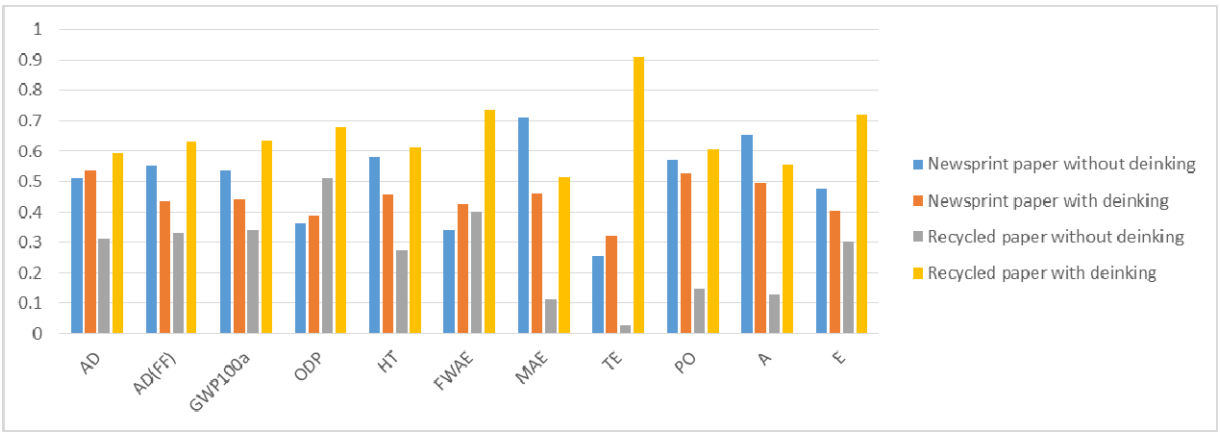

Fig. 5. Internal normalization - vector

5. REFERENCES

[1] Milani, A.S., Eskicioglu, C., Robles, K., Bujun, K., Hosseini Nasab, H.: *Multiple criteria decision making with life cycle assessment for material selection of composites*, Express Polymer Letters, 5, p.p. 1062–1074, 2011.

[2] Rogers, K., Seager, T.P.: *Environmental Decision Making Using Life Cycle Impact Assessment and Stochastic Multiattribute Decision Analysis: A Case Study on Alternative Transportation Fuels*, Environmental Science & Technology, 43, p.p. 1718–1723, 2009.

[3] Agarski, B., Kljajin, M., Budak, I., Tadic, B., Vukelic, D., Bosak, M., Hodolic, J.: *Application of multi-criteria assessment in evaluation of motor vehicles' environmental performances*, Tehnički Vjesnik, 19, p.p. 221-226, 2012.

[4] Hsu, C.W., Kuo, R.J., Chiou, C.Y.: *A multi-criteria decision-making approach for evaluating carbon performance of suppliers in the electronics industry*, International Journal of Environmental Science and Technology, 11, p.p. 775–784, 2014.

[5] Agarski, B., Budak, I., Vukelic, Dj., Hodolic, J.: *Fuzzy Multi-criteria-based impact Category Weighting in Life Cycle Assessment*. Journal of Cleaner Production, 112, p.p. 3256-3266, 2016.

[6] Rowley, H.V., Peters, G.M.: *Multi-criteria Methods for the Aggregation of Life Cycle Impacts, 6. Australian Conference on LCA*, ALCAS - Australian Life Cycle Assessment Society, Mebourne, 2009.

[7] Hermann, B.G., Kroeze, C., Jawjit, W.: *Assessing environmental performance by combining life cycle assessment, multicriteria analysis and environmental performance indicators*, Journal of Cleaner Production, 15, pp. 1787-1796, 2007.

[8] Myllyviita, T., Holma, A., Antikainen, R., Lahtenen, K., Leskinen, P.: *Assessing environmental impacts of biomass production chains e application of life cycle assessment (LCA) and multi-criteria decision analysis (MCDA)*, Journal of Cleaner Production, 29-30, pp. 238-245, 2012.

[9] Domingues, A.R., Marques, P., Garcia, R., Freire, F., Dias, L.C.: *Applying Multi-Criteria Decision Analysis to the Life-Cycle Assessment of vehicles*. Journal of Cleaner Production, 107, p.p. 749-759, 2015.

[10] Herva, M., Roca, E.: *Review of combined approaches and multi-criteria analysis for corporate environmental evaluation*, Journal of Cleaner Production, 39, p.p. 355-371, 2013.

[11] Guinee, J.B., Gorree, M., Heijungs, R., Huppes, G., Kleijn, R., de Koning, A. van Oers, L., Wegener Sleeswijk, A., Suh, S., Udo de Haes H.A., de Bruijn, H., van Duin, R., Huijbregts, M.A.J., Lindeijer, E., Roorda, A.A.H. Weidema B.P.: *Life cycle assessment; An operational guide to the ISO standards*; Parts 1, 2, and 3. Ministry of Housing, Spatial Planning and Environment (VROM) and Centre of Environmental Science (CML), Den Haag and Leiden, The Netherlands, 2001.

[12] Frischknecht, R., Jungbluth, N., Althaus, H.-J., Doka, G., Dones, R., Heck, T., Hellweg, S., Hischier, R., Nemecek, T., Rebitzer, G., Spielmann, M.: The ecoinvent database: *Overview and methodological framework*, International Journal of Life Cycle Assessment 10, 3–9, 2005.

Authors: Assis. prof. dr Boris Agarski[1)], Assoc. prof. dr Igor Budak[1)], M.Sc. Milana Ilic Micunovic[1)], Assis. prof. dr Nusret Imamovic[2)], Prof. dr Borut Kosec[3)], Prof. dr Milan Kljajin[4)], Assoc. prof. dr Djordje Vukelic[1)]

[1)] University of Novi Sad, Faculty of Technical Sciences, Trg Dositeja Obradovica 6, 21000 Novi Sad, Serbia, Phone.: +381 21 485 2350, Fax: +381 21 454-495.

[2)] Univerzitet u Zenici, Mašinski Fakultet u Zenici, Fakultetska 1, 72000 Zenica, Tel: +387 (0)32 449 141.

[3)] University of Ljubljana, Faculty of Natural Sciences and Engineering, Aškerčeva 12, 1000 Ljubljana, Slovenia, Phone.: +386 1 2000410, Fax: +386 1 4704560.

[4)] Sveučilište Josipa Jurja Strossmayera, Strojarski fakultet u Slavonskom Brodu, Slavonski Brod, Trg Ivane Brlić Mažuranić 2 , tel. +385 35 446 188, fax. +385 35 446 446

E-mail: agarski@uns.ac.rs
budaki@uns.ac.rs
milanai@uns.ac.rs
nimamovic@mf.unze.ba
borut.kosec@omm.ntf.uni-lj.si
mkljajin@sfsb.hr
vukelic@uns.ac.rs

Journal of Production Engineering
Vol.19 No.2
JPE (2016) Vol.19 (2) Original Scientific Paper
Santoši, Ž., Šokac, M., Ralević, N., Budak, I., Dramićanin, M.

APPLICATION OF FUZZY LOGIC AS A TOOL FOR IMPROVING THE QUALITY OF PHOTOGRAPHY BY SHAPE FROM FOCUS/DEFOCUS 3D DIGITIZATION

Received: 22 June 2016 / Accepted: 15 September 2016

Abstract: *Shape from focus/defocus presents one of the passive 3D digitizing methods. This method is based on a reconstruction of shapes and surfaces in space by capturing series of photographs of the same scene with different focus settings. Because of characteristics of optical devices for acquisition of photographs, which have adjustable depth of field, it is possible to capture adequate photographs for the application of this method. This paper will present the application of fuzzy logic rule-based approach as a tool to improve the quality of photographs by shape from focus/defocus 3D digitization.*
Key words: *image processing, fuzzy logic, 3D digitization*

Primena fazi logike kao alata za poboljšanje kvaliteta fotografija kod 3D digitalizacije fokusiranjem-defokusiranjem. *3D digitalizacija fokusiranjem-defokusiranjem je jedna od pasivnih metoda 3D digitalizacije. Zasniva se na rekonstrukciji oblika i površina u prostoru pomoću niza fotografija iste scene snimljene sa različitim podešavanjima fokusa. Zbog optičkih svojstava uređaja za akviziciju fotografija koje karakteriše mala dubinska oštrina moguće je napraviti podobne fotografije za primenu ove metode. U ovom radu će se predstaviti primena fazi logike zasnovane na logičkim pravilima kao alat za poboljšanje kvaliteta fotografija kod 3D digitalizacije fokusiranjem-defokusiranjem.*
Ključne reči: *obrada slike, fazi logika, 3D digitalizacija*

1. INTRODUCTION

Shape from focus/defocus presents a passive method used for 3D digitizing. It is based on reconstruction of shapes and surfaces in space by capturing series of photographs of the same scene with different focus settings [1, 2]. In order to capture a suitable input photographs, optical devices for photos acquisition have to enable very shallow depth of field and they must have a controlled displacement of the focal or reference plane. The best example of these devices is light microscope which is characterized by a very shallow depth of field, but in other hand with very little work space and it is suitable for small objects. But for larger objects, a digital camera can be used that possesses advanced optics, and therefore it can achieve a very shallow depth of field.

Depth of field is a term that is referring to the field of acceptable sharp focus in front, and behind of the actual focus point. The parameters that affect the size of the depth of field are lens focal length, aperture size and focus point distance. With different settings of these parameters it is possible to increase or decrease the size of the depth of field. To achieve the smallest depth of field it is necessary to adjust the maximum aperture, minimum focal length of the lens (if applicable) and set the object to the closest distance possible.

2. ACQUISITION OF PHOTOGRAPHS

For acquisition of photographs a light microscope with a digital camera was used. Figure 1 shows the principle of the acquisition of photographs and shape from focus/defocus 3D digitization method.

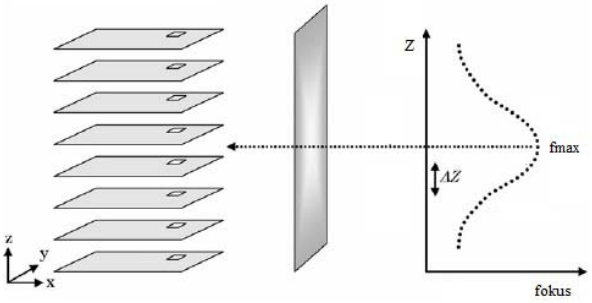

Fig. 1. Acquisition of photographs and shape from focus/defocus 3D digitization method

The camera that is mounted on the lens of the microscope allows digital recordings and capturing of images necessary for further processing. For experiment, a workpiece was used on which a four-sided pyramid footprint was obtained in order to measure Vickers hardness of the material. The angle of the top of the pyramid is 136°. Photographs are captured with a incremental step on the reference plane by 0,02 mm, and a total of 40 photographs were taken. The resolution of photographs was 2048x1536 pixels.

3. THEORETICAL BACKGROUND

Depending on the texture of the materials, with the sense of sight and touch that human posseses, it can be determined what kind of materials surfaces are in question. Visual texture has a key role in shape from focus/defocus 3D digitization. The materials with the

dynamic texture, characterized by expressed contrast and high entropy value and also visually clear and sharp edges (from a photographic point of view) are suitable for the application of this method. Sharp parts of the observed object on the photo, or parts that are within the scope of the depth of field, possess the aforementioned characteristics of dynamic textures, while parts outside the depth of field have significantly lower contrast and entropy values. With the known properties of visual texture and depth of field, the idea is to demonstrate the application of spatial filters for image processing and fuzzy logic in order to improve the quality of object regions on photographs that are within the scope of the depth of field.

The main objective of methods for improving image quality is the processing of the input photo and getting output image that is more suitable for further applications [3]. The algorithm for image processing is shown in Figure 2.

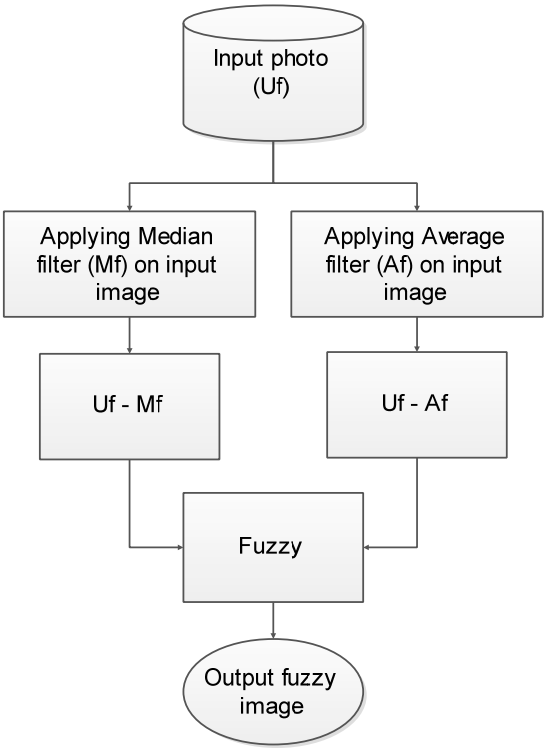

Fig. 2. Image processing algorithm

Input in algorithm for image processing is one photograph on which a nonlinear (median) filter and a linear average filter are applied. Characteristic of median filter is that it effectively removes impulsive noise, only if the presence of noise does not exceed 50% on the image. Principle of median filter is to replace a given pixel value with the median value of its neighboring pixels, as shown in Figure 3.

It depends on a size of local neighborhood that surrounds a value of given pixel, but it also depends on the value which will be replaced, as well as spatial filter operation that can be very diverse and have different purposes. For example, filtering in one direction only. Advantage of the median filter is that it keeps the edges of the object while it removes impulse noise on the image [3].

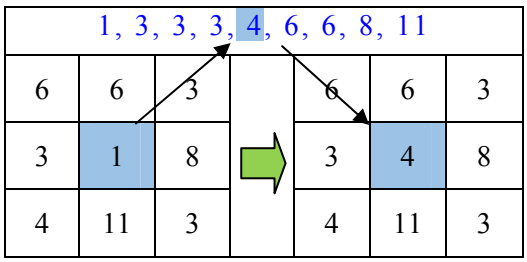

Fig. 3. Median filter principle

Average filter works by averaging local neighborhood of a targeted pixel value and replace that value with calculated average of the local neighborhood pixels [3]. Average filter is useful for removing grain noise from photographs. Also, local neighborhood size of selected pixel affect its outcome value (Figure 4).

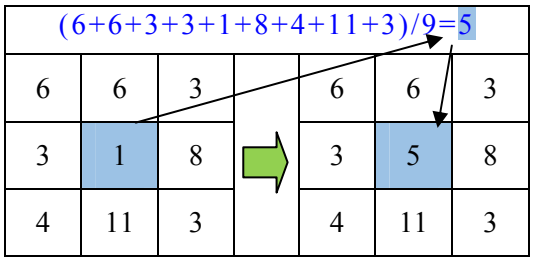

Fig. 4. Average filter principle

Both of these filters serve to blur the image (eliminate impulse and grain noise), and to smooth the sharp parts on the photograph. Because of the working principle of the median and average filters, regions on the image that have already been blurred in a large extent will not be affected, due to application of these filters. While the regions of the object on image, which are located within depth of field, will take significant loss in texture information and it will become blurred. After image processing, with the use of these filters next step is to apply basic arithmetic operations (subtraction) between input photo Uf and filtered images Mf and Af. These subtracted images represent inputs in the fuzzy image processing system.

3.1 Fuzzy logic

Fuzzy logic presents a tool that provides a mathematical model which allows the capability of human reasoning, up to a certain extent. With the use of fuzzy sets it is possible to model the uncertainty connected with the vagueness, imprecision and lack of information related to a given problem [4, 5]. Because of its characteristics, fuzzy logic has found wide use in various fields, such as regulation and control of devices in electronics, in image processing, in evaluation of environmental impact, etc. [2, 6, 7]. Fuzzy image processing generally can be divided into three main stages [5]:

- fuzzification,
- modification of member functions and
- defuzzification.

Beside of these three main stages, two more

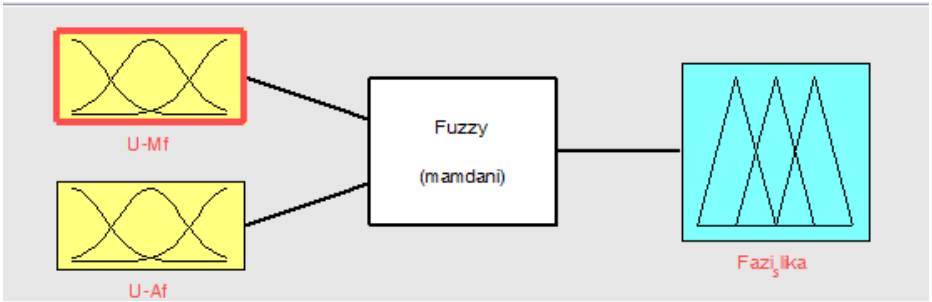

Fig. 5. Example of fuzzy system with two inputs and one output

additional stages can be added such as the theory of fuzzy sets and fuzzy logic and expert knowledge. This includes knowledge in the areas of expertise that are necessary in order to successfully solve the given problem, and in this case to determine which regions on the image are in focus and which are not. Figure 5. shows an example of fuzzy system consisting of two inputs and one output.

Input values are written in a clearly defined framework of the so-called crisp set. Crisp inputs values at first must go through fuzzification process and afterwards it will be converted into fuzzy domain, therefore appropriate membership functions will be defined next. After that, defined rules are applied (if and, then) on fuzzy inputs, defuzzification process occurs and it is returned to crisp domain.

The inputs in this case are filtered images in the spatial domain which are, for a specific pixel value, assigned to a corresponding membership function. Membership functions define in what degree a specified pixel value belongs, or does not belong to a given image.

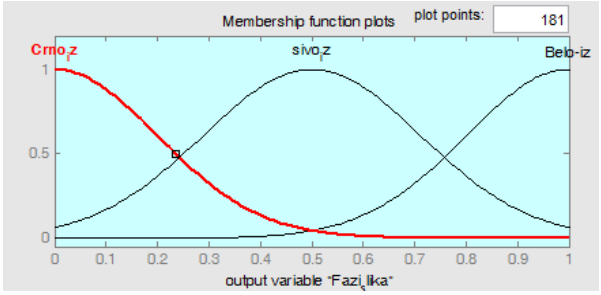

Fig. 6. Example of membership function plot

Figure 6. shows membership function plot and membership functions defined over the output image. Next, through defined rules (if and, then), and with combination of two input images, as a result output images are obtained. Graphic plot of membership functions of fuzzy system is shown in Figure 7. During the definition of rules, linguistic variables shown in Table 1. are used.

		Average filter		
		white	gray	black
Median filter	gray	white_out	gray_out	black _out

Table 1. Linguistic variables

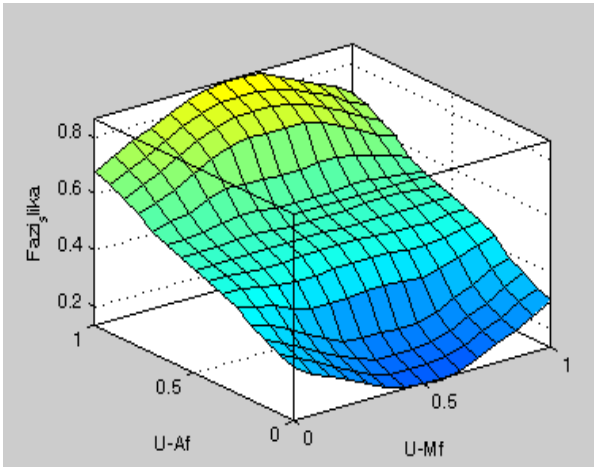

Fig. 7. Graphic plot of membership functions of fuzzy system

In the fuzzy domain for each pixel value from image a corresponding membership function is calculated, and on a basis on this value, intensity value for each pixel was calculated.

4. RESULTS

A large number of methods for improvement of image quality have empirical character and iterative nature, therefore it is very difficult to perform the quantification of results, ie. to assess how well image was improved. Basic indicators that are most commonly used for evaluation of image quality are the mean squared error (MSE) and peak signal to noise ratio (PSNR).

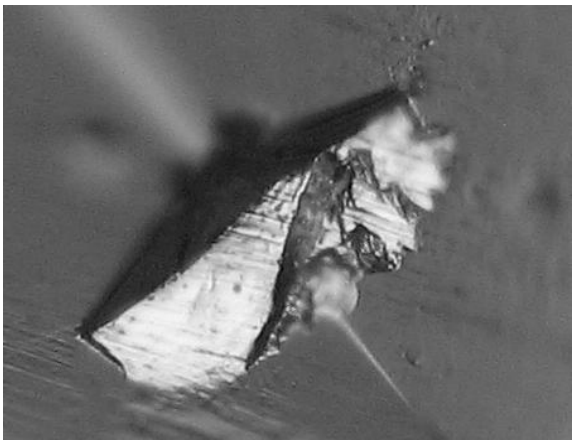
Fig. 8. Part of original image

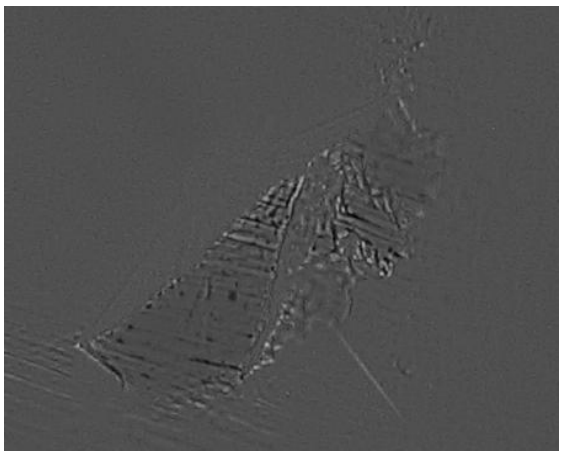

Fig. 9. Input image median filter

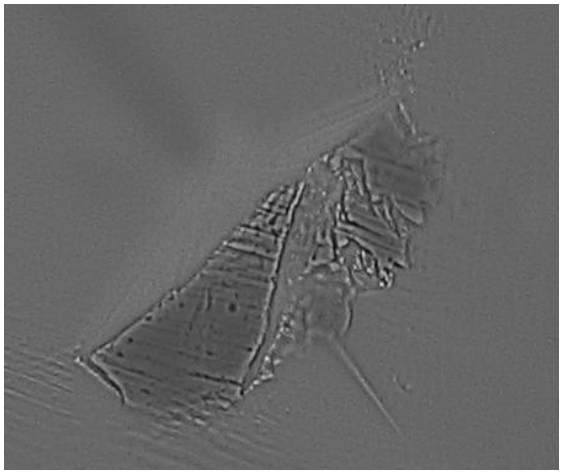

Fig. 10. Input image average filter

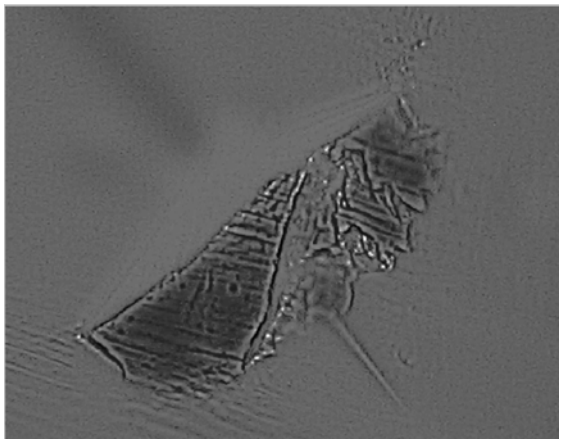

Fig. 11. Output fuzzy image

	MSE	PSNR
U-Mf	0.0170	17.6906
U-Af	0.0050	23.0234

Table 2. MSE (mean-squared error) and PSNR (Peak Signal-to-noise ratio) of the U-Mf and U-Af U in relation to the output fuzzy image

Figures 8, 9, 10 and 11 shows original image, input image median filter, input image average filter and output fuzzy image, respectively. Table 2 shows results of statistical parameters used for evaluation of image quality.

5. CONCLUSIONS

Fuzzy logic is a form of artificial intelligence which is a very powerful tool for mathematical description of problems and processes which people can easily describe and introduce. What should be emphasized is that as an approach which is connected with solving a problem of image processing has its advantages and disadvantages. This paper presents the use of fuzzy logic as a tool to improve the quality of input photographs, by shape from focus/defocus 3D digitization method. In the case of the photographs with parts of the object that are inside and outside of the depth of field, where transitions and boundaries from sharp to blur are not clearly defined, fuzzy logic finds a justification for the use. Further research should be oriented towards improving system phase by introducing additional rules and constraints in order to to ensure the best possible quality of output images.

6. REFERENCES

[1] Pertuz, S., Puig, D., Angel Garcia, M.: *Analysis of focus measure operators for shape-from-focus*, Pattern Recognition, vol. 46, pp 1415–1432, 2013.

[2] Malik, A., Nisar, H., Choi, T.: *A Fuzzy-Neural approach for estimation of depth map using focus*, Applied Soft Computing, vol. 11, pp. 1837–1850, 2011.

[3] Gonzalez, R.C.,Woods, R.E., Eddins, S.L.: *Digital Image Processing Using MATLAB*, New Jersey, Prentice Hall, 2003, Chapter 11.

[4] Negoita, V., Zadeh, A., Zimmermann, H.: *Fuzzy sets as a basis for a theory of possibility*, Fuzzy sets and systems 1, pp. 3-28. 1978.

[5] ---, „Fuzzy Logic Toolbox™ User's Guide“, Matlab, MathWork, R2015a

[6] Budak, I., Vukelić, Đ., Bračun, D., Hodolič, J., Soković, M.: *Pre-processing of point-data from contact and optical 3D digitization sensors*, Sensors, vol. 12, pp. 1100–1126, 2012.

[7] Agarski, B., Budak, I., Vukelic, Đ., Hodolic, J.: *Fuzzy multi-criteria-based impact category weighting in life cycle assessment*, J. Clean. Prod., vol. 112, pp. 3256–3266, 2016.

Authors: **M.Sc. Željko Santoši, M.Sc. Mario Šokac, Assoc. prof. Igor Budak, Prof. Nebojša Ralević, M.Sc. Miroslav Dramićanin.** University of Novi Sad, Faculty of technical sciences, Trg Dositeja Obradovića 6, 21000 Novi Sad, Serbia, Phone: +381 21 485 2350, Fax: +381 21 454-495.

E-mail: zeljkos@uns.ac.rs
marios@uns.ac.rs
budaki@uns.ac.rs
nralevic@uns.ac.rs
dramicanin@uns.ac.rs

Journal of Production Engineering
Vol.19 No.2
JPE (2016) Vol.19 (2) Original Scientific Paper
Brajlih, T., Irgolič, T., Kostevšek, U., Matin, I., Hadžistević, M., Balič, J., Drstvenšek, I.

ACCURACY INSPECTION OF CRANIAL IMPLANTS USING CT IMAGING AND CAQ SOFTWARE

Received: 27 June 2016 / Accepted: 11 September 2016

Abstract: *The main objective of the paper is to establish a method for testing how the post-operative cranial implant's position corresponds to the CAD designed position. The research is based on the segmentation of CT images which yield 3D data for CAI. Surface comparisons of the pre-operative and post-operative implants were made and the material thickness has been examined in order to determine occurring deviations and find the cause of them. The case analysis showed deviations in the locations that could be contributed to the silicone rubber moulding. The deviations were not exceeding the tolerance limits and the implant seemed to fit properly within expected procedure accuracy.*
Key words: *cranial implants, CAQ software, CT scanning, segmentation, surface comparison*

Tačnost inspekcije kranijalnih implanta korišćenjem CT-a i CAQ softvera. *Cilj rada je izbor metode za testiranje odnosno inspekciju položaja lobanjskih implantata nakon ugradnje sa odgovarajućim CAD modelom. Istraživanje je bazirano na segmentaciji CT snimaka neophodnih za CAI . Poređenje pre-operativne i post-operativnog površine modela i debljine je sprovedeno sa ciljem pronalaženja odstupanja i uzroka njihovog nastanka. Analiza slučaja je pokazala tačnu lokaciju devijacija nastalu procesom brizganja u alatu od silikonske gume. Dobijena odstupanja su u granicama tolerancije a tačnost sprovedenog postupka je zadovoljavajuća.*
Ključne reči: *kranijalni implant, CAQ softver, CT skeniranje, segmentacija, upoređivanje površina.*

1. INTRODUCTION

The main objective is to establish a method for testing how the post-operative implant's position corresponds to the CAD designed position. The data used for this purpose has been obtained through digital images made by a CT scanner and three dimensional CAD models are generated after the process of segmentation. It will be determined if the segmentation of these images yield enough 3D data for the actual inspection of dimensional accuracy and the position of the implant [1].

In most of the scientific articles concerning this subject, the focus is mainly on the mechanical properties of the implant both before and, most of the time, after the operation. Properties such as stress, strain... are being analyzed under the conditions of a certain applied force [2]. In this paper, the variations of cranial implants before and after surgery will be analysed based on the displacement, shape, positioning, etc. The position of the implant will also be compared to the CAD designed position.

2. DESCRIPTION OF THE PROBLEM

In order to be able to produce the physical model of the implant, a couple of steps need to be completed. At first, the patient will be selected and he will have to undergo a couple of scanning sessions. These images are a source of information regarding the contour of the cranial damage. This allows for a thorough evolution of the cranium before the operation takes place, making an implant of great precision possible. The data from these digital images will be processed and segmentation will be performed with software.

3. PRODUCTION PROCESS

For the design of cranial implants, two aspects must be taken into account: biocompatibility, which is determined by the choice of material and patient customization. For medical purposes, scans can either be made by computed tomography (CT) or magnetic resonance (MR). The images made with CT or MR are segmented to segregate the bone or tissue of interest from the rest. These images are converted in a file format called DICOM, which represents the 2D cuts and will be transferred to the additive manufacturing. DICOM file was imported in to the software for segmentation EBS (Ekliptik, Slovenia) [3], the two dimensional image data is used to generate a 3D model as indicated in Fig.1.

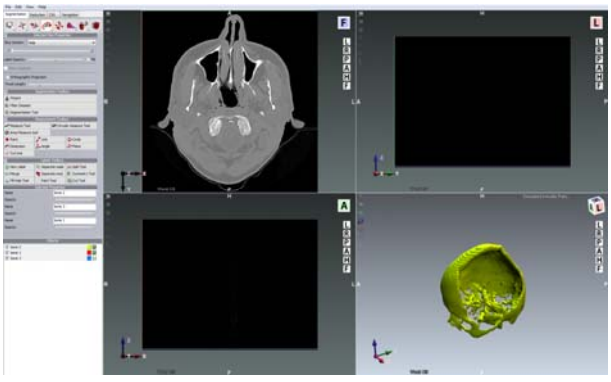

Fig. 1. EBS segmentation software

Another important factor for the generation of a three dimensional model is the Hounsfield value. The software, EBS, always gave a standard value of 150, which is a normal value for soft tissue. Using this value, the selected ROI (Region of Interest) surrounding the entire cranial tissue. When raising this value until +700 the ROI got smaller and the three dimensional model had thinner tissue, leaving even openings in this model. Raising the value until +1000, the skull was partially visible in both cases.

The step following the segmentation is to convert the DICOM file to an STL file (structure triangulation language) in order to generate a format usable for additive manufacturing. The software used for conversion in this case is also EBS. STL file approximates the surface of a solid model with mesh of triangles. For cranial implants, this is usually a polygon mesh. The purpose of these triangles is to depict as accurately as possible the geometry of the implant and the patient's cranium. The STL file contains data usable for the Additive Manufacturing system to produce the physical model.

The analysis of deviations has been performed with the help of GOM Inspect [4]. Displacements of the implant and the surrounding bone tissue can be visually interpreted based on colour-coded maps.

4. RESULTS

As seen in the picture, all of seven post-operative models have a different quality. Some of the models were built with the images stacked from bottom to top and others were generated from right to left as indicated in Fig.2.

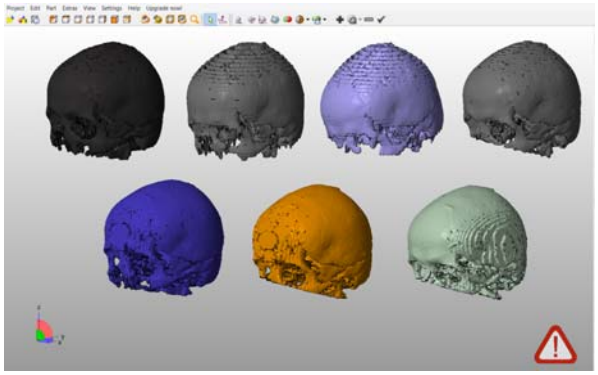

Fig. 2. Post-operative CT segmentation results

Models on the top rows looks quite good and usable for analysis, since the staircase shape is only visible at the top of the cranium and almost not on the implant. The left and middle models on the bottom row are stacked differently than the ones on the top row. They also have a distinct staircase shape, only that now it is placed in a different direction. For the one on the right slide, bottom row, it is visible that the slices were stacked differently than all of the previous models. In this article, the first model on the left on the top row was eventually chosen for further analysis in GOM inspect.

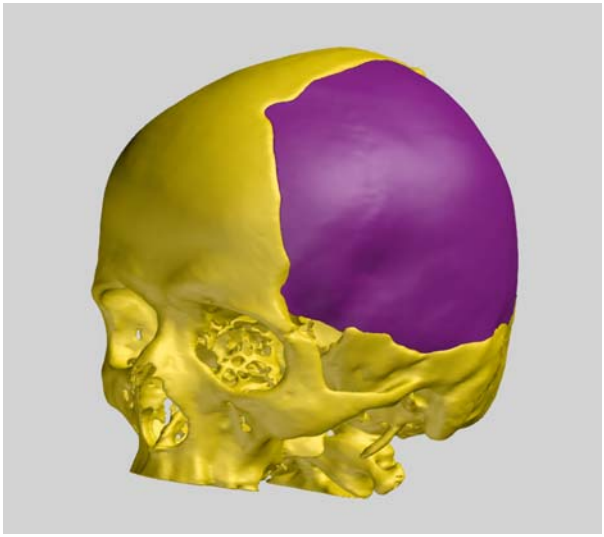

Fig. 3. Nominal CAD data

At first, there a surface comparison of the actual and nominal data was made (Figure 3) aligned with the global fit. The first maximum value that was put is 5 mm. The regions overall colored in green means that these areas there are not or only minor deviations. Yellow colored regions are visible on the implantant, which points out that there are minor- deviations in this region. It is normal to have some deviations due to the fact that the implantation itself can never be carried out exactly as planned with the pre-operative planning in the software.

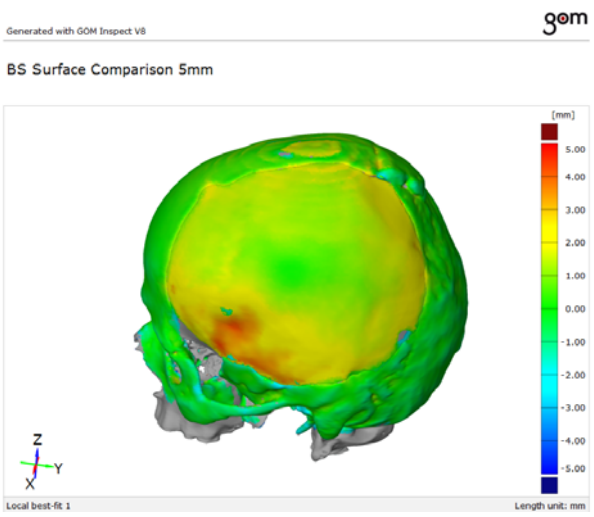

Fig. 4. Global best-fit comparison

There are no dark colored regions visible in either red or blue, which means there are no places where the deviations exceed the given maximum or minimum deviations and the implant was manufactured and fixed in a proper way. The second maximum value that was put is 3 mm. There are also dark colored regions, which mean there are places where the deviations exceed the given maximum deviations as indicated in Fig.4.

The yellow zone is also probably due to the fact that the implants are manufactures through silicone rubber moulding. Problem is that pressure is only being exerted from one direction, perpendicular on the base of the mould. Since the region in the middle of the

implant is being pressed against the base where there is almost no movement, it is located in the green zone.

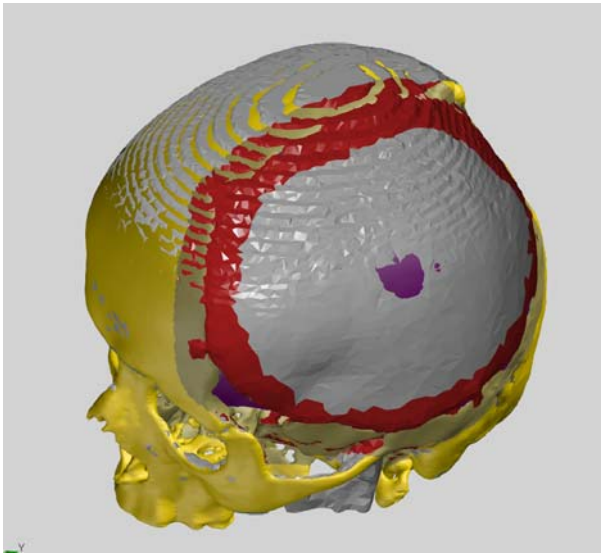

Fig. 5. Local best-fit area

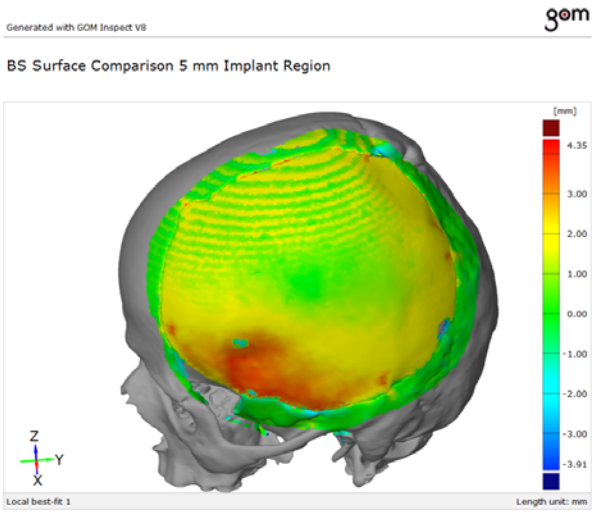

Fig. 6. Local best-fit surface comparison

All of these comparisons were made for global fits, but might as well be done for local fits. This means the selected area where the transition from skull to implant takes place (Figures 5 and 6).

There are no major differences in between the deviations if the global and local best-fit colored maps are compared to each other. The most critical region is still located around the temples and the deviations are in line with each other.

To get an even more precise view on the deviations on the implant, it is possible to leave the implant as nominal data. This means not the entire mesh will be used for analysis, but only the part corresponding to the implant as CAD-body. With the upper and lower limit put at 5 mm again, the corresponding surface comparison looks quite alike again (Figure 7 and 8). The only minor difference might be that at the top edge of the implant there are no or only negligible deviations.

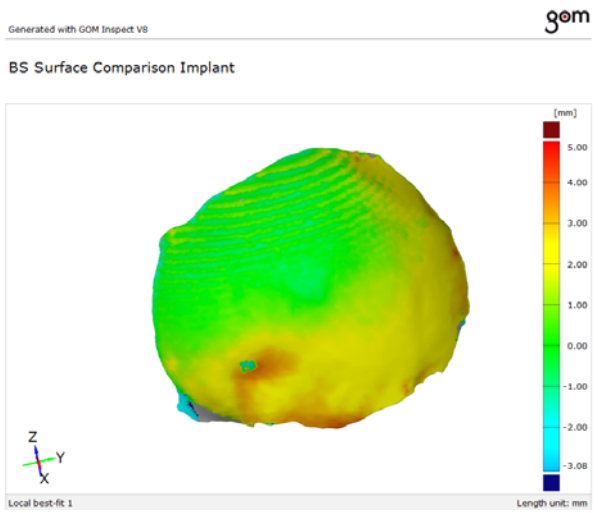

Fig. 7. Implant deviations (outside)

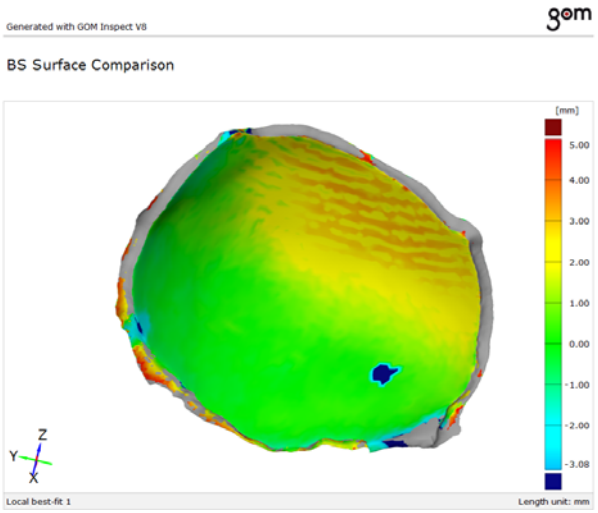

Fig. 8. Implant deviations (inside)

Since the implant has a concave shape, the pressure will deform the implant's shape and it will bend open on the sides. The more concave the implant is, the bigger the deformation will be. In these cases, the deformation is around 1 mm. A solution for future cases could be to exert pressure from the sides as well in order to equalize these deformations.

The deviations might also be the result of the material being too thick at certain places. If in future analysis of other cases with cranio maxillofacial surgery almost the same kind of deviations at almost the same places would return, it might be considered to check the manufacturing process. As in the surface comparison, it is also really easy to adjust the values of the upper and lower limits and get a clear visualization of this.

The area with a notably bigger deviation is located in the same place regardless of the registration method and could be due to bone growth, but this does not affect the functionality of the implant. Overall, the deviations are acceptable and guarantee a good fixation of the implant.

5. DISCUSSION

When taking a closer look to the results, there is one

visual aspect that returns in every one of the figures. It can be seen that the inside region of the cranial implant is colored in green, while the area towards the edges of the implant is yellow.

Although it is not possible to draw general conclusions from results of a single case, this is probably due to the fact that the implants are manufactured through silicone rubber moulding. In this process, the material is poured over the desired shape and pressure will be exerted. The problem is that this pressure is only being exerted from one direction, perpendicular on the base of the mould. Since the region in the middle of the implant is being pressed against the base where there is almost no movement, it is located in the green zone of the legend bar. On the sides of the mould there are only openings to drain the excess material.

Since the implant has a concave shape, the pressure will deform the implant's shape and it will bend open on the sides in a way that results in a flatter shape. The more concave the implant is, the bigger the deformation will be. In these cases, the deformation is around 1 mm which is quite big for something only due to the production process. A solution for future cases could be to exert pressure from the sides as well in order to equalize these deformations.

6. CONCLUSION

If the surface comparisons of future cases give the same deviations, thus the green coloured centre without deviations surrounded by a yellow region with occurring displacements, then the division of pressure on the mould in the production process can be reassessed. This would provide a more concave shape like intended instead of a flatter implant.

It can be concluded that if the results of the analyses of future cases would be comparable, the above described method could be used for trustworthy inspection of the dimensional accuracy and the implant its position.

7. REFERENCES

[1] Drstvensek, I., Ihan Hren, N., Strojnik, T., Brajlih, T., Valentan, B., Pogacar, V., Zupancis Hartner, T., Drstvensek, I.: *Applications of Rapid Prototyping in Cranio-Maxilofacial Surgery Procedures*, International Journal of Biology and Biomedical Engineering, Vol. 2, No. 1, pp. 34-35, 2008.

[2] Lohfeld, S., McHugh, P., Serban, D., Boyle, D., O'Donnell, D., Peckitt, N.: *Engineering Assisted Surgery: A route for digital design and manufacturing of customised maxillofacial implants*, Journal of Materials Processing Technology, Vol. 183, No. 2-3, pp. 333-338, 2007.

[3] Home website of Ekliptik company: [Internet]. Ekliptik d.o.o.. Avaliable at: http://www.ekliptik.si/client.en/index.php [11.02.2016].

[4] Home website of GOM company: [Internet]. Topomatika d.o.o. Avaliable at: http://www.gom.com/index.html [8.04.2016].

Authors:

Dr. Tomaž Brajlih, Dr. Tomaž Irgolič, Urška Kostevšek, Prof. dr. Jože Balič, Prof. dr. Igor Drstvenšek, University of Maribor, Faculty of Mechanical Engineering, Smetanova ulica 17, 2000 Maribor, Slovenia, Phone.: +386 2 220 7596, Fax: +386 2 220 7990.

Dr. Ivan Matin, Prof. dr. Miodrag Hadžistević, University of Novi Sad, Faculty of Technical Sciences, Trg Dositeja Obradovica 6, 21000 Novi Sad, Serbia, Phone.: +381 21 485 2350, Fax: +381 21 454-495.

E-mail: tomaz.brajlih@um.si
tomaz.irgolic@um.si
urska.kostevsek@um.si
joze.balic@um.si
igor.drstvensek@um.si
matini@uns.ac.rs
miodrags@uns.ac.rs

Journal of Production Engineering
Vol.19 No.2
JPE (2016) Vol.19 (2) Original Scientific Paper
Štrbac, B., Radlovački, V†., Ačko, B., Spasić – Jokić, V., Župunski, Lj., Hadžistević, M.

THE USE OF MONTE CARLO SIMULATION IN EVALUATING THE UNCERTAINTY OF FLATNESS MEASUREMENT ON A CMM

Received: 04 August 2016 / Accepted: 11 October 2016

Abstract: *Due to their flexibility, precision, accuracy and level of automation, coordinate measuring machines are a leader among measuring instruments in production metrology. As they are essentially based only on sampling coordinates of points, they can measure any macro- tolerance indicated on the drawing. Among different form tolerances, flatness tolerance is the one that is often present in technical documentation. Although CMMs have metrological characteristics of high quality, these measuring instruments are not without measurement error. Since measurement error is generally unknown in practice, measurement uncertainty is considered a quantitative indicator of measurement error. It is generally believed that Monte Carlo simulation is the best method for numerical evaluation of measurement uncertainty. This paper presents a developed model for the evaluation of measurement uncertainty in the process of measuring flatness on a CMM. The presented model is used with a concrete measuring machine and concrete workpiece.*
Key words: *flatness, measurement uncertainty, coordinate measurement machine, Monte Carlo simulation*

Primena Monte Karlo simulacije u oceni nesigurnosti merenja ravnosti na KMM. *Zbog svoje fleksibilnosti, preciznosti, tačnosti i nivoa automatizovanosti koordinatne merne mašine zauzimaju lidersku poziciju među mernim instrumentima u proizvodnoj metrologiji. Kako se u osnovi baziraju samo na uzorkovanju koordinata tačaka mogu da izmere bilo koju makro toleranciju naznačenu na crtežu. Među različitim tolerancijama oblika, toleranija ravnosti je često prisutna na tehničkoj dokumentaciji. Iako se odlikuju visokim metrološkim karakteristikama ovi merni instrumenti poseduju grešku merenja. Pošto je u praksi greška merenja generalno nepoznata, kao kvantitativni pokazatelj greške merenja daje se merna nesigurnost. Opšte je mišljenje da je Monte Karlo simulacije najbolji metod za numericko ocenjivanje merne nesigurnosti. U ovom radu će biti prikazan razvijeni model, za konkretnu mernu mašinu i radni predmet, za procenu merne nesigurnosti pri merenju ravnosti na KMM.*
Ključne reči: *ravnost, merna nesigurnost, koordinatna merna mašina, Monte Karlo simulacija*

1. INTRODUCTION

Due to their flexibility, precision, accuracy and level of automation, coordinate measuring machines (CMMs) are a leader among measuring instruments in production metrology. With adequate equipment, coordinate measuring machines can be used for measuring any macro- tolerance indicated in technical documentation since a CMM basically perceives only coordinates of those points which are on the surface of the measured object. When the coordinates of points have been determined, an independent software analysis is performed to determine associative geometry of the workpiece using basic geometric primitives (line, circle, plane, etc.) The associative elements are determined by means of applying appropriate algorithms to the coordinates of the sampled points.

Flat form is one of the most frequent forms whose specification has to be checked. After sampling the total number of points, flatness error can be determined according to two associative criteria: least squares (LS) and minimum zone (MZ) [1]. The LS method is more superior in comparison to the MZ method from the aspect of simplicity and duration of calculating. The LS generally overestimates the shape error which can result in dismissing good parts. On the other hand, the MZ tends to underestimate the shape error and is very sensitive to peaks which can, if they go unnoticed, lead to bad results. The LS does not follow the standards carefully and cannot guarantee that the minimum zone solution is specified in the standard [2, 3]. The standard recommends that the form tolerances should be evaluated based on the concept of the minimum zone, but it does not offer the methodology of evaluation, so the MZ solution is not uniform. There are more than ten different approaches to flatness evaluation based on the minimum zone method [4-6]. For the purpose of investigation in this paper, the LS method will be used. The evaluation will be performed using the LS method.
Every measurement is subject to uncertainty. The measurement result makes sense only when it is accompanied by a statement of uncertainty. GUM defines uncertainty as a parameter associated with the result of measurement that characterizes the dispersion of the values that could reasonably be attributed to the measurand [7]. Uncertainty can be described as a probability distribution of the values of the measured quantity which enables the determination of the limits of the measured quantity with any level of confidence. These limits define the so-called expanded uncertainty.
The evaluation of measurement uncertainty in CMM measurements is a complex task due to a number of factors and their interactions which affect it. It is

generally believed that Monte Carlo simulation is the best method for numerical evaluation of uncertainty. Therefore, this simulation method is applied in the evaluation of uncertainty when measuring flatness on a CMM.

2. METHODOLOGY

The use of Monte Carlo simulation for evaluating uncertainty of CMM measurements is currently in the focus of investigation. Numerous models and approaches have been developed for that purpose. A pioneer in the field is the VCMM (Virtual Coordinate Measuring Machine) developed by PTB (Physikalisch-Technische Bundesanstalt) [8]. The VCMM works on the principle of imitating the measuring strategy and physical behavior of a CMM in virtual reality (Figure 1). The role of Monte Carlo method is to randomly sample probability density functions that describe possible scenarios of the factors that influence measurement uncertainty. The result of this is several thousands of simulation measurement results whose 95% confidence interval represents the expanded measurement uncertainty. Input parameters are usually allocated an adequate probability density function. A similar principle has been applied in the development of the expert CMM [9]. Generally, the use of simulation tools for the evaluation of measurement uncertainty on a CMM is identical with the operation of a real CMM. Actually, its operation can be divided into two steps. The first step is determining the uncertainty of the sampled points, whereas the second step is the propagation of these uncertainties through the part program. Therefore, special attention is paid to the modeling of hardware errors of CMMs which are the commonest reason of uncertainty of a sampled point. In order to determine the uncertainty of sampled points, Gaska used the laser system Laser Tracker [10] for geometric errors of a CMM and for measuring the reference sphere for sensor errors. To define hardware errors of CMMs, Kruth used the measurement results obtained with a laser interferometer for twenty-one geometric errors and sensor errors from verification tests [11]. Although these models proved to be efficient in evaluating measurement uncertainty, their development is not simple since it requires time-consuming experiments. However, there are investigations whose focus was not on modeling point uncertainty, but Monte Carlo simulation was applied efficiently anyway. Dhanish introduced a simplification, considering that the uncertainties of the measurement points are independent, identical, characterized by normal distribution and equal to the specified standard uncertainty of a CMM [12]. Wen introduced the same assumption, with the uncertainty value being evaluated from the measuring equipment (CMM) and measurement environment [13].

After the first step has been defined, it is necessary to define a criterion for determining results, i.e. for determining associative geometry-step 2 (Figure 1). Unlike the previous models, in this paper, a simulation model for the evaluation of measurement uncertainty in measuring flatness was developed whose input quantities (x, y, z coordinates of the sampled points) are based on the repeatability of the sampled point. Namely, the uncertainty of coordinates of points is described by an adequate probability density function based on the repetition of the sampled point on the examined surface.

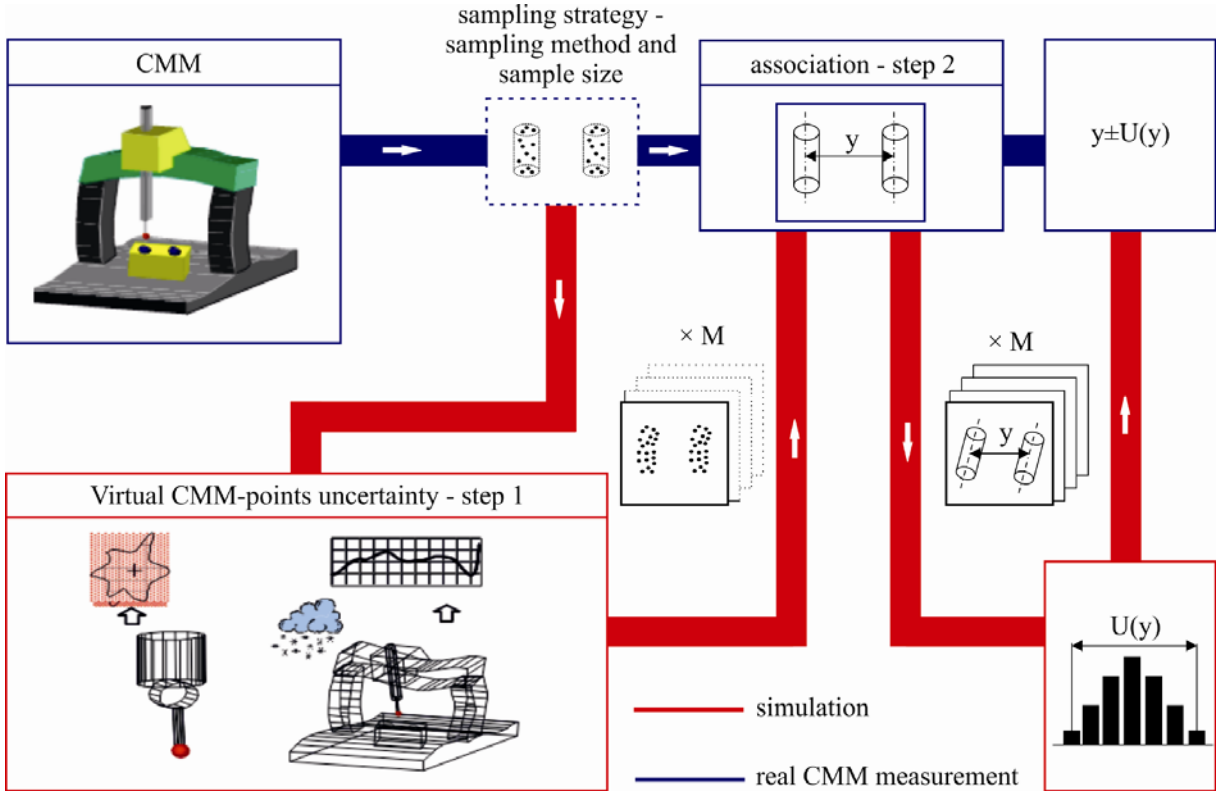

Fig. 1. Concept of Virtual Coordinate Measuring Machine

Likewise, the model involves the influence of shape error using an adequate distribution function. Earlier researches have shown that the shape error, in interaction with the number and position of the measured points, represents a factor that influences measurement uncertainty to a great extent [11, 14]. The inputs in the model which are defined this way will contain CMM hardware errors in the interaction with the environment. However, this pilot study is restricted to a concrete measurement location, measurement strategy and workpiece. Namely, the study was conducted on optical glass whose form error is defined in calibration certificate. For the defined number of points in the measurement strategy and the position of the workpiece in the measurement volume, each point was sampled ten times. Checking for normality showed that the repeatability of each point can be described using normal distribution. Added to this, a uniform distribution which describes the shape error of the workpiece was added to z variable. From the mentioned distributions, *N* Monte Carlo samplings were generated with the aim of obtaining N least squares reference planes from which *N* flatness error was determined. 2.5% quantile and 97.5% quantile were used to define the 95% interval of the expanded uncertainty. The difference of these percentages is the width of the uncertainty interval. The proposed model was tested according to ISO-15530-4 [15].

3. VERIFICATION OF THE PROPOSED MODEL

The model was tested on optical glass which represents the standard of flatness with *d*=50mm and specified flatness error y_{cal}=0.068µm. Flatness calibration was carried out with Zygo Verifier MST interferometer and the result was *Ucal*=0.02µm. The measurement was performed on Carl Zeiss UMS 850 coordinate measuring machine in the Laboratory for Dimensional Metrology at the Faculty of Mechanical Engineering in Maribor. The maximum permissible error (MPE_E) was 2.1+L/330 µm (*L* is the length expressed in mm). The workpiece was measured in ten points Based on *m* = 10 repeated measurements of coordinates for each point, normal distributions for x_i, y_i, z_i (*i*=1,2,3,...,10). Gaussian distributions were defined based upon the calculated mean values $\bar{x}_i$, $\bar{y}_i$, $\bar{z}_i$ and standard deviations σ_{x_i}, σ_{y_i}, σ_{z_i}. For each distribution, a sample of N elements (N=1000) was generated (simulated). For the first out of the total N sampled values of coordinates of points, from the defined distributions, an equation of the reference plane was determined by the method of least squares. Flatness error was then determined based on this equation (Figure 2). The next step was taking the second sampled value (x_1, y_1, z_1),..., (x_n, y_n, z_n) so the coordinates of new i points were obtained on the basis of which fitting was performed in order to find a new equation of the plane. A new flatness error for the new equation of the plane was determined by the least squares method.

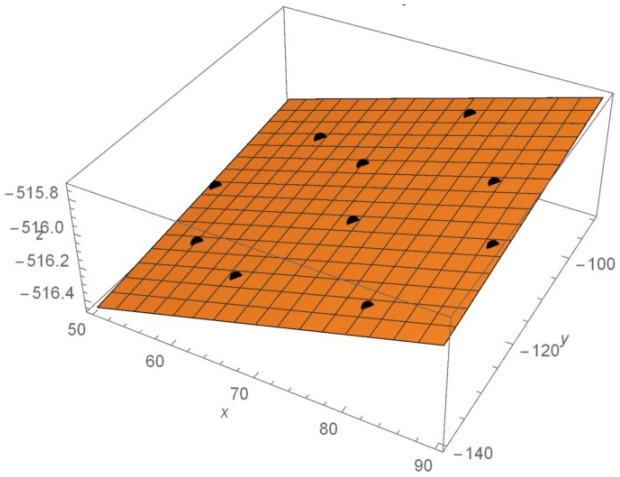

Fig. 2. Determination of LS reference plane and flatness error

The procedure was repeated for all *N* sampled values from the Gaussian distributions so the result was N equations of the plane and *N* values for flatness error. Based on the N values of flatness error, a histogram of frequencies was constructed (Figure 3). The measurement uncertainty amounted to *U* = 0.001135mm for 95% probability (*k*=2).

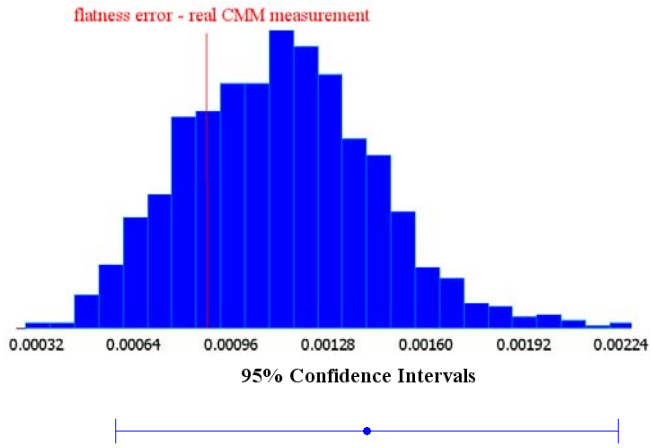

Fig. 3. Distribution of flatness errors from Monte Carlo simulation, 95% confidence interval and flatness error value obtained with a CMM software

3.1. Testing the proposed model

In accordance with ISO 15530-4:2011 recommendation which refers to the method of testing software for evaluation of uncertainty, the measurement results were tested in relation to the expanded uncertainties estimated by the proposed model. It was necessary to meet the following criterion:

$$\frac{\left|\bar{y} - y_{cal}\right|}{\sqrt{U_{cal}^2 + U^2}} = 0.69 \leq 1 .$$

According to the results of the experiment which involved measuring and evaluation of flatness error on a CMM several times with the aim of finding $\bar{y}$ the criterion was met. Thus, it can be concluded that the proposed model gives reliable evaluation of measurement uncertainty on a CMM.

4. CONCLUSION

A measurement result is incomplete if it is not accompanied by a statement of uncertainty and compliance/non-compliance with the specification cannot be proved without it. Monte Carlo method is a very efficient simulation tool for the evaluation of measurement uncertainty, especially in CMMs because of a number of factors and their interactions which affect uncertainty. The use of Monte Carlo method implies the development of a mathematical model of the measurement process. This paper includes a model developed for the evaluation of uncertainty in measuring flatness, based on the repeatability of the sampled coordinate of a point. The proposed model was verified on the standard for flatness - optical glass. The testing recommended by the standard proved the validity of the model. Further research will focus on the interaction of CMM uncertainty with the size of sampling, distribution of sampling and involving different shape deviations as characteristics of the production process.

5. REFERENCES

[1] ISO/TS 12781-2: *Geomatrical product specifications (GPS) – Flatness – Part 2: Specification operators*, ISO, Geneve, 2011.

[2] Badar, M.A., Raman, S., Pulat, P:S.: *Intelligent search – based selection of sample point for straightness and flatness estimation*, Journal of Manufacturing Science and Engineering, Vol. 125, p.p. 263-271, 2003.

[3] Samuel, G.L., Shunmugam, M.S.: „*Evaluation of straightness and flatness error using computational geometric techniques*“, Computer Aided Design, Vol. 31, p.p. 829–843, 1999.

[4] Calvo, R., Gomez, E., Domingo, R.: „*Vectorial method of minimum zone tolerance for flatness, straightness, i their uncertainty estimation*“, International Journal of Precision Engineering and Manufacturing, Vol. 15, p.p. 31-44, 2014.

[5] Weber, T., Motavalli, S., Fallahi, B., Cheraghi, S. H.: *A unified approach to form error evaluation*, Precision Engineering, Vol. 26, p.p. 269-278, 2002.

[6] Radlovački, V., Hadžistević, M., Štrbac, B., Delić, M., Kamberović, B.: *Evaluating minimum zone flatness error using new method - Bundle of plains through one point,* Vol. 43, p.p. 554–562, 2016.

[7] ISO/IEC Guide 98-3:2008: „*Uncertainty of measurement – Part 3: Guide to the expression of uncertainty in measurement (GUM:1995)*“. ISO/IEC, 2008.

[8] Trenk, M., Franke, M. & Schwenke, H.: *The "virtual CMM" a software tool for uncertainty evaluation - Practical application in an accredited calibration lab*, In ASPE Summer Topical Meeting on Uncertainty Analysis in Measurement and Design. State College, Pennsylvania, USA, 2004.

[9] Balsamo, A., Di Ciommo, M., Mugno, R., Rebaglia, B.I., Ricci, E., Grella, R.: Evaluation of CMM Uncertainty Through Monte Carlo Simulations, CIRP Annals - Manufacturing Technology Vol. 48, No. 1, pp. 425-428, 1999.

[10] Sladek, J., Gaska, A.: *Evaluation of Coordinate Measurement Uncertainty with Use of Virtual Machine model based on Monte Carlo Method*, Measurement, Vol.45, pp. 1565-1575, 2012.

[11] Kruth, J.P., Van Gestel, N., Bleys, P., Welkenhuyzen, F.: *Uncertainty determination for CMMs by Monte Carlo simulation integrating feature form deviations*, CIRP – Manufacturing Technology, Vol. 58, pp. 463-466, 2009.

[12] Dhanish, P.B., Mathew, J.: *Effect of CMM Point Coordinate Uncertainty on Uncertainties in Determination of Circular Features*“, Measurement, Vol. 39, p.p. 522-531, 2006.

[13] Wen, X-L., Zhu, X-C., Zhao, B-Y., Wang, D-X, Wang, F-L.: *Flatness error evoluation and verification based on new generation geometrical product specification (*GPS), Precision Engineering, Vol. 36, p.p. 70-76, 2012.

[14] Choi, W., Kurfess, T.R., Cagan, J.: *Sampling uncertainty in coordinate measurement data analysis*, Precision Engineering, Vol. 22, pp. 153-163, 1998.

[15] ISO, 2004. ISO/TS 15530-4:2011: *Geometrical Product Specifications (GPS) – Coordinate measuring machines (CMM): Technique for determining the uncertainty of measurement – Part 4: Evaluating task-specific measurement uncertainty using simulation*, ISO, 2011

Authors: **Assist. Štrbac Branko, MSc; Professor Hadžistević Miodrag, PhD,** University of Novi Sad, Faculty of Technical Sciences, Department of Production Engineering, Trg Dositeja Obradovića 6, 21000 Novi Sad, Serbia.
e-mail: strbacb@uns.ac.rs
miodrags@uns.ac.rs

Professor Spasić – Jokić Vesna, PhD; Research Trainee Župunski Ljubica, PhD University of Novi Sad, Faculty of Technical Sciences, Department of Power, Electronic and Telecommunication Engineering, Trg Dositeja Obradovića 6, 21000 Novi Sad, Serbia.
e-mail: svesna@uns.ac.rs
ljubicaz@uns.ac.rs

Assoc. Professor Radlovački Vladan, PhD, University of Novi Sad, Faculty of Technical Sciences, Department of Industrial Engineering and Management, Trg Dositeja Obradovića 6, 21000 Novi Sad, Serbia.
e-mail: rule@uns.ac.rs

Professor Ačko Bojan, PhD, University of Maribor, Faculty of Mechanical Engineering, Maribor, Slovenia.
e-mail: bojan.acko@um.si

Journal of Production Engineering
Vol.19 No.2
JPE (2016) Vol.19 (2) Original Scientific Paper
Puškar, S., Šokac, M., Milovančev, A., Budak, I.

APPLICATION OF MULTIDETECTOR COMPUTER TOMOGRAPHY IN ACQUISITION OF CORONARY ARTERIES

Received: 22 June 2016 / Accepted: 14 September 2016

Abstract: *MSCT coronary angiography is a noninvasive diagnostic procedure that allows an accurate and precise assessment of the degree of narrowing of the coronary vessels as well as the type of plaque. Further development of methods of recording the training apparatus, introducing the use of a scanner with the dual source technology as well as the proper selection of patients take to be more precise estimate of the degree of stenosis in coronary arteries.*
Key words: *Cardiology, multislice computed tomography, coronary angiography*

Primena tehnologije multidetektorskog skenera za snimanje koronarnih krvnih sudova. *MSCT koronarografija je neinvazivna dijagnostička procedura koja omogućava tačnu i preciznu procenu stepena suženja koronarnih krvnih sudova kao i vrste plaka. Dalje usavršavanje metode snimanja kroz usavršavanje aparata, uvođenjem u upotrebu skenera sa "dual source" tehnologijom kao i pravilan odabir pacijenata dovode do sve tačnije procene stepena stenoze koronarnih arterija.*
Ključne reči: *Kardiologija, multi-slajs kompjuterizovana tomografija, koronarna angiografija*

1. INTRODUCTION

Modern developments in the field of radiology enabled the improvement of diagnostic procedures in all areas of medicine.

The emergence of multi-slice computerized tomography (MSCT) with 16-slice and the subsequent 64, 128 and 256-slice devices with a multidetector scanners, and a possible layer thickness (resolution) of 0.3 to 0.6 mm, has led to significant changes in the diagnostic methods of coronary heart disease.

2. DEVELOPMENT OF MSCT

The first multi-slice CT scanner ELSCINT Twin was developed in 1991 [1]. It was a two-slice scanner, which is made during each rotation of the two sections. This technology has developed rapidly, and soon 4-slice was put into operation, then a 16-slice, 64, 128 and 256-slice [1]. The emergence of dual source technology, with two X-ray sources and the use of multislice detectors that are positioned opposite of each other and at a 90 degrees from each other, continually rotating around the patient during scanning, enabled shorter scanning time (and also the time in which is necessary that the patient holds his breath) and provided a better image of tested blood vessels (Figure 1) [2].

3. TECHNICAL BASICS OF MSCT TECHNOLOGY

CT scanners have an X-ray source and a detector placed opposite one another which are continuously rotating around the patient. Recordings (scans) are made when patient is moving through the opening apparatus (gentry), as shown in Fig. 2. A computer processes data obtained from images and, based on them, creates a three-dimensional (3D) volumetric model. Formed 3D object can then be seen from different angles, perspectives and different sections [3].

3D object that can be seen on a workstation is made up of a series of three-dimensional pixels (called voxels), the size of which depends on the resolution of the scanner. Voxel is shown in different shades of gray (from black to white) which represent the level of attenuation of X-rays, depending on the type of tissue through which the X-ray beam had passed. Bone and calcium (which is especially important in the diagnosis of coronary heart disease) imply a higher level of attenuation, which appears in white color on the image. The air is characterized by a very low level of attenuation, which represents voxels in black. A smaller voxel size corresponds to a higher resolution scanner as it depends on the X-ray sensor resolution, and not the number of sections. By increasing the number and size of the detector (multidetector MSCT), as well as speeding up the rotation apparatus (gentry) around the patient, images with better quality are obtained.

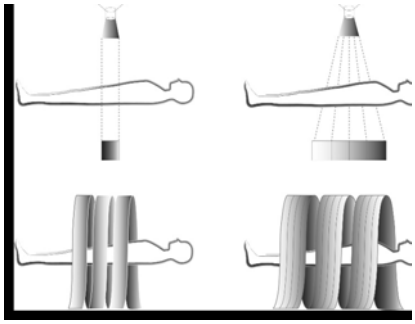

Fig. 1. The difference between single and multislice scanner

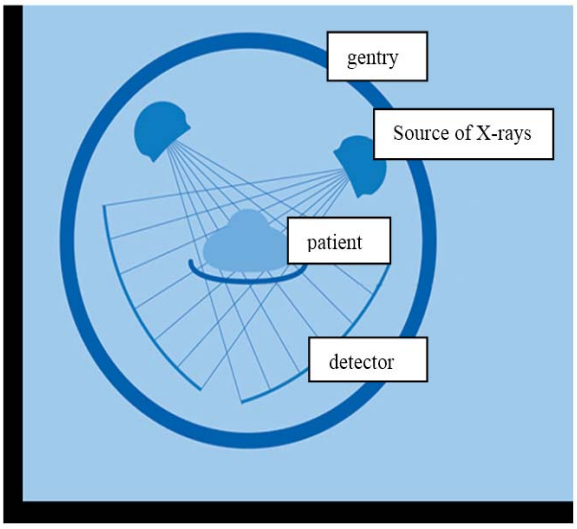

Fig. 2. ECG triggering and reducing radiation

4. APPLICATION OF MSCT SCANNERS IN CARDIOLOGY

The specificity of the coronary arteries imaging in relation to the recording of other organs lies in the fact that the heart and the organs keeps moving. For this reason, it is much harder to get an adequate image. To use this technology for shrinkage evaluation of the blood vessels, the scanning is performed only in a certain phase of the cardiac cycle - in late diastole. This is the phase where the heart muscle is least moving. For this reason ECG-triggering is introduced. Scanning in a certain part of diastole (late diastole) and cardiac triggering or ECG gating (Eng. Prim. Aut.) is a very important factor for obtaining high-quality images of coronary arteries (Fig. 3 and 4) [4].

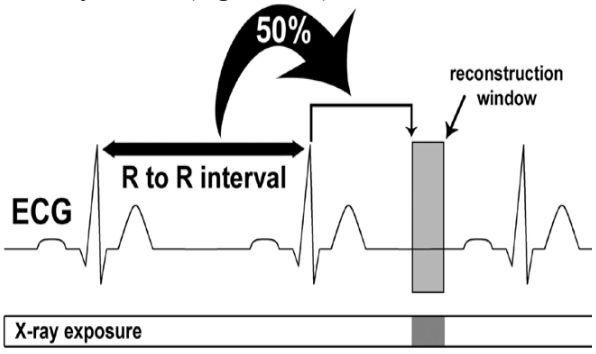

Fig. 3. ECG gating during CT coronary angiography

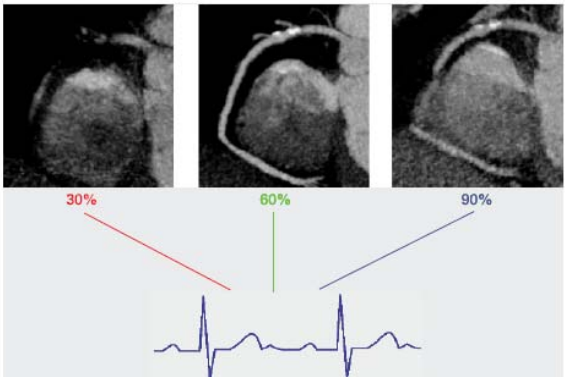

Fig. 4. The process of image reconstruction at various diastole stages

The apparatus registers R prong during the ECG (systole). Scanning is carried out after a certain (programmed) break, when the heart comes in late diastole, which results in rendered images with much less artifacts on them (Fig. 4).

5. RADIATION DOSES DURING MSCT CORONARY ANGIOGRAPHY

In the beginning of the application of MSCT technology, the level of radiation that the patient received was significantly higher, compared to conventional angiography (invasive coronary angiography), where the radiation dose was up to 21 mSv [5]. The "CORE" study in 2006 (comparing CT coronary angiography with invasive coronary angiography) showed a mean effective radiation dose of 16 mSv for men and for women 15 mSv [5]. In "PROTECTION I" study an average radiation of 12 mSv was obtained [5].

During the diagnostic invasive coronary angiography, moderate doses are ranging from 2.5 up to 10 mSv [5]. The introduction of EKG triggers technology during the MSCT coronary angiography, the scanning is performed only in a certain part of the cardiac cycle (diastole portion) and by reducing the voltage tube, it can achieve reduced radiation dose of up to 90% [5]. Typical effective doses of radiation at different diagnostic procedures are shown in Table 1.

PROCEDURE	Efective dose (mSv)
MSCT coronary angiography	6 – 25
Invasive coronary angiography	2.1 - 6
MSCT of the chest	5-7

Table 1. Effective radiation dose during various diagnostic procedures

6. THE IMPORTANCE OF MSCT CORONARY ANGIOGRAPHY IN CLINICAL PRACTICE

The tendency of modern medicine is that during the diagnostic procedure it resorts in less invasive procedures with the use of diagnostic and therapeutic methods that do not require hospitalization. MSCT coronary angiography, as a noninvasive diagnostic technique, enables evaluation of coronary vessels narrowing and different types of plaque, without hospitalization of patients and without any serious complications (death, acute myocardial infarction, cerebrovascular accident) and with a significant reduction in cost, in relation to invasive coronary angiography (ICA). Scientific research in the field of application of MSCT coronary angiography in which MSCT coronary angiography and ICA were compared, aimed at testing the degree of correlation of the findings of the two diagnostic procedures. MSCT coronary angiography, as a noninvasive procedure, has become the method of choice for the assessment of coronary circulation for certain patient groups (Fig. 5

and 6). Since the introduction of dual source MSCT coronary angiography technology, this method of visualization of the coronary arteries and the size and type of plaque in blood vessels, has an even more significant role in the diagnosis of patients with angina pectoris [6]. Sensitivity is thereby registered to 95% and specificity of 95% to 75% PPV, NPV 99% [7]. In the world every year a large number of ICA is performed in which there are no observed hemodynamically significant stenosis in the coronary arteries (according to some studies, up to 40%) [7].

In this way, on the one hand, patients are undergoing unnecessary hospitalization, risks and invasive diagnostic procedures with unnecessary costs for the health insurance system. MSCT coronary angiography in such cases could have a dual role. With high accuracy, sensitivity and specificity in younger patients and in patients who have a low Ca score, MSCT coronary angiography could replace the ICA in the diagnosis of coronary heart disease, or detection of stenosis in the coronary blood vessels that are not hemodynamically significant, and also reduce the number of unnecessary ICA procedures. By eliminating patients who have rhythm disturbances, primarily atrial fibrillation, followed by obese patients and those who can't hold their breath long enough, with adequate training of doctors who can read the findings of MSCT coronary angiography, this recording method allows obtaining high accuracy of the findings in assessing the degree of coronary stenosis artery.

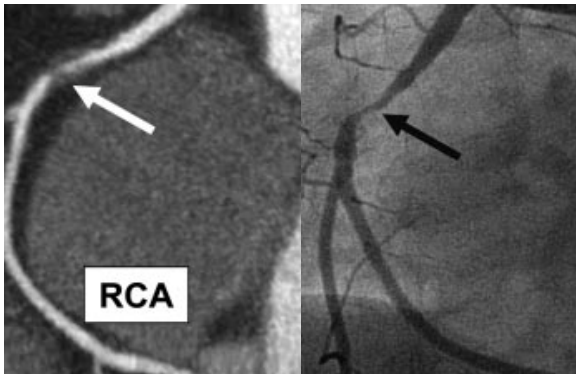

Fig. 5. Correlation between findings of constriction in the right coronary artery MSCT (left) and the ICA (right)

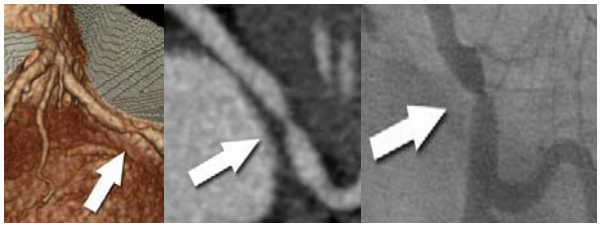
Fig. 6. Correlation between findings on coronary artery narrowing on MSCT (above) and the ICA (below)

The negative findings of MSCT coronary angiography with a high degree of probability excludes the existence of hemodynamically significant coronary artery disease, and patients with such findings should not run ICA. A certain degree of doubt exists with positive findings of MSCT coronary angiography because of the possibility of false positives, which ranges in different studies between 12-15% [8,9]. Further development of scanning methods and perfecting of the apparatus (128 and 256 slice units), with proper selection of patients in the future should lead to a reduction in false positives MSCT coronary angiography and therefore reduce the number of performing unnecessary invasive coronary angiography.

Extensive coronary artery calcification limits the possibility for successful visualization of the coronary blood vessels. Calcified plaques in the walls of blood vessels and high regard Ca score lead to the appearance of artifacts such as the effect of blooming and reflection, which significantly limit the quality assessment of the degree of narrowing of the blood vessel. The occurrence of artifacts is due to the fact that high-density objects (calcification) occupy a space that is greater than, or equal to the size of a voxel. As a consequence, it comes to overestimating the degree of stenosis [8]. So far, attempts were committed to reduce the interference in reading the findings, which are due to the presence of calcification. Advanced algorithms for image reconstruction were introduced, but without any significant effect. MSCT technology, image filters, increasing the tube voltage, to some extent reduce the interference. However, in clinical practice calcification in the walls of coronary arteries are still making it difficult to interpret the findings, suggesting that there is a need for further improvement of MSCT angiography for better applications, as well as different programs for better image processing. However, Ca score is closely linked with the emergence of significant hemodynamically narrowing of the blood vessels, so that the finding of calcification on MSCT shows the existence of a significant narrowing [10].

7. CONCLUSION

Multi-slice computed tomography of coronary arteries represents a reliable diagnostic method for the assessment of coronary blood vessels. It has a high sensitivity and specificity compared to conventional invasive coronary angiography. Further development of scanning methods, perfecting of the apparatus and by introducing the use of a scanner with the dual source technology as well as the proper selection of patients, are leading to a more precise estimation of the degree of stenosis of coronary arteries using MSCT technology.

8. REFERENCES

[1] Flohr, T.G., McCollough, C.H., Bruder, H.: First performance evaluation of a dual source CT (DSCT) system, Eur Radiol, Vol 16, p.p 256–68, 2006.

[2] Greuter, M.J.Q., Flohr, T., van Ooijen, P.M.A.: A model for temporal resolution of multidetector computed tomography of coronary arteries in relation to rotation time, heart rate and reconstruction algorithm, Eur Radiol,Vol 17, p.p 784–812, 2007.

[3] Roberts,W.T., Bax, J.J., Davies. L.C.: Cardiac CT and CT coronary angiography: technology and application, Heart, Vol 94, p.p.781-792, 2008.
[4] Leschka, S., Alkadhi, H., Plass, A., Desbiolles, L., Grunenfelder, J., Marincek, B., Wildermuth, S.: Accuracy of MSCT coronary angiography with 64-slice technology: first experience, Eur Heart J, Vol 26, p.p. 1482–1487, 2005.
[5] Hausleiter, J., Meyer, T., Hermann, F.: Estimated radiation dose associated with cardiac CT angiography, JAMA, Vol 7, p.p. 301:500, 2009.
[6] Andreini,D.: Comparison of the diagnostic performance of 64-slice computed tomography coronary angiography in diabetic and non-diabetic patients with suspected coronary artery disease, Cardiovascular Diabetology, Vol num 9, p.p. 80-90, 2010.
[7] Chow, C.K., Sheth, T.: What is the role of invasive versus non-invasive coronary angiography in the investigation of patients suspected to have coronary heart disease?, Internal Medicine Journal, Vol num 41, p.p. 5–13, 2011.
[8] Hassan, A., Nazir, S.A., Alkadhi, H.: Technical challenges of coronary CT angiography: Today and tomorrow. European Journal of Radiology, Vol num 79, p.p. 161-171, 2011.
[9] Puskar, S.; Test opterecenja, multi-slice kompjuterska tomografija koronarnih krvnih sudova i invazivna selektivna koronarna angiografija u dijagnostici pacijenata sa stabilnom anginom pectoris, PhD dissertation, University of Novi Sad, Medical faculty, Novi Sad, 2013.
[10] Ma, H., Wang, Y., Wen, Z., Liu, Y., Liu, J., Yang, J.: Challenge of coronary artery calcium by 64-multidetector computed tomography, Int J Cardiol, Vol num 168 (5), p.p. 5044- 5049, 2013.

Authors: **dr sci med Slobodan Puškar, dr Aleksandra Milovančev**, Institute for Pulmonary Diseases Vojvodina, Sremska Kamenica, Put dr Goldmana 4. 21000 Novi Sad, Serbia. Phone: +381 21 480 5284.
Assoc. prof. Igor Budak, M.Sc. Mario Šokac, University of Novi Sad, Faculty of Technical Sciences, Trg Dositeja Obradovica 6, 21000 Novi Sad, Serbia, Phone: +381 21 450-366, Fax: +381 21 454-495.

E-mail: puskarslobodan@yahoo.com
marios@uns.ac.rs
lesandra_5@yahoo.com
budaki@uns.ac.rs

Journal of Production Engineering
Vol.19 No.2
JPE (2016) Vol.19 (2) Original Scientific Paper
Reddy, Y.R.M., Prasad, B.S.

SIMULATION OF FORM TOLERANCES USING CMM DATA FOR DRILLED HOLES - AN EXPERIMENTAL APPROACH

Received: 25 August 2016 / Accepted: 15 October 2016

Abstract: *Drilling is one of the important processes for the production of a high-precision workpiece with quality holes. Main areas of application of drilling process are in the defense, aircraft, and automobile industries. In this study, the effect of cutting parameters on the hole quality and tool wear during the drilling of Al7075 and Ti-6Al-4V specimens with HSS and carbide insert drills have been investigated. The dynamic cutting force excites the cutting tool shaft, inducing a vibration/deflection which causes inaccuracy such as hole tolerances and circularity error. The cutting forces can cause tool/workpiece deflection and vibrations, and these vibrations will lead to errors in hole diameter, circularity and cylindricity. Hence, form tolerances in drilled holes need to be monitored and quantified; if not quality drilled holes will be affected. A coordinate measuring machine (CMM) is employed to measure the hole diameters, circularity, and cylindricity. A comparison has been made regarding the quality of the hole between cutting tools based circularity error and cylindricity error. It is observed that there is a decrease of agreement between tool performance and hole quality at high cutting speed and feed rate at different test combinations. A correlation is established between measured and simulated error results. Effect of spindle speed, feed rate, and the vibration amplitude on circularity and cylindricity are critically studied in the present work. The obtained results are quite encouraging, showing a correlation between measured and simulated values.*
Key words: *Coordinate measuring machine (CMM) Circularity error, cylindricity error, tool wear, surface metrology, simulation, drilling.*

Simulacija tolerancija oblika korišćenjem CMM podataka za bušene rupe – eksperimentalni pristup. *Bušenje je jedan od važnih procesa za proizvodnju radnih predmeta visoke preciznosti sa kvalitetnim rupama. Glavne oblasti primene procesa bušenja su u vojnoj industriji, avio industriji i automobilskoj industriji. U ovom radu je istraživan uticaj parametara obrade procesa bušenja na kvalitet rupe i habanje alata pri obradi materijala Al7075 i Ti-6Al-4V burgijama od brzoreznog čelika i tvrdog metala. Dinamična sila rezanja pobuđuje osovinu alata, uvodeći tako vibracije/odbijanje što uzrokuje netačnosti kao što su tolerancije rupe, kružnosti i greška cilindričnosti. Stoga se moraju pratiti tolerancije mera u bušenim rupama, inače će u suprotnom ispoštati kvalitet rupa. Koordinatna merna mašina (CMM) je korišćena radi merenja prečnika rupa, kružnosti i cilindričnosti. Napravljeno je poređenje kvaliteta rupa po kriterijumu greške kružnosti i greške cilindričnosti reznog alata. Primećeno je opadanje poklapanja između performansi reznog alata i kvaliteta rupa kod visokih brzina rezanja i pomaka kod različitih testiranih kombinacija. Uspostavljenja je veza između mernim i simuliranim vrednostima grešaka. Uticaj broja obrtaja, pomaka i amplitude vibracija na kružnost i cilindričnost su kritički istraživani u ovom radu. Dobijeni rezultati su ohrabrujući i pokazuju vezu između merenim i simuliranim vrednostima.*
Ključne reči: *koordinatna merna mašina (CMM), greška kružnosti, greška cilindričnosti, habanje alata, metrologija površina, simulacija, bušenje.*

1. INTRODUCTION

Drilling is one of the fundamental machining processes of making holes, and it is essentially for manufacturing industries like aerospace industry, manufacturing industry, and automobile industry. Especially drilling is necessary for industries in assembly related to mechanical fasteners where hole diameter and circularity error plays a very crucial role. At various machining conditions, quality of the drilling process is studied [1]. Particularly in automotive industry demand for quality requirements is increased high-frequency [2]. Cylindrical, circular, or spherical features are fundamental geometric features in engineering. As precision requirement becomes more stringent, it is not sufficient to consider only size tolerance of circular and cylindrical parts along with their tolerances as well [3]. The cylindrical conditions typically exhibit errors from the ideal design specifications in both the axial and radial directions [4]. The cylindricity error is essentially caused by the roundness error in cross section, the form error such as taper, barrel, banana, and concave in the axial section as well as the diametric variation in the cylindrical section [5].

In modern industry coordinate measuring machine become a basic instrument for modern metrology. It is a universal, fast and accurate device, applicable for various measurement tasks [6] low-frequency and free-form surface as well [7]. Chandrashekhar et al. [8] predicted the roundness error of the drilled workpiece based on helical grooves, but there were discrepancies between theoretical and experimental results. Turgay Kivak et al. [9] an experimental investigation is presented in which error from circularity of the holes is

the result of the deflection, vibration, lack of lubrication and increased tool wear. Azarhoushang and Akbari [10] studied the effect of ultrasonic assisted drilling on the circularity, cylindricity, surface roughness, and hole oversize in Inconel 738-LC work pieces.

Two different types of vibration can be distinguished in drilling, low-frequency vibrations associated with lobed holes and high-frequency vibration (chatter). One of the most common roundness problems in drilled holes is the existence of the spaced lobes [11]. It is also found that lobed hole profiles exist even in the absence of chatter and at very low cutting speed. The low-frequency vibration is significant for drilling because it directly affects hole quality. Circularity the s [12]. Now a day coordinate measuring machines (CMMs) are used extensively for carrying out on-line and off-line inspection with least measurement uncertainty. To yield critical geometric errors of the measured part, data obtained by a coordinate measuring machine must be analyzed or interpreted using suitable algorithms, which should confirm to the specifications laid down in the ISO/1101 standard [13]. In this study, a new roundness and cylindricity modeling of drilling using commercial surface metrology software TrueRond and its characteristics are investigated. By comparing with the experimental lobe results with simulated lobe profiles, the reliability of the proposed method proved. Complete features of drilling for the Al7075 and Ti-6Al-4V alloys with the different cutting tool and the accuracy of form tolerances for holes investigated. Modern mass production in the automotive industry is very sensitive towards fabrication tolerances [14]. In present day industries due to the high cost associated with materials like Ti-6Al-4V and Al7075A limited. Hence, it is required to develop an automatic evaluation method for form tolerance evaluation based on CMM data. The limited amount of literature is available on tolerance simulation methods to investigate the hole quality and stability of the machining processes.

As part of present work, simulations conducted must produce results that are closer to reality. For this purpose measurement data (CMM data) and simulation data (TrueRond) have to be compared to varying both work materials and cutting tools as well. This is important to get more know-how of simulations behavior to use the tools more precise. The present paper is organized as follows: circularity and cylindricity errors are measured using CMM based on the minimum zone solution method are formulated. Then tolerance simulations are generated using surface metrology software TrueRond for circularity and cylindricity error evaluation is proposed.

2. PROBLEM DEFINITION EXPERIMENTATION DESIGN AND PROPOSED METHODOLOGY

The ultimate objective of the present research is to evaluate the measured form tolerance errors with simulated profiles in the drilling operation. The simulated values are obtained by using form measuring software named TrueRond. It enables designers to analyze in measuring form errors that are caused due to vibrations and cutting forces in machining operation through PC rather than the shop floor using trial and error.Recently tolerance simulation has gained importance at the leading companies. Today's competitive pressures require companies to take advantage of every tool at their disposal.

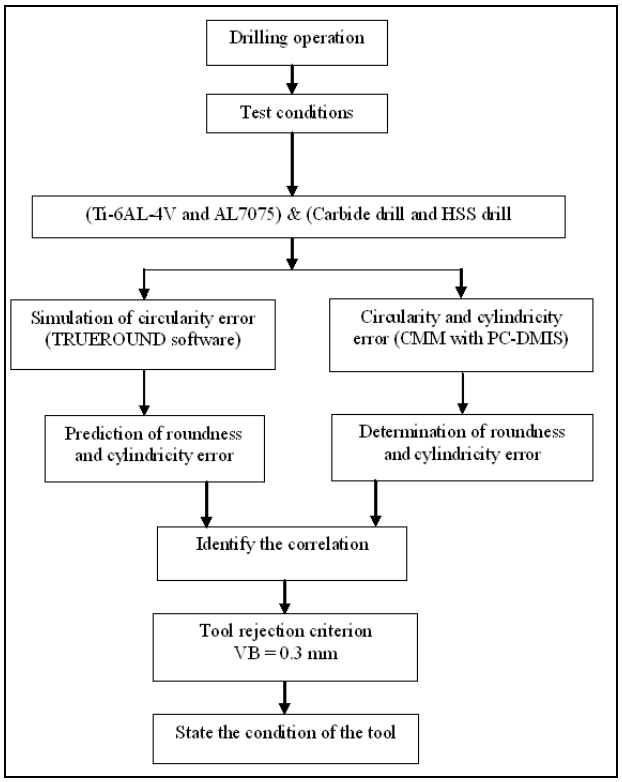

Fig. 1. Proposed methodology

Figure 1 gives the various stages in the present proposed research work. The drilling operation is carried out according to tool maker's recommendation for a specific workpiece and cutting tool combination. Global performance 070705 DEA CMM is employed to measure the circularity and cylindricity of drilled holes. Measured CMM data used as a basis for tolerance simulation using TrueRond software for evaluation of results. The procedures for the step by step simulation of form errors are showcased in the further chapters more clearly. The present work is aimed to predict the form errors in various work materials when drilled with HSS and WC with different materials drilled in combination.

3. EXPERIMENT DETAILS

Drilling tests were carried out with drills of 10 mm diameter using a radial drilling machine under dry cutting conditions, blind holes of 8 mm depth drilled by employing different test conditions. Regarding the hole diameters and the circularity measurements, a comparison is made relating to the quality of the hole between cutting tools. It is identified that there is a reduction in tool performance and hole quality at high cutting speed and feed rate combinations. A significant increase in tool wear is observed when increasing

cutting speed. The utmost wear type was seen in the form of flank wear and chisel edge wear. The purpose of experiments is to evaluate the measured and experimental roundness and cylindricity errors obtained under different drilling conditions as listed in Table 1.

Rotational speed (rpm)	Feed rate (mm/min)	Depth of cut (mm)
465	18 26	8
795	18 26	8
1250	18 26	8
1980	18 26	8
Workpiece materials	Al-7075(150mmX150mmX10mm) Ti-6Al-4V(150mmX150mmX10mm)	
Drilling bit	Carbide Tip (Ø10mm) HSS (Ø 10mm)	

Table. 1. Test conditions selected for experimental investigation

Most commonly used materials in aircraft and automobile industry such as titanium alloys (Ti-6Al-4V) and aluminum alloys (Al7075) of dimensions (150mmX150mm X10mm)are selected as specimens for experimental investigation. Both HSS and tungsten carbide drill bit of Ø10mm diameter are used as cutting tool materials. The details of test conditions and experimental set-up are given in Table 1.The tests are carried out on 38 mm cap radial drilling machine, manufactured by siddharupa machine tools, Gujarat, India. Major specifications include; Drill Capacity: 38 mm drill head, Spindle nose: MT 4, Spindle Travel: 220, the number of spindle speed: 8, Range of spindle speed: 62-1980 rpm, Range of Power feed (mm/Rev): 2, working table: 380mmx300mmx300mm. The cutting parameters are selected according to the tool supplier's recommendation for tool and workpiece combinations. Experimental tests are carried out at dry machining conditions. Cutting velocity and feed rates are selected based on the tool manufacturer's (Sandvik) recommendations for workpiece material and tool combination. The experimental setup for the drilling operations is shown in figure 2.

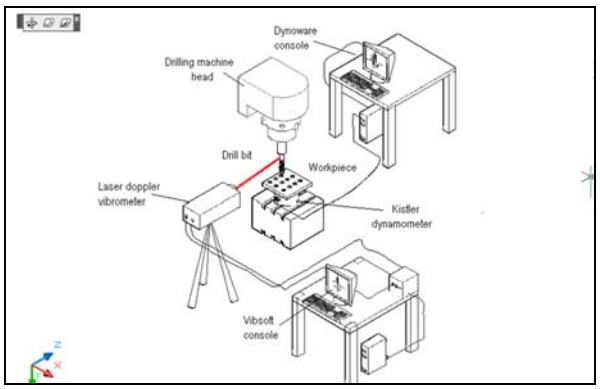

Fig. 2. Schematic representation of experimental setup for drilling process

Throughout the experiment, depth of cut is kept constant. Both cutting speed and feed rate are varied according to the design of experiments for different work piece-tool combination. A non-contact vibration transducer Laser Doppler Vibrometer PolyTec 100V with a data acquisition scheme is kept at a constant distance from the machining zone to measure the shift during the drilling process. To measure the developed cutting forces a Kistler® 9272 4-component dynamometer with a multi-channel analyzer is placed below the workpiece. Vibrations and cutting forces influence the hole quality and form tolerances, but discussion about these factors is intentionally not included in the present work. The form errors are measured along the length of drilled hole using a CMM, which utilizes the minimum zone circle method MZC to express a hole profile.

3.1 Measurement of the roundness for the hole profile based on MZC method using CMM

Various researchers have attempted to develop methods for establishing the reference feature and to evaluate the circularity error. Several measurement techniques are available to estimate the reference feature (circle). These include the Minimum Circumscribed Circle (MCC), the Maximum Inscribed Circle (MIC), the Minimum Zone Circles (MZC) and the Least Squares Circle (LSC). In the present work, roundness error is evaluated from the measured points using Minimum Zone Circles (MZC) method that one among the four internationally defined methods.

The MZC method is to determine a pair of concentric circles, the region between which contains all the measurement points with the minimum radius separation. The radius difference is defined as the roundness error, illustrated in Figure 3a. The hole roundness error is an index for hole quality, which can be examined only by experiments. The probe of the DEA CMM can be positioned independently in two or three axes simultaneously, and it is presented in figure 3b. This probe is either positioned manually, or automated positioning is intended by virtual display after the ruby ball probe is manually set to zero. The probe in finding the errors is brought in contact with four different points of a single hole as shown in figure 3 below. The probe is moved and brought into contact with four different points of a single hole in every test specimen. The measurement of roundness is done according to ISO 12181:2003.

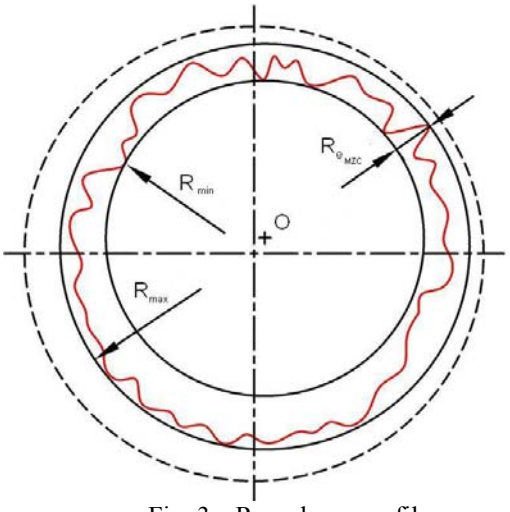

Fig. 3a. Roundness profile

Fig. 3b. Global performance DEA (070705) CMM

Then the roundness error $R_{e_{MZC}}$ is represented by

$$R_{e_{MZC}} = R_{max} - R_{min} \quad (1)$$

where R_{max} and min R_{min} is the maximum and minimum distance between the MZC circle and themeasured profile.Different combinations of workpiece materials and drill bit are used in the experiment.Specimens with drilled holes are inspected under DEACMM for hole diameter, circularity and cylindricity and it is presented in figure 4.

Fig. 4. Specimens used in the experiment

Figure 4 gives the different combinations of workpiece materials and drill bit and they used in the experiment.

3.2 Form tolerance error evaluation using PC-DMIS software

The fitting requirements of the cylindrical component are very important in the precision assemblies. The size tolerances and the form errors such as circularity error and cylindricity error all affect the fitting conditions. The PC-DMIS software interlinked generated the readings in.RTF and an online screen snap of real-time error generation. The tools in software are defined through symbols for an easy and efficient understanding of the application of software as shown in figure 5. Roundness error profile is presented in figure 5a, and figure 5b gives the cylindricity error profile. b. PC-DMIS software calculates the form errors using software tools in measuring cylindricity, roundness, concentricity, etc. The drilled holes are assigned an ID for each hole, i.e., CIR 1, CIR 2, CIR 3, CIR 4 as shown in figure 5.

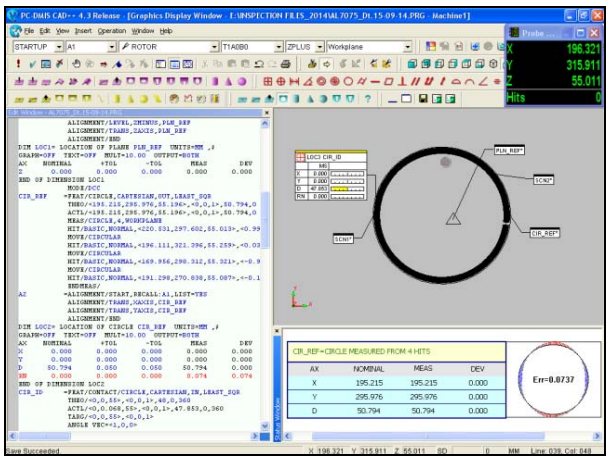

Fig. 5a. Roundness error profile

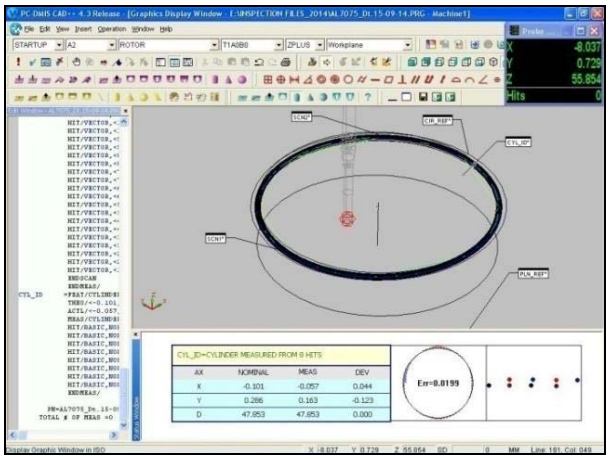

Fig. 5b. Cylindricity error profile

The Ruby probe is used as a stylus in the measuring machine. The roundness error is calculated for circle1 which is measured from four hits taken Ruby ball probe as a stylus. The process is repeated for all the four circles. When result observed, the circle1 having less error and when coming to the fourth circle the error is maximum since the due to vibration which affects the tool wear increasing in roundness error vice versa. Data obtained from CMM is used as input data for simulation in TrueRond software.

4. RESULTS AND DISCUSSIONS

TrueRond is highly interactive surface metrology software that provides a common user interface to operate and generate all of the gauging measurements. It generates profiles either of LIC, MZC, MIC and MCC of harmonic roundness in different machining processes. TrueRond can easily interface with metrology equipment (DEA CMM) and PC-DMIS software. It is possible to make the calculation of roundness and cylindricity along with all other form tolerances.

4.1 Evaluation roundnesserror and cylindricity error profileswith using TrueRond:

Figure 6presents the profile with roundness errors in cross sections that have three, four, and five lobes, respectively in one of the test conditions in the present

study. These profiles with lobes are generated based on measured data using CMM of the drilled holes in Ti-6Al-4V and Al7075 specimens. Figure 6 gives the typical profile of the drilled hole with a cylindricity error in microns. The roundness data collected at 4 or 5 levels in the depth of each drilled hole by using CMM. Based on this data, cylindricity error is simulated, and they presented in figure 7. Cylindricity profile shown in figure 7 is corresponding to the test case of the AL7075 specimen is drilled with HSS drill bit. It is observed that as the depth of the hole is increase the peak of the profile is observed to be deviated from the tolerance zone by maximizing the error.

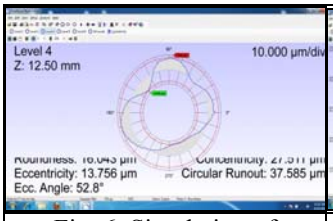

Fig. 6. Simulation of circularity profile with lobes in TrueRond

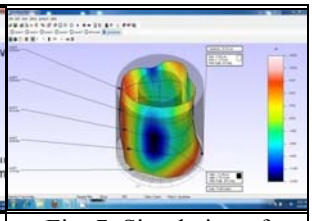

Fig. 7. Simulation of Cylindricity profile in TrueRond

In this section, simulation profiles with TrueRond are presented in figure 8a to figure 8d. Among this, figure 8a gives the roundness profiles when holes drilled on the Al7075 specimen by HSS drill bit and figure 8b shows the simulated profiles of roundness when Ti-6Al-4V specimen drilled with HSS drill bit. In Figure 8a, profiles have only roundness errors in cross sections that have three, four, and five lobes, respectively. It is found that in general, the harmonics from the second up to the fiftieth are sufficient to represent a circular profile satisfactorily by removing only the effect of measurement [15].

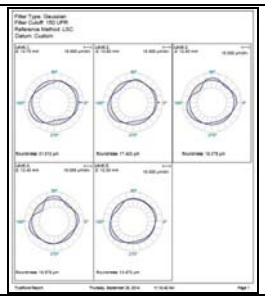

Fig. 8a. Roundness profile Al7075/HSS drill

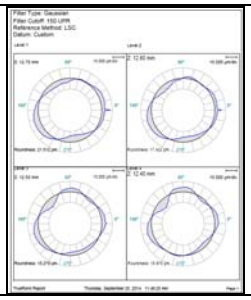

Fig. 8b. Roundness profile Ti-6Al-4V/HSS drill

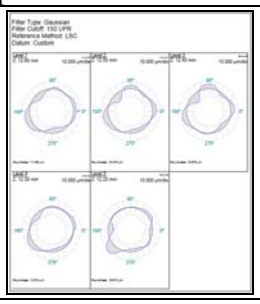

Fig. 8c. Roundness profile Al7075/Carbide drill

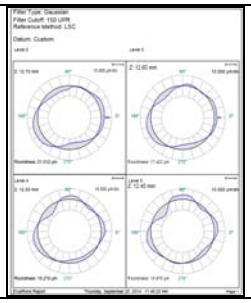

Fig. 8d. Roundness profile Ti-6Al-4V/Carbide drill

Figure 8c and figure 8d shows a hole roundness error recorded by simulated by TrueRond when carbide drill is used in drilling holes on Al7075 and Ti-6Al-4V specimens. The comparisons of values are made between simulated, and measured values by CMM are presented in Table 2. Figure 8c and figure 8d shows the influence of drill bit rotational speeds on the hole roundness error. It reveals that the higher the rotational speeds, the bigger the roundness error. The reason for this is the shaft vibration and whips at higher speeds.

Error from circularity of the holes is the result of deflection, vibration, lack of lubrication and wear. Errorfrom circularity means fluctuations on the surface. Similar to roundness error, cylindricity error needs to be evaluated for drilled holes as part of the present results evaluation. Cylindricity error is measured as the minimum radial separation between two coaxial cylinders enclosing all the cylindrical profiles. Figure 9ato figure 9d shows that variation in the simulated profiles of the cylindricity error for Ti-6Al-4V workpiece when drilled with HSS drill bit and tungsten carbide drill bit. Influence of feed rates on the hole cylindricity error at a constant depth of the hole is clearly evident in all cases presented in figure 9. It is observed that the higher the feed rate, the greater the roundness and cylindricity error. This is because at higher feed rate the chip load becomes larger and the tool bears greater cutting force. The trend conforms to the results reported by Chandrasekhar et al. [15]. Figure 9a presents the cylindricity error of Ti-6Al-4V/HSS drill bit combination and cylindricity found to be varied between 10 µm to 55µm. Moreover, the roundness errors at entry are higher but decrease with penetration depth. These may be due to the unstable beginning of drilling process.

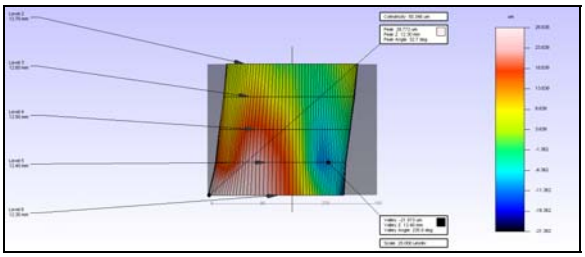

Fig. 9a. Simulated cylindricity profile Ti-6Al-4V/HSS drill bit

Figure 9b showed the simulated cylindricity profile when drilling operation carried out on Ti-6Al-4V workpiece with tungsten carbide drill bit as a cutting tool. Figure 9b shows the typical form errors in the axial direction in the cylinder, such as taper, banana, barrel, and hourglass.

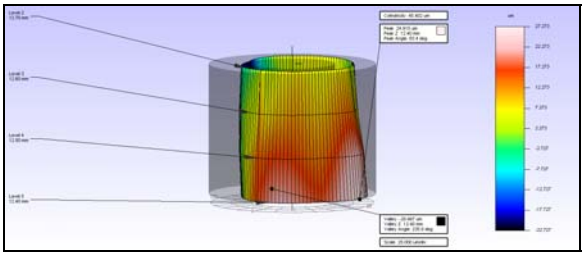

Fig. 9b. Simulated cylindricity profile Ti-6Al-4V/tungsten carbide drill bit

Simulation results of the Al7075 specimen are presented in figure 9c and figure 9d. Simulated cylindricity profile for Al7075, when drilled with HSS drill bit, is presented in figure 9c, and figure 9d gives the simulated profiles of the Al7075 specimen when is drilled with tungsten carbide drill.

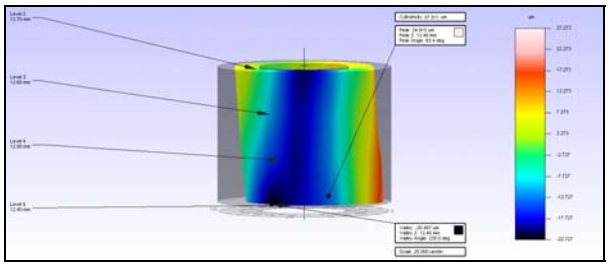

Fig. 9c. Simulated cylindricity profile Al7075/HSS drill bit

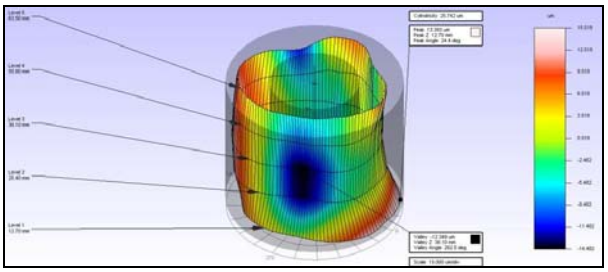

Figure 9d. Simulated cylindricity profile Al7075/Tungsten Carbide drill bit

The cylindricity error variation in carbide and HSS tools is examined clearly, and the wear difference is more with HSS tool. These results presented in Table 2 also indicate the same.Drill wear is measured with Opto mech vision inspection device, and this is presented in figure 10.

The relation between roundness error and different cutting speeds in all test conditions are presented in figure 11and figure 12 gives the progression of tool wear in relation with roundness error in the experiment.

Fig. 10 Drill wear under Opto mech vision inspection system

Figure 11 shows the influence of rotational speeds on the hole roundness error. It reveals that the higher the rotational speeds, the bigger the roundness error. Highest cylindricity error values are obtained in the drilling of Ti-6Al-4V with HSS drill bit and shown in Table 2 this is due to increased tool wear.

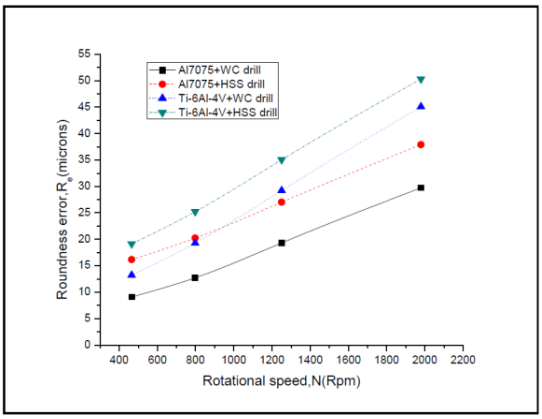

Fig. 11. Roundness errors versus rotational speed

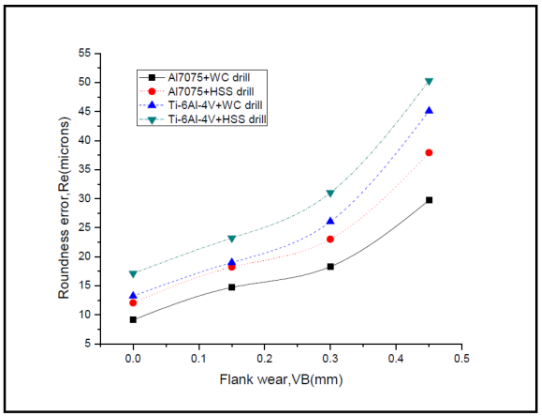

Fig. 12. Roundness error versus tool flank wear

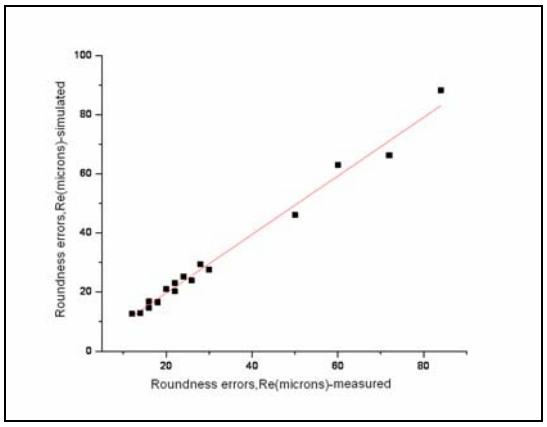

Fig. 13. Correlation between simulated and predicted roundness errors

Figure 13 presents the comparison graph from which the closeness of measured roundness errors (CMM data) with simulated values is presented. The difference between the measured and predicted response are illustrated in figures 13.

In other words, carbide drill bits showed a better performance than HSS drill bits concerning roundness error and cylindricity error. From the results table 2, it is found that an increase in cutting speed led to an increase in form tolerance due to increased tool wear on the cutting edge.

Hence, both the roundness error and cylindricity error values increased. Besides, it also observed that both roundness error and cylindricity error are influenced by feed rate.

Workpiece/Cutting tool	Al7075/HSS drill bit			Ti-6Al-4V/HSS drill bit		
Hole ID	Roundness error, CMM (μm)	TrueRond Error (μm)	Flank wear, VB(mm)	Roundness error, CMM (μm)	TrueRond Error (μm)	Flank wear, VB(mm)
CIR 1	16.15	17.76	0.09	19.15	20.83	0.168
CIR 2	20.22	23.99	0.126	25.23	27.17	0.198
CIR 3	27.02	28.91	0.188	35.05	38.16	0.287
CIR 4	37.91	41.13	0.213	50.3	55.32	0.356
Cylindricity error, Cz(μm)	25.32			Cylindricity error, CR(μm)	32.43	
Workpiece/Cutting tool	Al7075/carbide drill bit			Ti-6Al-4V/carbide drill bit		
Hole ID	Roundness error, CMM (μm)	TrueRond Error (μm)	Flank wear, VB(mm)	Roundness error, CMM (μm)	TrueRond Error (μm)	Flank wear, VB(mm)
CIR 1	9.11	9.92	0.06	13.24	13.96	0.103
CIR 2	12.72	13.80	0.091	19.28	20.55	0.143
CIR 3	19.31	20.75	0.138	29.25	31.81	0.246
CIR 4	29.74	32.20	0.165	45.1	48.65	0.305
Cylindricity error, Cz(μm)	17.72			Cylindricity error, CR(μm)	26.46	

Table. 2. Experimental and simulated results

The results of compared in figure 13 indicate the good level of agreement between data obtained from CMM with simulated data using TrueRond. The error percentage is found to be less than 10% between the two.

5. CONCLUSIONS

Present work involves the monitoring the drilled hole status of Al7075 and Ti-6Al-4V materials based on circularity and cylindricity, with tool rejection criterion parameter flank wear. Both experimental and simulated approaches used to monitor the drilled hole status based on output parameters. This paper described a method for evaluating roundness and cylindricity errors from the measured points by coordinate measuring machine, providing a solution for assessing the quality of drilled holes from the measured points within a region on the workpiece under test. The evaluation result is verified by comparing with the result given by TrueRond simulations. Experiments show that measured roundness and cylindricity error values agree well with the simulated values. This method can be applied to estimate the selected form tolerance errors in the production line, so as to assess the machining process. Form tolerances error evaluation with simulation method played a significant role in determining the accuracy of the evaluation of circularity and cylindricity error. Findings of the present work, demonstrate that the proposed method can be used to obtain very accurate and stable results for the evaluation of roundness and cylindricity.

6. REFERENCES

[1] Chyn-Shu Deng., Jih-Hua Chin., 2004, Roundness errors in BTA drilling and a model of waviness and lobing caused by resonant forced vibrations of its long drill shaft, Journal of Manufacturing Science and Engineering Transactions of the ASME, 126: 524-534.

[2] Beckmann A., Bohn M., Gust P., 2015, Tolerance simulation in the assembling process based on experimental data from series production, Proceedia CIRP, 27: 35 – 40.

[3] Cho N., Tu J F., 2002, Quantitative circularity tolerance analysis and design for 2D precision assemblies, International Journal of Machine Tools & Manufacture, 42(13): 1391-1401.

[4] Hemant R., Sudhon K., Sam A.,2009, An inspection advisor for form error in cylindrical features, International Journalof Advanced Manufacturing Technology, 40: 128–1434.

[5] Zhang XD.,2005, Unified functionaltolerancing approach for precision cylindrical components, International Journal of Production Research, 43: 25–47.

[6] Xiu-Lan Wen., Jia-Cai Huang., Dang-Hong Sheng., Feng-Lin Wang., 2010, Conicity and cylindricity error evaluation using particle swarm optimization, Precision Engineering, 34: 338–344.

[7] Chajda J., Grzelka M., Gapinski B., Pawłowski M., Szelewski M., Rucki M., 2014, Coordinate measurement of complicated parameters like roundness, cylindricity, gear teeth or free-form surface, 8th International conference on advanced manufacturing operations, 225-231.

[8] Chandra shekhar S., Sankar T S., Osman M O M.,1987, A Stochastic characterization of the machine tool workpiece system in BTA deep hole machining- part II: mathematical modelling and analysis, Advanced Manufacturing Processes, 2(1&2): 71–104.

[9] Turgay Kivak., KasimHabli., UlviSeker.,2012, The effect of cutting parameters on the hole quality and tool wear during the drilling of inconel 718, Gazi University Journal of Science, 25(2): 533-540.

[10] Azarhoushang B., Akbari J.,2007, Ultrasonic-assisted drilling of Inconel 738-LC, International Journal of Machine Tools and Manufacture, 47(7–8): 1027–1033.

[11] Pirtini M., Lazoglu I.,2005, Forces and hole quality in drilling, International Journal of Machine Tools and Manufacture, 45(11): 1271–1281.

[12] Chang-long Du., Chen-Xu Luo., Zheng-tong Han., Yong-she Zhu.,2014, Applying particle swarm optimization algorithm to roundness error evaluation based on minimum zone circle, Measurement, 52: 12–21.

[13] Julius Klingera F., Martin Bohna.,2013, Predicting dimensional deviations of structural vehicle body parts deep drawn from aluminum blanks, Proceedia CIRP, 7: 353 – 358.

[14] Chandra shekhar S., Osman M O M., Sankar T S.,1984, An analytical time domain evaluation of the cutting forces in BTA deep hole machining using the thin shear plane model, International journal of production research, 22(4): 697-721.

[15] Weihua Ni., Zhenqiang Yao., 2013, Cylindricity modeling and tolerance analysis for cylindrical components, International Journal of Advanced Manufacturing Technology, 64: 867–874.

Acknowledgment

This research is sponsored by Science and Engineering Research Board (SERB) with sanction order No. SB/FTB/ETA-0262/2013. The authors wish to gratefully acknowledge the financial support provided for this study by the Department of Science and Technology, Govt.of India, New Delhi. Authors also wish to thank Sri PVS Ganesh Kumar, Scientist-'G' from NSTL, Visakhapatnam who provided insight and expertise that greatly assisted in the research work.

Authors: **Y. Rama Mohan Reddy, Corresponding author,** Ph.D. scholar, Dept.of Mechanical Engineering, GITAM Institute of Technology, GITAM University, Visakhapatnam, India-530045, Tel: +91-0-9553214909, **Dr Balla Srinivasa Prasad, Research guide**, Associate Professor, Dept.of Mechanical Engineering, GITAM Institute of Technology, GITAM University, Visakhapatnam, India-530045, Tel.: +91-0-98483210710 Fax: (+381 21) 454-495

e-mail: yrmreddy.3749@yahoo.com**,**

bsp.prasad@gmail.com

Journal of Production Engineering
Vol.19 No.2
JPE (2016) Vol.19 (2) Original Scientific Paper
Babič, M.

A NOVEL APPROACH OF HYBRID METHOD OF MACHINE LEARNING AND STATISTICAL PROPERTIES IN PATTERN RECOGNITION

Received: 24 September 2016 / Accepted: 10 November 2016

Abstract: *In this article, we present new method of hybrid intelligent systems. Intelligent systems are very useful for prediction in any situation and are a new wave of embedded and real-time systems that are highly connected, with massive processing power and performing complex process. Here, we present a method of hybrid systems for prediction of the roughness of robot laser hardened specimens, if we cannot measure or calculate one of parameters in existing models of intelligent systems. Also, we have a model of intelligent systems for prediction of the roughness of hardened specimens, but we cannot calculate one parameter in this model. Thus, we develop a new method of hybrid intelligent systems to solve this problem. We develop a hybrid of genetic programming, neural network and multiple regression. In this article, we present new method for statistical pattern recognition. Statistical pattern recognition relates to the use of statistical techniques for analyzing data measurements in order to extract information and make justified decisions. This solution to the presented problem has applications for metallurgy and mechanical engineering. With the hybrid system intelligent system, we increase production of the process of laser hardening, because we decrease the time of the process and increase the topographical property of the materials. This paper explores the use of an intelligent system with a new hybrid method of intelligent systems to predict the mechanical properties of robot laser hardened specimens, if we do not know one parameter of the existing model.*
Key words: *Hybrid machine learning, pattern recognition, statistics*

Novi pristup hibridnog metoda mašinskog učenja i statističke osobine u prepoznavanju obrazaca. *U ovom radu je predstavljen novi način hibridnih inteligentnih sistema. Inteligentni sistemi su veoma korisni za predviđanje u svakoj situaciji i predstavljaju novi talas implementiranih i real-time sistema koji su uzajamno povezani, koji poseduju veliku snagu obrade podataka i obavljaju složen proces. Ovde ćemo predstaviti metodu hibridnih sistema za predviđanje hrapavosti delova ojačanih robotskim laserom, ako ne možemo izmeriti ili izračunati neki od parametara u postojećim modelima inteligentnih sistema. Takođe imamo i model inteligentnih sistema za predviđanje hrapavosti ojačanih delova, ali ne možemo izračunati jedan parametar pomoću ovog modela. Tako, razvijamo nove metode hibridnih inteligentnih sistema za rešavanje ovog problema. Razvijamo hibrid genetskog programiranja, neuronskih mreža i višestruke regresije. U ovom radu ćemo predstaviti novu metodu za statističko prepoznavanje oblika. Statističko prepoznavanje obrazaca se odnosi na primenu statističkih tehnika za analiziranje izmerenih podataka da bi se izvukle informacije i načinile opravdane odluke. Ovo rešenje predstavljenog problema ima primenu u metalurgiji i mašinstvu. Sa hibridnim inteligentnim sistemom, je povećana proizvodnost usled smanjenja vremena obrade i povišenja topografskih osobina materijala. Ovaj rad istražuje upotrebu inteligentnog sistema sa novom metodom hibridnog inteligentnog sistema za predviđanje mehaničkih svojstva ojačanih pripremaka robotskim laserom, u slučaju da nam nije poznat neki od parametara u postojećem modelu.*
Ključne reči: *Hibridno mašinsko učenje, prepoznavanje obrazac, statistika*

1. INTRODUCTION

In recent years there has been an explosion of available data in fields such as biology, computer vision, finance, medicine and social networking platforms. The challenge is to analyse these vast amounts of data by developing new ideas and implementing novel machine learning techniques [1]. Machine learning as a matter of perspective and emphasis is closely allied to, and contains elements of, a range of subjects including artificial intelligence, bioinformatics, data mining, evolutionary computation, information retrieval, machine intelligence, machine vision, pattern recognition and statistics. The modern world is full of artificial, abstract environments that challenge our natural intelligence. The goal of our research is to develop Artificial Intelligence that gives people the capability to master these challenges, ranging from formal methods for automated reasoning to interaction techniques that stimulate truthful elicitation of preferences and opinions. Another aspect is characterising human intelligence and cognitive science, with applications in human-computer interaction and computer animation. Machine Learning aims to automate the statistical analysis of large complex datasets by adaptive computing. A core strategy to meet growing demands of science and applications, it provides a data-driven basis for automated decision making and probabilistic reasoning. Machine learning applications at EPFL range from natural language and image processing to scientific imaging, as well as computational neuroscience. In

machine learning, we have sometimes difficult problems. Statistical pattern recognition is a term used to cover all stages of an investigation from problem formulation and data collection through to discrimination and classification, assessment of results and interpretation and is usage in bioinformatics, document classification, image analysis, data mining, industrial automation, biometric recognition, handwritten text analysis, medical diagnosis, speech recognition, GIS and many more. In Statistical method of Pattern Recognition each pattern is described in terms of features. One significant problem is how to predict the mechanical properties of robot laser hardened specimens with statistical pattern recognition [2] of SEM image. In this paper we use the method of intelligent systems to predict the roughness of robot laser hardened specimens. Robot laser surface hardening [3] heat treatment is complementary to conventional flame or inductive hardening. The energy source for laser hardening is the laser beam, which heats up very quickly and the metal surface area of ponds up to 1.5 mm. We use three methods to analyze images: calculate fractal dimensions in 2D space, 3D space and calculate the density of visibility graphs in 3D space. Finally, we use the new method of hybrid intelligent systems to predict the roughness of hardened specimens.

2. MATERIAL PREPARATION AND METHOD

We hardened tool steel with a robot laser cell. After hardening, we polished and etched all specimens. Detailed characterization of their microstructure before and after surface modifications was conducted using a JEOL JSM-7600F field emission scanning electron microscope (SEM). We used the program ImageJ (available from the National Institute of Health, USA) to analyze these pictures. We use the following method for pattern recognition: calculate fractal dimensions of 2D object with the box-counting method [4], the method for estimation of a Hurst exponent H for 3D objects [5], and the method of constructing a visibility graph in 3D Space [6]. Characterisation of surface topography is important in applications involving friction, lubrication, and wear. In general, it has been found that friction increases with average roughness. Roughness [7] parameters are, therefore, important in applications such as automobile brake linings and floor surfaces. A profilometer (available from the Institute Jožef Stefan, Slovenia) was used for measurement of the surface roughness parameter R_a (i.e. the arithmetic mean deviation of the roughness profile) and hardness of the robot laser hardened specimens. For analysis of the results, we used an intelligent system method [8], namely genetic programming, neural network and multiple regression. Genetic programming [9] may be more powerful than neural networks and other machine learning techniques, able to solve problems in a wider range of disciplines. In his ground-breaking book, Koza shows how this remarkable paradigm works and provides substantial empirical evidence that solutions to a great variety of problems from many different fields can be found by genetically breeding populations of computer programs. Genetic Programming contains a great many worked examples and includes a sample computer code that will allow readers to run their own programs. Computers are made to solve problems without being explicitly programmed; genetic Programming is inspired by biological evolution. It is a machine learning technique used to optimise a solution based on a fitness score. Solutions are represented by *chromosomes* encapsulating parameters, and these chromosomes change with iterations to get closer to a desired representation. Genetic programming starts with a primordial ooze of thousands of randomly created computer programs. This population of programs is progressively evolved over a series of generations. The evolutionary search uses the Darwinian principle of natural selection and analogues of various naturally occurring operations, including crossover, mutation, gene duplication, gene deletion. Fig. 1 presents one of the randomly generated mathematical models of genetic programming.

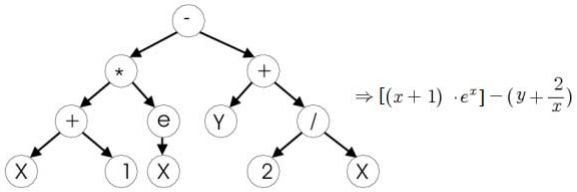

Fig. 1. Randomly generated mathematical models of genetic programming

The following evolutionary parameters were selected for the process of simulated evolutions: 500 for the size of the population of organisms, 100 for the maximum number of generations, 0.4 for the reproduction probability, 0.6 for the crossover probability, 6 for the maximum permissible depth in the creation of the population, 10 for the maximum permissible depth after the operation of crossover of two organisms, and 2 for the smallest permissible depth of organisms in generating new organisms. Genetic operations of reproduction and crossover were used. For selection of organisms, the tournament method with tournament size 7 was used. Researchers from many scientific disciplines design artificial neural networks, to solve a variety of problems in pattern recognition, prediction, optimisation, associative memory, and control. A series of algorithms that attempts to identify underlying relationships in a set of data using a process that mimics the way the human brain operates. Neural networks [10] have the ability to adapt to changing input so that the network produces the best possible result without the need to redesign the output criteria. The concept of neural networks is rapidly increasing in popularity in the area of developing trading systems. At one point in time, it would have seemed impossible to make a system that would be able to adapt to changing markets, but recent developments in technology have now made having these types of systems a reality. An artificial neural network (ANN) is a machine-learning approach that models the human brain and consists of a number of

artificial neurons. Neurons in ANNs tend to have fewer connections than biological neurons. Each neuron in an ANN receives a number of inputs. Fig. 2 presents a symbolic representation of the artificial neural network cell.

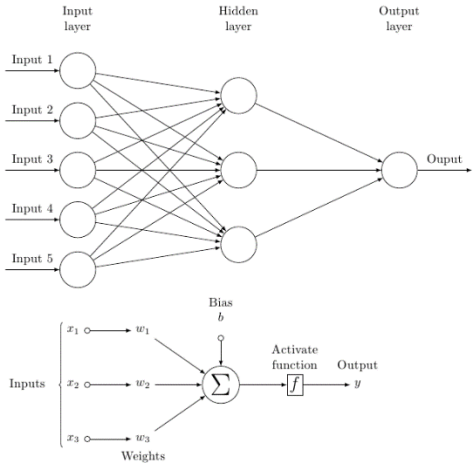

Fig. 2. Symbolic representation of the artificial neural network cell

Multiple regression analysis [11] is a powerful technique used for predicting the unknown value of a variable from the known value of two or more variables, also called the predictors. More precisely, multiple regression analysis helps us to predict the value of Y for given values of X_1, X_2, …,X_k. In general, the multiple regression equation of Y on X_1, X_2, …,X_k is given by:

$$Y = \alpha_0+\alpha_1\times X_1+\ldots+\alpha_6\times X_6 \quad (1)$$

Once a multiple regression equation has been constructed, one can check how good it is (in terms of predictive ability) by examining the coefficient of determination (R^2). R^2 always lies between 0 and 1.Multiple regression analysis is used when one is interested in predicting a continuous dependent variable from a number of independent variables. If the dependent variable is dichotomous, then logistic regression should be used. The major problem comes when we do not have one of the parameters of our models. Thus, we present a method of hybrid system of intelligent systems. The hybrid system method [12] of intelligent systems in machine learning is a robust method for solving complex global optimisation problems. It can be used in practical applications in industry, especially in laser technology of hardening. We present a built-in hybrid system of intelligent systems method. This means that we can insert one variable (that we cannot have or cannot measure for any reason) of the model into the second method of intelligent systems. The function *f* represents multiple regression, *g* genetic programming, and *h* the hybrid system.

$$f:R^6\rightarrow R,\ f(x_1,\ldots x_6)=\alpha_0+\alpha_1\times x_1+\ldots+\alpha_6\times x_6, \quad (2)$$

$$f:R^6\rightarrow R,\ g(x_1,\ldots x_6)=\beta_1\times x_1+\ldots+\beta_6\times x_6, \quad (3)$$

$$h:\ R^6\rightarrow R,\ h(x_1,\ldots,\ [f(x_1,\ldots x_6)-\alpha_0+\alpha_1\times x_1+\ldots+\alpha_6\times x_6]/\ \alpha_5,\ x_6)=\chi_1\times x_1+\ldots+\chi_6\times x_6, \quad (4)$$

3. RESULTS AND DISCUSSION

In Table 1, the parameters of hardened specimens that have an impact on roughness are presented. We mark specimens from P1 to P20. Parameters X_3, X_4 and X_5 presents statistical patterns of robot laser hardened specimens of SEM images. Parameter X_1 represents the parameter of temperature in degrees Celsius [C], X_2 represents the speed of hardening [mm/s], X_3 represents the fractal dimension in 2D space, X_4 represents the fractal dimension in 3D space, X_5 represents the density of the visibility graphs in 3D space, and parameter X_6 represents the basic roughness of the specimens. The final parameter Y is the measured surface roughness of laser-hardened robot specimens. Table 2 presents experimental and prediction data regarding the surface roughness of laser hardened robot specimens. In Table 2, symbol S represents the name of specimens, E experimental data, NM1 prediction with neural network with 30% learn set, NM2 prediction with neural network with 50% learn set, NM3 prediction with neural network with method one live out, R prediction with regression, GP prediction with genetic programming and HM prediction with hybrid method of intelligent systems. In Table 1, we can see that specimen P17 has the largest density of visibility graphs in 3D (0.2832), thus specimen P17 has the most complex graph. Specimen P4 has minimal roughness after hardening, i.e. 76 Ra. The measured and predicted surface roughness of robot laser hardened specimens is shown in the graph in Fig. 8. The genetic programming model is presented in Fig. 3. Under the model of genetic programming is presented the model of regression. The genetic programming model presents an 18.20% deviation from the measured data, which is less than the regression model, which presents a 76.66% deviation. The best neural network has a12.77% deviation from the measured data.

Model of regression

Y = −3345, 48 + 1, 21093×X1 − 78, 1663×X2 − 36, 2896×X3 + 445, 4794×X4 + 7449, 71×X5 + 1, 012724×X6

$$Y = X_5 * (X_1 + 2 * X_2 + \frac{X_1}{2*X_6-\frac{X_1}{2*X_4}-\frac{X_1+2*X_4}{X_6}} + \frac{X_1*2*X_6-\frac{X_1}{X_6}}{(-5{,}14505+X_4)*(2*X_6-\frac{X_1}{2+X_6-1})} - \frac{(X_4+X_6)*(X_4+2*X_6-\frac{(2*X_6-X_1)*(2*X_6*1*\frac{2*X_1}{X_6})*(4/X_6+X_4-1-\frac{X_1}{2*X_4})}{X_1*(X_1+X_4)})}{2*X_6-\frac{X_1}{X_6}} + \frac{X_6-\frac{X_1}{3*X_6-\frac{2*X_1}{X_4+X_6}}}{X_4} + \frac{X_6-\frac{X_1}{2*X_4+X_6-\frac{X_1}{X_4+X_6}}}{X_4} + \frac{X_6-\frac{X_1}{2*X_6-\frac{X_1}{X_4+X_6}}}{X_5})$$

Fig. 3. Model of genetic programming

S	X1	X2	X3	X4	X5	X6	Y
P1	1000	2	1,9135	2,304	0,1936	24	201
P2	1000	3	1,9595	2,264	0,2208	24	171
P3	1000	4	1,9474	2,258	0,2144	24	109
P4	1000	5	1,9384	2,341	0,2256	24	76
P5	1400	2	1,9225	2,222	0,2445	24	1320
P6	1400	3	1,9784	2,388	0,2221	24	992
P7	1400	4	1,954	2,250	0,2036	24	553
P8	1400	5	1,9776	2,286	0,2096	24	652
P9	1000	2	1,972	2,178	0,2352	201	337
P10	1000	3	1,858	2,183	0,2288	171	307
P11	1000	4	1,9784	2,408	0,2144	109	444
P12	1000	5	1,941	2,210	0,2352	76	270
P13	1400	2	1,9784	2,257	0,2208	1320	2350
P14	1400	3	1,581	2,265	0,232	992	1900
P15	1400	4	1,965	2,433	0,1984	553	661
P16	1400	5	1,8113	2,289	0,1904	652	759
P17	800	0	1,9669	2,232	0,2832	24	183
P18	1400	0	1,9753	2,235	0,2688	24	1330
P19	2000	0	1,9706	2,261	0,2416	24	1740
P20	950	0	1,9631	2,282	0,2128	24	502
P21	850	0	1,9537	2,319	0,2080	24	166

Table 1. Parameters of hardened specimens

S	E	NM1	NM2	NM3	R	GP	HM
P1	201	134	191	167	132	91	218
P2	171	188	123	153	237	114	229
P3	109	108	96	93	109	108	237
P4	76	125	128	111	152	119	240
P5	1320	1303	1284	1312	959	746	95
P6	992	1001	958	987	786	723	114
P7	553	623	549	585	509	671	51
P8	652	577	599	634	491	687	35
P9	337	266	333	348	563	335	143
P10	307	204	285	313	413	306	97
P11	444	114	420	435	261	420	13
P12	270	128	251	259	218	218	55
P13	2350	436	2345	873	2108	2404	3123
P14	1900	839	2292	1898	1799	1427	1157
P15	661	417	1762	660	1087	676	555
P16	759	244	1596	758	991	794	656
P17	183	575	194	173	680	188	144
P18	1330	1584	1598	1336	1300	793	149
P19	1740	1984	2306	1747	1836	1690	1059
P20	502	287	235	449	359	407	185
P21	166	161	303	241	219	112	153

Table 2. Experimental and prediction data

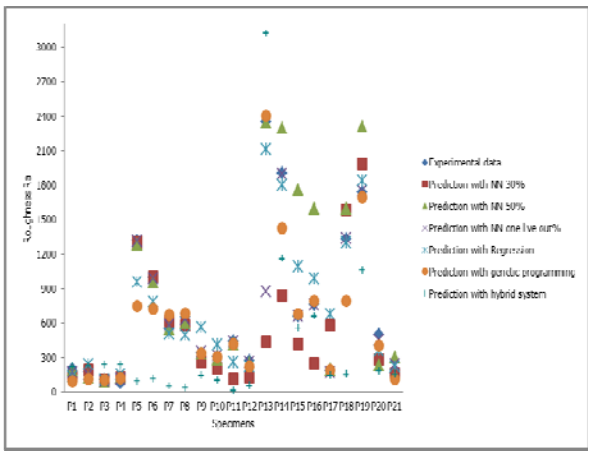

Fig. 4. Measured and predicted surface roughness of robot laser hardened specimens

The mathematical model hybrid system of the intelligent system is presented in Fig. 5. We express variable X_5 of multiple regression and insert it into the model of genetic programming.

$$Y = \frac{A*B+C}{B-7449,71}$$

$$A = -3345,45 + 1,21093 * X_1 - 36,2896 * X_3 + 445,4794 * X_4$$

$$B = X_1 + 2 * X_2 + \frac{X_1}{2*X_6-\frac{X_1}{2*X_4}-\frac{X_1+2*X_4}{X_6}} + \frac{X_1*(2*X_6-\frac{X_1}{X_6})}{(X_4-5,14505)*(2*X_6-\frac{X_1}{2*X_6-1})} - \frac{(X_4+X_6)*(X_4+2*X_6-\frac{(2*X_6-X_1)*(2*X_6*1*\frac{2*X_1}{X_6})*(4/X_6+X_4-1-\frac{X_1}{2*X_4})}{X_1*(X_1+X_4)})}{2*X_6-\frac{X_1}{X_6}} + \frac{X_6-\frac{X_1}{3*X_6-\frac{2*X_1}{X_4+X_6}}}{X_4} + \frac{X_6-\frac{X_1}{2*X_4+X_6-\frac{X_1}{X_4+X_6}}}{X_4}$$

$$C = 7449,71 * (\frac{X_6-\frac{X_1}{2*X_6-\frac{X_1}{X_4+X_6}}}{X_5})$$

Fig. 5. Model of hybrid machine learning system

Roughness is a good predictor of the performance of a mechanical component, since irregularities in the surface may form nucleation sites for cracks or corrosion. A statistically significant relationship was found between roughness, the parameters of the robot laser cell, topological property of visibility graphs in 3D, fractal dimension in 2D space and fractal dimension in 3D space. The fractal analysis in 2D and 3D space and topological property density of 3D visibility graphs of a series of digitized surface microstructures from the robot laser surface modified specimens indicated that useful correlations can be derived between the fractal dimensions and the surface microstructural features such as roughness. In addition, analysis of SEM images of the robot laser hardened specimens is an interesting approach. Methods of intelligent systems are very useful. In this study, we present three different methods of intelligent systems, namely genetic programming, neural network and multiple regression to predict topographical properties of robot laser-hardened specimens roughness. A statistically significant relationship was found between porosity measured using the method of determining the roughness from SEM images of the microstructure, the parameters of the robot laser cell and image analysis with fractal geometry and graph theory. The best property of roughness of the hardened specimen used the following

parameters of robot laser cell: speed 5 mm/s and temperature 1000° C. The neural network give us the best result. We use three methods: fractal geometry in 2D space, fractal dimension in 3D space and algorithm for constructing visibility graphs in 3D space to analyse the microstructure of the hardened specimens.The genetic programming model is better than the regression model and as good as the neural network. The density (X_5) of the visibility graph in 3D space has the maximum impact on variables in the regression model. In a model of genetic programming, we see the equal situation. The hybrid system method of intelligent systems presents a 56.04% deviation from the measured data, which is less than the regression model, which presents a 76.66% deviation.

4. CONCLUSSION

The paper presents new method using the mathematical methods of graph theory, fractal geometry and its application in the robot laser hardening process.We present a hybrid method of intelligent systems to predict the roughness of robot laser hardened specimens. The main findings can be summarised as follows:

1. We use the method visibility graph in 3D space, the method of calculation of fractal dimensions of 2D and 3D objectsto analysis robot laser hardened specimens.
2. We describe the topographic properties of the hardened specimens using the topological properties of the visibility graphs in 3D space and fractal dimensions.
3. We describe the relationship between hardness and the parameters of the robot laser cell using the topological properties of the 3D visibility graphs and fractal dimensions. This finding is important with regard to certain alloys that are hard to mix, because they have different melting temperatures; however, such alloys have better technical characteristics. By varying different parameters (e.g., temperature), robot laser cells produce different patterns with different topological properties of 3D visibility graphs and fractal dimensions.
4. For prediction of the hardness of hardened specimens we use neural networks, genetic algorithm and multiple regression.
5. We predict the mechanical properties of robot laser hardened specimens with statistical pattern recognition of SEM image.
6. With the hybrid method of intelligent systems, we increase production of the process of laser hardening, because we decrease the time of the process and increase topographical properties of materials.

5. REFERENCING

[1] Mehryar Mohri, Afshin Rostamizadeh, Ameet Talwalkar (2012). Foundations of Machine Learning, The MIT Press. ISBN 9780262018258.

[2] Bishop, Christopher M. (2006). Pattern Recognition and Machine Learning. Springer. p. vii. Pattern recognition has its origins in engineering, whereas machine learning grew out of computer science. However, these activities can be viewed as two facets of the same field, and together they have undergone substantial development over the past ten years.

[3] J. Grum, P. Žerovnik, R. Šturm: Measurement and Analysis of Residual Stresses after Laser Hardening and Laser Surface Melt Hardening on Flat Specimens; Proceedings of the Conference "Quenching ’96", Ohio, Cleveland, 1996.

[4] Mandelbrot, B. B. The fractal geometry of nature. New York: W. H. Freeman, 1982:93.

[5] Babič, Matej, Kokol, Peter, Guid, Nikola, Panjan, Peter. A new method for estimating the Hurst exponent H for 3D objects. Materias and technology, ISSN 1580-2949, 2014, letn. 48, 2, 203-208.

[6] Matej Babič. Doctoral dissertation. 2014.

[7] Jean M. Bennett, Lars Mattsson, Introduction to Surface Roughness and Scattering, Optical Society of America, Washington, D.C.

[8] Beverly Woolf, "Intelligent Tutoring Systems: A Survey," in Exploring Artificial Intelligence: Survey Talks from the National Conferences on Artificial Intelligence, ed. by Howard E. Shrobe and the American Association for Artificial Intelligence (San Mateo, CA.: Morgan Kaufmann, 1988), 1-43.

[9] John R. Koza. "36 Human-Competitive Results Produced by Genetic Programming". retrieved 2015-09-01.

[10] Graves, Alex; and Schmidhuber, Jürgen; Offline Handwriting Recognition with Multidimensional Recurrent Neural Networks, in Bengio, Yoshua; Schuurmans, Dale; Lafferty, John; Williams, Chris K. I.; and Culotta, Aron (eds.), Advances in Neural Information Processing Systems 22 (NIPS'22), December 7th–10th, 2009, Vancouver, BC, Neural Information Processing Systems (NIPS) Foundation, 2009, pp. 545–552.

[11] Box, G. E. P. (1954). "Some Theorems on Quadratic Forms Applied in the Study of Analysis of Variance Problems, I. Effect of Inequality of Variance in the One-Way Classification". The Annals of Mathematical Statistics **25** (2): 290. doi:10.1214/aoms/1177728786.

[12] Vadlamani Ravi, Nekuri Naveen, Mayank Pandey. Hybrid classification and regression models via particle swarm optimization auto associative neural network based nonlinear PCA. International Journal of Hybrid Intelligent Systems. 10 (3), (2013).

Author: **Dr. Matej Babič, Bs. M.**
Jožef Stefan Institute, Ljubljana, Slovenia
E-mail: babicster@gmail.com

Journal of Production Engineering
Vol.19 No.2
JPE (2016) Vol.19 (2) Original Scientific Paper
Djordjic, D., Djuric, S., Hadzistevic, M.

ANALYSIS AND TREATMENT OF WASTE MOTOR AND TRANSFORMER OILS FOR ENVIRONMENTAL PROTECTION

Received: 04 August 2016 / Accepted: 11 October 2016

Abstract: *In order to conduct safe and efficient flow management of motor or transformer oil, it is necessary to implement specific waste oil analysis and treatment in order to protect the environment and people's health and safety. The study presents analysis and treatment of waste oil in the electric power distribution companies, showing some data of the MH "ERS" ZEDP "Elektro-Bijeljina" joint-stock company Bijeljina and describing the basic treatments of motor and transformer waste oil. The concluding observations are also given.*
Key words: *motor oil, transformer oil, waste oil treatment, environmental protection, analysis of material flows.*

Analiza i tretman otpadnog motornog i transformatorskog ulja u funkciji zaštite životne sredine. *Radi bezbednog postupanja i efikasnog upravljanja tokovima motornog i transformatorskog ulja, neophodna je realizacija određenih analiza i tretmana otpadnog ulja u funkciji zaštite životne sredine, te bezbednosti i zdravlja ljudi. U radu je prezentovana analiza i postupanje sa otpadnim uljima u elektrodistibutivnim preduzećima, pri čemu su prikazani određeni podaci iz preduzeća MH "ERS" ZEDP "Elektro-Bijeljina" a.d. Bijeljina, opisani osnovni tretmani otpadnog motornog i transformatorskog ulja, te data zaključna razmatranja.*
Ključne reči: *motorno ulje, transformatorsko ulje, tretman otpadnog ulja, zaštita životne sredine, analiza tokova materijala.*

1. INTRODUCTION

Waste motor and transformer oils generated from the process of motor vehicle maintenance, reconstruction, repair, maintenance and replacement of power equipment, as well as other activities of power distribution companies, are qualified as hazardous waste, for which the companies are required to carry out analysis and other required activities, as defined by laws and bylaws, as well as ISO 14001 and other standards.

Required preventive and corrective measures for environmental protection, fire protection, safety and health at work are to be applied during different waste oil management.

2. MATERIALS AND METHOD

2.1 Waste motor oil

Using various types of motor oil during the exploitation of motor vehicles results in the formation of waste motor oil.

The basic functions of motor oil are: to lubricate the engine (whose cross-section is shown in Figure 1), to reduce friction and wear off of its moving parts, to provide good sealing of cylinder-piston assembly, to protect the engine from corrosion, to provide efficient cooling of the engine, to keep the engine clean and functional, to prevent the formation of deposits and impurities in the parts of the engine. [1]

Changing the motor oil in vehicles and operating machines is done in either authorized institutions or companies' workshops.

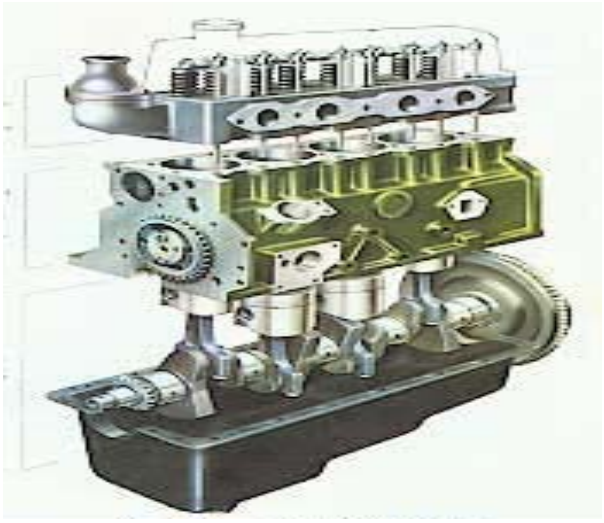

Fig. 1. Cross section of IC engines (internal combustion engines) [1]

2.2 Waste transformer oil

Transformer oil in the transformer (Figure 2) provides insulation, refrigeration, assists in extinguishing sparks, dissolves gases formed during the degradation of oil, dissolves gases and moisture from the cellulose insulation and the atmosphere [2].

Quantities of transformer oil in the transformers of associated power facilities (power substations of 35/10 kV voltage level) in the area of responsibility of the "Elektro-Bijeljina" joint stock company, are shown in Table 1. Waste transformer oil is formed in the following situations:

- if the results of analysis of transformer oil sample

are of unsatisfactory quality, replacement with new oil follows and

- if the damage to the power transformer caused discharge of transformer oil into the oil pit or the environment. [3]

Fig. 2. A transformer installed in a power grid in a substation [3]

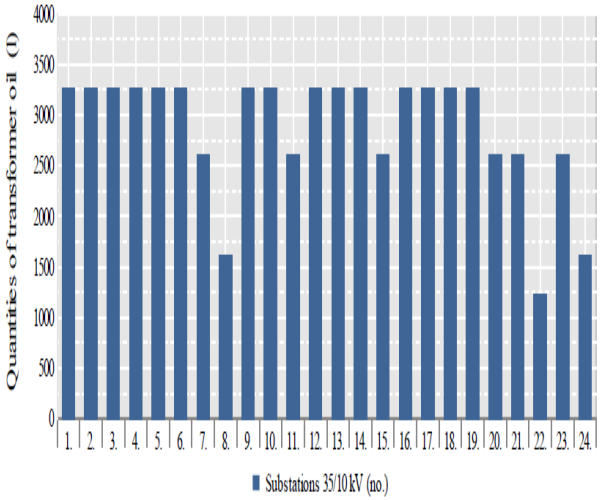

Table 1. Quantity of transformer oil in power facilities [3]

In case of oil replacement during the overhaul of power transformer in authorized institutions, the management of waste oil is under the jurisdiction of that particular institution. If the institution does not operate in accordance with ISO 14001 standards, it is the responsibility of the power distribution company to manage waste oil. [4]

2.3 MFA material flow analysis

MFA - material flow analysis is a systematic approach to presenting the material and supplies flows within the spatial and temporal limits of the system. It extends the analysis of inputs/outputs, which normally identifies only flows of inputs and outputs within defined limits. [5] MFA provides a comprehensive range of information. Balancing inputs and outputs for each process and finding the material through the system offer the following features:

- Identification of a source of existing flows (e.g: environmental loads, waste flows).
- Precise accumulation or discharging of materials within the process.

Aiming at more transparent interpretation of the results, defined are the conditions that have been met in accordance with the analysis and the issues related to the management of the flow of waste motor and transformer oils in the power company.

According to the ISO 14001 standard, the Environmental Management System (EMS) is a part of the company (enterprise) management system.

MFA is a current asset, which is applied in many branches of engineering, especially in complex systems. MFA is a tool for analyzing substances in connection with the processes and flows, after defining the spatial and temporal limits of the system. MFA is based on certain scientific laws and principles. Unlike other EMS tools, MFA is based on the law of conservation of mass.

In order to be able to select the most effective strategies for reduction and prevention, "stock & flow" diagrams enable the insights into the flows relevant to resources and environmental aspects. [6]

In order to assess the results, MFA should be combined with assessment system, which means that quantitative information on physical flows should be interpreted from the perspective of ecological knowledge and socio-economic value systems.

To create a MFA, the following procedures have been optimized:

- definition of problem and appropriate targets.
- selection of limits of systems, processes and materials.
- presentation of quantified results by using an appropriate diagram.

MFA modeling simplifies and reduces realistic complexity of the system. For the purpose of feasibility, MFA illustrates only the basic processes and flows. Defining the MFA system requires the following steps:

- Definition of spatial and time limits of the system.
- Definition of processes and flows.

2.3.1 MFA system limits

Definition of spatial limits of system

The spatial system limit is defined by the scope of this Study which, among other things, deals with the power distribution.

Definition of time limit of system

Due to the specific structure and the business operation of the power distribution companies themselves, as well as the business operation method, adopted time limit for the purpose of this analysis is 1 years.

2.3.2 Definition of processes and flows

The entire system of the Elektro-Bijeljina company, as a power distribution enterprise, is divided into 5 sub-systems, which are the work units (stations).

Model according to which the grouping has been done is the same for all distribution stations-work units

of the "Elektro-Bijeljina" joint stock company Bijeljina, where the processes are linked through the corresponding flows.

3. RESULTS AND DISCUSSION

Waste oil is hazardous waste and a major polluter of the environment. Therefore it is necessary to collect waste oil in an organised manner and, if possible, to recycle it because the waste oil is important secondary raw material which can be used for the production of lubricating oils or as a suitable heating fuel. Hence the oil enjoys such great ecological and economic significance. [7]

Given that oil may be contaminated with polychlorinated biphenyls (PCBs), one of the most toxic substances to man and wildlife, transformer oil treatment deserves special attention.

Devices filled with PCB fluids, which are in operation, are subject to special maintenance regulations and fall under the category of special waste after the use. [8]

In order to partially or completely neutralize characteristics of hazardous waste, various types of treatments have been developed, possibly followed by disposal in landfills that are specially equipped for the above mentioned function.

Today, after a long experience in tending to harmonize the hazardous waste system with environmental requirements as high as possible, created are the additional options for managing hazardous waste, which are related to the advancement of technologies that generate smaller amounts of waste, the substitution of hazardous substances with less hazardous, recycling and reuse of the existing hazardous waste and similar. [9]

Flow analysis of motor and transformer oils, and its management must be implemented in a safe and efficient manner in order to avoid environmental pollution and harm to human health. MFA - material flow analysis is the basis for monitoring new and generated waste oil.

The negative impact of improper waste oil management is multifaceted.

The most frequent is the contamination of waterways and land.

The contamination of surface waters is reflected in the creation of oil film on water surface, which prevents the penetration of oxygen into the water and thus reduce the living conditions of a large number of plants and animal species, microorganisms intoxication and toxic substances.

The presence of oil in the water flow of the so-called sanitary protection zone used for supplying communities and industrial area with the water of high quality is particularly dangerous.

Micro flora of water surface under the influence of waste oil becomes dead for plant life for a long period of time.

Results of waste oil analysis in the "Elektro-Bijeljina" company show that the share of generated quantities in the waste oil flows per work stations is: 43% in Vlasenica, Bratunac 33%, 20% in Bijeljina and Zvornik 4% [3], as shown in Figure 3. These results of waste oil analysis are logical, given that the overhaul of certain power plants, which belong to the above mentioned work stations, was done in the period analyzed.

After hazardous waste is generated, it is usually temporarily stored, which means the storing of hazardous waste on its way to the treatment plants and final disposal.

Due to the accumulation of large quantities of hazardous waste in one place, this phase is a major challenge in terms of organization in order to prevent possible accidents. Therefore the constant control is required by not only directly responsible participants, but also by the competent national authority [10].

Further functioning of the hazardous waste management usually includes its transport to the treatment plant, which significantly increases the risk of accidents and threat to the population and environment in the broader areas, along the route to be used.

3.1. Waste oil treatment plant

Waste oil quality substantially equal to some groups of base oils and lubricants production can be restored. This process is commonly called "Re-refining".

The main processes used in the waste oils treatment are: mixing, separation and chemical treatment and distillation.

In all waste oil treatment processes, the economic and energy value of waste oil are improved to varying degrees.

Two main techniques used are:

- re-refining and
- incineration (mainly in cement factories/plants),

each making approximately 30% of the total amount for re-use. The reprocessing makes remaining third, which is typically used for hydraulic oils. [11]

3.2 Re-refining

Less than 5% of the total base oil demand in Europe in 2000 was produced by re-refining [11].

In recent years, the level of regeneration has noticeably decreased in some EU countries which were the pioneers in using it, such as France, Germany, Italy and others, as well as Great Britain. This is mitigated by the fact that there are some new projects in France, Germany, Italy and Spain.

Known installed capacity for re-refining of base oils in Europe is just over 500 kt/year, and the number of plants is shown in Table 2. Currently, there are about 400 re-refining facilities worldwide, with total capacity of 1800 kt/year. [11]

The waste oils can generally be used as fuel, i.e. waste oil from ships, for tank cleaning, waste oil from crude oil / water separators, waste oil from emulsion etc.

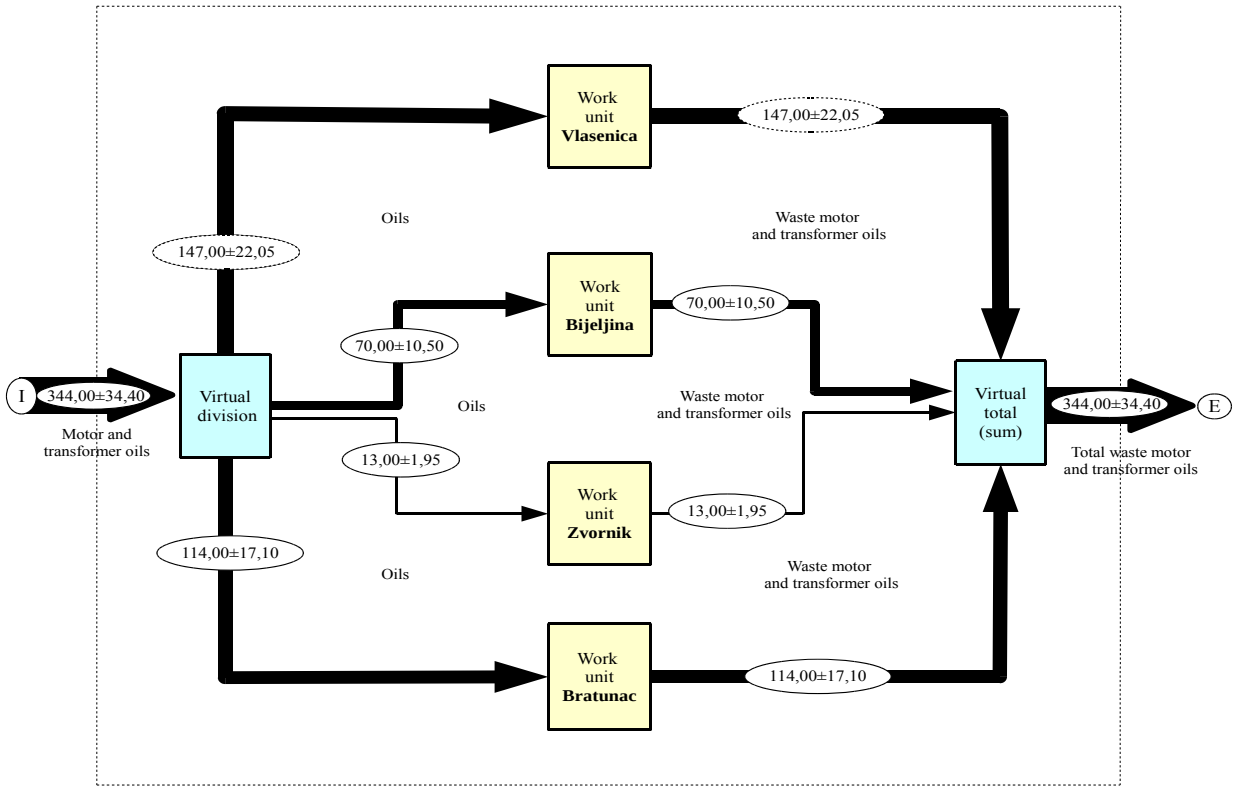

Fig. 3. The analysis and graphical display of the flows of motor and transformer oils per organizational units of the "Elektro-Bijeljina" joint stock company (1/year).

Remark: The management of waste oils generated in the work station Ugljevik is the responsibility of an authorized institution, specialised in oil change and waste oil treatment, in accordance with the legislation.

Country	Number of known plants	%
Belgium	2	5,71
Denmark	1	2,86
Germany	8	22,86
Greece	1	2,86
Špain	2	5,71
France	2	5,71
Italy	7	20,00
Malta	2	5,71
Poland	1	2,86
Finland	5	14,29
United Kingdon	3	8,57
Yugoslavia	1	2,86
Total	**35**	**100,00**

Table 2. Waste oil reprocessing plants in European countries [11].

In 1999, approximately 400 kt of waste oil was incinerated in cement plants in Europe, which represents about 17% of the total volume of waste oils, with a rate that varies greatly among different countries. This is the main way of exploitation in France, Greece and Sweden, but only one of several alternative manners in Austria, Belgium, Italy and the UK. [11] Some sectors in EU using the waste oil as fuel are:

- furnaces (e.g. Belgium),
- brick kilns (e.g. Spain),
- ceramic kilns (e.g. Spain),
- large combustion plants (e.g. Spain),
- lime kilns (e.g. Spain and Belgium),
- for new fuels production (e.g. Belgium),
- plant for the conversion of waste oil in marine fuels (e.g. Serbia),
- incineration (e.g. Belgium),
- space heaters (e.g. service stations and greenhouses),
- asphalt base.

Table 3 shows the quantity of used oil incinerated in the EU member states.

Inceneration option	Quantity of waste oil (kt)	%
Cement plants	307	41,94
Mixed with light destillate oil	213	29,10
Incinerators	52	7,10
Garage heaters	40	5,47
Others	120	16,39
Incinerated in total	**732**	**100,00**

Table 3. The quantity of waste oil incinerated in EU member states per year [11].

The figures correspond to: Denmark, Finland, France, Germany, Italy, Netherlands, Norway, Spain and the United Kingdom.

3.2.1 Waste oil re-refining

There are two main options for waste oil treatment.

- One option is a waste oil treatment in order to produce a material that will be used primarily as a fuel or for other purposes (e.g. absorbent etc.). This includes treatments such as: waste oil cleaning, thermal cracking, gasification.
- Another option is to treat waste oils that can be used as base oil for producing lubricants. [11]

Subsequently, lubricant producers add substances to meet the specifications of new products.

3.2.2 Technologies used for waste oil re-refining

Re-refining treatments may be different depending on the technology used for one or more of the following procedures:

- pre-treatment,
- cleaning,
- fractionation and
- final treatment. [11]

Waste oil pre-treatment

The purpose of pre-treatment is to remove water, small remnants and traces of fuel, such as crude oil, etc., including sediment removal. Water and sediment are removed from the waste oil by a simple physical - mechanical treatment.

Sedimentation is used in some cases for removal of water and sludge from waste oil and waste water through the oil and substances removal treatments. Generally, the treatment is carried out by using the gravitational effect, but the centrifuges or distillation may also be used.

Waste oil cleaning

Cleaning includes removal of the residues of: heavy metals, polymers, additives, and degradation compounds. Distillation and the addition of acids are typically main ways to achieve cleaning results.

Waste oil fractionation

Fractionation includes the separation of base oil by virtue of their different boiling point to yield two or three fractions of distillation.

Final treatment of waste oil

Final cleaning of various distilled fractions is carried out to achieve the required product specifications (e.g, enhanced colour, odor, thermal and oxidation stability, viscosity, etc.). Treatment may include removal of PAHs (polycyclic aromatic hydrocarbons) in the case of severe hydrocracking (high temperature and high pressure), or solvent extraction (low temperature and low pressure). Alkaline treatments KOH (potassium hydroxide) or NaOH (sodium hydroxide) are used to improve the colour properties. Bleaching is a treatment to remove the black colour from the oil (due to the dissolution of carbon additives). New objectives set for the implementation of upcoming specifications for motor oil of a passenger vehicle cannot be achieved. [11] In particular, the colour of produced oil is darker.

3.2.3 Physico-chemical treatment of special waste oil

Treatment of PCB-contaminated oil

It is dehalogenation process of PCB (Polychlorinated biphenyl) - contaminated oil from power transformers. The process eliminates low boiling point compounds and oxidation products, which are responsible for the low dielectric properties of the contaminated oil. At the end of this process, the filtration process is carried out in order to eliminate the by-products of the reaction. The concentration range mentioned in the applicability section, is typical range which defines whether the technique is economically viable. Technically, the application at higher concentrations is not a problem, but other types of PCB treatments have been defined with the necessary economic sustainability. [11]

Implementation driving force

There are mobile systems that may be applied on transformers in operation without the need for moving them. One example is operational in Italy. [11]

3.2.4 Selection of waste oil for recycling

Waste oils suitable to be recycled are:

- motor (black) oils with homogeneous features;
- black industrial oils are potentially suitable for the regeneration, but due to the presence of additives and other substances, they are generally not preferred for re-refining;
- light industrial oils, which are relatively clean, can be refined on the spot or be reused for other purposes. Their market is very specific and independent of the classical recycling pathway. [11]

If regeneration treatments are properly done, waste disposal phase could be entirely avoided. By disabling this phase, the waste motor, transformer and other oils become the waste usually incinerated in cement plants or disposed.

4. CONCLUSION

Based on the analysis results and synthesis of the data presented, the general conclusion is that striving to regeneration and reuse of waste motor and transformer oil is a priority. The decision on the selection of technology for treatment and disposal of oil should be made upon the analysis of each case. In this way, the realisation of one of the basic principles presented in the EU directives starts, which points to the need for self-sufficiency of each member state in addressing hazardous waste issue [10].

There are no waste oil and other hazardous waste treatment plants, including PCB waste treatments plant,

in most of the developing countries, thus the safe storage of such materials is the only solution for the temporary control of such waste; according to European regulations, this is also treated as a temporary measure before the final selection of treatment [10].

Developing countries need to rapidly start with the construction of required number of plants for either a certain type of treatment or a disposal of waste motor and transformer oils or other hazardous waste.

It is essential to make as many people as possible aware of the waste oils and other substances that are listed as hazardous substances and hazardous waste. This includes education about the dangers caused by these substances, measures to be taken in the event of contact with such substances, as well as on how to act in accident situations. Employees who come into contact with hazardous substances and wastes must use and apply personal protective equipment and complete appropriate training [12, 13, 14, 15].

The competent authorities must have open communication and possible cooperation among themselves as well as with the responsible individuals and the public that are indispensable links with the future system. In this regard, it is necessary to provide adequate training and continuous control afterwards, which will ensure the implementation of the established hazardous waste management principles.

Implementation of analysis, treatments, recommendations and activities for safe management of motor and transformer oils, especially in developing countries, must be realised systematically and in accordance with applicable legal standards, the requirements of applicable standards, environmental objectives and priorities of the optimal waste management.

Unpolluted and safe environment is an advantage of every country that plans fundamentally and works comprehensively according to the formula of integration of all protection aspects, in order to provide healthy conditions and environment for future generations.

5. REFERENCES

[1] Zoran Pesic, Bogdan Nedic: *Physical and tribological properties of lubricating oil*, the Faculty of Mechanical Engineering, Kragujevac, 8th International Conference on Tribology International, Belgrade, 2003.

[2] Anita Petrovic Gegic, Dragan Zivkovic: *Safe disposal of transformer oil*; Higher Education Technical School of Professional Studies Novi Sad, Transmission System and Market Operator "Elektromreza Srbije" Belgrade, 2010.

[3] Technical and other documentation of MH "ERS" ZEDP "Elektro-Bijeljina" joint-stock company Bijeljina.

[4] Technical regulations and manuals for the maintenance of power plants and distribution stations, MH Power Distribution Enterprise "Elektroprivreda RS", Banja Luka, 2008.

[5] Brunner, P. H. and H. Rechberger. *Practical handbook of material flow analysis*. Boca Raton, FL, USA: CRC Press., 2004.

[6] N. Stanisavljevic, PH Brunner, *Combination of material flow analysis and substance flow analysis: A powerful approach for decision support in waste management*. Waste Management & Research, 0734242X14543552, 2014.

[7] Proceedings of the 7th Symposium "*Recycling Technologies and Sustainable Development"* with international participation, University of Belgrade, Technical Faculty in Bor, Soko Banja, 2012.

[8] Sladjana Gavrancic, Dejan Skala: P*olychlorinated biphenyls - features, applications and decomposition technology,* Professional Papers, Technology and Metallurgy, University of Belgrade, 2000.

[9] Todorovic Maja, Bakrac Sasa: *The integration of environmental risk assessment process in the evaluation process of the environmental protection impact - methodological approach*; the Singidunum University, the Ministry of Defence of the Republic of Serbia, Belgrade, 2010.

[10] Milena Panic: *Hazardous waste management, planning, organization, operation system*, Special edition; Serbian Academy of Sciences and Arts, Belgrade, 2010.

[11] Reference Document "BREF" on best available techniques for industrial waste treatment, *Integrated environmental prevention and control of environmental pollution*, European Commission, 2006.

[12] The Law on Waste Management ("Official Gazette of RS" no. 111/13).

[13] The Law on Environmental Protection ("Official Gazette of RS" no. 71/12).

[14] The Law on Protection at Work ("Official Gazette of RS"no. 01/08 i 13/10).

[15] The Law on Fire Protection ("Official Gazette of RS" no. 71/12).

Authors: **Dragisa Djordjic Specialist in Environmental Engineering, Prof. dr Slavko Djuric, Prof. dr Miodrag Hadzistevic**, the University of Novi Sad, the Faculty of Technical Sciences, Department of Environmental Engineering and Occupational Safety, Trg Dositeja Obradovića 6, 21000 Novi Sad, Serbia, Phone : +387 65 738 060
E-mail: **zastitad@gmail.com**

Journal of Production Engineering
Vol.19 No.2
JPE (2016) Vol.19 (2) Original Scientific Paper
Adekunle, A. S., Olusegun, H. D., Dada, A. T., Adebiyi, K. A.

INHIBITIVE INFLUENCE OF GREEN PLANT LEAVES EXTRACT ON AISI 4137 STEEL

Received: 24 September 2016 / Accepted: 10 November 2016

Abstract: *Inhibition of corrosion on AISI 4137 steel in H_2SO_4 using Cascabela thevetia and Jatropha curcas leaves as inhibitor was studied using gravimetric and gasometric analysis. It was found that the leaves extract of both plants act as a good corrosion inhibitor for AISI 4137 steel in all concentrations of the extract ranging from 0.3 - 1.5 g/l and the inhibitive efficiency increases with increasing concentration of inhibitor. Cascabela thevetia has better surface coverage than Jathropha curcas with their surface coverage been 0.68 and 0.61 respectively. As the concentration of the inhibitors increases the evolution of the gas decreases with the highest evolution been 23 cm^3 and 22 cm^3 at 0.3 g/l concentration for both Cascabela thevetia and Jathropha curcas respectively in 7 minutes. Cascabela thevetia and Jatropha curcas leaves extract are recommended for use in industries as a replacement for toxic chemical inhibitors.*

Key words: *Corrosion inhibitor, Cascabela thevetia, Jathropha Curcas, Surface coverage, gasometric, gravimetric and inhibition efficiency*.

Inhibitivni uticaj ekstrakta zelenih biljnih listova na čelik AISI 4137. *Inhibicija korozije na čeliku AISI 4137 u H_2SO_4 korišćenjem listova Cascabela thevetia (žuti oleander) i Jatropha curcas (Barbadoski orah) kao inhibitora, je istraživano pomoću gravimetrijske i gasometrijske analize. Utvrđeno je da je ekstrakt listova obe biljke dobar inhibitor korozije na čeliku AISI 4137 u svim vrednostima koncentracijama ekstrakta, od 0,3 – 1,5 g/l s tim da se efikasnost inhibitivnosti povećava sa povećanjem koncentracije inhibitora. Cascabela thevetia poseduje bolju površinsku pokrivenost nego što ima Jatropha curcas, sa površinskom pokrivenošću 0,68 i 0,61 respektivno. Kako se povećava koncentracija inhibitora, evolucija gasova se smanjuje i gde je najveća evolucija 23 cm^3 i 22 cm^3 kod koncentracije 0,3 g/l pri Cascabela thevetia i Jatropha curcas u vremenskom intervalu od 7 minuta. Ekstrakt lišća Cascabela thevetia and Jatropha curcas se preporučuje za korišćenje u industriji kao zamena za toksične hemijske inhibicione supstance.*

Ključne reči: *Inhibitor korozije, Cascabela thevetia, Jatropha curcas, površinska pokrivenost, gasometrijska, gravimetrijska i inhibiciona efikasnost.*

1. INTRODUCTION

The deterioration of materials due to their chemical or electrochemical interactions with the surrounding environment is generally understood as corrosion. This is as a result of the natural tendency for metals to revert to more stable mineral form in its natural state [1]. Virtually all metals, with the exception of gold and platinum, will corrode in an oxidizing environment forming compounds either in their oxides, hydroxides or sulphides state. Even though it is a natural process for metallic materials to corrode, the speed at which it occurs depends greatly on the type of environment to which the material is exposed [2]. Corrosion processes are responsible for numerous losses in the industrial scope. Quite a number of ways have been deployed in controlling corrosion via material selection, coatings, designs, inhibitors and cathodic protection. The use of inhibitors has been one of the most practical methods for protection against corrosion in acidic environment [3]. Basically, there are various types of corrosion inhibitors such as anodic inhibitors, cathodic inhibitors, mixed inhibitors and volatile corrosion inhibitors [4]. There are also classification based on synthetic (organic), metallic (inorganic) and green inhibitors (natural product). A number of organic compounds are known to be applicable as corrosion inhibitors for carbon steel in acidic environments. Such compounds typically contain nitrogen, oxygen or sulphur conjugated system and function via adsorption of the molecules on the metal surface creating a barrier to the corrodent attack [5,6]. Research has confirmed that some of the synthetic and inorganic inhibitors are toxic thereby causing failure of kidney and liver as well as mutation of the enzymes [7]. However, because of the toxic nature, high cost, non-renewable, strict environmental regulations and disruption of ecosystem of some of these synthetic and inorganic inhibitors, the exploration of natural product of plant origin as corrosion inhibitor is currently receiving attention. The use of corrosion inhibitor is one of the best and most useful method in the industry [8,9].

Corrosion inhibitors are substances that are added in small concentrations to corrosive media to decrease or prevent the reaction of the metal in the media [7,10]. The availability of organic compounds, such as tannins, saponins, alkaloids, in the natural plants is what is majorly responsible for the inhibitive traits that are found in the green inhibitors [11]. Several plants extracts, have been tested as corrosion inhibitors for metals. A few of them are karanj (Pongamiapinnata), Kalmegh (Andrographis paniculata), Xylopia

ferruginea, Occimumviridis, Hibiscussubdariffa, henna, Acalyphaindica, Phyllanthusamarus, Jathropha carcus, tobacco, neem leaf and ginkgo [12,13,14]. Historically, inhibitors had great acceptance in the industries due to excellent anti-corrosive proprieties. However, many showed up a secondary effect which damaged the environment and this had led the scientific community to begin to research for friendly environmentally inhibitors, like the organic inhibitors. The exploration of natural products origin as corrosion inhibitors is becoming the subject of extensive investigation due principally to the low cost and eco-friendliness of these products, and is fast replacing the synthetic and expensive hazardous organic inhibitors [15]. Plant extracts constitute several organic compounds which have corrosion inhibiting abilities. The yields of these compounds as well as the corrosion inhibition abilities vary widely depending on the part of the plant and its location [16]. The extracts from the leaves, seeds, heartwood, bark, roots and fruits of plants have been reported to inhibit metallic corrosion in acidic media [17]. As a contribution to the current interest on environmentally friendly corrosion inhibitors, this present research aims at broadening the application of plant extracts for metallic corrosion inhibition by investigating the inhibitive properties of leaves extracts of *Cascabela thevetia* and *Jatropha Curcas* on AISI 4137 steel using weight loss (gravimetric) and gasometric techniques.

2. MATERIAL AND METHOD

Cascabela thevetia leaves, *Jathropha curcas* leaves, Methanol, Digital Electronic Weighing Balance, Standard Flat Bottom Flask, Beakers, Emery Papers, Buckner flask, stopwatch and Delivery tube. The spectrometric analysis of the steel used shows the following chemical composition by weight, Table 1.

Composition	C	Si	S
Composition (wt%)	0.370	0.230	0.060
Composition	Ni	Cr	Mo
Composition (wt%)	0.120	0.100	0.02
Composition	W	As	Sn
Composition (wt%)	0.003	0.006	0.006
Composition	Pb	Co	Zn
Composition (wt%)	-0.002	0.010	0.004
Composition	Mn	Cu	Al
Composition (wt%)	0.790	0.260	- 0.007
Composition	P	V	Fe
Composition (wt%)	0.050	0.003	97.95

Table 1: Compositional Analysis of AISI 4137

Rectangular steel specimen of 1mm thick was mechanically pressed cut into coupons of 35mm x 20mm x 1mm with a drilled hole of 3mm on each coupon for the purpose of suspension. The exposed area of each coupon was abraded with emery paper of different grades, polished and degreased with Ethanol The steel coupons was cleaned with acetone and kept inside desiccators. The leaves of cascabela thevetia and Jatthropha curcas were washed and sliced into pieces separately; the prepared leaves was then room dried, pulverized into powdery form and soaked with methanol for 48 hours. The solution was filtered and methanol was evaporated from the filtrate in order to get the needed inhibitive extract. The extract was weighed with digital electronic weighing balance. The phytochemical analysis of the inhibitive extract for both cascabela thevetia and Jatthropha curcas leaves was carried out using plant tissue homogenization technic.

2.1 Gravimetric analysis

Extract of cascabela thevetia and Jatthropha curcas ranging from 0.3g, 0.6g, 0.9g, 1.2g and 1.5g were dissolved in separate beakers each filled with 1 litre of sulphuric acid solution as the inhibited environments. The pre-treated steel coupons were taken out of the desiccator, weighed with a digital electronic weighing balance of ±0.01g accuracy and the corresponding weight, W_1) was noted. The prepared coupons was immersed by suspension into the prepared environment and removed from each of the environments i.e. the blank (uninhibited) and the inhibited environments at an interval of 7 days. Each of the removed coupons at the end of the stated interval was washed with Ethanol and Acetone, then weighed again and the weight (W_2) noted. The whole experiment lasted for 28 days. The differences in weights of the coupons (weight loss) in both the blank and the inhibited environments were recorded with the periods of immersion and the inhibitor concentrations noted. The values recorded were used accordingly to calculate the weight loss, corrosion rate, surface coverage and inhibitive efficiency of each inhibitor concentration by the following equations:

$$\Delta W = W_1 - W_2 \quad (1)$$

Where,

W_1 = Initial weight of each coupon before immersion in both media (g)

W_2 = Final weight of each coupon after immersion in both media (g)

$$\text{Corrosion Rate } (CR) = \frac{\Delta W}{AT} \quad (2)$$

Where,

A = Area of the coupon, mm^2

T= Time spent in both media, hrs.

$$\text{Surface Coverage } (\Theta) = \frac{(CR_1 - CR_2)}{CR_1} \quad (3)$$

and,

Inhibitive Efficiency (I.E.) = Θ x 100% (4)

Where,

CR_1 = Corrosion Rate in the blank environment at the same interval

CR_2 = Corrosion Rate in the inhibited environment at the same interval

2.2 Gasometric analysis

Gasometric experiments were conducted on the steel coupons of dimension 15mm x 10mm x 1mm. The gasometric (gas-volumetric) technique provides a rapid and reliable means of ascertaining any perturbation by the inhibitor with regards to gas evolution at the

corroding interphase. Each specimen was dropped into the Buckner flask containing 4.0M H_2SO_4 solutions in the presence of the various extract concentrations (0.3 – 1.5 g/l) for *Cascabela thevetia and Jathropha curcas* extract and one without an inhibitor (blank) at room temperature. The initial volume of the hydrogen gas was noted as v_1. The setup was allowed to be in rest position for seven minutes and the volume of hydrogen gas evolved per minute was noted as v_2. The whole experiment lasted for 24 hours.

The change in volume (ΔV), rate of evolution of the gas (RV_H), surface coverage (Θ) and inhibitive efficiencies (I.E %) was determined using the equations below:

$$\Delta v = v_1 - v_2 \qquad (5)$$

Where,

v_1 = initial volume of the hydrogen gas

v_2 = final volume of the hydrogen gas

$$\text{Rate of gas evolved, } (RV_H) = \frac{\Delta V}{AT} \qquad (6)$$

Where,

A = Area of the coupon (mm^2)

T = Time spent in both media (min)

$$\text{Surface Coverage } (\Theta) = \frac{(RV_1 - RV_2)}{RV_1} \qquad (7)$$

Inhibitive Efficiency (I.E.) = Θ x 100%

Where,

RV_1 = rate of gas evolved blank

RV_2 = rate of gas evolved inhibited

3. RESULTS AND DISCUSSION

The phytochemical analysis of both *Cascabela thevetia and Jathropha curcas* leaves showed the presence of the following compounds tannins, saponins, flavonoids, alkaloids, phenol and terpenoids while nicotine is absent. However, tannins, saponins and alkaloids are the most active constituents of the inhibitor Table 2. The weight losses for both the blank and that of the inhibited environment using *Cascabela thevetia and Jathropha curcas* increase with exposure time Fig 1 and Fig 2. The highest weight loss for blank in both cases for a period of 14 days is 5.18g while the lowest is 6.12 g in 28 days. However, in the inhibited environment, the weight losses increases within 21 days for both inhibitors with highest weight loss of 5.43 g occurring in a concentration of 0.3 g/l and lowest weight loss of 5.43 g occurring in a concentration of 1.5 g/l for the *Cascabela thevetia* while for the *Jathropha curcas* is 5.2 g for the lowest and 4.07g for the highest at the same concentrations. This was as a result of the formation of the protective film layer on the surface of the mild steel in the inhibited environment. Beyond 21 days for both inhibitors, the weight loss decreases with a weight loss of 5.88 g in 0.3 g/l and 4.36 g in 1.5 g/l for *Cascabela thevetia;* 5.84 g in 0.3 g/l and 4.66g in 1.5 g/l for the *Jathroha curcas* thereby maintaining the same concentration order as earlier stated.

The weight loss of mild steel using both inhibitors shows that within 7-14days at a high concentration of 0.9-1.5 g/l , *Jathropha curcas* is a better inhibitor compared to *Cascabela thevetia* but within 14-21 days, *Jathropha curcas* shows the least weight loss irrespective of the concentration been used. Thus, Jathropha *curcas* appears to be a better inhibitor within 21days than *Cascabela thevetia.*

Phytochemical constituent	*Cascabela thevetia*	*Jathropa curcas*
Tanins	+	+
Saponins	+	+
Phenol	-	+
Flavonoids	+	+
Alkaloids	+	+
Terpenoids	+	+
Nicotine	-	-

Key: + is present - is absent

Table 2. Phytochemical constituents of the inhibitors

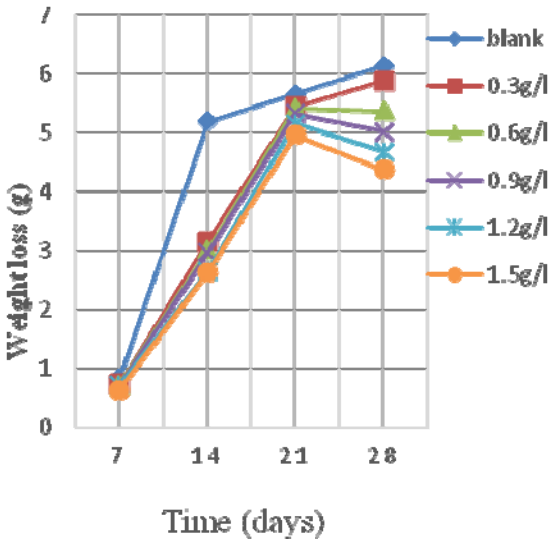

Fig. 1. Weight loss of steel in H_2SO_4 with varied concentrations of *Cascabela thevetia* as inhibitor

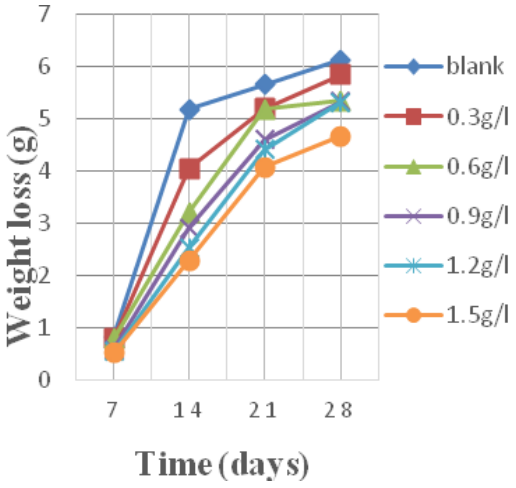

Fig. 2. Weight loss of steel in H_2SO_4 with varied concentrations of *Jathropha curcas as* inhibitor

Furthermore, the corrosion rate for both *Cascabela*

thevetia and *Jathropha curcas* increase as the exposure time increases within 21 days and 14 days respectively Fig 3 and Fig 4. The maximum corrosion rate for *Cascabela thevetia* is $1.54x10^{-5}$ g/mm^2/hr. in 0.3 g/l and lowest is $1.4x10^{-5}$ g/mm^2/hr. in 1.5 g/l while for *Jathroha curcas* it was $1.72x10^{-5}$ g/mm^2/hr. in 0.3 g/l and $0.974x10^{-5}$ g/mm^2/hr. in 1.5 g/l. In general, the corrosion rate for both inhibitors at different concentration irrespective of the concentration was lesser than that of the blank.

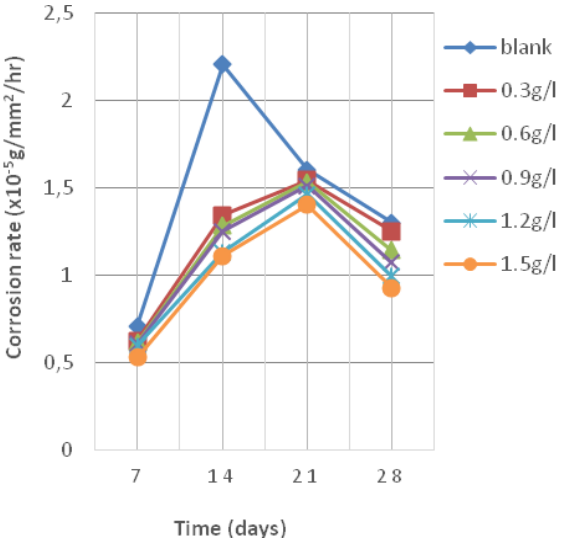

Fig. 3. Corrosion rate of steel in H_2SO_4 with varied concentrations of *Cascabela thevetia* as inhibitor.

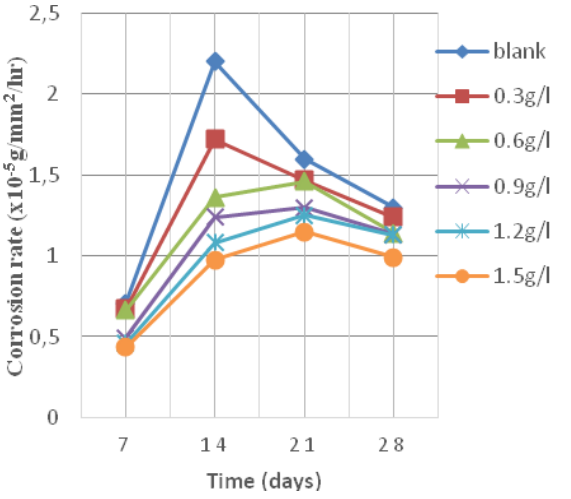

Fig. 4. Corrosion rate of steel in H_2SO_4 using varied concentrations of *Jathropha curcas* inhibitor.

The decrease in corrosion rate of the inhibited environments could be due to increase in inhibitor concentrations as a result of adsorption of organic compounds onto the surface of the coupons which developed the protective film layer that reduced the permeability of the H_2SO_4 onto the surface of the mild steel. Beyond 21 days for *Cascabela thevetia and 14days for Jathropha curcas* the inhibitor has no inhibitive effect irrespectively of the concentration. This could be due to the dissolution of H_2SO_4 into H_2 gas and SO_4^{2-}, with H_2 gas evolving the media becomes less corrosive since SO_4 is a base. Thus, *Jathropha curcas* has more effect as an inhibitor than *Cascabela thevetia.*

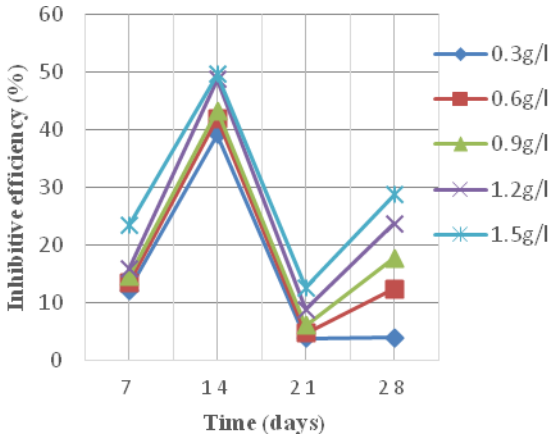

Fig. 5. Inhibitive efficiency using varied concentrations of *Cascabela thevetia* as inhibitor

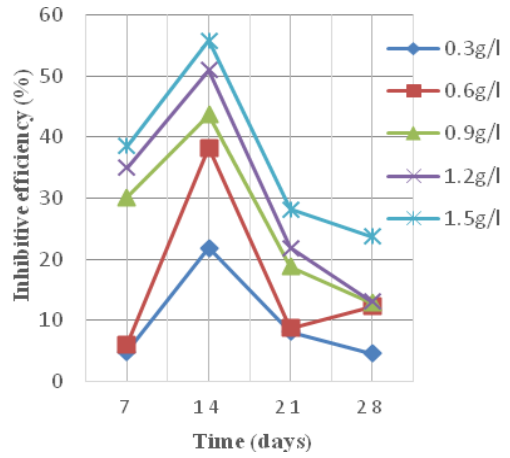

Fig. 6. Inhibitive efficiency using varied concentrations of *Jathropha curcas as* inhibitor

Fig 5 and Fig 6 shows the inhibitive efficiency of the inhibitor on mild steel in different concentrations of the inhibitor in H_2SO_4. The results showed that within the first 14days, the inhibitive efficiency increases as the concentration of the inhibitor increases for both *Cascabela thevetia and Jathropha curcas.* The maximum inhibitive efficiency of the inhibitor were found to be 49.6% and 55.8% at 1.5 g/l for *Cascabela thevetia and Jathropha curcas* respectively. This might be due to increase in the thickness of the protective film layer formed as the inhibitor concentration was increasing which could be caused by adsorption of phytochemical constituents (organic compounds such as tannins, alkaloids, flavonoids, terpenoids etc.) that are present in the inhibitors as shown in Table 2 formed on the surface of the mild steel that consequently reduced the permeability of H_2SO_4 onto the metal surface. However, the lowest inhibitive efficiency of the inhibitors was 39.2% and 21.9% at 0.3 g/l for *Cascabela thevetia and Jathropha curcas* respectively. Beyond 14 days, the inhibitive efficiency for both *Cascabela thevetia and Jathropha curcas* decrease irrespective of the concentration.

3.1 Gasometric

In the *Cascabela thevetia and Jathropha curcas* inhibitors, the rate of evolution of hydrogen gas decreases linearly as the time increases but not at a fast rate as the blank Fig7 and Fig 8. This shows that the presence of inhibitors *(Cascabela thevetia and Jathropha curcas)* slow down the rate and the volume of hydrogen gas that is evolved. Also, the evolution of the gas is directly dependent on the concentration of the inhibitors, hence as the concentration of the inhibitors increases the evolution of the gas decreases for both inhibitors. Highest gas evolved in 7 minutes was 23 cm^3 and 22 cm^3 at 0.3 g/l concentration for both *Cascabela thevetia and Jathropha curcas* inhibitors respectively while the least gas was 49 cm^3 at 1.5 g/l concentration for both *Cascabela thevetia and Jathropha curcas* inhibitors at 1minute.

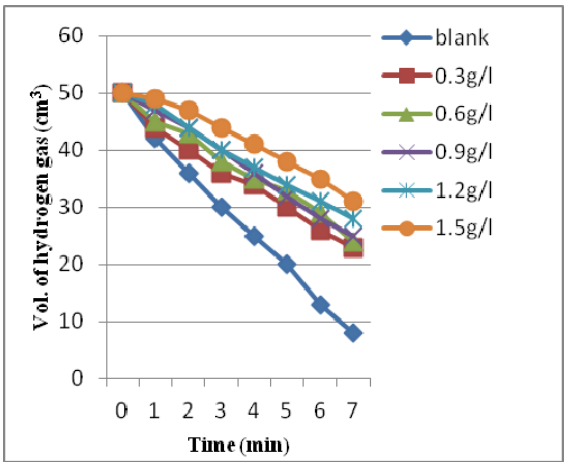

Fig. 7. Volume of hydrogen gas evolved using Cascabela thevetia as inhibitor

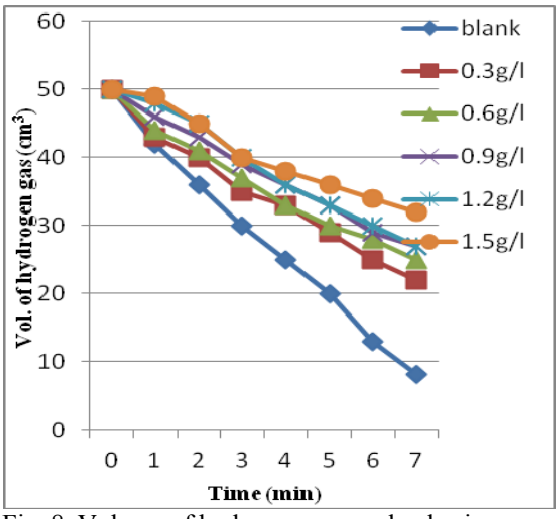

Fig. 8. Volume of hydrogen gas evolved using Jathropha curcas as inhibitor

The surface coverage for both *Cascabela thevetia and Jathropha curcas* increases as the concentration increases Fig 9. This was as a result of the phytochemical constituents that was rapidly reacting with the H_2SO_4 thereby reducing the rate at which the acid reacts with the mild steel and consequently reducing the rate at which the metal would corrode. The highest surface coverage for *Cascabela thevetia and Jathropha curcas* as inhibitors was 0.68 and 0.61 respectively at 1.5 g/l concentration and the least surface coverage was 0.31and 0.27 for *Cascabela thevetia and Jathropha curcas* respectively at 0.3 g/l concentration. This shows that *Cascabela thevetia* has a better surface coverage compared to *Jathropha curcas* and invariably would inhibit better for a shorter period of time however as the time increases, Jathropha curcas would inhibit better and more efficiently as shown earlier in the gravimetric analysis.

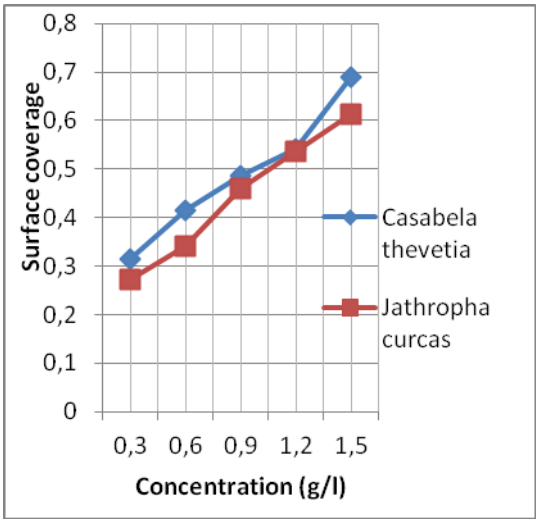

Fig. 9. Surface coverage of the inhibitors

The inhibitive efficiency of *Cascabela thevetia and Jathropha curcas* inhibitors increases with increase in the inhibitors concentration Fig 10. The highest efficiency for both inhibitors were 68% and 61% for *Cascabela thevetia and Jathropha curcas* respectively at 1.5 g/l and the least inhibitive efficiency for both inhibitors were 31% and 27% for *Cascabela thevetia and Jathropha curcas* respectively at 0.3 g/l. This suggests that the phytochemical components of the inhibitors are adsorbed on the mild steel–solution interface. Similar trend was observed in 0.5 M H_2SO_4 fpr the weight loss measurements up to 14days which showed that *Jathropha cucas* would inhibit better at a prolonged time.

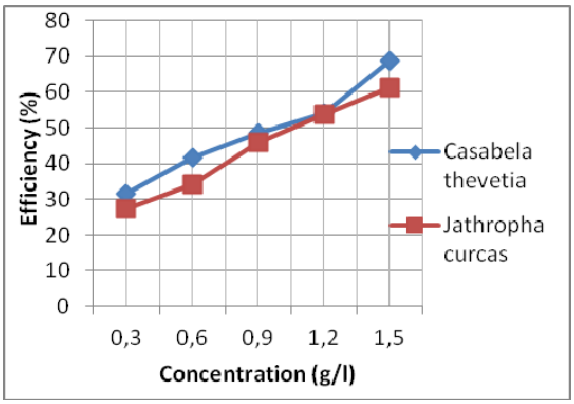

Fig .10. Efficiency of inhibitors

The trend in inhibition efficiency with concentrations of the various inhibitors used indicates the chemisorption of the phytochemical constituents of

the inhibitors on the surface of the metal. This observed trend of the corrosion of mild steel in the H_2SO_4 solutions with increase in the inhibitors concentration was due to the adsorption of the components of the inhibitors on the metal surface. The inhibitive action of organic molecules was regarded as a simple substitution process, in which an inhibitor molecule (*I*) in the aqueous phase substitutes an *x* number of water molecules adsorbed on the surface:

$$I(aq) + xH_2O(ads) \leftrightarrow I(ads) + xH_2O(aq)$$

which will in turn inhibit further metal dissolution.

4. CONCLUSION

In the analysis carried out in this work using the gravimetric and gasometric approach, the following conclusions were drawn:

1) The extracts of Cascabela thevetia and Jathropha curcas leaves at 1.5g/l concentration in H_2SO_4 gave an inhibitive efficiency of 49.59% and 55.77% respectively after 28days while the gasometric analysis gave an efficiency of 68.9% and 61.3% respectively.

2) As the concentration of the inhibitors increased in the H_2SO_4 medium, the weight loss, corrosion rate and hydrogen gas evolved decreased.

3) Cascabela thevetia has better surface coverage than Jathropha curcas and thus inhibit better in short period of time but for prolonged time Jathropha curcas inhibit best.

4) The evolution of the gas is directly dependent on the concentration of the inhibitors, hence as the concentration of the inhibitors increases the evolution of the gas decreases with the highest evolution of 23 cm^3 and 22 cm^3 at 0.3 g/l concentration for both Cascabela thevetia and Jathropha curcas inhibitors respectively in 7minutes.

5) Cascabela thevetia and Jathropha curcas were seen to be active as inhibitors as a result of active phytochemical constituents present in them.

5. REFERENCES

[1] Vasant, P. C., Bansal, G. K. An Investigation into the Environmental Impacts of Atmospheric Corrosion of Building Materials. *International Journal of Chemical Sciences and Applications*, 4(1), pp1 – 6, 2013.

[2] Barbara, S., Robert, K. *What is corrosion?* The electrochemical society interface, 6, pp24-26, 2006.

[3] Ansari, K. R., Yadav, D. K., Ebenso, E. E., Quraishi, M. A. *Novel and Effective Pyridyl Substituted 1, 2,4- Triazole as Corrosion Inhibitor for Mild Steel in Acid Solution*. International. Journal of Electrochem. Science, 7, pp4780 – 4799, 2012.

[4] Agarwal P., Landolt D. *Effect of anions on the efficiency of aromatic carboxylic acid corrosion inhibitors in near neutral media: Experimental investigation and theoretical modeling.* Corrosion Science, 40(4-5), pp673 – 691, 1998.

[5] Ebenso, E.E., *Effect of halide ions on the corrosion inhibition of mild steel in H_2SO_4 using methyl red.* bulletin of electrochem. 19(5): pp209-216, 2003.

[6] El-Ashry, H.E., El-Nemr, A., Esawy, S.A., Ragab, S. *Corrosion inhibitors: Quantum chemicals studies on the corrosion of mild steel in acidic medium by some triazole oxadiazole and thiadiazole derivatives*. Electrochem Acta 51: pp3957-3968, 2006.

[7] Singh, A., Ebenso, E. E., Qurashi, M. A. *Corrosion Inhibition of carbon steel in HCl solution by some plant extracts*. International Journal of Corrosion. pp1-20, 2012.

[8] Eddy, N.O., Odoemelam, S.A. *Effect of pyridoxal hydro-chloride-2,4-dinctrophenyl hydrazone on the corrosion of mild steel in HCl*. Journal of surface science technology 24(1-2), pp1-14, 2008

[9] Al-Otaibi, M.S., Al-Mayouf, A. M., Khan M., Mousa, A. A., Al-Mazroa, S. A., Alkhathlan, H. Z., *Corrosion inhibitory action of some plant extracts on the corrosion of mild steel in acidic media*. Arabian Journal of Chemistry, pp. 1-7, 2012.

[10] Hubert, G., Elmar-Manfred, H., Hartmut, S., Helmut S. *Corrosion Ullmann's Encyclopedia of Industrial Chemistry,* Wiley-VCH, Weinheim, 2002.

[11] Raja, K., Rajendra, S., Saranya, R. *Allum sativum (Garlic) extract as non-toxic corrosion inhibitors*. Journal of Chemistry, pp1 – 4, 2013.

[12] Oguzie, E.E. *Inhibition of acid corrosion of mild steel by telfaria ocidentalis extract*. Pigment and Resin Technol, 34(6), pp321-326, 2005

[13] Abiola, O.K., N.C. Ebenso, E.E., Nwinuka, N.M. *Ecofriendly corrosion inhibitors: inhibitive action of delonix regia extract for the corrosion of aluminium in acidic medium*. Anti-corr meth. Mater 54(4), pp219-224, 2009.

[14] Rajalakshmi, R., Prithiba, A., *Leelavathi S. An overview of emerging scenario in the frontiers of eco-friendly corrosion inhibitors of plant origin for Mild Steel*. Journal of Chemical, Acta 1, pp6 – 13, 2012.

[15] Eddy, N.O., Ebenso E.E. *Adsorption and inhibitive properties of ethanol extracts on musa sapientum peels as a green corrosion inhibitor for mild steel in H_2SO_4.* African Journal of pure Applied chemistry, 296, pp046-054, 2008.

[16] Okafor, P.C., Ikpi, M.E., Uwah, I.E., Ebenso, E.E., Ekpe, U.J., Umoren S.A., Corrosion Science 50, pp2310, 2008.

[17] Umoren, S.A., Obot, I. B., Ebenso E. E., Okafor, P. C., Ogbobe, O., Oguzie, E. E., Anti-Corrosion Meth. Material 53, pp27, 2006.

Authors: Senior Lecturer. Dr. **Adebayo S. Adekunle**[1], Prof. **Henry D. Olusegun**[2], Research Student. **Akinola Timothy Dada**[1], Prof. **Kazeem A. Adebiyi**[3].

[1]University of Ilorin, Department of Mechanical Engineering, P.M.B. 1515, Ilorin, Nigeria. Phone: 234-8033591465, 234-7039113639.

[2]Federal University of Technology Minna, Department of Mechanical Engineering, Minna, Nigeria, Phone: 234-8034501122.

[3]Ladoke Akintola University of Technology, Ogbomoso, Department of Mechanical Engineering, P.M.B. 4000, Ogbomoso, Nigeria. Phone: 234-8033616099.

E-mail: adekunlebayo@yahoo.com olusegunhenry@yahoo.com, haykay4c@gmail.com, engradebiyi@yahoo.com

Journal of Production Engineering
Vol.19 No.2
JPE (2016) Vol.19 (2) Original Scientific Paper
Ajao, K. S., Ohijeagbon, I. O., Adekunle, A. S., Olusegun, H. D.

DEVELOPMENT OF PAVING TILES COMPOUNDED WITH PULVERIZED CORNCOB CHARCOAL

Received: 01 November 2016 / Accepted: 03 December 2016

Abstract: *The current trend all over the world is to minimize environmental pollution through wastes recycling. Thus, paving tiles' specimens of dimensions 198mm x 98mm x 56mm were produced in the laboratory using various mix ratios of granite particles and pulverized corncob charcoal. Wood charcoal dust was used as control and cement as binder. Batching was by volume and a constant water/cement ratio of 0.7 was used. The tiles' physical and mechanical properties were determined. Results obtained showed that as the percentage of pulverized corncob charcoal in the mixture aggregate increases, the flexural strength, compressive strength and bulk density of the tiles decreases, while a progressive increase was experienced in water absorption for 20% and 15% cement addition. Significant similarities were observed in the properties of experimental tiles produced with addition of pulverized corncob charcoal and those with addition of wood charcoal dust which was used as control. 30% and 10% addition of pulverized corncob charcoal for 20% and 15% cement content tiles respectively were recommended. Recycling of corncob as a constituent material of paving tiles is feasible.*
Key words: *Paving Tiles, Granite Particles, Corncob Charcoal, Environmental Pollution, Recycling*

Razvoj elemenata za popločavanje obogaćenih sa usitnjenim izgorelim oklascima. *Aktualni trend u celom svetu je smanjenje zagađenja životne sredine primenom reciklaže otpada. S tim ciljem su u laboratoriji izrađeni elementi za popločavanje, dimenzija 198mm x 98 mm x 56mm, korišćenjem raznih vrsta odnosa granitnih čestica i usitnjenih izgorelih oklasaka. Usitnjen ćumur je korišćen u svrhu kontrole a cement kao vezivno sredstvo. Svaka šarža je bila iste zapremine i konstantnog odnosa voda/cement koji je iznosio 0,7. Fizičke i mehaničke osobina elemenata za popločavanje su bili određivani. Dobijeni rezultati pokazuju smanjenje savojne čvrstoće, otpornosti na sabijanje i gustine elemenata za popločavanje sa povećanjem procenta udela usitnjenih izgorelih oklasaka, dok je zabeleženo progresivno povećanje apsorpcije vode kod 20% i 15% cementne smeše. Velike sličnosti su bile primenćene u osobinama eksperimentalnih popločavajućih elemenata napravljenih sa dodatkom usitnjenih izgorelih oklasaka i onih sa dodatkom usitnjenog ćumura koji je bio korišćen kao kontrolni element. Na osnovu studije se preporučuje 30% i 10% dodatka usitnjenih izgorelih oklasaka na 20% odnosno 15% sadržaja cementa u elementima za popločavanje. Takođe je pokazana mogućnost reciklaže oklasaka kao materijala za izradu popločavajućih elemenata.*
Ključne reči: *elementi za popločavanje, granitne čestice, usitnjeni izgoreli oklasci, zagađenje životne sredine, reciklaža*

1. INTRODUCTION

In the effort of producing food for the world's growing population through agricultural activities, various agricultural residues are generated. Their indiscriminate disposal or open burning results in environmental pollution with emission of irritating smells and hazardous gases that poses serious challenges to sustainable healthy environment [1]. Thus, many researchers have attempted utilizing agricultural residues for various applications such as building construction material, in an environmentally and economically sustainable manner [2, 3, 4]. Corncob is one of the residues left over after extracting the corn. Large quantity of corncob is being discarded as waste into the environment most especially during harvest season because corn planting is predominantly focused on for the use of the kernel (grain).

Over the last few years, there has been an increase in the production of corn globally owing to intensive agricultural activities in the wake of population growth. Consequently, significant increase was observed in the quantity of corncob discarded as waste into the environment. During the year 2001-2011, global production of corn rose from 599.35 million metric tonnes to 867.52 million metric tonnes [5]. Nigeria production of corn in the year 2013 was estimated at 10.4 million metric tonnes and for every one tonne of corn produced, about 160 – 180 kg corncob is generated [2, 6]. In the year 2013, 1.664 – 1.872 million metric tonnes of corncob was generated in Nigeria and recycling of this waste is therefore imperative. Research has shown that corncob can be used in the production of activated carbon [7, 8] which can be briquetted and used as alternative cooking fuel [9, 10], corncob ash can also be used as cement replacement in concrete work [3, 11, 12]. However, large proportion of corncob generated annually is not utilized and as such a proactive means of solving the problem of environmental pollution associated with its indiscriminate disposal is to explore further use that would bring about its large

scale deployment. Thus, utilization of corncob as constituent material of paving tiles could provide a better way of evacuating it from the environment and eventually results in a sustainable economic benefit.

Paving tiles are manufactured concrete products, made in different shapes and sizes, used to finish off a paved area outside buildings, warehouses, museums, art galleries, commercial garages, halls, factories, walkways etc. for decorative and aesthetic purposes. Apart from providing aesthetic, they can also be used to aid drainage and level out a specific area so that excess water is drained away [13]. They are loosely laid and adhesives are not required in their installations; as a result, they can be removed and positioned as the need arises. The growth of paving tiles production in recent time is unprecedented due to continual development of infrastructure as a consequence of growing population and modernization.

The core material used in the production of paving tiles in Nigeria is granite particles popularly known as stone dust, usually sourced from quarry sites. The aim of this study is to harness corncob for use as a constituent material of paving tiles in order to reduce environmental pollution and increase the spectrum of value addition to farm produce. There had been several research efforts on the use of various agricultural residues and other wastes materials to obtain construction products. Semanda *et al.*, [14] investigated the feasibility of using plastic and egg shell wastes together with white cement in the production of floor tile materials. Pinto *et al.,* [15] worked on a lightweight concrete using granulated corncob as aggregate. Techniti *et al.,* [4] conducted a complete characterization of ten different agricultural by-products, including corncob, with a view to using agricultural residues as secondary raw materials of construction. Mujedu *et al*., [11] studied the use of corncob ash and sawdust ash as cement substitute in concrete works with a view to enhancing the reduction of corncob and sawdust wastes and also reduce the cost of concrete production. However, detailed potentials of corncob are yet to be fully explored as large proportion still remains unused and discarded as waste into the environment. This study therefore investigates the feasibility of using corncob as partial replacement of granite particles in the production of paving tiles.

2. MATERIALS AND METHOD

2.1 Materials

The corncobs used for this study was sourced in dry form from a corn threshing site in Ilorin south, Kwara State, Nigeria; and then carbonized to remove non-carbon elements. A metallic drum of about 90cm in height and 60cm diameter was used as kiln; the fabrication of the kiln was based on the method used by D-Lab charcoal process [16]. The kiln was designed to create an environment that has limited supply of oxygen, so that the burning corncobs inside the kiln can carbonize and the resultant corncob charcoal was pulverized using mortar and pestle. Wood charcoal dust, which is a waste from production and sales of wood charcoal, was used as control; this was collected from a charcoal merchant in Ilorin south. Other materials that were used are ordinary Portland cement (Dangote 3X brand), granite particles (stone dust) and potable water.

Samples of experimental paving tiles were produced from the mixture of granite particles and pulverized corncob charcoal in varying proportions with 20% and 15% cement content. Similarly, samples of paving tiles with varying proportions of granite particles and wood charcoal dust with 20% and 15% cement content were produced to serve as control. The mixture proportions of granite particles, pulverized corncob charcoal and wood charcoal dust are as presented in tables 1 and 2 for 20% and 15% cement addition respectively..

Granite particles (%)	Pulverized charcoal		Average mass (kg)
	Corncob (%)	Wood (%)	
80	-	-	2.38
70	10	-	2.25
60	20	-	2.14
50	30	-	1.93
40	40	-	1.73
80	-	-	2.38
70	-	10	2.25
60	-	20	2.15
50	-	30	2.01
40	-	40	1.71

Table 1. Aggregate mix of experimental paving tiles with 20% cement content

Granite particles (%)	Pulverized charcoal		Average mass (kg)
	Corncob (%)	Wood (%)	
85	-	-	2.29
75	10	-	2.17
65	20	-	2.04
55	30	-	1.87
45	40	-	1.67
85	-	-	2.29
75	-	10	2.17
65	-	20	2.12
55	-	30	1.89
45	-	40	1.77

Table 2. Aggregate Mix of Experimental Paving Tiles with 15% Cement Content

2.2 Moulding of the experimental paving tiles

The aggregate mixes of each batch of experimental paving tiles according to the proportion outlined in tables 1 and 2 were thoroughly mixed together so that homogeneity of the aggregated materials is achieved before the addition of potable water. The moulds were washed before the commencement of moulding so as to get rid of impurities that could lead to poor strength of the tiles. Also, the inner surfaces of the moulds were lubricated with a mixture of engine oil and diesel to ease removal of the tiles after production practiced by Enohuean and Omo-Irabor [17].

To achieve good surface finish of the products, cement mortar was firstly poured into the lubricated moulding containers and allowed to even out on the inner surfaces before the aggregate mixes were poured. The cast products were left for twenty-four hours to set and cure properly before they were removed from the moulds. After production, the experimental paving tiles were cured by sprinkling water on it morning and evening for seven days to prevent rapid drying which could lead to shrinkage cracking, dried under room temperature for sixteen days and sun-dried for five days [18]. This suggests that the experimental paving tiles were treated for twenty-eight days to attain adequate strength and free from cracks before the physical and mechanical properties tests were conducted on them.

2.3 Physical properties tests of experimental paving tiles

2.3.1 Determination of water absorption

The mass of each specimen of experimental paving tiles was determined firstly with weighing balance and their values recorded, as the dry mass, M_d. Each specimen was then submerged in cold water for twenty-four hours, after which the specimens were taken out and their surfaces wiped with a piece of cloth to remove excess water. The new mass of each specimen was determined with weighing balance and recorded as the saturated mass, M_s, the percentage water absorbed, otherwise known as "water absorption" was calculated using the relation in equation 2.1 [18].

$$A = \frac{M_s - M_d}{M_d} \times 100\% \qquad (2.1)$$

Where, A = Water absorption

2.3.2 Determination of bulk density

Experimental paving tiles specimens were dried to constant mass after curing, and the dry mass, M_d, was determined. The bulk density, B (in grams per cubic centimeter), of a specimen is the quotient of the dry mass divided by volume of the specimen. The volume, V, was determined from the surface dimensions, and physical geometry of the specimen namely length, width and thickness. The bulk density was calculated using the relation in equation 2.2 [19].

$$B = \frac{M_d}{V} \qquad (2.2)$$

2.4 Mechanical properties tests of experimental paving tiles

2.4.1 Flexural strength

The flexural strength test was conducted with a universal testing machine (Avery Dennison, England), 600kN capacity. Each of the tested experimental paving tiles specimens was placed horizontally and centrally on the two knife-edge vertical supports in an overlapping manner and the distance between the supports was noted. The specimen was then loaded centrally through a vertical indenter on the machine until failure occurred. The flexural strength in N/mm^2 (MPa), expressed as modulus of rupture, was calculated using the relation in equation 2.3 [20].

$$M = \frac{8PL}{\pi T^3} \qquad (2.3)$$

Where, M is the modulus of rupture (MPa), P is the load at rupture (N), L is the distance between supports (mm), and T is the average thickness of the specimen tested (mm).

2.4.2 Compressive strength

Each of the experimental paving tiles specimens was compressed with a compression testing machine and the load on the specimen at failure was noted. The compressive strength of each specimen was determined as the quotient of the average load on the specimen at failure to the area of bearing surface on the test specimen and calculated using the relation in equation 2.4 [20].

$$C_s = \frac{P_c}{A_c} \qquad (2.4)$$

Where,
C_s = Compressive strength of the specimen, MPa
P_c = Average load on the specimen at failure, N
A_c = Calculated area of the bearing surface on the test specimen, mm^2

3. RESULTS AND DISCUSSION

3.1 Physical Properties of Raw Materials

The physical properties of the aggregated materials used for the production of the paving tiles investigated were determined and presented in table 3 below.

Physical properties	Granite particles	Corncob charcoal	Wood charcoal
Colour	Ash	Black	Black
Density (g/cm^3)	1.69	0.40	0.67
Moisture content (%)	0.08	3.15	5.10
Maximum mass retained on sieve (%)	35.0	37.7	52.3
Mesh size of occurrence (mm)	0.00	0.50	0.00

Table 3. Physical properties of raw materials

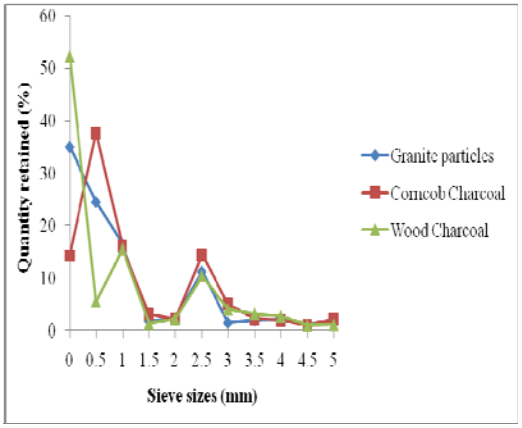

Fig. 1. Sieve analysis of aggregated materials

From the results of sieve analysis of raw materials, 91.6% granite particles, 87.8% pulverized corncob charcoal and 87.6% wood charcoal dust were retained within the 2.5mm sieve size. Hence, maximum particles size of 2.5mm was used for all aggregated materials to ensure maximum materials utilization.

3.2 Physical and mechanical properties of the experimental paving tiles

The experimental paving tiles developed were subjected to various physical and mechanical properties test to study the effects of varying granite and pulverized corncob charcoal contents on the bulk density, water absorption, drying shrinkage, flexural strength (modulus of rupture) and compressive strength of the tiles respectively.

The results of these tests were analyzed to determine the feasibility of using pulverized corncob charcoal as partial replacement of granite particles in the manufacturing of paving tiles. Three (3) samples per batch were tested for each of the properties determined, and the average values were recorded.

3.2.1 Bulk density

Figure 2 shows the variation of bulk density of the experimental paving tiles with the percentage granite particles, pulverized corncob charcoal and wood charcoal dust content for 20% and 15% cement addition respectively**.** A progressive decrease in bulk density was experienced as the percentage of pulverized corncob charcoal and wood charcoal dust content in the aggregate mix increases with decreasing percentage of granite particles content. The decreasing bulk density of the tiles was as a result of lower densities of the pulverized corncob charcoal and wood charcoal dust compared to that of granite particles, which was reducing as the pulverized corncob charcoal and wood charcoal dust content was increasing in the mixture aggregate. Samples produced with 20% cement content had a slightly higher bulk density compared to those produced with 15% cement content. This was as a result of higher bonding strength developed in the 20% cement content tiles, as there is tendency of more peripheral particles to be lost in the 15% cement content tiles during production process than in the 20% cement content tiles.

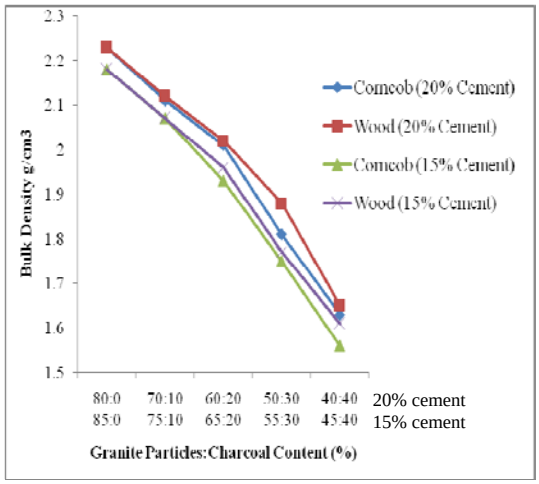

Fig.2. Variation of bulk density withtiles composition

Also, the bulk density of the granite particles/wood charcoal dust samples were slightly higher than that of the granite particles/pulverized corncob charcoal samples of equal mixture aggregate. This was attributed to higher density of the wood charcoal dust compared to that of the pulverized corncob charcoal.

3.2.2 Water absorption

The water absorption results obtained after 24 hours of soaking experimental paving tiles in water showed that water absorption capacity increased with increased percentage of pulverized corncob charcoal and wood charcoal dust content and with decreasing percentage of granite particles content in the mixture aggregate Fig. 3. The increased water absorption experienced in the tiles indicated that the pulverized corncob charcoal and wood charcoal dust were more porous compared to the granite particles. It was also observed that 15% cement content samples absorbed more water compared to 20% cement content samples. This was consistent with the finding of Semanda et al. [14]. The reduced water absorption rate of the 20% cement content samples was due to increased interfacial bonding between cement and aggregated materials but the reduced porosity was as a result of more cement content in the mixture, which might have lead to better curing process. The granite particles/pulverized corncob charcoal samples had slightly higher water absorption rate compared to that of granite particles/wood charcoal dust samples. This may be traced to difference in their particle size distribution as indicated in the sieve analysis results (table 3 and figure 1). The pulverized corncob charcoal used is coarser than the wood charcoal dust used as control, resulting in more porosity in the pulverized corncob charcoal tiles' samples.

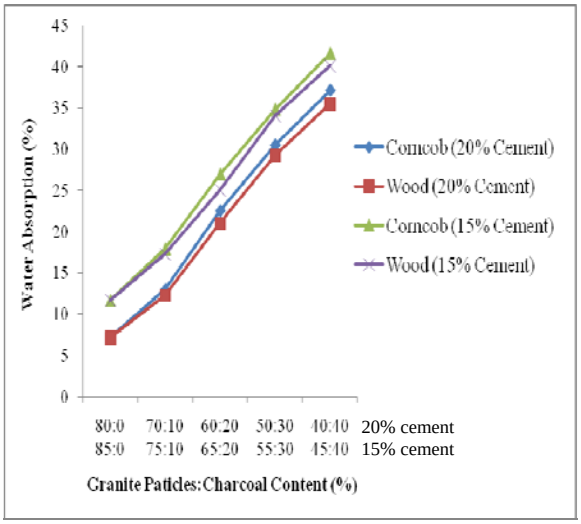

Fig. 3. Comparison of water absorption with tiles composition

3.2.3 Flexural strength

Figure 4 shows the variation of flexural strength of the experimental paving tiles with the percentage granite particles, pulverized corncob charcoal and wood charcoal dust content for 20% and 15% cement addition respectively**.** The flexural strength of the

experimental tiles was observed to decrease with increasing percentage of pulverized corncob charcoal and wood charcoal dust content and with decreasing percentage of granite particles content in the mixture aggregate. This was attributed to the reduction in cohesive forces between granite particles as the percentage of pulverized corncob charcoal and wood charcoal dust content increases in the mixture aggregate.

Granite particles/wood charcoal dust samples had slightly higher flexural strength compared to that of granite particles/pulverized corncob charcoal samples. The higher flexural strength in the wood charcoal dust samples was as a result of better interfacial bonding developed in the tiles due to the finer particles size of the wood charcoal dust compared to the pulverized corncob charcoal samples as indicated in the sieve analysis results. Also, the flexural strength of the 20% cement tiles was higher than that of 15% cement tiles.

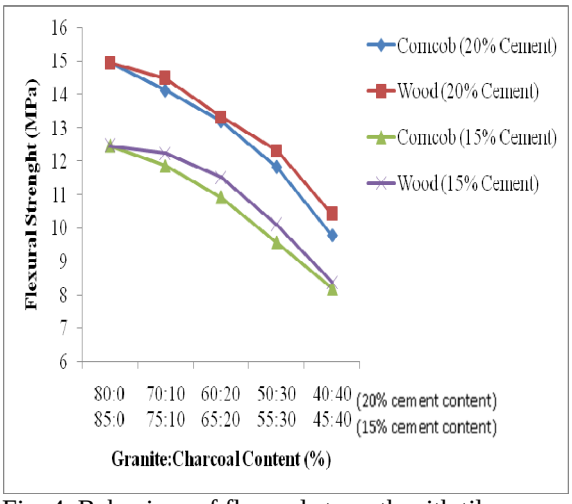

Fig. 4. Behaviour of flexural strength with tiles composition

3.2.4 Compressive strength

The variation of compressive strength of the experimental paving tiles with the percentage granite particles, pulverized corncob charcoal and wood charcoal dust content for 20% and 15% cement addition respectively was depicted in Fig. 5**.** The compressive strength of the experimental tiles was observed to decrease with increasing percentage of pulverized corncob charcoal and wood charcoal dust content with decreasing percentage of granite particles content in the mixture aggregate. The decrease in the compressive strength of the tiles with the addition of pulverized corncob charcoal and wood charcoal dust is due to the fact that pulverized corncob charcoal and wood charcoal dust does not have the compression qualities of the conventional aggregates.

Paving tiles with higher cement content exhibited higher compressive strength because of better curing and hardening process that occurred in the tiles compared to that of lower cement content. Results obtained showed that granite particles/wood charcoal dust samples had a compressive strength slightly higher than that of the granite particles/pulverized corncob charcoal samples. This was attributed to the finer particles size of the wood charcoal dust compared to pulverized corncob charcoal used, or lower density of the pulverized corncob charcoal compared to the wood charcoal dust.

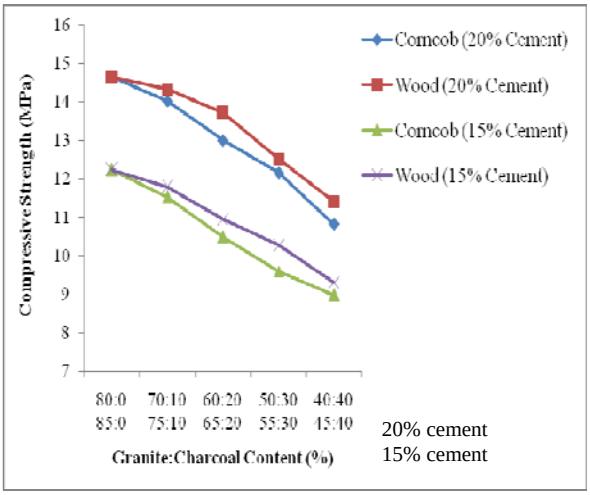

Fig. 5. Variation of compressive strength with tiles composition

4. CONCLUSION

Based on the results obtained from this study, the conclusions drawn can be summarized by the following points:

1. Better mechanical and physical properties namely: flexural strength, compressive strength and water absorption were obtained in the 20% cement content paving tiles compared to 15% cement content paving tiles.
2. As the percentage of pulverized corncob charcoal in the mixture aggregate increases, the flexural strength, compressive strength and bulk density of the tiles decreases, while a progressive increase was experienced in water absorption.
3. Pulverized corncob charcoal samples compared favorably in both physical and mechanical properties with wood charcoal dust samples used as control.
4. The compressive strengths of samples produced with 30% and 10% addition of pulverized corncob charcoal with 20% and 15% cement content are 12.15MPa and 11.53MPa respectively as against 12.86MPa obtained for field samples from selected commercial producers in Ilorin which were found to be produced with average cement content of 15.17% [21].
5. 30% and 10% addition of pulverized corncob charcoal for 20% and 15% cement content respectively are suitable for acceptable strength paving tiles.
6. Recycling of corncob as a constituent material of paving tiles is a viable means of addressing the challenge of environmental pollution caused by its improper disposal.

5. REFERENCES

[1] Agrawal, S., Trivedi, R. C., and Sengupta, B. *Air pollution due to burning of agriculture residue,* Indian Journal of Air Pollution Control, Vol.8(1), pp. 51-59, 2008.

[2] Pinto, J., Paiva, A., Varum, H., Costa, A., Cruz, D., Pereira, S., Fernandes, L., Tavares, P. and Agarwal, J. *Corn's cob as a potential ecological thermal insulation material.* Energy and Buildings, 43, pp. 1985-1990, 2011.

[3] Ettu, L. O., Osadebe, N. N. and Mbajiorgu, M. S. W. *Suitability of Nigerian agricultural by-products as cement replacement for concrete making.* International Journal of Modern Engineering Research (IJMER), Vol.3(2), pp. 1180-1185, 2013.

[4] Techniti, S., Anastasiadou, K., Vamvuka, D. and Gidarakos, E. *Investigating the recycling of agricultural biomass waste in construction materials.* Third International Conference on Industrial and Hazardous Waste Management, Crete-Chania, Greece. 2012.

[5] Zhang, Y., Ghaly, A. E., and Bingxi, L. *Physical properties of corn residues.* American Journal of Biochemistry and Biotechnology, Vol.8(2), pp. 44-53, 2012.

[6] Food and Agricultural Organization of United Nations [on-line], Accessed 30th November, 2015. http://faostat3.fao.org

[7] Kazmierczak, J., Nowicki, P. and Piertrzak, R. *Sorption properties of activated carbons obtained from corncobs by chemical and physical activation.* Open Access-Springerlink.Com, Vol.19, pp. 273-281, 2013.

[8] Adie, D. B., Lukman, S., Saulawa, B. S. and Yahaya, I. *Comparative Analysis of Filtration using Corncob, Bone char and Wood chippings.* International Journal of Applied Science and Technology, Vol. 3(3), pp. 146-152, 2013.

[9] Zubair, A., and Gana, S. A. *Production and characterization of briquette charcoal by carbonization of agro-waste.* Journal of Energy and Power, Vol.4, No.2, pp. 41-47, 2014.

[10] Oladeji, J. T. *Fuel characterization of briquettes produced from corncob and rice husk residues.* The Pacific Journal of Science and Technology, Vol.11(1), pp. 101-106, 2010.

[11] Mujedu, K. A., Adebara, S. A., and Lamidi, I. O. *The use of corncob ash and sawdust ash as cement replacement in concrete works.* The International Journal of Engineering and Science, Vol. 3(4), pp. 22-28, 2014.

[12] Raheem, A. A. and Adesanya, D. A. *A study of thermal conductivity of corncob ash blended cement mortar.* The Pacific Journal of Science and Technology, Vol. 12(2), pp. 106-111. 2011.

[13] Kumar, R. S. *Clay pavers – An external flooring material*. International Journal of Physical and Social Sciences, Vol. 2(5), pp. 145-160, 2012.

[14] Semanda, J., Mutuku, R. N., and Kakuli, J. W. "The Effect of Cement-Waste Mixes on the Physical and Strength Properties of Floor Tiles" European International Journal of Science and Technology, Vol. 3,(9), pp. 32-43, 2014.

[15] Pinto, J., Vieira, B., Pereira, H., Jacinto, C., Vilela, P., Paiva, A., Pereira, S. and Varum, H. *Corncob lightweight concrete for non-structural applications*. Construction and Building Materials, Vol. 34, pp. 346-351, 2012.

[16] D-Lab Charcoal Process [on-line], copyright @ Massachusetts Institute of Technology, Accessed 14th August, 2015. http://d-lab.mit.edu

[17] Enohuean, M. N. and Omo-Irabor, I. E. *Students work experience programme: Terrazzo flooring and moulding of interlocking tiles*. Journal of Advancement in Engineering and Technology, Vol. 2(2), pp. 1-5, 2015.

[18] Ohijeagbon, I. O., Olusegun, H. D., Adekunle, A. S., Adewoye, O. S., and Oladiji, A. O. *Impact of suitable replacement of granite particles on interlocking tiles.* Journal of Engineering Science and Technology Review, Vol. 5(2), pp. 51-56, 2012.

[19] Ohijeagbon, I. O. and Adeyemi, M. B. *Properties of clay/silica/cement tiles.* Nigerian Journal of Technological Development, Vol. 3(2), pp. 102-107, 2003.

[20] Olusegun, H. D., Adekunle, A. S., Ogundele, O. S., and Ohijeagbon, I. O. *Composite analysis of laterite-granite concrete tiles*. Epistemics in Science, Engineering and Technology, Vol. 1(1), pp. 53-59, 2011.

[21] Ogundipe, O. L. *Comparative analysis of locally produced interlocking tiles.* B.Eng. Project Report, Mechanical Engineering Department, University of Ilorin, Ilorin, Nigeria. (2010).

Authors: **Lecturer. Suleiman K Ajao,** University of Ilorin, Department of Materials and Metallurgical Engineering, P.M.B. 1515, Ilorin, Nigeria. Phone:234-8141849056.

Senior Lecturer. Dr. Idehai O Ohijeagbon, University of Ilorin, Department of Mechanical Engineering, P.M.B. 1515, Ilorin, Nigeria. Phone:234-7030092411.

Senior Lecturer. Dr. Adebayo S. Adekunle, University of Ilorin, Department of Mechanical Engineering, P.M.B. 1515, Ilorin, Nigeria. Phone:234-8033591465. **Professor. Prof. Henry D. Olusegun,** Federal University of Technology Minna, Department of Mechanical Engineering, Minna, Nigeria, Phone: 234-8034501122.

e-mail: suleimanajao@gmail.com
idehaiohi@yahoo.com
adekunlebayo@yahoo.com
olusegunhenry@yahoo.com

Journal of Production Engineering
Vol.19 No.2
JPE (2016) Vol.19 (2) Original Scientific Paper

Mohapatra, C. R.

A COMPUTATIONAL INVESTIGATION ON THERMAL CONDUCTIVITY OF PINE WOOD DUST FILLED EPOXY COMPOSITES

Received: 03 June 2016 / Accepted: 28 September 2016

Abstract: *Experimental and computational investigation on the thermal conductivity in particulate filler filled (pine wood dust) epoxy composites have been studied in the present work. The thermal conductivity of particulate filled polymer composite is calculated experimentally using Unitherm Model 2022. This study shows that the incorporation of wood dust results in reduction of conductivity of epoxy resin and there by improves its thermal insulation capability. Further the thermal conductivity of particle filled composites has been calculated computationally using fuzzy logic approach. The value of effective thermal conductivity obtained for various composite models using Fuzzy logic are in reasonable agreement with the experimental values for a wide range of filler contents from about 6.5 Vol% to 35.9 Vol%.*

Key words: *Epoxy-Wood dust composite, Thermal Conductivity, Unitherm Model 2022 , Fuzzy logic approach.*

Računarsko istraživanje toplotne provodljivosti kompozita punjenih piljevinom borovog drveta. *Eksperimentalna i računarska istraživanja toplotne provodljivosti česticama ispunjenog (piljevinom bora) epoksi kompozita su prikazani u ovom radu. Toplotna provodljivost kompozitnog polimera ispunjenog česticama je izračunata eksperimentalno koristeći Unitherm model 2022. Ova studija pokazuje da ubacivanje drvene piljevine rezultra smanjenjem provodljivosti čime se poboljšavaju sposobnosti toplotne izolacije. U nastavku rada je predstavljen način dobijanja vrednosti toplotne provodljivosti korišćenjem fazi logike. Vrednosti efektivne toplotne provodljivosti dobijene pomoću fazi logike za različite modele kompozita su u prihvatljivom slaganju sa eksperimentalnim vrednostima za širok spektar udela ispune kompozita (od 6,5 vol % do 35,9 % vol).*

Ključne reči: *Epoksi-Drvena piljevina kompozit, Toplotna provodljivost, Unitherm model 2022, model fazi logika.*

1. INTRODUCTION

The rapid progress in the environmental consciousness around the world has drawn attention of many towards natural fibre reinforced polymer composites related research. The availability of natural fibres and ease of manufacturing have attracted researchers and scientists to try locally available inexpensive fibres and to study their feasibility for reinforcement purposes. With easy availability, light weight, ease of separation, enhanced energy recovery, high toughness, non-corrosive nature, low density, low cost, good thermal properties, reduced tool wear, reduced dermal and respiratory irritation, natural fibre presents a good renewable and biodegradable alternative to the most common synthetic reinforcement such as glass fibre.

The improvement of the insulating properties of composites can be determined by measuring their thermal properties i.e. the values of thermal conductivity. Generally thermal conductivity is a property which has ability to conduct heat of materials. It plays an important role in determining their heat conduction/insulation capability. For porous materials, several researchers derived effective thermal conductivity like Stein hagen [1] reviewed the thermal conductivity of wood from -40^0C to 100^0C and found that thermal conductivity of wood increases in a linear manner with temperature and density. Little difference was found between its value in tangential and radial directions. Kamke [2] tested nine types of commercial wood panels using a guarded heat-flux method and concluded that the thermal conductivity of wood-based panels varies proportionally with both specific gravity and moisture content Suleiman et al. [3] investigated the thermal conductivity of wood in both longitudinal and transverse directions in the temperature range of 20^0C to 100^0C. Their results showed that thermal conductivity is about 1.5 times more in the longitudinal direction than in the transverse direction due to non-homogenous nature of wood. Fu and mai. [4] predicted the effective thermal conductivity of short fibre reinforced polymer composites. It was observed that the thermal conductivity of the composites increases with mean fibre length but decreases with mean fibre orientation angle with respect to the measured direction. Abdul Razak et al .[5] studied the electrical and thermal properties of epoxy- carbon black composites. It was observed that the epoxy-carbon black composites have better thermal properties than the neat epoxy. Mounika et al. [6] investigated the thermal conductivity characterization experimentally by a guarded heat flow meter method. The results showed that the thermal conductivity of the composite decreased with increase in fibre content and quite opposite trend was observed with respect to temperature. A various methods have used fuzzy logic method for identification of effective thermal conductivity of the polymeric composites. In their work VeisehSefidgar et al. [7] utilized the Artificial

Neural Networks (ANN) in order to predict the effective thermal conductivity of expanded polystyrene with specific temperature and moisture content. The experimental data was used for training and testing ANN. It was found that the results obtained from the ANN method gave good agreement with experimental data. Nandi et al. [8] made an attempt to model the equivalent thermal conductivity (ETC) of 2-phase particle reinforced polymer composites (PRPCs) on a genetic fuzzy approach. The model performance was rigorously tested in three stages to establish its practical applicability. Estimations of ETC by the proposed model were reasonable, even better compared to existing models and suggesting a generic model applicable to a wide range of 2-phase PRPCs. Agarkar [9] approached fuzzy logic technique for the gas identification.The identification rules were taken from the data obtained from microcontroller in form of IF-THEN rules for fuzzy controller to form membership of the functions. The results of the fuzzy logic will be shown to provide gas identification according to variation in different parameters such as gas concentrations, variation in sensor's resistance and output volt of microcontroller at room temperatures. Manocha et al [10] developed a fuzzy logic approach for the prediction of appropriate Thermal Comfort Level (TCL) considering Sol Air Temperature (SAT) and Overall Thermal Transmittance (OTT) as input constraints. A comprehensive clarification of the relevance uniting linguistic approach to the optimization under numerous principles was presented in this study. In comparison to other predictive modeling teqniques; fuzzy models have the advantage of being simple due to Fuzzy Inference System (FIS) capability to deal with problems that are based on user knowledge and experience.

In the present work the wood dust (Pine wood dust) has been considered as reinforced filler because of its low cost, easily available in nature, insulating characteristic and the most important factor is that it is eco-friendly material. Since this work aims at developing some kind of a light, cheap and insulating material, epoxy emerged as the first choice for the matrix material. Epoxy is chosen primarily because it happens to be the most commonly used polymer and because of its insulating nature (low value of thermal conductivity about 0.363W/m- ^{0}K). This work also reports the estimation of the equivalent thermal conductivity of particulate polymer composite system using fuzzy logic approach.

2. EXPERIMENTAL DETAILS

2.1. Matrix Material (Epoxy)

Epoxy(LY 556) resin and the corresponding hardener (HY 951) are mixed in a ratio of 10:1 by volume supplied by Hindustan Ciba Geigy (India) Ltd.

2.2. Filler Material (Pine wood Dust)

Pine wood dust has chosen as the filler material mostly for its very low thermal conductivity (0.068 W/m-^{0}K) and low density (0.52 gm/cc). It is also renewable, eco-friendly, available at low cost, non toxic and basically considered as waste product.

2.3. Composite Preparation

The low temperature curing epoxy resin and corresponding hardener were mixed in a ratio of 10:1 by weight as recommended. Pine wood dust (PWD) particles with average size 200µm were reinforced in epoxy resin (density 1.1 gm/cc) to prepare the composites. The fabrication of these composite was done by conventional hand – lay – up technique. The fillers were mixed thoroughly in the epoxy resin . A stainless steel mould having dimensions of 210 × 210 × 40 mm was used for this purpose. Silicon spray was used to facilitate easy removal of the composite from the mould after curing. The cast of each composite was cured under a load of about 50kg for 24 hours before it was removed from the mould. Then this cast was post cured in air for another 24 hours.

2.4. Determination of thermal conductivity

A guarded heat flow meter has been developed for thermal conductivity measurements. This is achieved by using a thermal conductivity testing system Unitherm Model 2022. (Fig.1) The tests are in accordance with ASTM-E-1530 standard. The sample and a heat flux transducer (HFT) shown in (Fig. 2) are sandwiched between two flat plates controlled at different temperatures to produce a heat flow through the stack. A cylindrical guard surrounds the test stack and is maintained at a uniform mean temperature of the two plates, in order to minimize the lateral leak of heat. In Unitherm 2022 the heat flux transducer measures the Q value. At steady state, the difference in temperature between the surfaces contacting the specimen is measured with temperature sensors embedded in the surfaces along with output from the heat flow transducer.

Fig.1 The Unitherm 2022

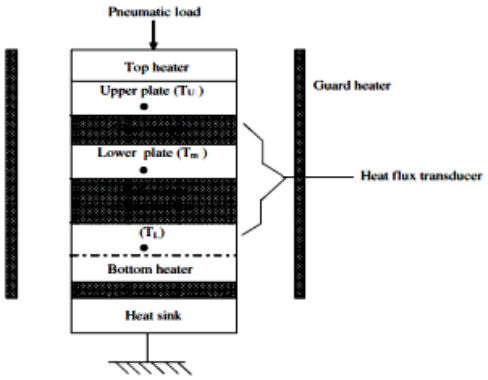

Fig. 2. Schematic model showing the testing arrangement

Taking these values with known cross sectional area and the sample thickness, the thermal conductivity is calculated using equation 1.

$$Q = KA[\frac{T_1 - T_2}{L}].....(1)$$

3. FUZZY LOGIC APPROACH

Fuzzy logic is one of the soft computing techniques that play a significant role in input-output matrix relationship. It is a superset of conventional (Boolean) logic that has been extended to handle the concept of partial truth i.e., truth values between completely true and completely false. This technique emulates the human decision making process in which not every decision is discrete. There is a certain amount of indecision, fuzziness in the decision and it deals with uncertainty. The basic elements of fuzzy logic are linguistic variables, fuzzy sets and fuzzy rules. The linguistic variables are words specifically adjective like very low, low, medium, high and very high.

3.1 Fuzzy Inference System

Fuzzy inference system is the process of formulating the mapping from a given input to an output using fuzzy logic. The mapping then provides a source from which decision can be made. The process of fuzzy inference involves the following elements: Membership Functions, Logic Operations and IF-THEN Rules. A general fuzzy inference system is shown in fig.3. It consist of crisp input, fuzzifier, Rule base, Inference engine, Defuzzifier and crisp output. The fuzzy inference system (FIS) take a crisp input and determines the degree to which they belong to each of the appropriate fuzzy sets through membership functions. A membership function is a curve that defines how each point in the input space is mapped to a membership value or a degree of truth between 0 and 1. The most common shape of a triangular membership functions although gaussian, trapezoidal and bell curves are also used. The fuzzifier then measures the value of input variables and performs a scale mapping that transfers the range of values of input variables into corresponding universes of discourse. The rule base contains linguistic rules that are provided by expert. It is also possible to extracts rules from the numerical data. Inference engine is used for fuzzy reasoning and to generate fuzzy values and the defuzzifier converts the fuzzy sets into crisp output. Fuzzy inference systems have successfully applied in fields such as automatic control, data classification, decision analysis, expert systems, and computer vision. Because of its multidisciplinary nature, fuzzy inference systems are associated with a number of names, such as fuzzy-rule-based systems, fuzzy expert systems, fuzzy modeling, fuzzy associative memory, fuzzy logic controllers, and simplyfuzzysystems.

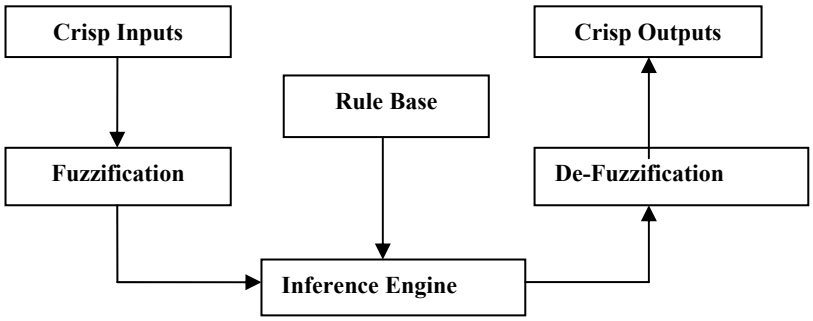

Fig. 3. Basic structure of FIS

3.2 The proposed model

In the proposed model, the input stages consist of two input variables i.e. particulate (PWD) and thermal conductivity. These two major factors are considered for the prediction of reduction thermal conductivity which are shown in figure 4.For fuzzification of these factors, the linguistic variables Low, Medium, High and Very high are used for the input and output. With the fuzzy sets defined, it is possible to associate the fuzzy sets in the form of fuzzy rules.

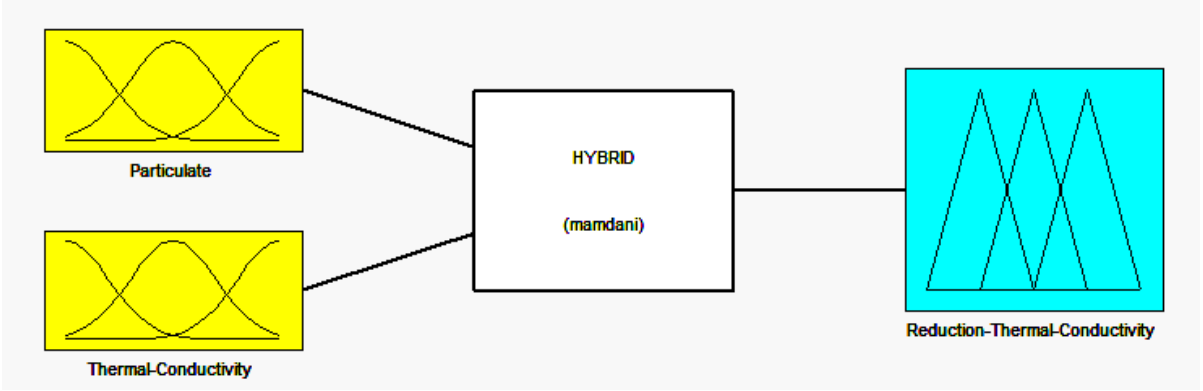

Fig. 4. The proposed Fuzzy Inference Engine for Hybrid functio

3.3 Membership function

Fuzzy membership functions are the mapping functions for the fuzzy data containing linguistic terms, fuzzy sets or fuzzy members to crisp data. For membership function, a large class of function can be taken viz. Triangular, Gaussian, Hybrid, Trapezoidal and Bell functions. In the present work, Hybrid function is taken into consideration. In this work, each input and output parameters have four membership functions like Low, Medium, High and Very high. We have used particulate (PWD) and thermal conductivity as input variables and reduction thermal conductivity as output variables. The input variables have been partitioned according to the experiment parameter ranges. Membership functions of fuzzy set input variables are shown in figure 5 and 6. Output variables are shown in figure 7.

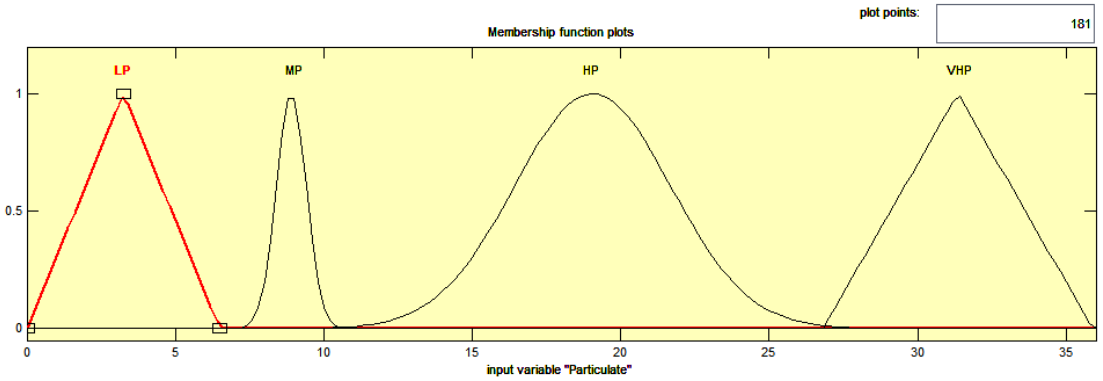

Fig. 5. Membership function of particulate for Hybrid function

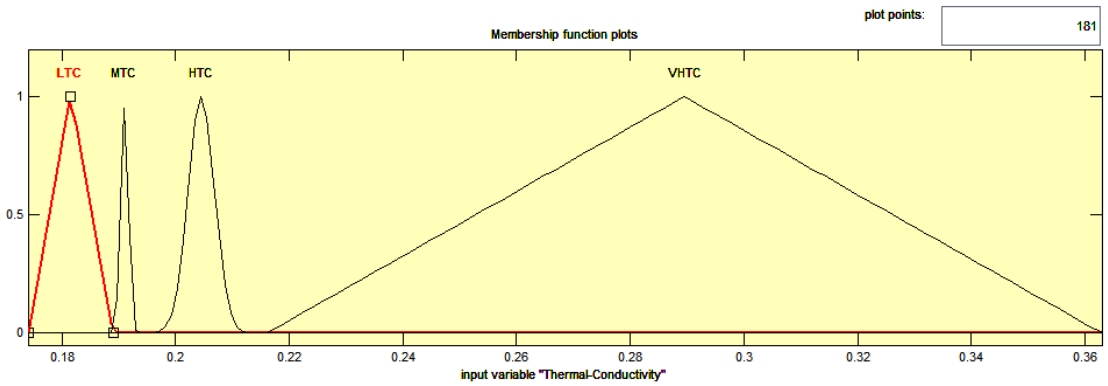

Fig. 6. Membership function of thermal conductivity for Hybrid function

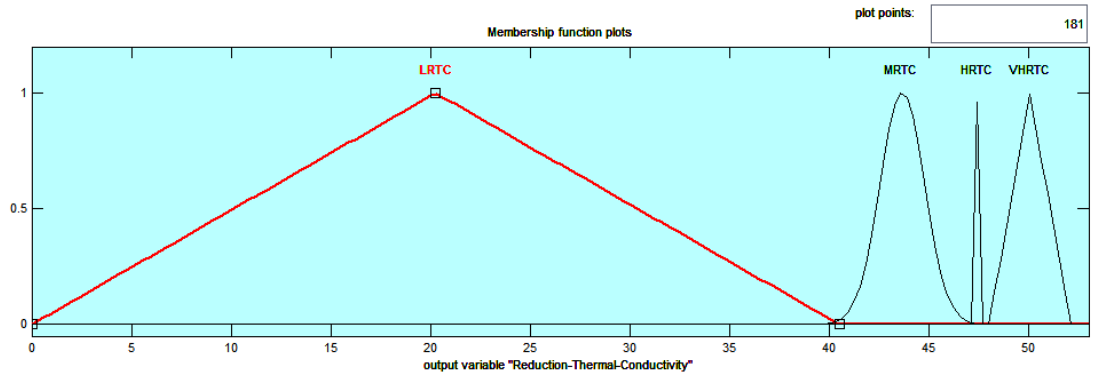

Fig. 7. Membership function of reduction thermal conductivity for Hybrid function

3.4 Rule-based Fuzzy relation

Fuzzy rules are the set of linguistic statements which establishes the relation between the input and the output in a fuzzy system. They are defined based on experimental work. The number of fuzzy rules in a fuzzy system is related to the number of fuzzy sets for each input variables. In this study, four study rules with two input variables are considered which is shown in Table-1. This is because of having an effective and an efficient modeling with fuzzy logic; it would be more acceptable to use least number of rules which can get a good result instead of using all possible rules that can be implemented. Experimental results are simulated in the Matlab software on the basis of Mamdani fuzzy logic. Table-1 presents the fuzzy inference system and gives the fuzzy rules presented in following type. IF “Condition 1”, AND “Condition 2”, THEN “Condition 3”.

No	Rule definition
1	If (Particulate is LP) and (Thermal conductivity is VHTC) then (Reduction Thermal conductivity is LRTC)
2	If (Particulate is MP) and (Thermal conductivity is HTC) then (Reduction Thermal conductivity is MRTC)
3	If (Particulate is HP) and (Thermal conductivity is MTC) then (Reduction Thermal conductivity is HRTC)
4	If (Particulate is VHP) and (Thermal conductivity is LTC) then (Reduction Thermal conductivity is VHRTC)

Table 1. Rules for the fuzzy inference system

3.5. Decision surface

Once all the variables of particulate (PWD) and thermal conductivity get executed by the fuzzy inference system. A decision surface can generate showing the value of output variable i.e. reduction thermal conductivity. Figure 8 presents a three dimensional curves representing the mapping from particulate and thermal conductivity as inputs (axis X & Y) and reduction thermal conductivity as an output (axis Z). In varying conditions of particulate and thermal conductivity parameters, the maximum value of reduction thermal conductivity likely to be changed accordingly that depends on fuzzy inference system.

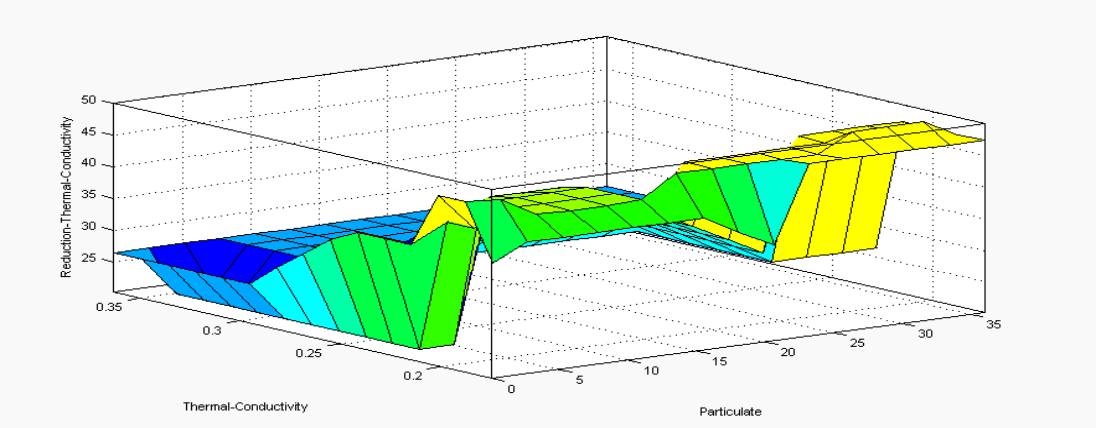

Fig. 8. Decision surface for Hybrid function

4. RESULTS & DISCUSSION

According to the fuzzy inference rule, Reduction thermal Conductivity is an output of the corresponding values of Particulate and Thermal Conductivity shown in Fig. 9 and Fig. 10 respectively. There is a strong relationship between the Particulate, Thermal Conductivity and Reduction Thermal Conductivity. The nature of curves in Fig. 9 shows that when Particulate content increases, Reduction Thermal Conductivity is increased, there by improves its insulation capability. On the other hand, the nature of Fig. 10 shows that as the Thermal conductivity increases, the Reduction Thermal Conductivity decreased which shows the improvement of its insulation capability. Table 2 and table 3 present the relation between particulate, thermal conductivity and reduction thermal conductivity (Hybrid) respectively.

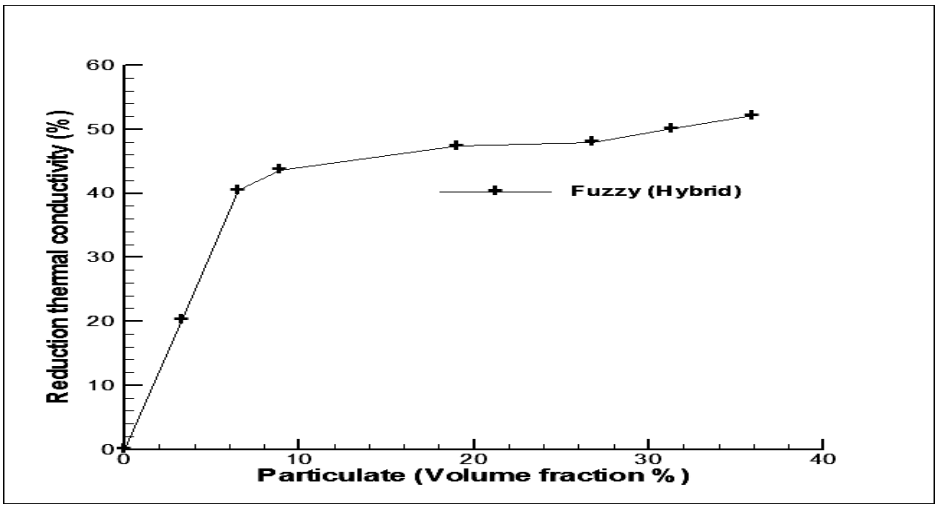

Fig. 9. Relation between Particulate and Reduction Thermal conductivity (Hybrid)

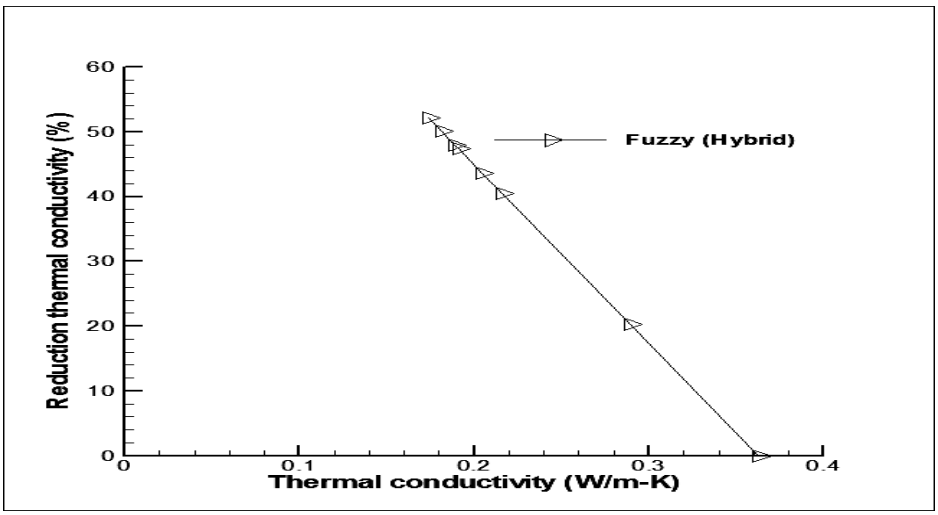

Fig. 10. Relation between Thermal Conductivity and Reduction Thermal conductivity (Hybrid)

Particulate (Volume fraction %)	Reduction thermal conductivity (%)
0	0
3.25	20.25
6.5	40.5
8.9	43.65
19.05	47.4
26.8	48
31.5	50.05
35.9	52.1

Table 2. Particulate vs. Reduction thermal conductivity (Hybrid)

Thermal conductivity (W/m-^{0}K)	Reduction thermal conductivity (%)
0.363	0
0.2895	20.25
0.216	40.5
0.2045	43.65
0.191	47.4
0.189	48
0.1815	50.05
0.174	52.1

Table 3. Thermal conductivity vs. Reduction thermal conductivity (Hybrid)

Fig. 11. shows a comparison between experimental results using Unitherm Model 2022 and Fuzzy logic over a wide range of volume fraction of particulate (PWD) between 0 to 35.9%.The figure shows that the incorporation of particulate results in reduction of thermal conductivity of composites and there by improves its insulation capability. It is also found that the results obtained from fuzzy logic with Hybrid function is very close to the experimental results. On comparison, it had found that the errors associated with fuzzy logic with respect to the experimental ones lie in the range of 0 to 3.62. Table 4 presents the values of thermal conductivity and % of error associated with the experimental and Fuzzy logic method for individual composite i.e. epoxy and pine wood dust.

Sample	Particulate (Vol.%)	Effective thermal conductivities of composites (W/m-K)		% of error with respect to Experimental value
		Hybrid	Experimental	
1	0	0.363	0.363	0
2	6.5	0.216	0.216	0
3	11.3	0.200	0.193	3.62
4	26.8	0.189	0.189	0
5	35.9	0.174	0.174	0

Table 4. Thermal conductivity values of composites & % of errors obtained from different methods

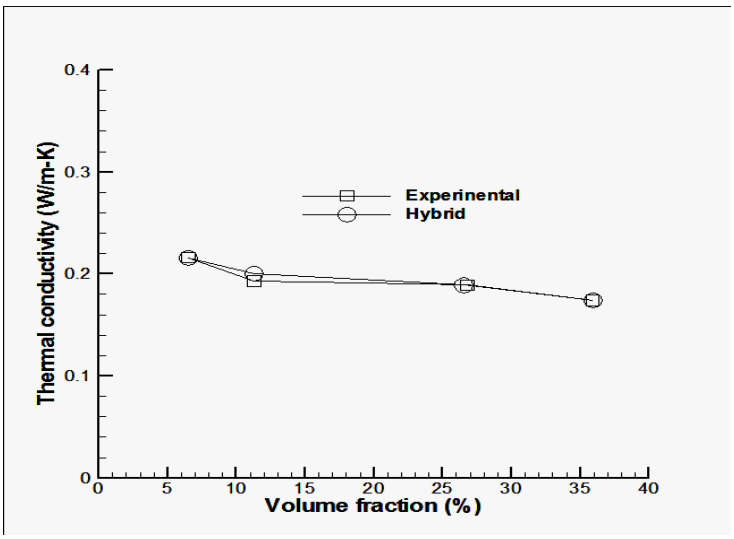

Fig. 11. Comparison of thermal conductivity values of hybrid model and experimental for PWD filler

5. CONCLUSION

In this present investigation on thermal conductivity of wood dust filled epoxy composites have led to the following conclusions:

1. Wood dust is an environmental friendly waste product which can be gainfully utilized for preparation of composites.

2. A successful fabrication of a wood dust filled epoxy composites with different types of wood is possible by hand lay- up technique.

3. A reduction in thermal conductivity was observed with increasing filler content in the mixture due to presence of air voids during preparation of composites and also presence of interfacial material having low thermal conductivity (PWD) which increase the interfacial resistance between the epoxy resin and filler.

4. In corporation of wood dust results in reduction of thermal conductivity of epoxy resin and there by improves its thermal insulation capability.

5. Fuzzy logic method can be gainfully employed to determine effective thermal conductivity of these composites with different amount of filler content.

6. The value of effective thermal conductivity obtained for various composite models using Fuzzy logic are in reasonable agreement with the experimental values for a wide range of filler contents from about 6.5 Vol% to 35.9 Vol%.

6. REFERENCING

[1] Steinhagen, H. P., "Thermal Conductivity Properties of Wood, Green or Dry, from -40^{0}C to +100^{0}C: a literature review," In: Gen. Tech. Re FPL-09, U.S. Department of Agriculture Forest Service, Forest products Laboratory, Madison WI., 1977.

[2] Kamke F. A., "Effects of Wood-based Panel Characteristics on Thermal Conductivity," Forest Prod.. J. Vol.39 (5), 1989, pp. 19-24.

[3] Suleiman, B. M., Larfeldt, J., Leckner, B. and Gustavsson,M.,"Thermal Conductivity and Diffusivity of Wood," Wood Sci. Technol. Vol. 33 (6), 1999, pp. 465-473.

[4] Fu, S. Y. and Mai, Y.W., "Thermal conductivity of Misaligned Short Fibre Reinforced Polymer Composites," J. Appl. Polymer Sci., Vol.(88), 2003, pp. 1497-1505.

[5] Abdul Razak, A. A., Salah, N J. and Kazem, W, A., "Electrical and Thermal Properties of Epoxy Resin Filled with Carbon Black," Eng. & Tech. J. Vol. 27, No. 11, 2009.

[6] Mounika, M., Ramaniah, K., Prasad, A.V. Ratna, Rao, K. Mohana, Reddy, K. Hema Chandra, Mater J.. "Thermal Conductivity Characterization of Bamboo Fiber Reinforced Polyester Composite". Environ. Sci. 3 (6),2012, pp.1109-1116.

[7] Veiseh, S. and Sefidgar, M.. "Prediction of Effective Thermal Conductivity of Moistened Insulation Materials by Neural Network," Asian Journal of Civil Engineering (Building and Housing) Vol. 13 (3),2012, pp. 319-330.

[8] Nandi Arup Kumar, Deb Kalyanmoy, Dutta Shubhabrata, Orkas Juhani, "A Genetic Fuzzy Based Modeling of Effective Thermal Conductivity for Polymer Composites," Journal of Intelligent & Fuzzy Systems: Applications in Engineering and Technology, Vol.25(2), 2013, pp. 259-270.

[9] Agarkar, Poonam T., "A Gas Sensing System Using Multisensors Data and Fuzzy Technique," International Journal of Application or Innovation in Engineering &Management, 2013.

[10] Manocha,Sandeep Kumar, Singh,Hari Kumar, Yadav,P.K.,andSuman, B.M. "Prediction of Indoor Thermal Comfort Level Using Fuzzy Logic," IOSR Journal of Mechanical and Civil Engineering (IOSR-JMCE), Volume 11, Issue 3,2014, pp. 25-33.

Author: **Ramesh Chandra Mohapatra Reader,** Mechanical Department, Department of Mechanical Engineering, Government College of Engineering, Keonjhar, Odisha, India, Phone No. 9438551072
E- mail: rameshmohapatra75@gmail.com

Journal of Production Engineering
Vol.19 No.2
JPE (2016) Vol.19 (2) Preliminary Note
Ambedkar, B.R.K., Naidu, G.S., Sreenivasarao, T., Varahalanaidu, G.

STUDIES ON PRODUCTION OF STEEL WITH IMPROVED CLEANLINESS AND ITS EFFECT ON MECHANICAL PROPERTIES

Received: 28 August 2016 / Accepted: 11 October 2016

Abstract: *Clean Steel refers to steels that have low levels of the solute elements like Oxygen, Hydrogen, Nitrogen, Phosphorus, Sulfur and some inclusions of oxygen, sulphur etc. A study on Cleanliness in steel was carried and it was observed that, it was best achieved through a variety of operations during steel making which are mentioned. This paper gives the brief observation about the procedure followed in Vizag Steel Plant(RINL-VSP,INDIA) and how best the cleanliness in steel is obtained at RINL-VSP. Few suggestions are also mentioned for further improvement in the process of clean steel making.*
Key words: *steel, metallic inclusions, steel processing, slag*

Istraživanje proizvodnje čelika sa povišenom čistoćom i njegov efekat na mehaničke osobine. *Pod čistim čelikom se podrazumevaju niski nivoi rastvarajućih elemenata kao što je kiseonik, vodonik, azot, fosfor, sumpor i uključaka kao npr. kiseonik, sumpor itd. Istraživanje čistoće kod čelika je sprovedeno a rezultati pokazuju da je najbolji rezultat postignut kombinacijom operacija tokom proizvodnje. Ovaj rad pruža kratko zapažanje o procesu proizvodnje u Vizag Steel Plant-u (RINL-VSP,INDIA) i način dobijanja najbolje čistoća u RINL-VSP. Nekoliko sugestija je predloženo u smislu poboljšanja procesa proizvodnje čistog čelika.*
Ključne reči: *čelik, metalini uključci,proizvodnja čelika, šljaka*

1. INTRODUCTION

Steel cleanliness is the one unifying theme in all steel plants as problems in steel cleanliness can lead to internal rejects or customer dissatisfaction with steel products. Thus all steel plants are continuously attempting to improve their practices to produce more consistent products. Besides operating conditions inputs such as coke, iron ore, hot metal and additions in the convertor. In addition to product consistency, it is now clear that fatigue resistance and tool and die life correlate strongly with steel cleanliness and that improvement in steel cleanliness will result in further improvements in steel performance [1]. The future of steelmaking and casting will be to continue to reduce the total oxide inclusion mass in liquid steels and to ensure that the remaining inclusion chemistry and size distribution is closely controlled. This work done by us will give you what developments in the processes can be made so that it will give consistent steels with high cleanliness [1-5].

2. CLEAN STEEL

Steel cleanliness is an important factor of steel quality and the demand for cleaner steels increases every year. The so-called clean steel generally is the steel in which the content of impurity elements, such as phosphorus, sulfur, total oxygen, nitrogen, hydrogen (including carbon sometimes) and inclusions are very low. The improvement of steel cleanliness has therefore become a more and more important subject in the development of ferrous metallurgical technology, and also an important task for the iron and steel producers.

The demand for better mechanical properties of steels was urging steel producers to improve cleanliness of their final products. In order to obtain the satisfactory cleanliness of steel it is necessary to control and improve a wide range of operating practices throughout the steelmaking processes like de-oxidants and alloy additions, secondary metallurgy treatments, shrouding systems and casting practice.

It has been well known that the individual or combined effect of carbon [C], phosphorus [P], sulfur [S], nitrogen [N], hydrogen [H] and total oxygen (T.O.) in steel can have a remarkable influence on steel properties, such as tensile strength, formability, toughness, weld ability, cracking-resistance, corrosion-resistance, fatigue-resistance, etc. Also, clean steel requires control of non-metallic oxide inclusions and controlling their size distribution, morphology and composition.

The control of the elements mentioned above is different for different performance demands. Those impurity elements also vary with different grades of steel [3,4]. Some element in steel is harmful to certain steel grades, but may be less harmful or even useful to another steel grades. The following table shows the influence of impurities over mechanical properties.

As we mentioned before, steel cleanliness depends on the amount, morphology and size distribution of non-metallic inclusions [5-7]. The inclusions generate many defects and many applications restrict the maximum size of inclusions so the size distribution of inclusions in steel products is also important. For certain applications where stringent mechanical properties are required the internal cleanliness of steel is very important. The cleanliness requirements for various steel grades are as follows, Table 2.

Element	Form	Mechanical Properties Affected
S, O	Sulfide and oxide inclusions	Ductility, Charpy impact value, anisotropy Formability (elongation, reduction of area and bendability) Cold forgeability, drawability Low temperature toughness Fatigue strength
C, N	Solid solution	Solid solubility (enhanced), hardenability
	Settled dislocation	Strain aging (enhanced), ductility and toughness (lowered)
	Pearlite and cementite	Dispersion (enhanced), ductility and toughness (lowered)
	Carbide and nitride precipitates	Precipitation, grain refining (enhanced), toughness (enhanced) Embrittlement by intergranular precipitation
P	Solid solution	Solid solubility (enhanced), hardenability (enhanced) Temper brittleness Separation, secondary work embrittlement

Table 1. The influence of impurities over mechanical properties.

Steel cleanliness is controlled by a wide range operating practices throughout the steelmaking processes. These include the time and location of de-oxidant and alloy additions, the extent and sequence of secondary metallurgy treatments, stirring and transfer operations, shrouding systems, tundish geometry and practices, the absorption capacity of the various metallurgical fluxes, and casting practices.

3. NON-METALLIC INCLUSIONS

Non-metallic inclusions, which are undesirable components of all steels, play an important role with respect to their effect on the steel properties. Controlling inclusions in steel is closely connected with the concept of "clean steel". The improvement in steel properties by control of non-metallic inclusions plays an important part in defending the applications of steel against newer competitive materials. The aims of the metallurgist are to eliminate undesirable inclusions and control the nature and distribution of the remainder to optimize the properties of the final product.

Generally, non-metallic inclusions in steel normally have a negative contribution to the mechanical properties of steel, since they can initiate ductile and brittle facture. Among various types of nonmetallic inclusions, oxide and sulfide inclusions have been thought harmful for common steels.

3.1 Classification of non-metallic inclusions:

Non-metallic inclusions are divided by chemical and mineralogical content, by stableness/stability and origin. By chemical content non-metallic inclusions are divided into the following groups:

1. Oxides (simple: FeO, MnO, Cr_2O_3, TiO_2, SiO_2, Al_2O_3 etc.; compound: $FeOFe_2O_3$, $FeOAl_2O_3$, $MgO\ Al_2O_3$, $FeOCr_2O_3$ etc.)
2. Sulphides (FeS, MnS, CaS, MgS, Al_2S_3 etc.; compound: FeSFeO, MnSMnO etc.)
3. Nitrides (simple: TiN, AlN, ZrN, CeN etc.; compound: Nb(C, N), V(C, N) etc, which can be found in alloyed steels and has strong nitride-generative elements in its content: Titanium, Aluminum, Vanadium, Cerium etc.)
4. Phosphides (Fe_3P, Fe_2P etc.)

Steel product	Maximum allowed impurity fraction	Maximum allowed inclusion size
IF steels	[C]≤30 ppm, [N]≤40 ppm, T.O.≤40 ppm [C]≤10 ppm, [N]≤50 ppm	
Automotive and deep-drawing Sheets	[C]≤30 ppm, [N]≤30 ppm	100 μm
Drawn and Ironed cans	[C]≤30 ppm, [N]≤40 ppm, T.O.≤20 ppm	20 μm
Alloy steel for Pressure vessels	[P]≤70 ppm	
Alloy steel bars	[H]≤2 ppm, [N]≤20 ppm, T.O.≤10 ppm	
HIC resistant steel sour gas tubes	[P]≤50 ppm, [S] ≤10 ppm	
Line pipes	[S]≤30 ppm, [N]≤50 ppm, T.O.≤30 ppm	100 μm
Sheets for continuous annealing	[N]≤20 ppm	
Plates for welding	[H]≤1.5 ppm	
Bearings	T.O.≤10 ppm	15 μm
Tire cord	[H]≤2 ppm, [N]≤40 ppm, T.O.≤15 ppm	10 μm
Non-grain-orientated Magnetic Sheets	[N]≤30 ppm	
Heavy plate steels	[H]≤2 ppm, [N]=30-40 ppm, T.O.≤20 ppm	Single inclusion 13 μm Cluster 200 μm
Wires	[N]≤60 ppm, T.O.≤30 ppm	20 μm

Table 2. The cleanliness requirements for various steel grades

4. CONTROL OF INCLUSIONS IN STEEL

The indigenous non metallic inclusions which can precipitate as discrete phases during solidification of

steel for example sulphides and oxides. These inclusions are influenced by the steel making techniques at various stages in steel making shop. Various steel refining processes are developed for the inclusion control in steels and these processes are called Secondary Steel Making processes [8]. The final operations of refining, degassing, alloying and temperature adjustment are carried out in secondary steel making.

Molten steel stream after treatment in the ladle is teemed into tundish and then from tundish to mould in the continuous casting. Teeming of steel form ladle to tundish requires shrouding of molten steel stream in order to avoid re-oxidation. Here macro-inclusions rich in FeO and MnO can form. However the dissolved oxygen increases and forms inclusions during solidification. Use of shrouded and submerged nozzles will help control inclusion formation.

One of the best ways to reduce sulphide and oxide inclusions is INJECTION LADLE METALLURGY. Most commonly used injection powder is Calcium Silicide (30% Ca). However, it is necessary to inject Ca-Si deep into the bath for best recovery of Ca. The $CaO-CaF_2$-Al powder is very suitable for desulfurization of low silicon steels.

Tundish flux should be selected such that it can easily absorb inclusions floating in the tundish .At the same time flux should also cover molten steel to prevent oxidation.

Another way to decrease the inclusions in steel is by bubbling or stirring with Argon through the bottom of the steel bath [8, 9]. The rising gas bubbles carry non-metallic inclusions which are ultimately absorbed in the slag. This Argon stirring also homogenizes both bath composition and temperature.

Vacuum arc degassing (VAD) also effectively reduces non-metallic inclusions. In VAD consists of Argon stirring from bottom and also electric arc to increase the temperature of steel bath. This is an example of Ladle Metallurgy.

5. OBSERVATIONS AND CONCLUSIONS

The following are some observations which shows us how we can improve steel quality and what must be avoided to obtain the steel with improved cleanliness.

- SLAG CARRY OVER: While tapping the steel from the converter into the ladle there will be a chance of BOF slag to enter the ladle. This slag which is going to come inevitably along with molten steel is going to be termed as the carry over slag. This carry over slag is deleterious as it may leads to phosphorous reversion.
- OPEN TEMPERATURES: The opening temperatures also termed as tapping temperatures fluctuates more and more for heat to heat which is blown in the converter. This may results in phosphorous reversion from the slag into the metal. The following table will show a detailed study over opening temperatures and the amount of phosphorous:
- LADLE REFINING FURNACE: Only few heats, only limited to special grades, from the converter are sending to ladle furnace. But to achieve the best quality steel more heats should be sent to LF. The ladle furnace itself has certain advantages over ARS as it has more control over super heat and alloying additions over ARS.
- RINSING TIME**:** The ideal rinsing time for the best quality steel is 12 minutes which yields better homogeneity in composition and temperature. But at VSP the rinsing times are limited to 8 minutes.
- SUPERHEAT AND CASTING SPEED: The superheat maintained in the ladle and the casting speed is not consistent. This leads to decrease in the productivity rate of the steel to be manufactured.
- VACUUM DEGASSING: Vacuum degassing itself has various advantages over conventional Argon rinsing and Ladle furnace operations. Adopting an RH or a DH degasser will help in close control over the impurities and inclusions.
- DESULPHURISATION: Though the charging materials have low contents of sulphur but if the sulphur varies there is no treatment for the sulphur removal through any secondary metallurgy operations in VSP.
- EMS and TERRITORY METALLURGY**:** Adopting territory metallurgy treatments and an Electric Magnetic Stirrer will help to achieve the best quality grade with accurate cast structure i.e. with more equiaxed grains.

6. REFERENCES

[1] Peiweihan, Ping Mei , Yi-Fei Lin, Shaojunchu, Oxide inclusions in ferromanganese and its influence on the quality of clean steels

[2] Balakrishnan, A. and brown, s., 1996, Process planning for aluminium tubes: an engineering-operations perspective.

[3] Portmann, M. C., Vignier, A., Dardilhac, D. and Dezalay, D., 1998, Branch and bound crossed with ga to solve hybrid ow shops. European journal of operational research.

[4] Rajendran, C. and Chaudhuri, D., 1992, A multi-stage parallel-processor owshop problem with minimum owtime. European journal of operational research, 57.

[5] Tang, L. X., Liu, J. Y., Rong, A. Y. and Yang, Z. H., 2000, A mathematical programming model for scheduling steelmaking-continuous casting production scheduling. european, Journal of Operational Research.

[6] Tang, L. X., Liu, J. Y., Rong, A. Y. and Yang, Z. H., 2001, A review of integrated planning & scheduling systems and methods for integrated steel production. European journal of Operational research, 133.

[7] Vignier, A., Billaut, J. C. and Proust, C., 1999, Hybrid owshop scheduling problems: state of the art. Rairo-recherche operationnelle-operations research, 33.

[8] Portal of CISR - Carnegie Mellon university center of iron and steel research (US)

[9] Journal of Phase Equilibria (IIM india)

Authors: **Bula Ratna Kumar Ambedkar, Dr G. Swami Naidu, T. Sreenivasarao, G. Varahalanaidu**, Dept. of Metallurgical engineering, JNTUK-UCEV, Vizinagaram, Andhra pradesh, India

E-mail: ambi3639@gmail.com

Journal of Production Engineering
Vol.19 No.2
JPE (2016) Vol.19 (2) Preliminary Note

Kádárová, J., Kočišová, M.

PERFORMANCE MEASURES OF INDUSTRIAL COMPANIES BASED ON BALANCED SCORECARD

Received: 01 November 2016 / Accepted: 03 December 2016

Abstract: *Companies exist or are created mainly because of the achievement of one or more strategic goals. To ensure continued success, they should monitor its performance with respect to them. In practice the performance of a company is often evaluated by estimating its performance indicators. This paper discusses the company's performance management cycle and production performance evaluation system, which is based on the internal processes of an industrial company.*
Key words: *performance measures, industrial companies, Balanced Scorecard*

Ocena performansi industrijskih preduzeća na osnovu sistema uravnoteženih pokazatelja. *Preduzeća postoje ili se stvaraju, uglavnom zbog postizanja jednog ili više strateških ciljeva. Da bi se osigurao kontinualni uspeh, trebali bi se meriti performance u odnosu na njih. U praksi se često performance ocenjuju određivanjem pokazatelja performansi. U ovom radu je prikazano upravljanje performansama preduzeća i sistem ocene proizvodnih performasi, koje su zasnovane na internim procesima industrijskih preduzeća.*
Ključne reči: *ocene performansi, industrijska preduzeća, uravnoteženi pokazatelji*

1. INTRODUCTION

Businesses have become more and more widespread and diverse and aim their strategies for enhancing the long term growth, success and performance (Figure 1).

As a production process becomes more complex, the availability and exchange of information become more critical to the efficiency of the business. The correlation of planning, production, sourcing, distribution, finance and work force information in near real time is a proven way to empower both management and staff to reduce errors and increase production efficiency. People are often talking about different ways of business performance measurement and control.

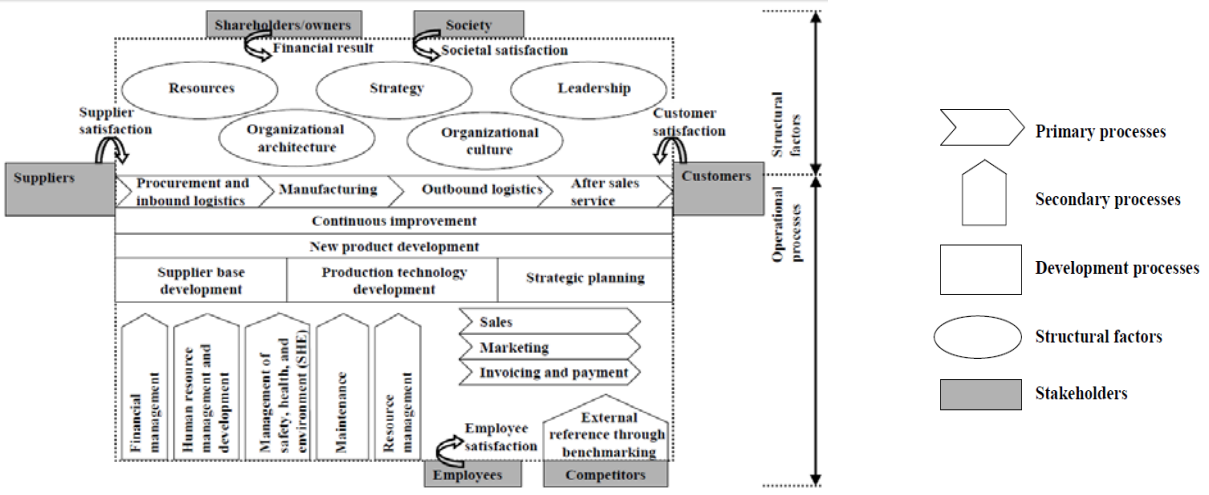

Fig. 1. A business model [1]

With the Balanced Scorecard (BSC), business owners and top management implement company strategy into business processes [2]. The BSC is a well known business performance management concept and translates strategy in terms of objectives, measures and targets in the four perspective – financial, customer, learning and growth and internal processes [3]. Environmental and social aspects can also be subsumed under the four existing BSC perspectives.

2. BUSINESS PERFORMANCE MANAGEMENT

Businesses have become more and more widespread and diverse and aim their strategies for enhancing the long term growth, success and performance [4].

As a product development process and production process becomes more complex, the availability and exchange of information become more critical to the

efficiency of the business [5]. The correlation of planning, production, sourcing, distribution, finance and work force information in near real time is a proven way to empower both management and staff to reduce errors and increase production efficiency [6]. People are often talking about different ways of business performance management (Figure 2).

This methodology implements a small feedback loop among the three major steps of performance management cycle - set goals, model, and plan [3].

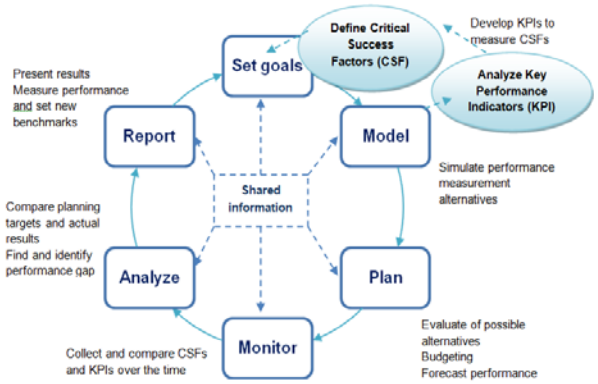

Fig. 2. An improved model of business performance management cycle [5]

Probably the best known, the most sophisticated and in terms of implementation the most successful performance measurement system used in industrial companies and based on performance management cycle is called Balanced Scorecard (BSC). It is instrument for strategic communication which translates strategy in terms of strategic goals, success factors and performance indicators in the four main perspectives – financial, customer, learning and growth and internal processes and two another perspectives staff satisfactions, and community and environment. So, the main idea of this measurement model is linking company's financial objectives with operational aspects of business such as customers, internal processes, learning and development [7].

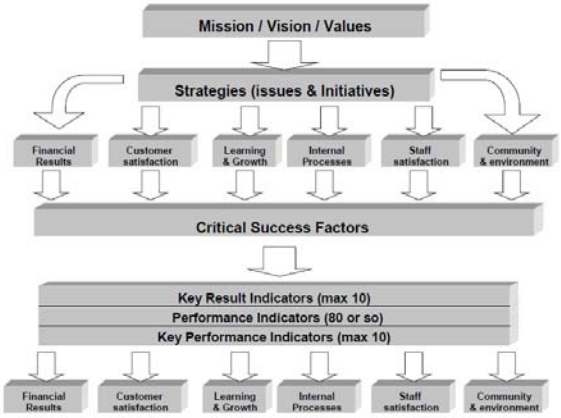

Fig. 3. Balanced Scorecard model

According to Figure 3, industrial design of company performance starts with the company's vision, mission, strategy, objectives, and appears in performance indicators [8].

Company's strategic goals are based on the mission, which describes the company's main objective for existence. For reaching the goal, company may use a variety of strategies. Strategy is developed thanks to analyze of the company operating environment, which allows describing the current situation and forecasting the future. Strategy is based on the company's core purpose, core values and vision [4].

Unfortunately, generally and abstractly formulated vision, mission and strategic goals depend on the verbal formation, that can be influenced by wishful thinking of the management. It is important to establish connections between the development and formulation of corporate strategy and its implementation [9].

Two different strategies can be distinguished when setting objectives and formulating strategy for industrial companies [4]:

- **Revenue growth strategy** - puts the emphasis on the market, products, customers and market segments. Origin for the revenue growth strategy development is in the sales department;
- **Productivity growth strategy** - puts the emphasis on the company`s manufacturing operations and on improving efficiency through the optimization of manufacturing processes, and improving technologies and the response to appearing problems.

3. CRITICAL SUCCESS FACTORS

Critical Success factors (CSFs) are the parameters which are vital for the success of a project or success of a business [10]. They monitor if a company or project achieve its mission.

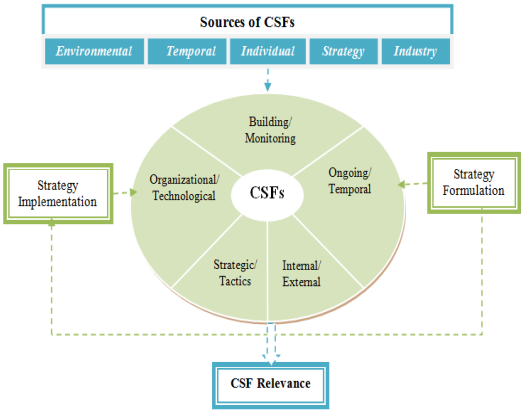

Fig. 4. Sources of CSFs

The advantages of identifying CSFs are that they are simple to understand and they can be used in concert with strategic planning methodologies. Clarifying the priority order of CSFs, measuring results, and rewarding superior performance will improve the odds for long-term success as well (Fig. 4).

4. KEY PERFORMANCE INDICATORS

Key performance indicators (KPIs) are quantifiable measurements that reflect the critical success factors of a project or business. KPIs are measures that quantify objectives and enable the measurement of strategic performance. They reflect the CSFs of a company. The application of KPI provides business executives with a

high-level, real-time view of the progress of a project or company (Figure 5). Types of KPIs are the following [11]:

- **Leading** - (typically financial) tell us how the company has performed in the past (revenue, cost, margin, etc.)
- **Lagging** – (non-financial) tell us how the organization is performing now, predict likely future financial performance (number of returns, on-time delivery, market share, etc.)
- **Input** - measure assets and resources invested in or used to generate business results.
- **Process** - measure the efficiency or productivity of a business process.
- **Output** - measure the financial and nonfinancial results of business activities.
- **Outcome** - reflect overall results or impact of the business activity in terms of generated benefits, as a quantification of performance.
- **Qualitative** - A descriptive characteristic or an opinion. They find out by customer or employee satisfaction through surveys. While the survey data itself is quantitative, the measures are based on a subjective interpretation of a customer's or employee's opinions.
- **Quantitative** - measurable characteristics, resulted by counting, adding, or averaging numbers. Quantitative data is most common in measurement and therefore forms the backbone of most KPIs.
- **Functional** - is relevant for an organizational main capability and is valid across multiple organization typed and industries.
- **Industry** - is specific for a particular line of operations or industry.

Careful analysis of the risk also enables the organization to convert the same to performance inputs and link them directly with the business goals and achieve higher business distinction. The Key Risk Indicators (KRI) and KPI can be made to work in direct collaboration with each other to facilitate business two different sides of the same coin. The KRI provide an early warning signal to the management regarding the impending risks involved in a particular activity, the KPI provide quantifiable inputs to enhance performance and enumerate the critical success factors vital to success in the company [12].

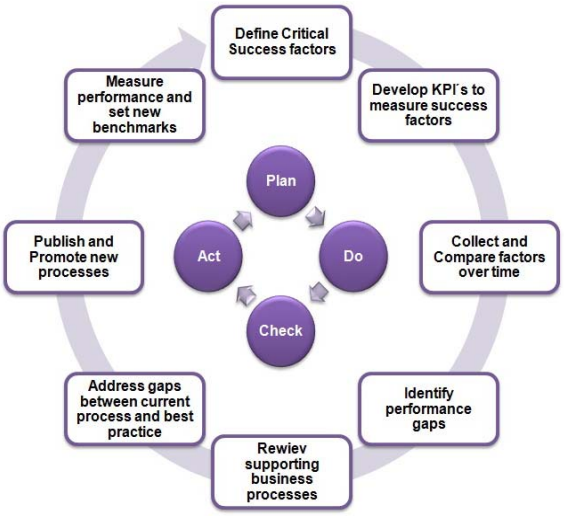

Fig. 5. KPI Identification Process [3]

1	**Strategic Objective** Which strategic objective is this indicator relating to?
2	**Key Performance Question (KPQ):** What Question do you want to have an answer to? What are our information needs?
3	Who is asking this question? Who is the information customer?
4	What will they do with the information? Why are they asking?
Performance indicator basics:	
5	KPI ID
6	KPI Name
7	KPI Owner
How will the data be collected	
8	What is the data collection method?
9	What is the source of the data?
10	What is the formula / scale / assessment method?
11	How often, when and for how long do we collect the data?
12	Who collects the data?
Target	
13	What is the target or performance threshold(s)?
Good measures tests	
14	How well is the indicator measuring performance?
15	What are the costs for collecting the data? Justified?
16	What dysfunctional behavior could this indicator trigger?
Reporting	
17	Who is the primary and secondary audience for this indicator
18	Reporting frequency (when and for how long will this indicator be reported?)
19	Reporting channel (which channels will be used to report this indicator?)
20	Reporting formats (in which formats will the information be reported?)

Table 1. Key Performance Indicator template [6]

The key risk indicators provide an early warning signal to the management regarding the impending risks involved in a particular activity, the key performance indicators provide quantifiable inputs to enhance performance and enumerate the critical success factors vital to success in an organization [13]. KRI and KPI, both are vital to company planning and objective strategy along with the CSF and hence, must be accounted for in the designing the long term plans of the company [14].

To help select appropriate KPIs, company should create a KPI assessment template (Table 1) that lists information of KPIs, how they affect the project, and how you can ensure meet the targets. 20-point Indicator Design Template has been created and used successfully in many companies.

The first four elements of the performance indicator design template address the purpose of the indicator. Then we look at some basics and at the more technical aspects of the data collection. Instead of just selecting any existing measurement method it is important to consider the strengths, weaknesses, and appropriateness of different data collection methods [1,15]. Targets should be:

- specific and time bound,
- stretching and aspirational but achievable,
- based on good information.

Than we check how well the KPI we have designed. Here we look at how well the indicator is actually measuring what it is supposed to measure, the costs versus benefits, and explore any undesirable consequences or cheating behavior this indicator might encourage.

In the final section of the indicator design template the designer of an indicator identifies the way the performance indicator is reported [16]. It identifies the audience, access restrictions, the reporting frequency, the reporting channels and reporting formats.

5. CONCLUSIONS

Key Performance Indicators are one of the most powerful tools available to enable companies to achieve performance improvement which should be a core goal of any performance management system. But using KPIs appropriately comes replete with challenges. KPIs should be primarily deployed for learning and improvement and not for command control. When KPIs are used inappropriately they also become the most resisted of management tools.

6. REFERENCES

[1] Hudáková-Stašová, L., & Bajus, R. (2015). Process controlling and its software solution. Actual problems of economics, 3(165), 492-503.

[2] KPI. (2014). On Key Performance Indicators (KPIs), KPIs…naturally, Australia. (smartKPIs, Ed.) Cit. 2015. Dostupné na Internete: http://www.smartkpis.com/key-performance-indicator-KPI

[3] Kaplan, R. S., & Norton, D. P. (1996). Translating Strategy Into Action: The Balanced Scorecard (1 ed.). Boston: Harvard Business Scool Press.

[4] Lavin, J., & Randmaa, M. (2012). 8th International Conference of DAAAM Baltic Industrial Engineering. Relations between business objectives and the actual outcome of the business, (pp. 19-21). Tallinn, Estonia.

[5] Jafari, M., Shahanaghi, K., & Tootooni, M. (2014). Developing a Robust Strategy Map in Balanced Scorecard Model Using Scenario Planning. (Hindawi, Ed.) Mathematical Problems in Engineering, 1-9.

[6] Marr, B. (2010, June 6). How to Design Key Performance Indicators, API White Paper. Retrieved 2015, from http://www.ap-institute.com/media/3970/how_to_design_key_performance_indicators_indicators.pdf

[7] Niven , R. P. (2006). Balanced Scorecard: Step by step (2 ed.). New York: John Wiley & Sons.

[8] Marr, B. (2015). What is a Key Performance Indicator (KPI)?, Key Performance Indicators. (A. BWMC, Ed.) Retrieved from http://www.ap-institute.com/Key%20Performance%20Indicators.html

[9] Rovnak, M., Chovancova, J., & Bednarova, L. (2013). 13th International Multidisciplinary Scientific Geoconference, SGEM 2013, Book Series: International Multidisciplinary Scientific GeoConference-SGEM. Managing environmental risks in production companies, (pp. 651-658). Albena, BULGARIA.

[10] Parmenter, D. (2008). Klíčové ukazatele výkonnosti: Rozvíjení, implementování a využívání vítězných klíčových ukazatelů výkonnosti. Česká společnost pro jakost. (1, Ed.) Praha, Cech Republic: Grada.

[11] Wagner, J. (2009). Merění výkonnosti, Jak měrit, vyhodnocovat a využívat informace o podnikové výkonnosti. (1, Ed.) Praha, Cech Republic: Grada.

[12] Rigby, D. K. (2011a). Management Tools 2011, An Executive's Guide, Boston. (Bain&Company, Ed.) Retrieved from http://www.bain.com/Images/Bain_Management_Tools_2011.pdf

[13] Rigby, D., & Bilodeau, B. (2011). Management Tools and Trends 2011. (Bain&Company, Ed.) Retrieved 2015, from http://www.bain.es/management_tools/Management_Tools_and_Trends_2011_Final_Results.pdf

[14] Nývltová, R., & Marinič, P. (2010). Finanční řízení podniku, Moderní metódy a trendy. Praha, Cech Republic: Grada.

[15] Hudáková-Stašová, L., & Bajus, R. (2015). Cost management using the activity based costing model. Actual problems of economics, 164(2), 373-387.

[16] Mixtaj, L., Nascakova, J., & Weiss, E. et al. (2012). Evaluation of return on investment for proposed use of solar systems in Poland. Metallurgy & Metallurgical Engineering, 51(3), 361-364.

Acknowledgements

This contribution is the result of the projects implementation: Project VEGA 1/0741/16 Controlling innovation of the industrial companies for the sustaining and improving their competitiveness.

Authors: **doc. Ing. Jaroslava Kádárová, PhD. Ing. Michaela Kočišová, PhD. MBA.** Technical University of Košice, Department of Industrial Engineering and Management, Němcovej 32, 042 00, Košice, Slovak Republic, Phone.: +421 55 602 3242

E-mail: jaroslava.kadarova@tuke.sk
michaela.kocisova@tuke.sk

IN MEMORIAM

Prof. Dr Janko Hodolič (1950–2015)

Prof. dr Janko Hodolič was born on 09. August 1950 in Pivnice, Republic of Serbia. He graduated at the Faculty of Mechanical Engineering in Novi Sad, while he defended his master and doctor of science thesis at the Faculty of Technical Sciences in Novi Sad. After graduation he started to work as assistant, in scientific field of machine tools, and later as assistant for subject: automatic machine handling at Faculty of Technical Sciences in Novi Sad. In June 1989 he was elected for the position of assistant professor for scientific field of machine tools, flexible technological systems and automation of design processes at Faculty of Technical Sciences in Novi Sad. For the same scientific field and for subjects: Flexible technological systems and Machine tools, he was elected for the position of associate professor in June 1994. In June 1997 was elected for the position of full professor in scientific field of metrology and fixtures, for subjects: Measurement and control and Fixtures. His scientific and research activities were mostly oriented on application of computer technologies in various fields of mechanical engineering (FTS, CAD, CAM, CAQ). Since 2000 he actively dealt with aspects of measurement and quality in field of environmental engineering, and from 2008 in field of biomedical engineering.

For a great contribution to scientific development, in 2006 he was promoted to honorary doctor of science at the Technical University in Kosice (Dr.h.c.). In the same period he was elected for the position of visiting professor at the Slovak Technical University in Bratislava and the Central European College in Skalica, Slovakia. He performed lectures on number of subjects, including: machine tools, automated management of machine tools, FTS, fixtures, fixture design accessories and measuring machines, measurement and quality, computer integrated manufacturing - CIM, information technologies in plastic design, environmental technologies and systems, ecodesign, measurement and control of pollution, and mechanical engineering in environmental protection. Most of these subjects, he conceived and developed with his closest associates.

He published over 450 scientific papers as author and co-author, of which about half were published at the international level, in monographs, journals and at conferences. He reviewed a number of books and numerous scientific papers from his scientific fields. He participated in realization of more than 50 scientific and research national and international projects, including projects of technological development of Republic of Serbia, projects of importance for the technological development of AP Vojvodina, CEEPUS, TEMPUS, bilateral, multilateral, etc. At more than 20 projects he was the manager or coordinator. As mentor or member he participated in commissions for the defense of a large number of a graduate, master's theses and doctoral dissertations at universities in Serbia, Slovenia and Slovakia. At the same universities he participated in a number of electing commissions for the professor positions.

Already as a student he showed an affinity for social engagement. He was President of the International Cooperation Student Association of Mechanical Engineering and Vice President of Student Association. After the employment, he served as a President of the Council OOUR, director of the Institute for Production Engineering, vice dean for finances and vice dean for science and international cooperation at the Faculty of Technical Sciences. He was also the head of the study program environmental management at doctoral studies at the Central European College in Skalica, Slovakia, where he also was the vice-rector for research. On the Slovak Technical University in Bratislava he was elected as a member of the Scientific and Academic Council.

Professor Hodolic was a member of several national and international scientific professional associations (JUSK, DAAAM, SETAC, etc.), editorial boards of national and international journals, as well as organizational, program, and scientific committees of national and international conferences. He is the founder of scientific conference ETIKUM and CASE LCA network of scientific LCA centres of Central and Eastern Europe. For outstanding contribution to the field of production engineering he was awarded with "Prof. Dr. Pavle Stanković" plaque and charter.

IN MEMORIAM

Prof. Dr Ljubomir Borojev (1945–2016)

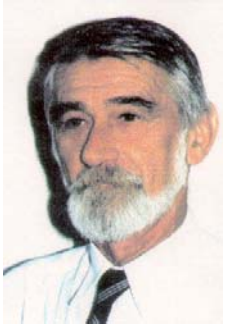

Our esteemed Dr Ljubomir Borojev, retired full professor of the Faculty of Technical Sciences in Novi Sad, suddenly died on Sunday, 4th of September 2016.

Ljubomir Borojev was born on 11th of June 1945 in Pancevo. He finished his Primary and Secondary School education in Novi Sad. He graduated from the Faculty of Mechanical Engineering in Novi Sad in 1970. and completed postgraduate studies for the degree of Master of Science from the Faculty of Technical Sciences in Novi Sad. His Master's thesis entitled “Hydrostatic support of the machine tools elements for finishing machining," was completed in 1980, and doctoral thesis entitled "Contribution to the development of design methodology of modern machine tools on the basis of experimental and computer modeling of the hydrostatic bearings for the high-precision spindles " was done at the same Faculty in 1994.

After graduation in 1970, he joined the Mechanical Engineering Department of the Faculty of Technical Sciences as an assistant at the Department of metal cutting machining. He became Assistant Professor in 1994, Associate Professor in 2000 and a Full Professor for the scientific field "Machine tools, flexible manufacturing systems and automation of process designing" in July 2005.

He has achieved a remarkable and enviable academic career during 40 years of working at the Faculty. In the course of his career at the Faculty of Technical Sciences, he conducted a large number of practical classes and lectures within the courses of Machine tools, Exploitation of machine tools, Processing and Technological Systems and Automatic flexible technological systems, which are remembered by his students for an interesting way of presenting as well as inspiration they were performed with. He also performed lectures for postgraduate courses, including Modern Machining Systems and Selected Chapters in Automatic Flexible Manufacturing Systems. During all those years he actively worked on improving the teaching process, gained a significant experience as a teacher and became extremely appreciated lecturer by both his colleagues and students. According to many, he was and will always remain one of the best lecturers of the Faculty of Technical Sciences.

Prof. Borojev gave a great contribution to the development of young scientists. Under his primarily teaching methods as well as his professional and scientific leadership, dozens of students gained their professional qualification of mechanical engineer. He also participated in management and in the committees for the defense of master's and doctoral theses at the Faculty of Technical Sciences. It can be said that Prof. Borojev dedicated his whole life to his work commitment at the Faculty, Institute, Department, Laboratory and his work with students.

It can be considered that Professor Borojev was one of the pioneers, and one of the few researchers in the world dealing with the problems of hydrostatic and aerostatic bearing of main spindles for grinding machine tools. His scientific and technical work is included in over 100 scientific papers published in journals and conference papers in the country and abroad, over 40 research projects studies, several monographic scientific publications, textbooks, scripts, and more than 50 technical papers in the form of projects, feasibility studies and specialized publications. In many companies of the metal complex Vojvodina he was always very welcomed as a product development consultant, especially in the field of experimental testing of processing systems.

During his professional career at the Faculty, he performed a large number of social functions, including: Director of the Institute for Production Engineering, President of the Council of the Institute for Production Engineering, Member of the Council of the Faculty of Technical Sciences, Head of the Laboratory for Machine Tools, Flexible Technological Systems and Automation of Process Design. He was repeatedly commended and rewarded for his work.

We, his friends and associates, colleagues, former students, will always remember Professor Ljubomir Borojev with utmost respect.

Journal of Production Engineering

PUBLICATION ETHICS AND PUBLICATION MALPRACTICE STATEMENT

The statement is based on the worldwide recognized Elsevier's Publishing ethics resource kit (http://www.elsevier.com/ethics/toolkit) and on the Committee on Publication Ethics (COPE) Code of Conduct (http://publicationethics.org/resources/guidelines). Full detailed guidelines of international standards for authors and editors can be found here: http://publicationethics.org/international-standards-editors-and-authors.

1. Authors' duties

Reporting standards. Authors of original research reports should present an accurate account of the work performed as well as an argumentatively coherent discussion of its significance. Underlying data should be represented accurately in the paper. A paper should contain sufficient detail to permit others to judge the academic and scientific merits of the work. Fraudulent or knowingly inaccurate statements constitute unethical behaviour and are unacceptable.

Data access and retention. Authors may be asked to provide the raw data in connection with a paper for editorial review, and should be prepared to provide public access to such data, if practicable, and should in any event be prepared to retain such data for a reasonable time after publication.

Originality and plagiarism. The authors should ensure that they have written entirely original works, and if the authors have used the work and/or words of others that this has been appropriately cited or quoted. Plagiarism takes many forms, from 'passing off' another's paper as the author's own paper, to copying or paraphrasing substantial parts of another's paper (without attribution), to claiming results from research conducted by others. Plagiarism in all its forms constitutes unethical publishing behaviour and is unacceptable.

Multiple, redundant or concurrent publication. An author should not in general publish manuscripts describing essentially the same research in more than one journal or primary publication. Submitting the same manuscript to more than one journal concurrently constitutes unethical publishing behaviour and is unacceptable. In general, an author should not submit for consideration in another journal a previously published paper.

Acknowledgement of sources. Proper acknowledgment of the work of others must always be given. Authors should cite publications that have been influential in determining the nature of the reported work. Information obtained privately, as in conversation, correspondence, or discussion with third parties, must not be used or reported without explicit, written permission from the source.

Authorship of the paper. Authorship should be limited to those who have made a significant contribution to the conception, design, execution, or interpretation of the reported study. All those who have made significant contributions should be listed as co-authors. Where there are others who have participated in certain substantive aspects of the research project, they should be acknowledged or listed as contributors. The corresponding author should ensure that all appropriate co-authors and no inappropriate co-authors are included on the paper, and that all co-authors have seen and approved the final version of the paper and have agreed to its submission for publication.

Disclosure and conflicts of interest. All authors should disclose in their manuscript any financial or other substantive conflict of interest that might be construed to influence the results or interpretation of their manuscript. All sources of financial support for the project should be disclosed.

Fundamental errors in published works. When an author discovers a significant error or inaccuracy in his/her own published work, it is the author's obligation to promptly notify the journal editor or publisher and cooperate with the editor to retract or correct the paper.

2. Editors' duties

Publication decisions. The editors of a peer-reviewed journal are responsible for deciding which of the articles submitted to the journal should be published. The editors may be guided by the policies of the journal's editorial

board and constrained by such legal requirements as shall then be in force regarding libel, copyright infringement and plagiarism. The editors may confer with other editors or reviewers in making this decision.

Fair play. An editor should evaluate manuscripts for their intellectual content without regard to race, gender, sexual orientation, religious belief, ethnic origin, citizenship or political philosophy of the authors.

Confidentiality. The editors and any editorial staff must not disclose any information about a submitted manuscript to anyone other than the corresponding author, reviewers, potential reviewers, other editorial advisers, and the publisher, as appropriate.

Disclosure and conflicts of interest. Unpublished materials disclosed in a submitted manuscript must not be used in an editor's own research without the expressed written consent of the author. Privileged information or ideas obtained through peer review must be kept confidential and not used for personal advantage.

3. Reviewers' duties

Contribution to editorial decisions. Peer review assists the editors in making editorial decisions and through the editorial communications with the author may also assist the author in improving the paper.

Promptness. Referees who feel unqualified to review the research reported in a manuscript or knows that a prompt review will be impossible, should notify the editor and excuse themselves from the review process.

Confidentiality. Any manuscripts received for review must be treated as confidential documents. They must not be shown to or discussed with others except as authorized by the editors.

Ethics. Reviews should be written respectfully. Personal criticism of the author is inappropriate. Referees should express their views clearly with supporting arguments. Sweeping general remarks that disfavour the author's paper is unacceptable and such remarks needs to be backed up with clear arguments and concrete references to the content of the paper reviewed.

Acknowledgement of sources. Reviewers should identify relevant published work that has not been cited by the authors. Any statement that an observation, derivation, or argument had been previously reported should be accompanied by the relevant citation. A reviewer should also call to the editors' attention any substantial similarity or overlap between the manuscript under consideration and any other published paper of which they have personal knowledge.

Disclosure and conflict of interest. Unpublished materials disclosed in a submitted manuscript must not be used in a reviewer's own research without the express written consent of the author. Privileged information or ideas obtained through peer review must be kept confidential and not used for personal advantage. Reviewers should not consider manuscripts in which they have conflicts of interest.

INSTRUCTIONS FOR CONTRIBUTORS

No. of pages:	4 DIN A4 pages
Margins:	left: 2,5 cm
	right: 2 cm
	top: 2 cm
	bottom: 2 cm
Font:	Times New Roman
Title:	Bold 12, capitals
Abstract:	Italic 10
Headings:	Bold 10, capitals
Subheadings:	Bold 10, small letters
Text:	Regular 10
Columns:	Equal column width with 0,7 cm spacing
Spacing:	Single line spacing
Formulae:	Centered and numerated from 1 in ascending order. Equations must be typed in Equation Editor, with following settings: Style>Math – Times New Roman Size>Full 12pt, Subscript/Superscript 7pt, Symbol 18 pt
Figures:	High quality, numerated from 1 in ascending order (e.g.: Fig.1, Fig. 2 etc.); Figures and tables can spread over both two columns, please avoid photographs and color prints
Tables:	Numerated from 1 in ascending order (e.g..: Tab. 1, Tab. 2, etc.)
References:	Numerated from [1] in ascending order; cited papers should be marked by the number from the reference list (e.g. [1], [2, 3] ...)
Submission:	**Papers prepared in MS Word format should be e-mailed to: pkovac@uns.ac.rs, savkovic@uns.ac.rs**
Notice:	**Papers are to be printed in Journal of Production Engineering** Sample paper with detailed instructions can be found at: **http://www.jpe.ftn.uns.ac.rs/**

FOR MORE INFORMATION, PLEASE CONTACT:

Prof. Pavel Kovač, PhD, MEng.
Assist. Prof. Borislav Savković, PhD, MEng.
FACULTY OF TECHNICAL SCIENCES
Department for Production Engineering
Trg Dositeja Obradovica 6
21000 Novi Sad
Serbia

Tel.: (+381 21) 485 23 24; 485 23 20 ; 450 366;
Fax: (+381 21) 454 495
E-mail: pkovac@uns.ac.rs, savkovic@uns.ac.rs
http://www.jpe.ftn.uns.ac.rs/